

Crude Oil Families in the Euphrates Graben Petroleum System



Berlin Institute of Technology (TU Berlin)

**Helmholtz Centre Potsdam – GFZ German Research
Centre for Geosciences**

Crude Oil Families in the Euphrates Graben Petroleum System

وَقَدْ عَلِمْنَا



... to the soul of my great mother who has traveled from this world
without saying GOOD-BYE MY LITTLE this work is dedicated

Contents

| | |
|---|------------|
| Contents | i |
| ABSTRACT | v |
| ZUSAMMENFASSUNG | vii |
| Acknowledgements | ix |
| List of Figures | x |
| List of Tables | xiv |
| 1 Introduction and Background | 1 |
| 1.1 Petroleum Geochemistry | 1 |
| 1.1.1 Petroleum Origin and Generation | 3 |
| 1.1.2 Petroleum Migration and Accumulation | 6 |
| 1.1.3 Petroleum Systems and Oil Families | 7 |
| 1.2 Regional Petroleum Geology | 10 |
| 1.3 The Study Area | 15 |
| 2 Goals and Objectives | 23 |
| 3 Experimental Methods | 25 |
| 3.1 Oil Samples Analysis | 25 |
| 3.1.1 Whole Oil Gas Chromatography (GC-FID) | 28 |
| 3.1.2 Single Ion Monitoring - Gas Chromatography - Mass Spectrometry (SIM-GC-MS) | 30 |

| | | |
|----------|---|------------|
| 3.1.3 | Compound Specific Stable Isotopes | 30 |
| 3.2 | Rock Samples Analysis | 34 |
| 3.2.1 | Solvent Extraction | 34 |
| 3.2.2 | Gas Chromatography of Saturates GC-FID | 36 |
| 3.3 | Oil and Source Rock Samples Analysis | 36 |
| 3.3.1 | Medium Pressure Liquid Chromatography MPLC | 36 |
| 3.3.2 | Gas Chromatography - Mass Spectrometry GC-MS | 37 |
| 3.3.3 | Metastable Reaction Monitoring MRM-GC-MS-MS | 39 |
| 4 | Results | 55 |
| 4.1 | Oil Samples | 55 |
| 4.1.1 | Bulk Properties | 55 |
| 4.1.2 | Molecular Composition | 62 |
| 4.1.3 | Aliphatic Biomarkers Characteristics | 73 |
| 4.1.3.1 | Hopanes | 74 |
| 4.1.3.2 | Steranes | 77 |
| 4.1.4 | Diamondoids | 87 |
| 4.1.5 | Aromatic Hydrocarbons | 93 |
| 4.1.6 | Stable Isotopes | 101 |
| 4.1.6.1 | Stable Carbon Isotopes | 102 |
| 4.1.6.2 | Stable Hydrogen Isotopes | 107 |
| 4.2 | Rock Samples | 117 |
| 4.2.1 | Source Rock Quality | 117 |
| 4.2.2 | Normal Alkanes | 119 |
| 4.2.3 | Biomarker Characteristics of Rock Extracts | 119 |
| 5 | Discussion and Interpretation | 133 |
| 5.1 | Oil-Oil Correlation | 133 |
| 5.1.1 | Oil Families: Classification and Identification | 138 |
| 5.1.2 | Oil Families: Maturity Variations | 146 |
| 5.1.3 | Oil Families: Stable Isotopic Composition | 148 |
| 5.1.4 | Oil Families: Geographic and Stratigraphic Distribution | 153 |
| 5.2 | Oil-Source Rock Correlation | 156 |

| | | |
|----------|---|------------|
| 5.2.1 | Source Rock Distribution | 156 |
| 5.2.2 | Geochemical Oil-Source Rock Correlation | 158 |
| 5.2.3 | Possible Oil Migration Pathways | 160 |
| 5.3 | Oil Mixing Potential | 165 |
| 5.4 | Petroleum Biodegradation | 175 |
| 6 | Summary and Conclusions | 191 |
| | Bibliography | 197 |
| | Appendices | 227 |
| A | GCFID Fingerprints of Crude Oils | 229 |
| B | Geochemical Data of Analysed Oils | 243 |
| C | Oil Families Geochemistry | 255 |
| D | Mixing Model Calculations | 259 |
| E | Concentration of Crude Oil Constituents | 261 |

ABSTRACT

Located in the northern part of Arabian Peninsula, Syria is one of the Middle East oil countries. The most petroliferous province in Syria is the Euphrates Graben system in the eastern part of the country. Oil and gas have been discovered in this graben in the mid 1980's by Shell E&P and its partners. Since then no comprehensive study has been performed to investigate the origin of crude oils produced from more than 60 oil fields in the area. This study deals with this issue from a petroleum geochemistry perspective and tries to answer open questions regarding the source of light and heavy oils produced over the Euphrates Graben. Eighty two oil samples in addition to 37 rock samples have been analysed geochemically in order to investigate the molecular composition of hydrocarbons and the maturation degree of their associated source rocks. Routine geochemical analysis in addition to stable isotopes and diamondoid analyses were carried out for 30 oil samples. Based on gross composition, biomarker and non-biomarker characteristics, oil-oil correlation identified three oil families in the study area: Family 1, Family 2A and Family 2B. Crude oils of Family 1 have been found to be generated from a marine, clay-rich and highly mature source rock. The related source rock is older than Jurassic in age based on age-related biomarker parameters. Maturity-related parameters (aliphatic biomarkers) and non-biomarkers (like diamondoids) imply that a highly mature source rock is responsible for generating Family 1 crude oils. These features fit very well to Palaeozoic Tanf Formation (Abba group) which is equivalent to Lower Silurian Hot Shales found elsewhere in the Middle East and North Africa. However, the Upper Cretaceous R'mah Formation and Shiranish

Formation were found to be responsible for generating the remaining crude oils studied here. Compositional and molecular differences between families 2A and 2B were attributed to facies and subtle maturation variations. Geochemical oil-source rock correlation supported the classification of oil families that Family 2A was most likely generated from the Shiranish Formation, while the R'mah Formation was the source rock for Family 2B oils. According to the very complex tectonic situation of this rift basin and, additionally, the lack of geological data, it was not possible to definitely retrace the migration pathways for oils from source rocks to reservoirs. However, an attempt to figure out the potential migration fairways is presented by concepts for trap configurations for specific areas especially for crude oils found in shallow Miocene reservoirs. To predict to which extent these oil families could mix with each other, oil mixing mathematical models have been applied for crude oils which have different signatures from different sources. The results of the theoretical mixing were promising and showed that some oils in the southeastern part of the graben generated principally from the Upper Cretaceous R'mah Formation, and have got significant contribution from a Silurian source rock. These findings about petroleum mixtures could support the attempts to find more hydrocarbon plays in the Palaeozoic section in south- and northeastern part of the graben by retracing possible oil migration routes. Secondary alteration processes influenced the petroleum composition particularly in shallow reservoirs. Geochemical investigations for crude oils in the northwestern part of the graben showed that biodegradation took place resulting in lower API gravities and poorer light ends.

ZUSAMMENFASSUNG

Syrien, im nördlichen Teil der arabischen Halbinsel gelegen, ist eines der wichtigsten erdölproduzierenden Länder des Nahen Ostens. Eine der erdölhöfigsten Provinzen ist das Euphrat-Graben-System im östlichen Teil des Landes, in dem im Laufe der 80er Jahre Erdöl und Erdgas durch Shell E&P und seine Partner entdeckt wurden. Seit damals wurden keine weiterführenden Studien durchgeführt, welche die Herkunft der aus mehr als 60 Ölfeldern stammenden Rohöle eindeutig belegen könnten. Die vorliegende Arbeit widmet sich dieser Wissenslücke mit einem petroleum-geochemischen Ansatz und versucht, offene Fragen bezüglich der Herkunft der im Bereich des Euphrat Grabens geförderten Leicht- und Schweröle zu beantworten. 82 Ölproben und 37 Gesteinsproben wurden geochemisch analysiert, um die molekulare Zusammensetzung der geförderten Kohlenwasserstoffe zu untersuchen und den Reifegrad der jeweiligen Muttergesteine festzustellen. Für 30 ausgewählte Ölproben wurden zusätzlich stabile Isotope und Diamantoiden analysiert. Durch Öl-Öl Korrelation, basierend auf der Gesamtzusammensetzung, sowie Charakteristika von Biomarkern und Nicht-Biomarkern, wurden drei Ölfamilien im Studiengebiet identifiziert: Familie 1, Familie 2A und Familie 2B. Für die Rohöle der Familie 1 kann gezeigt werden, dass diese von einem marinen, tonreichen Muttergestein stammen, welches, nach Analyse reifeabhängiger Biomarker (aliphatische Biomarker) und Nicht-Biomarker (Diamantoiden), von hoher Maturität sein muss. Unter Zuhilfenahme altersabhängiger Biomarker-Parameter kann ein prä-jurassisches Alter abgeleitet werden. Basierend auf diesen Charakteristika kann auf die Tanf Formation (Abba Gruppe) als Muttergestein geschlossen werden, die

ein Äquivalent zu den "Hot Shales" des unteren Silurs im Nahen Osten und Nordafrika darstellt. Des Weiteren wird gezeigt, dass die in der Oberen Kreide abgelagerten R'mah Formation und Shiranish Formation verantwortlich für die Genese der übrigen untersuchten Rohöle sind. Kompositionelle und molekulare Unterschiede zwischen Familie 2A und 2B könnten auf Fazies- und geringfügige Reifeunterschiede zurückgeführt werden. Geochemische Erdöl-Muttergesteins-Korrelationen unterstützen die Klassifikation in ölfamilien dahingehend, dass die Familie 2A der Shiranish Formation und die Familie 2B der R'mah Formation zuzuordnen sind. Aufgrund der sehr komplexen tektonischen Situation und dem Fehlen relevanter geologischer Daten war es im Rahmen dieser Arbeit nicht möglich, einen eindeutigen Migrationsweg der Rohöle vom Muttergestein zum Reservoir nachzuvollziehen. Trotzdem werden hier potentielle Migrationswege unter Zuhilfenahme skizzenhafter Fallenstrukturen und Konfigurationen für spezifische Gebiete aufgezeigt, insbesondere für Rohöle aus den flachen Reservoiren des Miozäns. Um vorherzusagen, in welchem Ausmaß sich diese ölfamilien untereinander vermischen, wurden statistische Mischungsmodelle für öle mit unterschiedlichen Signaturen und Muttergesteinen erarbeitet. Die Ergebnisse dieses theoretischen "Mixing"-Ansatzes sind vielversprechend und zeigen, dass einige Öle aus dem südöstlichen Teil der Grabenstruktur zusätzlich zu ihrer primären Herkunft, der oberkretazischen R'mah Formation, signifikante Anteile aus silurischen Muttergesteinsintervallen aufweisen. Diese Ergebnisse könnten neue Explorationsansätze unterstützen, da durch Kenntnis möglicher Migrationsrouten zusätzliche Kohlenwasserstoffvorräte im paläozoischen Intervall im süd- und nordöstlichen Teil des Grabens zu finden sein können. Sekundäre Alterationsprozesse hatten ebenfalls, vor allem in flach gelegenen Reservoiren, einen signifikanten Einfluss auf die Erdölzusammensetzung. Geochemische Untersuchungen von Rohölen aus dem nordwestlichen Teil des Grabens zeigen, dass Biodegradation stattgefunden hat, was sich in einer höheren öldichte und einer geringeren Konzentration an kurzkettigen Kohlenwasserstoffen niederschlägt.

Acknowledgements

I would like to thank Prof. Brian Horsfield and Prof. Wilhelm Dominik for their expert supervision and kind support during the course of this project. My gratitude goes also to PD Dr. Heinz Wilkes and Dr. Hans-Martin Schulz for valuable discussions and their critical comments and feedbacks.

I am so thankful to the entire team at GFZ Potsdam - Section of Organic Geochemistry for the excellent working and supporting atmosphere.

Many thanks to our industry partners Shell International E&P and Al Furat Petroleum Company AFPC for providing the samples set and related data and for their permission to present the results of this study in the international conferences. Special thanks to Dr. Peter Nederlof who always supported the study.

My brothers, Hatem and Alaa, and lovely sisters and relatives . . .
Thanks all of you!!

Unlimited thanks to my divine wife Ranya who supported me throughout the whole PhD time by finding many different ways to keep me going on. She brought me sweet and vital gifts "Fatima, Ghassan, and Bilal".

List of Figures

| | | |
|------|--|----|
| 1.1 | Petroleum geochemistry improves forecasting efficiency. Modified after (Murriss, 1984). | 2 |
| 1.2 | The main stages of petroleum formation: diagenesis, catagenesis and metagenesis. Modified after (Horsfield & Rullkotter, 1994a). | 4 |
| 1.3 | The main geological elements of the petroleum system. Modified after (Magoon & Dow, 1994). | 8 |
| 1.4 | Oil and gas fields in the Middle East region adopted from (Konert <i>et al.</i> , 2001). | 11 |
| 1.5 | Oil and gas fields location in Syria adopted from (Brew <i>et al.</i> , 2001a). | 13 |
| 1.6 | Topography and the major tectonic zones of Syria. | 14 |
| 1.7 | Generalized stratigraphy and selected structural elements in various hydrocarbon provinces in Syria. Proven features related to hydrocarbon accumulation are shown as solid lines; dashed lines where uncertain. Adopted from (Brew <i>et al.</i> , 1997b) | 16 |
| 1.8 | Location map of the study area showing the wells from which the analysed oil samples come from. | 17 |
| 1.9 | Schematic cross section in the study area of AB profile in perpendicular to the graben axes (see Fig.1.8 for profile location). Modified after (de Ruiter <i>et al.</i> , 1995) | 19 |
| 1.10 | The stratigraphic column in the Euphrates Graben showing the main source rock and reservoir horizons. | 20 |

| | | |
|------|--|----|
| 3.1 | Example of a whole oil chromatogram of NSO (Norwigen Standard Oil). A full range of n -alkanes up to n - C_{35} was observed. . | 32 |
| 3.2 | Ion chromatograms displaying the distribution of adamantanes and diamantanes in oil sample G002961 (see Tab.3.3 for peak assignments) | 44 |
| 3.3 | Schematic view of a GC-C-IRMS-system for compound-specific isotope analysis. The separation of complex mixtures is done by gas chromatography. At a temperature of 940 °C separated compounds are oxidized to CO_2 and H_2O catalytically. The reduction interface eliminates nitrogen oxides and the water is separated from the carrier gas by a <i>Nafion</i> membrane in the water removal device. The remaining CO_2 is ionized and detected in the mass spectrometer. From the ratio of $^{44}CO_2$ to $^{45}CO_2$ the $\delta^{13}C$ value can be calculated. | 45 |
| 3.4 | Ion chromatogram displaying the distribution of alkyl benzenes in oil sample G002963. Tab.3.5 for peak assignments. | 46 |
| 3.5 | Ion chromatogram displaying the distribution of naphthalenes. Tab.3.6 for peak assignments. | 47 |
| 3.6 | Ion chromatogram displaying the distribution of phenanthrenes. Tab.3.7 for peak assignments. | 47 |
| 3.7 | Ion chromatogram displaying the distribution of dibenzothiophenes. Tab.3.8 for peak assignments. | 48 |
| 3.8 | Ion chromatogram displaying the distribution of monoaromatic steroids. Tab.3.9 for peak assignments. | 48 |
| 3.9 | Ion chromatogram displaying the distribution of triaromatic steroids. Tab.3.10 for peak assignments. | 49 |
| 3.10 | Ion chromatograms displaying the distribution of hopanes in the aliphatic fraction determined by GC-MS-MS. Tab.3.11 for peak assignments. | 49 |
| 3.11 | Ion chromatogram displaying the distribution of steranes in the aliphatic fraction determined by GC-MS-MS. Tab.3.12 for peak assignments. | 50 |

| | | |
|------|---|----|
| 3.12 | Ion chromatogram displaying the distribution of 21-, 24, 27-norcholestanes and 24-, 27-nordiacholestanes in the aliphatic fraction analysed by GC-MS-MS. Tab.3.13 for peak assignments. | 52 |
| 4.1 | Percent of sulfur versus API gravity for selected oil samples from the study area. | 58 |
| 4.2 | Cross plot showing nickel and vanadium concentrations for some Syrian oils. G002978, G002993, and G003005 have the highest V and N contents. | 59 |
| 4.3 | Bulk oil properties comparison for Syrian oil samples. API gravity decreases proportionally with increasing sulfur, vanadium, and nickel content. | 60 |
| 4.4 | Ternary diagram showing gross composition of oil samples. . . . | 61 |
| 4.5 | GC fingerprints for two oils from the study area. The dissimilarity can probably be attributed to different sources. | 63 |
| 4.6 | Crude oil sample (G002972) showed fewer gasoline range components, compared to the rest of the data set. This may be an indication of evaporative loss of the lighter ends during storage. | 64 |
| 4.7 | GC profile of G002997 oil sample showing loss in <i>n</i> -alkanes with a large hump of unresolved components giving them the appearance of biodegraded oils. | 68 |
| 4.8 | Cross plot showing that LHCPI values increase with increasing maturity. | 69 |
| 4.9 | Pristane and phytane formation from phytol, which is derived from the chlorophyll side chain. | 70 |
| 4.10 | The plot of $Pr/n-C_{17}$ vs. $Ph/n-C_{18}$ can be used to infer the oxicity and the organic matter type (Peters <i>et al.</i> , 1999b). . . . | 71 |
| 4.11 | The specific components used in calculating the saturates correlation parameters: where: $n-C_5$ = <i>n</i> -pentane, $n-C_6$ = <i>n</i> -hexane, $n-C_7$ = <i>n</i> -heptane, MCH = methylcyclohexane, Pr= pristane, Ph = phytane, CPI= carbon preference index. | 72 |

| | | |
|------|--|----|
| 4.12 | Plot of aromaticity (B) versus paraffinicity (F) ratios referring to several reservoir alteration processes after (Talukdar <i>et al.</i> , 1990). | 73 |
| 4.13 | Molecular structures of hopanes and steranes. | 74 |
| 4.14 | m/z 191 mass fragmentograms showing the three types (tri-, tetra-, and pentacyclic) of terpanes observed within the samples set. (a) shows a significant dominance of hopanes (C_{29} and C_{30}), (b) represents a different patterns of tricyclic and pentacyclic terpanes, (c) has no recognizable compounds to be identified. . . | 75 |
| 4.15 | Molecular structures of C_{27} 18α -trinorneohopane (18α -22,29,30-trinorneohopane <i>or</i> Ts) and C_{27} 17α -trinorhopane (17α -22,29,30-trinorhopane <i>or</i> Tm). | 76 |
| 4.16 | m/z 217 mass fragmentograms showing the sterane and diasterane distributions observed within the samples set. (a) shows a relative dominance of diasteranes over steranes compounds, (b) has different distribution of steranes and diasteranes, (c) represents regular steranes dominance. | 79 |
| 4.17 | C_{28}/C_{29} $\alpha\beta\beta$ sterane ratio as an age-related biomarker. Low values (below 0.7) for G002954, G002959, G002982, and G002988 oil samples indicate probably to Palaeozoic origin. | 80 |
| 4.18 | The structures of 21-, 24-, and 27-norcholestane and 24- and 27-nordiacholestane compounds identified in the crude oils. . . . | 83 |
| 4.19 | The $24/(24+27)$ -nordiacholestane ratio as an effective source-age parameter to distinguish oils originating from different eras. . . | 84 |
| 4.20 | Molecular structures of $20R$ (biological epimer) and $20S$ (geological epimer) for the C_{29} $5\alpha, 14\alpha, 17\alpha(H)$ -steranes. | 85 |
| 4.21 | Cross plot of sterane maturity parameters based on apparent isomerization of asymmetric centers in the C_{29} steranes. | 86 |
| 4.22 | Triangular plot illustrating the relative abundance of C_{27} , C_{28} , and C_{29} regular steranes [$5\alpha, 14\alpha, 17\alpha(H)$ $20S + 20R$ and $5\alpha, 14\beta, 17\beta(H)$ $20S + 20R$] in the saturate fractions of crude oils. The arrow illustrates the decreasing C_{29} concentration through geological time; after (Grantham & Wakefield, 1988). | 87 |

| | | |
|------|---|-----|
| 4.23 | Molecular structures of diamondoids (adamantane and diamantane). | 88 |
| 4.24 | Cross plot of sum of the concentration of the entire range of diamantanes (ppm) versus the sum of the concentration of the entire range of adamantanes (ppm). Arrow refers to increasing maturity. | 90 |
| 4.25 | Cross plot of methyladamantane index (MAI) versus methyl-diamantane index (MDI). Limits of X and Y axis are obtained from (Chen <i>et al.</i> , 1996). No significant trend could be recognized. . . | 91 |
| 4.26 | Cross plot of dimethyl diamantane index-1 (DMDI-1) versus dimethyl diamantane index-2 (DMDI-2), where DMDI-1 typifies silica type II source and DMDI-2 typifies carbonate type II source (Schulz <i>et al.</i> , 2001). | 92 |
| 4.27 | Mass chromatograms of m/z 253 showing the distribution of the monoaromatic steroid hydrocarbons in three oil samples. Labeled peaks are identified in Tab.3.9 | 94 |
| 4.28 | Mass chromatograms of m/z 231 showing the distribution of the triaromatic steroid hydrocarbons in three oil samples. Labeled peaks are identified in Tab.3.10 | 95 |
| 4.29 | Mass chromatograms of m/z 184+198+212+226 showing the distribution of the alkyl-DBT hydrocarbons in three oil samples. Labeled peaks are identified in Fig.3.7 and Tab.3.8 for peak assignments | 98 |
| 4.30 | 4-MDBT/1-MDBT (MDR) versus $Ts/(Ts+Tm)$ showing a very good correlation suggesting that type (II+III) organic matter generated these oils. | 99 |
| 4.31 | Plot of carbon number versus $\delta^{13}C$ value for n -alkanes ($n-C_9$ - $n-C_{27}$) in the Euphrates Graben crude oils. Due to contamination with water, GC-C-IRMS measurements for sample G002968 were not possible. | 104 |

| | | |
|------|--|-----|
| 4.32 | Carbon isotopic composition of pristane and phytane in individual oil samples. A linear correlation with certain deviations was recognized. | 105 |
| 4.33 | Plots of carbon isotopic signature of pristane (a) and phytane (b) versus number versus dia/reg C_{27} - C_{29} steranes. A slight negative trend could be recognized. | 106 |
| 4.34 | Plots of carbon isotopic signature of pristane (a) and phytane (b) versus number versus the sum of adamantene hydrocarbons concentration. A slight negative trend could be recognized especially for pristane. | 106 |
| 4.35 | Plot of δ D value versus carbon number for n -alkanes (n - C_6 - n - C_{27}), pristane and phytane in the Euphrates Graben crude oils. Due to contamination with water, GC-C-IRMS measurements for G002968 crude oil were not possible. | 109 |
| 4.36 | Hydrogen isotopic composition of pristane and phytane in individual oil samples. A very good linear correlation could be recognized, that is much better than that one of carbon isotope shown in Fig.4.32. | 110 |
| 4.37 | Plots of hydrogen isotopic signature of pristane (a) and phytane (b) versus dia/reg C_{27} - C_{29} steranes. Increasing biomarker ratio is in agreement to gradual elevating of D-enrichment. It could be recognised that the correlation of this biomarker is better in pristane than in phytane case. | 111 |
| 4.38 | Plots of hydrogen isotopic signature of pristane (a) and phytane (b) versus the sum of adamantene concentration. Good correlation is observed as an exponential trend especially for pristane. . | 112 |
| 4.39 | Cross plot showing the correlation of diamondoid-based maturity parameter to the calculated difference of summed δ D values of pristane and phytane and the sum for δ D values of n - C_{17} and n - C_{18} | 114 |

| | | |
|------|---|-----|
| 4.40 | δD values of <i>n</i> -alkanes (<i>n</i> - C_9 to <i>n</i> - C_{25}), pristane and phytane from three crude oils. (a) G002959: offset 8‰, (b) G002963: offset 24‰, and (c) G002973: offset 30‰. Different maturation levels could be recognized looking at the different offset values (shown in parenthesis) as discussed in text. | 123 |
| 4.41 | A maturity profile of the average δD values of <i>n</i> -alkanes, and δD values of pristane and phytane for investigated oil samples. Some samples were not plotted (e.g. G002993 and G002997) as they have possible biodegradation effect. | 124 |
| 4.42 | TOC content in analysed rock samples from three different potential source rocks (R'mah, Abba, and Shiranish Formations). . . | 125 |
| 4.43 | Showing: (left) hydrogen index (HI) versus oxygen index (OI) values for the analysed sample set, and (right) hydrogen index (HI) versus (Tmax) values for the analysed sample set. | 126 |
| 4.44 | Total organic carbon content of 70 Silurian rock samples investigated in Al Furat Petroleum Company laboratory (Frijihoff <i>et al.</i> , 2006). | 127 |
| 4.45 | Vitrinite reflectance equivalent % R_o from graptolite reflectance measurements for Silurian Tanf Formation rock samples (Frijihoff <i>et al.</i> , 2006). | 127 |
| 4.46 | Saturate fraction gas chromatograms of the potential source rock samples. | 128 |
| 4.47 | Pr/ <i>n</i> - C_{17} vs. Ph/ <i>n</i> - C_{18} cross plot of the investigated rock samples. | 129 |
| 4.48 | Ternary diagram showing the relative abundance of C_{27} , C_{28} and C_{29} regular steranes in saturated hydrocarbon fractions of source rock samples (R'mah in red, Shiranish in blue, and Tanf/Abba in green). A distinction between Upper Cretaceous R'mah and Shiranish source rocks is relatively obvious. | 130 |
| 4.49 | Ternary diagram showing the relative abundance of C_{27} , C_{28} and C_{29} diasteranes in saturated hydrocarbon fractions of source rock samples (R'mah in red, Shiranish in blue, and Tanf/Abba in green). | 131 |

| | | |
|-----|--|-----|
| 5.1 | Three-dimensional Euclidean space. The point (x,y,z) is determined; like every point in such system, by three coordinates X, Y, Z. | 135 |
| 5.2 | Dendrogram of light hydrocarbon parameters listed in Tab.4.2 for 62 investigated oil samples from the Euphrates Graben. Hierarchical clustering distinguishes seven different groups of crude oils. Colored dots represent the oil samples selected for further geochemical analysis. | 137 |
| 5.3 | Geographic distribution of 62 oil samples representing the seven general crude oil groups identified in the study area. Symbol colors coincide with cluster colors illustrated in previous Fig.5.2. | 138 |
| 5.4 | Geographic distribution of 30 oil samples which have been selected for biomarker and stable isotope analyses. It is obvious that this sub set of samples is very well representing the whole sample set not only from the geochemical signature point of view but also from geographical distribution pattern in the study area. | 139 |
| 5.5 | Dendrogram shows genetic relationships among oils based on chemometric analysis of 23 source-related geochemical parameters (Appendix.C). Cluster distance is measure of genetic similarity indicated by the vertical distance from any two samples on the bottom to their branch point on the top. Family 1 (in blue) is probably generated from the Silurian Tanf Formation. Oils from Family 2A (in green) are most likely attributed to Upper Cretaceous source rocks. | 141 |
| 5.6 | Cross-plot shows $Pr/n-C_{17}$ against $Ph/n-C_{18}$ for the different families. Family 1 crude oils (blue triangles) have relatively low values of $Pr/n-C_{17}$ and $Ph/n-C_{18}$ which are attributed probably to the high maturity level of the source rock. | 142 |
| 5.7 | Ternary diagrams of C_{27} , C_{28} , and C_{29} sterane and diasterane composition for analysed oils based on MRM-GC-MS-MS. The identified three oil families are clearly distinguished. Dashed lines are only for visual reference. | 143 |

- 5.8 Cross-plot of dimethyldiamantene index DMDI-1 versus DMDI-2 (see equations Eq.4.1 and Eq.4.2 for identification) illustrates that Silurian oils (blue triangles) are identified to originate from a clay-rich source. Some oils from Family 2B (red circles) are located below the dashed line referring to a clear input of clay-rich source to these basically calcareous oils. 144
- 5.9 C_7 oil correlation star diagram (C_7 OCSD) clarifies the distinguishable signature of Family 1 crude oils (blue lines) from the Family 2A (green lines) and Family 2B (red lines) oils. It can be recognized that red lines are in an intermediate state between blue and green ones implying the assumption for red-colored oils to be a mixture from Silurian and Upper Cretaceous source rocks. 145
- 5.10 Cross plot based on diamondoids concentration illustrating the maturity variation of identified oil families. 147
- 5.11 Hydrogen isotopic profiles of n -alkanes from n - C_6 to n - C_{26} for different oil families, where Family 1 in blue, Family 2B in red, and Family 2A in gray. 149
- 5.12 Cross plots of δD versus $\delta^{13}C$ values for different hydrocarbons n - C_7 , n - C_{10} , n - C_{15} , n - C_{20} , Pristane, and Phytane. 150
- 5.13 Cross plots of pristane versus phytane δD values. 151
- 5.14 Cross plots of pristane δD values versus sum of adamantane concentration. 152
- 5.15 Geographic distribution of the main genetic oil families in the Euphrates Graben. Numbers near dots represents the oil samples code G00xxxx (e.g. 3017 is G003017) 154
- 5.16 Figure shows a combination of the distribution of identified oil families and the probable spread of potential source rocks across the study area. Very good correlation is obvious between the oil families and the probable associated source rocks. 157
- 5.17 Plot of pristane/ n - C_{17} vs. phytane/ n - C_{18} for oil samples of Family 2A and Family 2B and associated potential source rocks (Upper Cretaceous Shiranish and R'mah). 159

| | |
|---|-----|
| 5.18 Ternary diagram showing the relative abundance of C_{27} , C_{28} and C_{29} regular steranes in saturated hydrocarbon fractions of oils (families 2A and 2B) and extracted source rocks (R'mah and Shiranish). | 160 |
| 5.19 Ternary diagram showing the relative abundance of C_{27} , C_{28} and C_{29} diasteranes in saturated hydrocarbon fractions of oils (families 2A and 2B) and extracted source rocks (R'mah and Shiranish). | 161 |
| 5.20 Schematic sketch shows the possible migration routes of Family 2B from R'mah source rock to the accumulations. | 162 |
| 5.21 Schematic sketch illustrates the potential secondary migration pathways of Family 2A crude oils from the source rocks into the main reservoirs and the re-migration from Cretaceous into the Miocene accumulations. | 163 |
| 5.22 The theoretical structure of matrices used for mixing calculations, where G resembles the main matrix includes data of the end-members, d refers to the data of proposed mixed oil, and f is the proportion of each end-member in the mixed oil. | 170 |
| 5.23 Calculation result when applied for a (pure) Silurian oil. | 172 |
| 5.24 Mixing calculation results for proposed mixed oil samples (for oil sample locations see Fig.5.15). | 173 |
| 5.25 Schematic mechanisms of biodegradation within a petroleum reservoir. | 176 |
| 5.26 Generalized sequence of the removal of selected molecular groups at increasing levels of biodegradation, modified from (Wenger <i>et al.</i> , 2001). | 177 |
| 5.27 Biodegradation leads to the deterioration of crude oil quality as indicated by API gravity. | 178 |
| 5.28 Sulfur, nickel, and vanadium contents increase with decreasing API gravity as an indication of the biodegradation effect. | 179 |

| | | |
|------|---|-----|
| 5.29 | Whole oil GC-FID chromatograms for selected non-biodegraded (pink) and biodegraded (blue) oil samples. Different distribution of saturated hydrocarbons can easily be recognized. | 180 |
| 5.30 | Plot of conventional biodegradation parameters $i-C_5/(i-C_5+n-C_5)$ vs. $3MP/(3MP+n-C_6)$ showing different signatures of the proposed biodegraded oils (in blue). | 181 |
| 5.31 | Cross plot of the ratios $Pr/n-C_{17}$ vs. $Ph/n-C_{18}$. The increased values of the blue samples can be interpreted as a result of biodegradation effects. | 182 |
| 5.32 | Whole-oil chromatogram of G002998 sample shows higher biodegradation degree in comparison with other biodegraded oil samples. | 184 |
| 5.33 | C_7 oil transformation star diagram (C_7 OTSD) shows that G002997, G002993, and G003011 oil samples have suffered from alteration processes as having relatively low values of Tr's as interpreted according to (Halpern, 1995). | 185 |
| 5.34 | Plot of the conventional biodegradation parameter $Ph/n-C_{18}$ vs. the <i>mean degradative loss</i> (MDL) for biodegraded oil samples. . | 187 |
| 5.35 | Whole-oil chromatogram of G003005 sample shows no significant appearance of biodegradation effect. | 188 |
| 5.36 | Stable carbon isotopic profiles of n -alkanes ($n-C_9$ - $n-C_{26}$) for biodegraded (blue) and non-biodegraded (orange) oil samples. . . . | 189 |
| 5.37 | Stable hydrogen isotopic profiles of n -alkanes ($n-C_6$ - $n-C_{26}$) for biodegraded (blue) and non-biodegraded (orange) oil samples. . | 190 |
| A.1 | illustrates the GC fingerprints for analyzed crude oils from the study area. | 242 |

List of Tables

| | | |
|------|---|----|
| 3.1 | List of the analysed 82 Oil samples | 28 |
| 3.2 | List of the light and saturated hydrocarbons, which were identified by gas chromatography flame ionization detection. Also given are abbreviations used in the chromatogram that is shown in Fig.3.1. | 30 |
| 3.3 | Adamantanes and diamantanes identified in Syrian crude oil sample. Peak series correspond to those in Fig.3.2 | 31 |
| 3.4 | List of 37 rock samples analysed in the current study with different analytical methods. | 35 |
| 3.5 | Alkylbenzenes identified in Syrian crude oil samples. Peak series correspond to those in Fig.3.4. | 38 |
| 3.6 | Naphthalenes identified in Syrian crude oil samples. Peak series correspond to those in Fig.3.5. | 39 |
| 3.7 | Phenanthrenes identified in Syrian crude oil samples. Peak series correspond to those in Fig.3.6. | 40 |
| 3.8 | Dibenzothiophenes identified in Syrian crude oil samples. Peak series correspond to those in Fig.3.7. | 41 |
| 3.9 | Monoaromatic steroids identified in Syrian crude oil samples. Peak series correspond to those in Fig.3.8. | 42 |
| 3.10 | Triaromatic steroids identified in Syrian crude oil samples. Peak series correspond to those in Fig.3.9. | 42 |
| 3.11 | Individual hopanes identified in the aliphatic fraction of Syrian crude oil samples analysed by GC-MS-MS. | 43 |

| | | |
|------|---|----|
| 3.12 | Identified steranes in the aliphatic fraction of Syrian crude oil samples analysed by GC-MS-MS. | 51 |
| 3.13 | Nor- and nordiacholestanes identified in Syrian crude oil samples. | 52 |
| 3.14 | C_{30} methylsteranes identified in Syrian crude oil samples by MRM GC-MS-MS. | 53 |
| 4.1 | Bulk geochemical composition for a suite of Syrian oil samples. where: Sat % = percent saturated hydrocarbons, Arom % = percent aromatic hydrocarbons, NSO % = percent hetero compounds (resins and asphaltenes), S % = percent sulfur content, V (ppm) = vanadium concentration [part per million], N (ppm) = nickel concentration [part per million], sat/arom = saturate to aromatic hydrocarbon ratio. | 57 |
| 4.2 | Light hydrocarbon parameters. Pr/Ph = pristane over phytane ratio; Pr/ n - C_{17} = pristane over heptadecane ratio; Ph/ n - C_{18} = phytane over octadecane ratio; F (paraffinicity) = n -heptane over mch ratio; B (aromaticity) = toluene over n -heptane ratio; I (<i>iso</i> -heptane ratio) = [(2mh _{ex} + 3mh _{ex}) / (c13dmcp + t13dmcp + t12dmcp)]; H (heptane ratio) = [(100x n - C_7) / ((ch _{ex} + 2mh _{ex} + 23dmp + 11dmcp + 3mh _{ex} + c13dmcp + t13dmcp + t12dmcp + 3ep + 224tmp + n - C_7) + mch _{ex})]; LHCPI (light hydrocarbon preference index) = [n - C_{17} + n - C_{18} + n - C_{19}] / [n - C_{27} + n - C_{28} + n - C_{29}]; see Tab.3.2 for compounds abbreviations | 67 |
| 4.3 | Classification of oils on the basis of light hydrocarbon compositions. | 70 |
| 4.4 | Hopane biomarker parameters of crude oils, where: Mo/(Mo+Ho) = moretane/(moretane+hopane); HHI = C_{35} homohopane index; GI = gammacerane index; HH iso. = homohopane isomerization ratio | 78 |

- 4.5 Sterane biomarker parameters of crude oils, where: C_{28}/C_{29} = the C_{28}/C_{29} $\alpha\beta$ sterane ratio; Dia/Reg C_{27} - C_{29} = the ratio of diasteranes over steranes from C_{27} to C_{29} ; $\beta\beta/(\beta\beta+\alpha\alpha)$ = $\beta\beta/(\beta\beta+\alpha\alpha)$ C_{29} steranes; $\alpha\alpha$ $20S/(20S+20R) = \alpha\alpha$ $20S/(20S+20R)$ C_{29} steranes, $24/(24+27) = 24/(24+27)$ C_{26} nordiacholestanes. 81
- 4.6 Diamondoid-related parameters, where: Σ Adam. = sum of adamantane concentrations (ppm), Σ Dia. = sum of diamantane concentrations (ppm), 3- +4-Mdia = sum of 3- and 4-methyldiamantane concentrations (ppm), MAI = methyladamantane index = 1-methyladamantane/(1-methyladamantane + 2-methyladamantane), MDI = 4-methyldiamantane/(4-methyldiamantane + 1-methyldiamantane + 3-methyldiamantane), DMDI-1 = dimethyldiamantane index 1 = 3-, 4-dimethyldiamantane/(3-, 4-dimethyldiamantane + 4-, 9-dimethyldiamantane), DMDI-2 = dimethyldiamantane index 2 = 4-, 8-dimethyldiamantane/(4-, 8-dimethyldiamantane + 4-, 9-dimethyldiamantane). 89
- 4.7 The calculated parameters based on Polycyclic Aromatic Hydrocarbons PAHs. * where: MPI-1 = $[1.5(2\text{-MP} + 3\text{-MP}) / (P + 1\text{-MP} + 9\text{-MP})]$; % Rc = calculated Vitrenite Reflectance which is inferred from MPI-1 values by the formulas given in the text (Eq.4.4 and Eq.4.5); MDR = 4-MDBT/1-MDBT; MA I/(I+II) = monoaromatic steroids I/(I+II); TA I/(I+II) = triaromatic steroids I/(I+II) 96
- 4.8 δD values of parameters used in Figs.4.36-4.41, where: Iso.Ave=the average δD values of pristane and phytane, iso-alkane=the calculated difference of summed δD values of pristane and phytane and the sum for δD values of n - C_{17} and n - C_{18} , Alkanes.Ave.=the average δD values of n -alkanes in the range from n - C_9 to n - C_{25} , $\Delta\delta D$ =the offset in hydrogen isotopic signature between the average in δD values of isoprenoids (pristane and phytane) and n -alkanes (in the range from n - C_9 to n - C_{25}). 113

| | | |
|------|---|-----|
| 4.9 | Rock-Eval data of the analysed samples of three potential source rocks plotted in Fig.4.43. | 118 |
| 4.10 | Hydrocarbon parameters obtained from analysis of rock extracts saturated fractions using GC-FID | 120 |
| 4.11 | Saturate biomarker parameters for analysed rock extracts. . . . | 122 |
| 5.1 | The concentration (ppm), carbon and hydrogen isotopic values (‰) for each compound in the three end-members. | 168 |
| 5.2 | The concentration (ppm), carbon and hydrogen isotopic values (‰) for each compound in the proposed mixed oils. | 169 |
| 5.3 | No units for these data because they result from multiplying the hydrogen isotopic value with the normalized concentration value. The normalized concentration values result from dividing the concentration of each compound by the lowest concentration of that compound in the sample set. | 171 |
| 5.4 | Mean degradative loss (MDL %) values and molecular parameters used to assess the biodegradation extent for some crude oil samples in the study area, where $iso-/n\text{-alkane} = i\text{-}C_5 / (i\text{-}C_5 + n\text{-}C_5)$, $br.-/n\text{-alkane} = 3MP / (3MP + n\text{-}C_6)$. N-D is non-degraded oil. nd = no data. | 183 |
| B.1 | Concentrations [$\mu\text{g/g}$ oil] for adamantane and diamantane compounds. Compound names and numbers are shown in Fig.3.2 and Tab.3.3 | 245 |
| B.2 | $\delta^{13}\text{C}$ values [‰] for $n\text{-}C_3$ to $n\text{-}C_{31}$ in the studied crude oils. G002968 is contaminated with water, hence, no data can be provided. | 249 |
| B.3 | $\delta\text{ D}$ values [‰] for $n\text{-}C_3$ to $n\text{-}C_{31}$ in the studied crude oils. G002968 is contaminated with water, hence, no data can be provided. | 253 |

| | | |
|-----|---|-----|
| C.1 | Source-related parameters used to classify the oil samples into main genetic oil families shown Fig.5.15. $CPI = ([n-C_{25}H_{52}] + [n-C_{27}H_{56}] + [n-C_{29}H_{60}] + [n-C_{31}H_{64}]) / (0.5[n-C_{24}H_{50}] + [n-C_{26}H_{54}] + [n-C_{28}H_{58}] + [n-C_{30}H_{62}] + 0.5[n-C_{32}H_{66}])$, % C_{27} St, % C_{28} St, and % C_{29} St are the relative abundance of regular steranes, % C_{27} dia, % C_{28} dia, and % C_{29} dia are the relative abundance of rearranged steranes, $Dia/Reg = \beta\alpha$ diasterane / $(\alpha\alpha + \beta\beta)$ regular sterane for $C_{27}-C_{29}$ | 256 |
| C.2 | Source-related parameters used to classify the oil samples into main genetic oil families shown Fig.5.15. C_{22}/C_{21} ; C_{24}/C_{23} ; C_{26}/C_{25} TT=tricyclic terpanes, $C_{28}/C_{29} = C_{28}/C_{29}$ $\alpha\beta\beta$ sterane, $HHI = C_{35} / (C_{31}-C_{35})(S+R)$ homohopanes, GI= gammacerane index, St./H= $C_{29}-C_{33}$ steranes/17 α (H) hopanes, $24/(24+27) = C-24/(C-24+C-27)$ norcholestane | 257 |
| C.3 | Source-related parameters used to classify the oil samples into main genetic oil families shown Fig.5.15. $24d/(24d+27d) = C-24/(C-24+C-27)$ nordiacholestane, DMDI-1= dimethyl diamantane index 1= $3,4DMD/(3,4DMD+4,9DMD)$, DMDI-2= dimethyl diamantane index 2= $4,8DMD/(4,8DMD+4,9DMD)$, EAI= ethyl-diamantane index= $2EA/(2EA+1EA)$, % 4,9 DMD= $4,9DMD/(4,9-+4,8-+3,4DMD)$, % 4,8 DMD= $4,8DMD/(4,9-+4,8-+3,4DMD)$, % 3,4 DMD= $3,4DMD/(4,9-+4,8-+3,4DMD)$ | 258 |
| E.1 | | 262 |
| E.2 | Concentrations (ppm) of crude oil constituents used in Eq.5.17 to calculate the mean degradative loss to assess the degree of biodegradation after (Elias <i>et al.</i> , 2007). | 263 |

Chapter 1

Introduction and Background

1.1 Petroleum Geochemistry

Petroleum Geochemistry is an established science concerned with the utilization of chemical principles to the study of the *formation, migration, accumulation* and the *alteration* of petroleum and the application of this understanding in the exploration and recovery of oil and gas. In this context, petroleum geochemistry has its useful modern applications in exploration and production of "*conventional*" hydrocarbons and also supports the development of "*unconventional*" resources like shale gas. In oil exploration, geochemistry enlarges exploration effectiveness by accounting for many of the factors that control the volumes of petroleum available in a trap, including source quality and richness, thermal maturity, and the timing of generation-migration-accumulation relative to entrapment formation. Fig.1.1 shows that when geochemical parameters are coupled with structural and reservoir data, the exploration efficiency will be more than double in comparison to only using the available geophysical data (Murris, 1984).

In this framework, petroleum geochemistry is applied in exploration for instance in (1) petroleum systems and exploration risk assessment (Hunt, 1996; Murris, 1984), (2) molecular composition, biological markers, isotope chemistry and chemometric analysis for genetic oil-oil and oil-source rock correlation (Dahl *et al.*, 1993; MacKenzie, 1984; Mackenzie *et al.*, 1983;

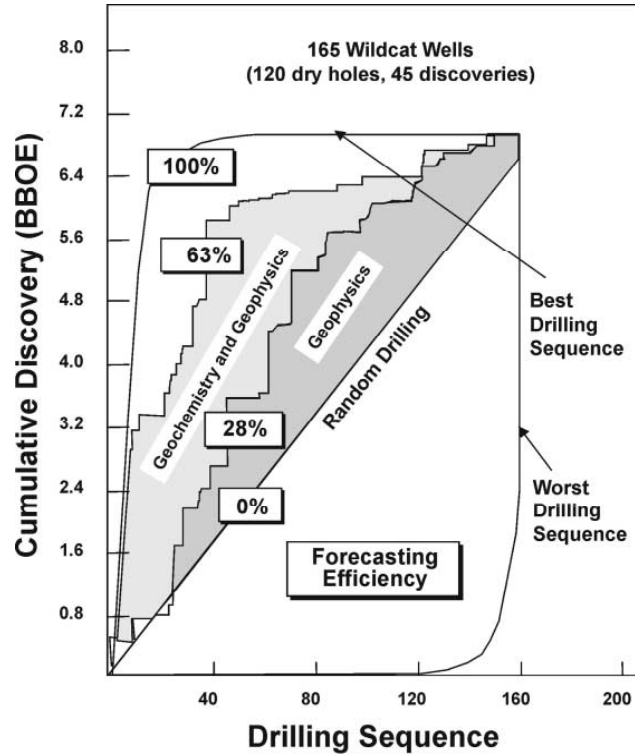


Figure 1.1: Petroleum geochemistry improves forecasting efficiency. Modified after (Murris, 1984).

Peters *et al.*, 1994; Peters & Moldowan, 1993; Peters *et al.*, 1986b; Philp, 1985), (3) 3D basin modeling (Peters *et al.*, 2000a; Welte *et al.*, 1997), and (4) secondary alteration effects on petroleum composition (Behar *et al.*, 1997; Connan, 1984; Horsfield *et al.*, 1992; Tissot & Welte, 1984; Wilkes *et al.*, 2008). In phase of oil production and development of producing fields, petroleum geochemistry complements information of reservoir engineering to solve reservoir-related problems that can result in increasing the recoveries of the huge amounts of petroleum deserted in the traps as unrecoverable. It has useful applications in reservoir management such as (1) reservoir continuity assessment (Halpern, 1995; Nederlof *et al.*, 1994; Ross & Ames, 1988; Slentz, 1981), (2) analysing the commingled production from multiple zones (Hwang *et al.*, 2000; Kaufman & Ahmed, 1990), (3) evaluating the oil mixing potential from multiple sources (Chen *et al.*, 2003b; McCaffrey *et al.*, 1996; Zhang *et al.*, 2003), (4) prediction of oil quality in accumulations (Bement *et al.*, 1996; Baskin & Jones, 1993), and (5) prediction of gas-oil and oil-water contacts (Baskin *et al.*, 1995). The following

sections describe the basic principles of petroleum geochemistry.

1.1.1 Petroleum Origin and Generation

Petroleum is defined as a complex mixture of hydrocarbons derived from degradation of organic matter buried in sedimentary rocks. The organic matter in sediments derives from the remains of extant organisms including algae, bacteria and higher plants. By accumulation and lithification of sediments, sedimentary rocks are formed. The potential petroleum *source rocks* are fine-grained sedimentary rocks rich in organic matter and have been empirically correlated with shales having >0.5% total organic carbon (TOC) content (Philippi, 1965). The transformation process of organic matter into petroleum (oil and gas) is divided into three main stages called *process of maturation* and includes: *diagenesis*, *catagenesis*, and *metagenesis* as illustrated in Fig.1.2 (Horsfield & Rullkotter, 1994a; Killops & Killops, 1993; Tissot & Welte, 1984).

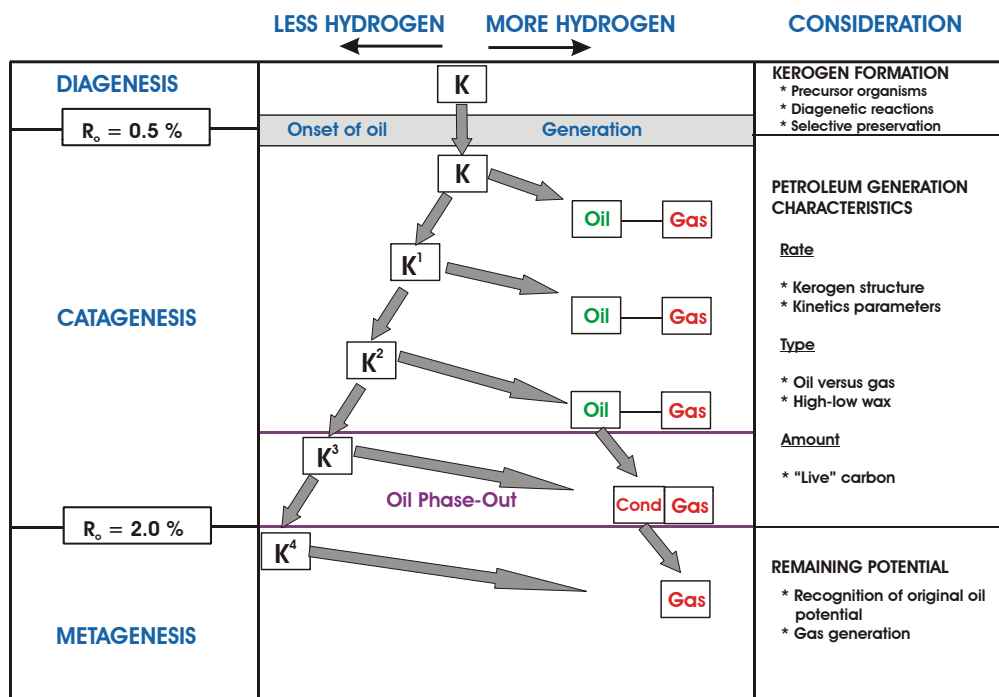


Figure 1.2: The main stages of petroleum formation: diagenesis, catagenesis and metagenesis. Modified after (Horsfield & Rullkotter, 1994a).

Diagenesis of organic matter refers to biologically, chemically, and phys-

ically induced changes in the organic matter composition that occur in the subsurface in sedimentary rocks at an equivalent *vitrite reflectance* of 0.5% (Hunt, 1996; Peters *et al.*, 2005). Actually, these changes begin before organic matter reaches the sediments as organic matter sinking through the water column is fed upon by both the macrofauna and (aerobic) bacteria. Indeed, a significant proportion of the organic matter reaching the sediment does so in form of residues of the living organisms and/or higher plants. Decomposition occurs once the organic matter reaches the sediment surface. Burial by subsequently accumulating sediment eventually isolates it from water. Where the burial flux of organic matter is high enough, oxygen is eventually consumed and as the organic matter is buried to a progressively greater depth, it is attacked by a series of bacterial communities utilizing a progression of electron receptors (oxidants). Under these conditions a series of zones exists where nitrogen, iron and sulfate reduction occur (anaerobically) (Killops & Killops, 1993). The bulk of the organic matter in sediments exists in solid form, yet only dissolved compounds can cross cell membranes and be a useful source of nutrition of microbes. For this reason, bacteria release enzymes that first break insoluble complex organic molecules into smaller soluble ones. Complex organic molecules usually cannot be oxidized completely by a single organism, because no single organism is likely to produce all the necessary enzymes. Instead, these molecules are broken down by consortia of bacteria. Thus proteins, carbohydrates, and lipids are broken down into amino acids, simple sugars, and long-chain fatty acids. At the same time there are very complex compounds which are not easy to decompose (bio-macromolecules). These bio-macromolecules will be preserved and/or condensed into geopolymers to form the so-called *kerogen* which is the principle product of diagenesis (Tissot & Welte, 1984). Kerogen is defined as sedimentary organic matter that is insoluble in water and organic solvents. It is usually accompanied by a smaller fraction of soluble organic matter called *bitumen*. Kerogen is usually classified into one of three types, based on bulk H/C and O/C ratios. *Type I* kerogen is rich in lipids especially long-chain aliphatics, and has high petroleum potential.

It is derived primarily from algal and bacterial remains, often deposited in lacustrine environments. *Type II* kerogen is the most common type. It is derived primarily from planktonic and bacterial remains deposited in marine environments (though remains of higher plants can contribute as well) (Tissot & Welte, 1984; Espitalie *et al.*, 1977). Its lipid content and oil potential are somewhat lower than *Type I* kerogen. *Type III* kerogen is rich in aromatic and poor in aliphatic structures. It is formed principally from the remains of vascular plants. Its oil potential is poor, but it can be a source of gas (Horsfield & Rullkötter, 1994a; Hunt, 1996). As sedimentary organic matter is buried, it experiences progressively higher temperatures and pressures. Although most bacterial decomposition occurs quickly, in the upper meters or so (diagenesis depth), it may continue at a much slower pace indefinitely. Indeed, bacteria have been found in subsurface source rocks at temperatures up to 75 °C and a depth of nearly 3 km. As bacterial activity ceases, a number of new reactions begin as the organic matter attempts to come to equilibrium with higher pressures and temperatures. These reactions, in which kerogen breaks down into a variety of hydrocarbons and a refractory residue, are collectively called catagenesis. In the oil-generating stage of catagenesis called *oil window*, which is the point where maximum hydrocarbon generation occurs, vitrinite reflectance is typically in the range of 0.6 to 1.3 %. During catagenesis heteroatom bonds are the first to be broken as they generally are weaker than carbon-carbon bonds. Hydrocarbons released during this stage are thus those attached to the kerogen structure with heteroatoms or merely trapped within it. Thus the hydrocarbon fraction of bitumen in immature kerogen is dominated by "*geochemical fossils*" or *biomarkers*, i.e. molecules that have lost their functional groups but whose basic skeleton is preserved (Peters & Moldowan, 1993; Killops & Killops, 1993). As temperature increases, carbon-carbon bonds are also broken, a process called *cracking*. Carbon-carbon bonds in the centre of chains are slightly weaker than those at the ends. As these begin to break, hydrocarbon fragments are released that progressively dilute biomarkers. Also because of this effect, the size of hydrocarbons evolved decreases with

increasing maturity. Thus the hydrocarbons generated in the oil window of catagenesis show a maximum abundance at relatively low carbon number ($\sim C_{10}$) and steadily decreasing abundance with increasing carbon number (Peters *et al.*, 2005). As temperatures approach and exceed 150 °C, even smaller hydrocarbons ($\lesssim C_5$) become dominant. These are gases at surface temperature and pressure. Dissolved in them, however, are lesser amount of longer chains ($\gtrsim C_5$). These condense to liquids upon reaching the surface and hence are called *condensates*. Hydrocarbons that are gas-dominated yet contain a significant amount of longer hydrocarbons are called *gas condensates*, and this stage of catagenesis, corresponding roughly to 150 to 180 °C is called the *wet gas zone*. At higher temperatures, the liquid hydrocarbons are completely eliminated by C-C bond breaking. Eventually, all C-C hydrocarbon bonds are broken, leaving methane (CH_4) as the sole hydrocarbon, accompanied by nearly a pure carbon residue. This stage of evolution is referred as metagenesis or the *dry gas zone* (Horsfield & Rullkötter, 1994a; Bordenave, 1993).

1.1.2 Petroleum Migration and Accumulation

Most petroleum source rocks are fine-grained. Subjected to pressure of burial, their porosities are quite low, hence liquid and gaseous hydrocarbons are expelled once the source rock becomes saturated; this process is called *primary migration*. The mechanisms of migration of hydrocarbons are not fully understood, but probably involve both passage through microfractures and diffusion through the kerogen matrix. Expulsion efficiencies vary with kerogen type. The quality and quantity of the petroleum generated depends largely on the type of organic matter. Since petroleum tends to migrate out of the source rock as it is created, it is difficult to judge the amount of petroleum generated from field studies. However, both mass balance calculations on natural depth sequences (Schmoker, 1994) and laboratory pyrolysis experiments on immature kerogen will give some indication of the petroleum generation potential (di Primio & Horsfield, 1996; Dieckmann *et al.*, 2000 1998; Horsfield & Dueppenbecker, 1991).

Migration will continue until the petroleum reaches either a trap or the surface (called *secondary migration*). Secondary migration of petroleum in carrier beds is controlled by buoyancy forces, hydrodynamic fluid flow and capillary forces (Bordenave, 1993; Hunt, 1996; Tissot & Welte, 1984). Distances covered by secondary migration ranges from a few kilometers to more than one hundred kilometers. Hydraulic fracture, tectonism, trap failure, or through capillary supplies petroleum from reservoirs into new carrier beds what is called *tertiary migration* resulting in new secondary reservoirs or surface seeps. The more water soluble components of petroleum may dissolve in water, either flowing through the reservoir or encountered by migrating petroleum. This process, called *water washing*, will deplete the petroleum in these water-soluble components. Aerobic bacteria encountered by petroleum can metabolize petroleum components, a process called *biodegradation*. Long, unbranched alkyl chains are preferentially attacked, followed by branched chains, cycloalkanes, and acyclic isoprenoids. Aromatic steroids are the least affected. Finally, further *thermal evolution* can occur after migration, resulting in an increase in methane and aromatic components at the expense of aliphatic chains.

1.1.3 Petroleum Systems and Oil Families

The *Petroleum System* is a unifying concept that encompasses all of the disparate elements and processes of petroleum geology. A petroleum system includes a pod of active source rocks and all genetically related oil and gas accumulations. It contains all the geologic elements and processes that are essential if an oil and gas accumulation is to exist (Magoon & Dow, 1994). To fully characterize the petroleum system the following elements must be identified: source rock, reservoir rock, seal rock and overburden rock. On the other hand the petroleum systems have two processes: trap formation, and generation, migration, accumulation of hydrocarbons (see Fig.1.3).

A petroleum system investigation identifies names (source rock and reservoir rock) and maps the geographic, stratigraphic and temporal extent of a petroleum system (Demaison & Huizinga, 1991). The investigation

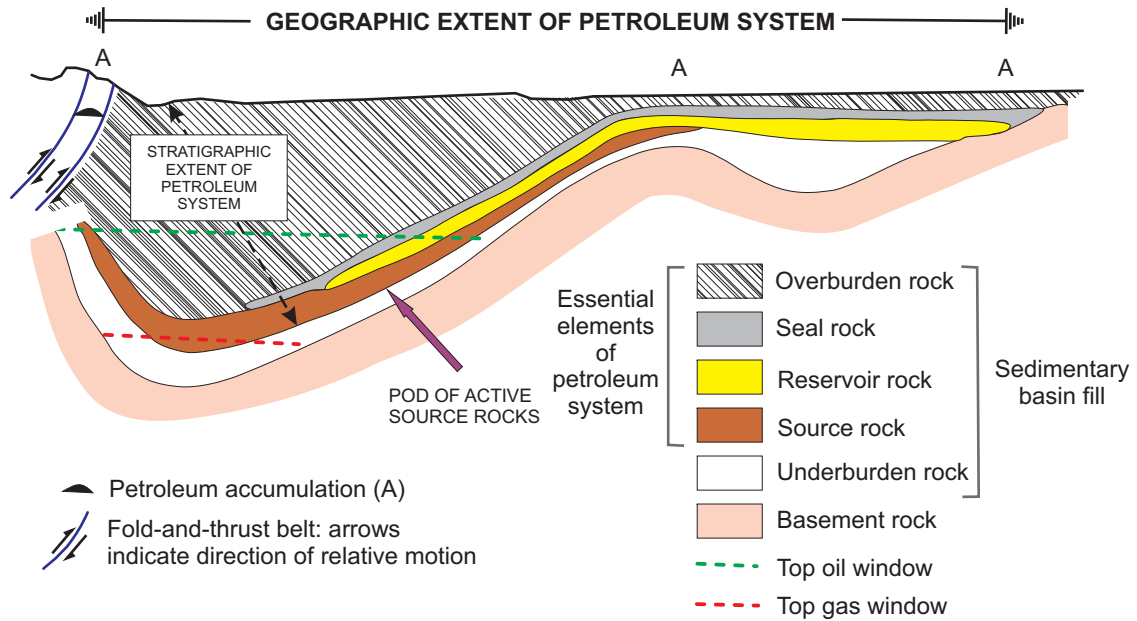


Figure 1.3: The main geological elements of the petroleum system. Modified after (Magoon & Dow, 1994).

includes certain components:

- Petroleum-petroleum geochemical correlation
- Petroleum-source rock geochemical correlation
- Burial history chart
- Petroleum system map
- Petroleum system cross section
- Events chart
- Table of hydrocarbon accumulations
- Determination of generation-accumulation efficiency

For the Middle East, the focus of the current thesis, some studies have been published dealing with the petroleum systems of different oil provinces. The Palaeozoic and Jurassic petroleum systems of Saudi Arabia, for instance, have been studied intensively by (Abu-Ali & Littke, 2005; Abu-Ali *et al.*, 1999; Cole *et al.*, 1994ab; Survey, 2002). Petroleum systems of Iraq

were analysed in different papers (Aqrawi, 1998; Fox & Ahlbrandt, 2002; Verma *et al.*, 2004). Some studies have been also performed for Oman petroleum systems (Grantham *et al.*, 1987; Terken, 1999; Terken *et al.*, 2001). Petroleum systems of Adaiyaman, central and SE Turkey were analysed in (Demirel, 2004; Demirel & Guneri, 2000; Demirel *et al.*, 2001; Hu-vaz, 2009; Soyulu *et al.*, 2005). In Syria the petroleum provinces have been analysed in some papers like (de Ruiter *et al.*, 1995; Abboud *et al.*, 2005; Kent & Hickman, 1997). Petroleum systems characterization involves classification of oil families and detailed oil-source rock correlation based on geochemical parameters including biomarkers, stable isotopic composition of individual compounds and diamondoids (Peters *et al.*, 2005). A distinct oil family could be defined as a group of crude oils produced from different reservoirs and are genetically-related as they have been generated from a single source rock in the sedimentary basin. Oil families classification is based principally on oil-oil and oil-source rock geochemical correlation to find the genetic relationships among these oils (Greene *et al.*, 2004; Osadetz *et al.*, 1992; Sarmiento & Rangel, 2004; Sharaf *et al.*, 2007; Zhang & Huang, 2005a; Peters *et al.*, 1994).

1.2 Regional Petroleum Geology

The Middle East region has the most prolific petroleum provinces in the world where it contains about two thirds (755.325 billion barrel oil Bbbl, 60.97 %) of the world's remaining oil reserves and over one third (2585.351 trillion cubic feet TCF, 41.10 %) of its remaining gas reserves (Ahlbrandt *et al.*, 2000; BP, June 2008). On the other hand one-third (25,878 million barrel per day Mbbl/d) of the world oil production takes place in the Middle East. Conversely, the rest of the world accounts for as much as two-thirds of production, with only one-third of total reserves being attributed to it (EIA, 2010). Additionally, the Middle East has several of super giant oil fields in the world which have more than 30 Bbbl petroleum reserves the like Ghawar oil field (90 Bbbl) in Saudi Arabia, Burgan in Kuwait (86 Bbbl),

and Magnon in Iraq (30 Bbbl).

The reasons of the productive oil abundance are due to the following geological key factors (Alsharhan & Nairn, 1997; Beydoun, 1998; Beydoun & Dunnington, 1975):

- A long history of quiet and almost continuous sedimentation.
- A very large volume of predominantly marine sediments.
- Extensive, excellent and often very thick reservoirs, principally carbonates but also sandstones.
- Deposition of organically-rich source rocks under anoxic conditions in the right juxtaposition with very permeable extensive reservoirs.
- Capable and broadly spread seals over several intervals of geological time.
- The existence of extremely large anticlinal traps coincident with peak oil generation and migration.
- The absence of prolonged erosional intervals and strong tectonics.

The Middle East hydrocarbon habitats can be subdivided into three main basins: the Arabian Platform, the Zagros Basin, and the Oman Oil Basin (Ahlbrandt *et al.*, 2000; Alsharhan & Nairn, 1997) (see Fig.1.4). This subdivision coincides with the age of the oil fields.

- The petroleum systems in the Arabian Platform are composed of Jurassic and Cretaceous source rocks and reservoirs (Christian, 1997; Murris, 1980; Newell & Hennington, 1983), but also Palaeozoic hydrocarbon systems occur (Abu-Ali *et al.*, 1991 1999; Al-Husseini, 1991).
- Younger basins are attributed to Cenozoic age on the Zagros Basin as a result of the late Cenozoic tectonics which forms the Zagros Belt

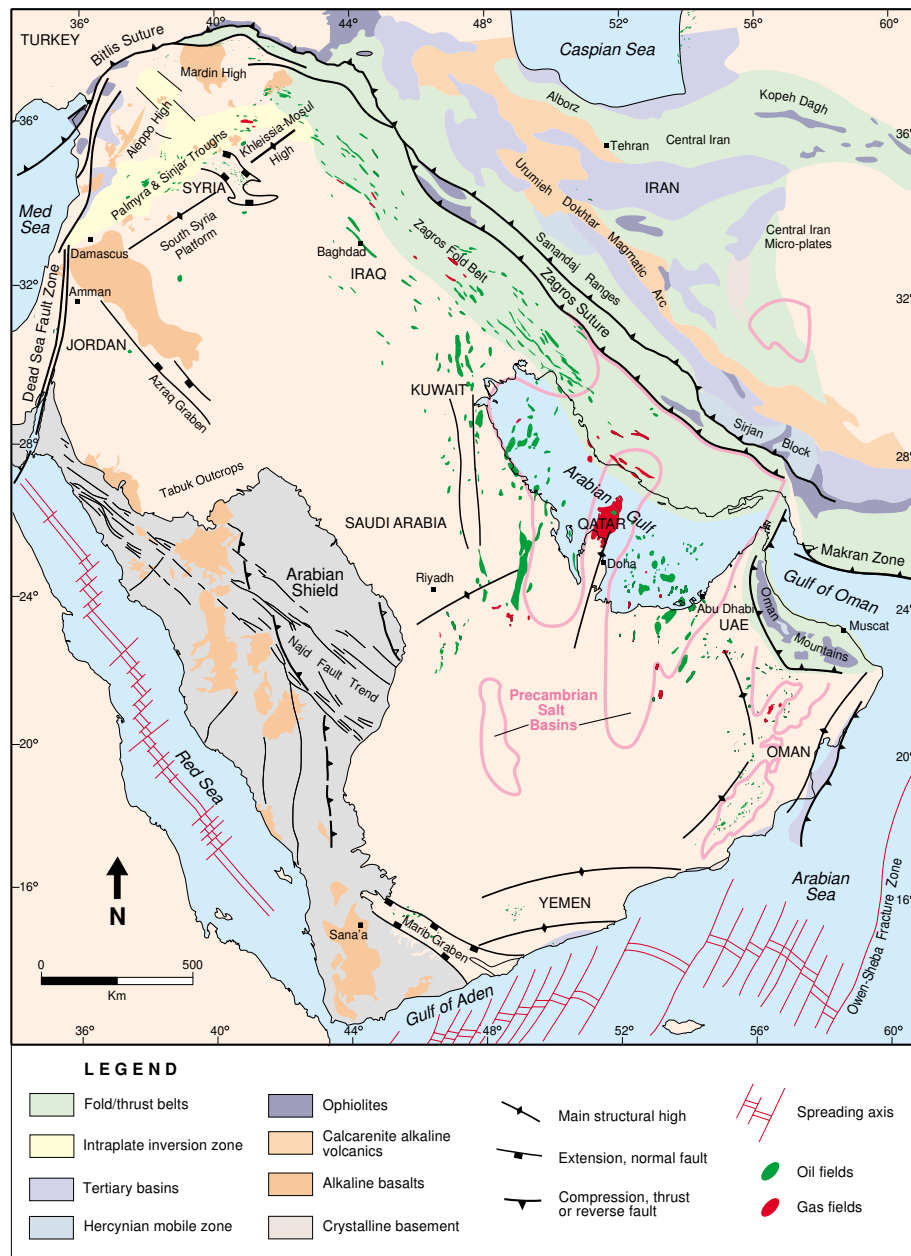


Figure 1.4: Oil and gas fields in the Middle East region adopted from (Konert *et al.*, 2001).

(Ala *et al.*, 1980; Alsharhan & Nairn, 1997; Pitman *et al.*, 2004; Al-Habba & Abdullah, 1989; Metwalli *et al.*, 1974; Sadooni & Aqravi, 2000; Verma *et al.*, 2004).

- The Oman Oil Basin contains Infracambrian, Paleozoic, and Cretaceous hydrocarbon systems (Droste, 1997; Grantham *et al.*, 1987; Terken *et al.*, 2001).

Anticlinal traps are the most common structural type, which are probably related to the basement-controlled structures as in offshore Abu Dhabi, Kuwait, Saudi Arabia, Bahrain and Qatar Arch. Other types of hydrocarbon traps are associated with salt structures as in Yemen and with domal structures with either E-W or S-N trends in the Cretaceous of the United Arab Emirates (U.A.E) and offshore Qatar. Other petroleum accumulations are linked to rift-type basins (e.g. Euphrates Graben in Syria and the Red Sea). A few stratigraphic traps are found in Saudi Arabia and Kuwait (Alsharhan & Nairn, 1997; Ahlbrandt *et al.*, 2000).

Syria, which is situated in the northern part of the Arabian Plate, has oil reserves of 4.2 Bbbl (0.36 % form world reserves) and 10.6 TCF of natural gas (0.17 % form world reserves) (OAPEC, 2010). Crude oil production of Syria in 2008 was 390 Tbbl/d (about 0.5 % of the world production) (OAPEC, 2010). The petroleum exploration history in Syria began in 1934 in northeastern Syria and the first exploration well has been drilled in 1939. The first petroleum shows have been realized in Jebissa and Ghouna (NE part of Syria) during the late '30s and '40s by the Iraq Petroleum Company (IPC) in association with the state-owned petroleum company (the later Syrian Petroleum Company SPC). The first major discovery, the Karatchok Field, was made in 1956 by the U.S American independent Menhall Company, followed by a second discovery of the Suwaidiyah Field in 1959 by the German company Concordia. Subsequently, in 1962, the discovery of the Rumailan Field by the Syrian Petroleum Company followed the nationalization of all oil operations. In 1975, the Syrian government began to award production-sharing contracts to foreign operators. In mid-1980s the significant discoveries have been made in the Euphrates Graben which is located in the southeastern part of the country. Fig.1.5 shows the oil and gas fields of Syria in the late '90 of the 20th century. Crude oils produced from oil fields are transported through the Syrian pipeline to the both refineries in Homs and Banyas in addition to the Tartus Port for exporting (Alsharhan & Nairn, 1997; Aldahik, 2003).

Tectonically, Syria consists of relatively stable and unstable blocks. The

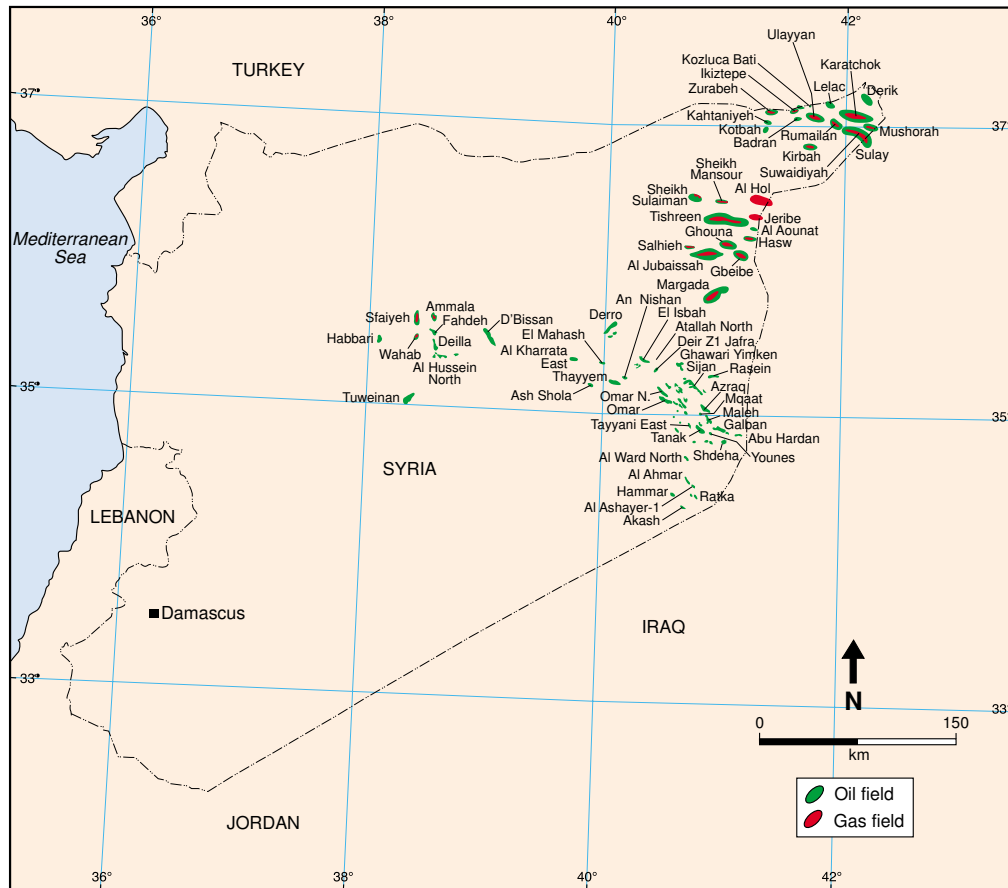


Figure 1.5: Oil and gas fields location in Syria adopted from (Brew *et al.*, 2001a).

stable sector includes the Aleppo Plateau, the Rutbah Uplift, and the Rawda (Khleissa) High. Meanwhile, the unstable sector includes the Dead Sea Fault System, Palmyride Fold Belt, the Euphrates Fault System, and Abd El Aziz - Sinjar Uplift (Barazangi *et al.*, 1993; Best *et al.*, 1993; Brew *et al.*, 1999 1997b; Chaimov *et al.*, 1993) (see Fig.1.6).

Only three tectonic provinces are considered to be hydrocarbon-bearing zones: the Palmyride Fold Belt, the Euphrates Fault System, and the Abd El Aziz - Sinjar Trough (Al-Saad *et al.*, 1992; Alsharhan & Nairn, 1997; Brew *et al.*, 1999 1997a; Jamal *et al.*, 2000; May, 1991; Kent & Hickman, 1997).

In general, the late Palaeozoic-Mesozoic extension, Mesozoic extension, and late Cenozoic compression are the main causes of forming the source

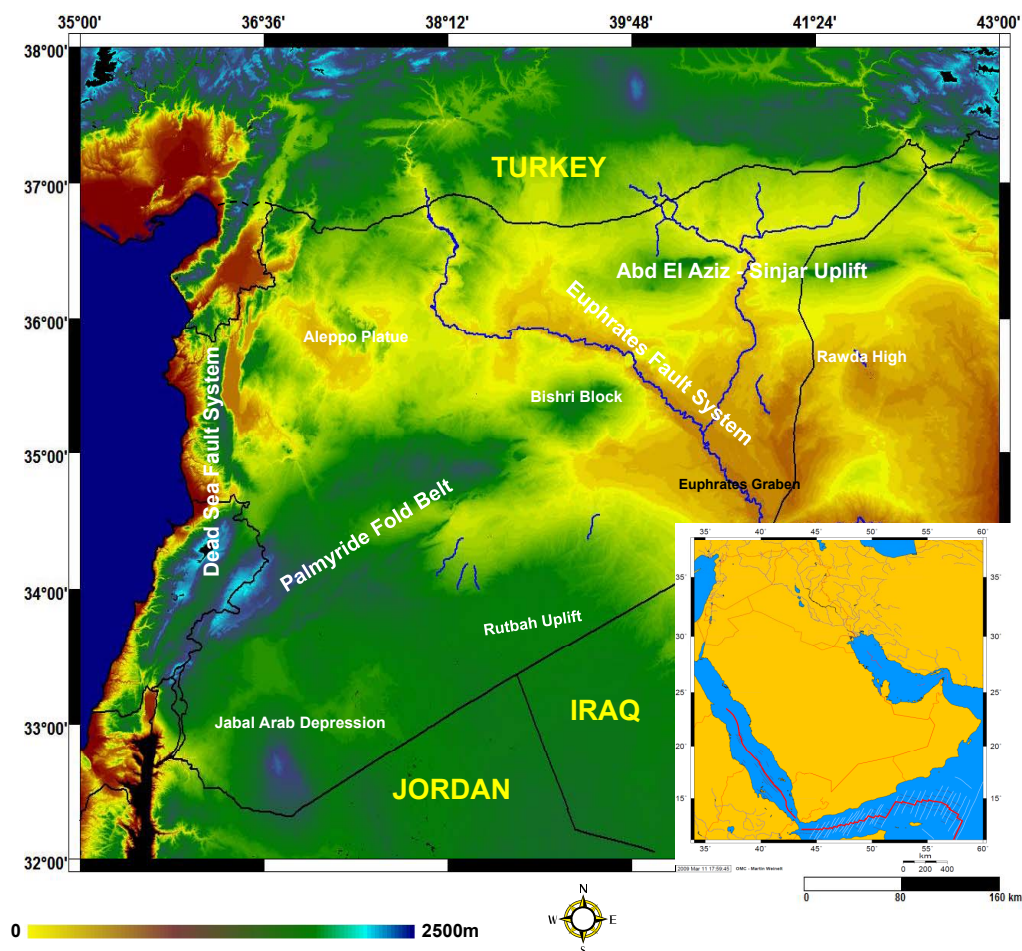


Figure 1.6: Topography and the major tectonic zones of Syria.

and reservoir rocks in Syria (Alsharhan & Nairn, 1997; Brew *et al.*, 1997a).

In the Palmyride Fold Belt, the source rocks are buried deeper than elsewhere in Syria. This deep burial results gas and condensates being generated that are accumulated mostly in the Middle Triassic Kurrachine Dolomite which is sealed by the Kurrachine Anhydrite formation (Jamal *et al.*, 2000; Salel & Seguret, 1994; Searle, 1994) (see Fig.1.7). The Upper Carboniferous Markada sandstone is considered as another reservoir target. It is believed that the late Palaeozoic-Mesozoic fault blocks and the folds created during structural inversion and shortening are responsible for trap formation in this zone.

In the Bishri Block in the transition zone between Palmyride and Euphrates Graben (Alsdorf *et al.*, 1995) a combination of oil and gas is pro-

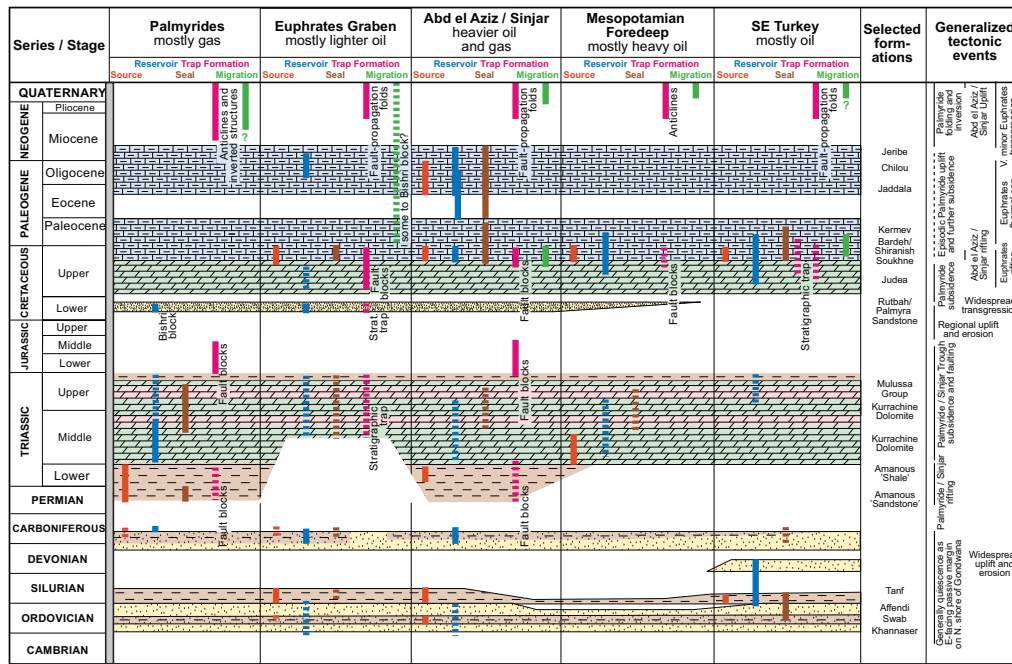


Figure 1.7: Generalized stratigraphy and selected structural elements in various hydrocarbon provinces in Syria. Proven features related to hydrocarbon accumulation are shown as solid lines; dashed lines where uncertain. Adopted from (Brew *et al.*, 1997b)

duced. Hydrocarbons found in the Lower Cretaceous sandstones are thought to be the result of westward migration of petroleum generated in the Euphrates Graben. The potential Upper Cretaceous source rocks (Arak marl and Shiranish Formation) may not have been sufficiently buried to reach full maturity in the Bishri Block (Illiffe *et al.*, 1998).

In the Mesopotamian Foredeep the source rocks are attributed to Late Cretaceous and Triassic strata charging the traps formed by folded Late Cretaceous (Massive Limestone) and Cenozoic (Chilou and Euphrates) sediments (Abboud *et al.*, 2005; Kent & Hickman, 1997; Aldahik, 2001) (see Fig.1.7).

1.3 The Study Area

With more than one billion barrel of proven recoverable oil reserves and lesser amount of natural gas found since mid-1980's (Litak *et al.*, 1998),

the Euphrates Graben is considered as the most prolific and prospective oil province in the Syrian Arab Republic. The Euphrates Graben fault system, extending from the Iraq border in the southeast towards the Turkish border to the northwest (Fig.1.8), extends over an area of about 160 x 90 km (Guyot & Zeinab, 2000; Litak *et al.*, 1998) and has an estimated maximum extension of about 6 km (Litak *et al.*, 1997). The Euphrates Graben is kind a rift basin which consists of grabens, half grabens and flower structures (Litak *et al.*, 1997; Sawaf *et al.*, 1993). This rift basin is comparable to the Gulf of Suez rifting basin due to the surfacial area (c.a. 14400 km^2), recoverable hydrocarbon amount (c.a. 1 Bbbl oil), and even due to the orientation (southeast-northwest) [(Alsharhan, 2003) and the references herein]. The Euphrates Graben, located in the SE Syria, is part of a system of rifts which developed during in the Late Cretaceous (Caron-Cecile & Jamal-Maher, 2000; de Ruiter *et al.*, 1995; Sawaf *et al.*, 1993). In the latest Maastrichtian, the rifting in the Euphrates Graben ceased due to the continental-continental collision along the northern Arabian Plate associated with emplacement of ophiolites along the margins (Litak *et al.*, 1998; Sawaf *et al.*, 1993). As a result of this rifting, about 2.5 km of Cretaceous sediments have been deposited in the central graben and thin towards the northeast and southwest margins (Fig.1.8).

Two distinct fault populations are noted in the study area:

- west-northwest-striking normal faults with relatively large throws in the northwestern part of the study area, which may initially have formed in response to Late Cretaceous stresses (Litak *et al.*, 1998).
- steeply dipping, northwest-striking flexures and strike-slip faults nearer to the Iraqi border (see Fig.1.8), which might be related to the northwest trending late Proterozoic Najd fault system exposed in Saudi Arabia (Beydoun, 1991).

As a standard rifting basin, the stratigraphical history of the Euphrates Graben could be subdivided into three major units: pre-rift, syn-rift, and post-rift sequences (Fig.1.9).

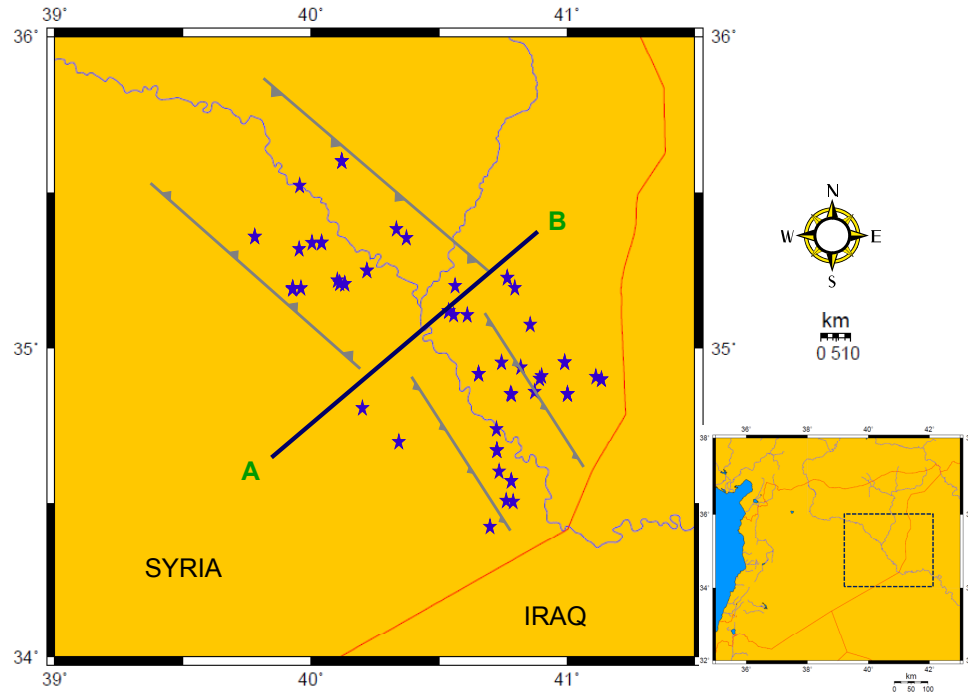


Figure 1.8: Location map of the study area showing the wells from which the analysed oil samples come from.

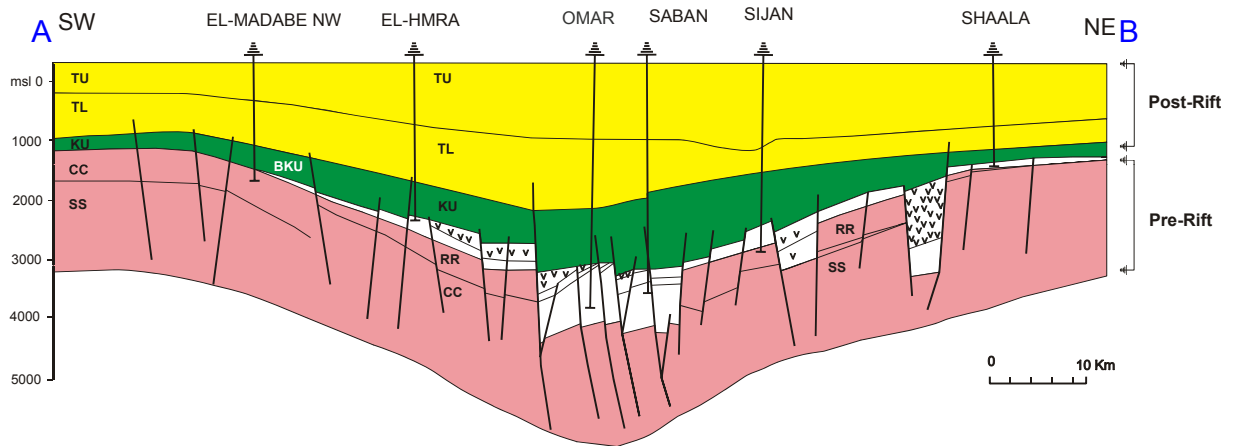


Figure 1.9: Schematic cross section in the study area of AB profile in perpendicular to the graben axes (see Fig.1.8 for profile location). Modified after (de Ruiter *et al.*, 1995)

- **Pre-rift:** Since the rifting onset was in the Late Cretaceous, the pre-rift unit is composed of strata ranging from Paleozoic to Early Cretaceous (de Ruiter *et al.*, 1995). The Early Paleozoic section consists of alternations of shallow-marine clastics of Ordovician age (Khabour Fm) (Ala & Moss, 1979) followed by Lower Silurian shales

(Tanf Fm.) (Lababidi & Hamdan, 1985) deposited by repeated regressive and transgressive cycles (Beydoun, 1991; Brew *et al.*, 1999) (see Fig.1.10). The Upper Silurian and Devonian formations are absolutely absent in the study area because of a proposed regional uplift (Brew *et al.*, 1999; Sawaf *et al.*, 1993). Periods of maximum transgression resulted in carbonates distribution in the middle part of Carboniferous, Triassic and Lower Cretaceous sections (Ziegler, 2001). In terms of petroleum geology, the pre-rift section contains the organic matter-rich marine shale of the Lower Silurian Tanf Fm. which is considered as one of the two main source rocks in the study area charging the Paleozoic reservoirs e.g. Doubayat Fm. (Alsharhan & Nairn, 1997; Brew *et al.*, 1997b; de Ruiter *et al.*, 1995; Frijhoff *et al.*, 2006). This Tanf Fm. is equivalent to the Lower Silurian "Hot Shale" in North Africa and Arabia (Luning *et al.*, 2000 2005; Konert *et al.*, 2001). The most prolific reservoirs in the Euphrates Graben are also part of the pre-rift unit (de Ruiter *et al.*, 1995). They are: (1) the Lower Cretaceous shallow marine Rutbah Fm.; (2) the Post Judea Sand (PJS); and (3) the fluvial Triassic Mulussa F (Alsharhan & Nairn, 1997) (see Fig.1.10).

- **Syn-rift:** The (Coniacian) Derro Formation couplet of red beds is the first deposited sediment in the syn-rift sequence (de Ruiter *et al.*, 1995), followed by the occurrence of the lagoonal cherty limestone R'mah Formation (equivalent to Soukhne) and carbonate of the Ereik Formation. The deposition of the Lower Shiranish Fm. is also part of the syn-rift section.

This syn-rift sequence includes the most prolific source rock (R'mah Fm.) in the Euphrates Graben charging the pre-rift Triassic and Lower Cretaceous beds (Beydoun, 1986; de Ruiter *et al.*, 1995; Serreya, 1990). However, the shallow to open marine Lower Shiranish Fm. could play a binary role as a source and reservoir rock simulta-

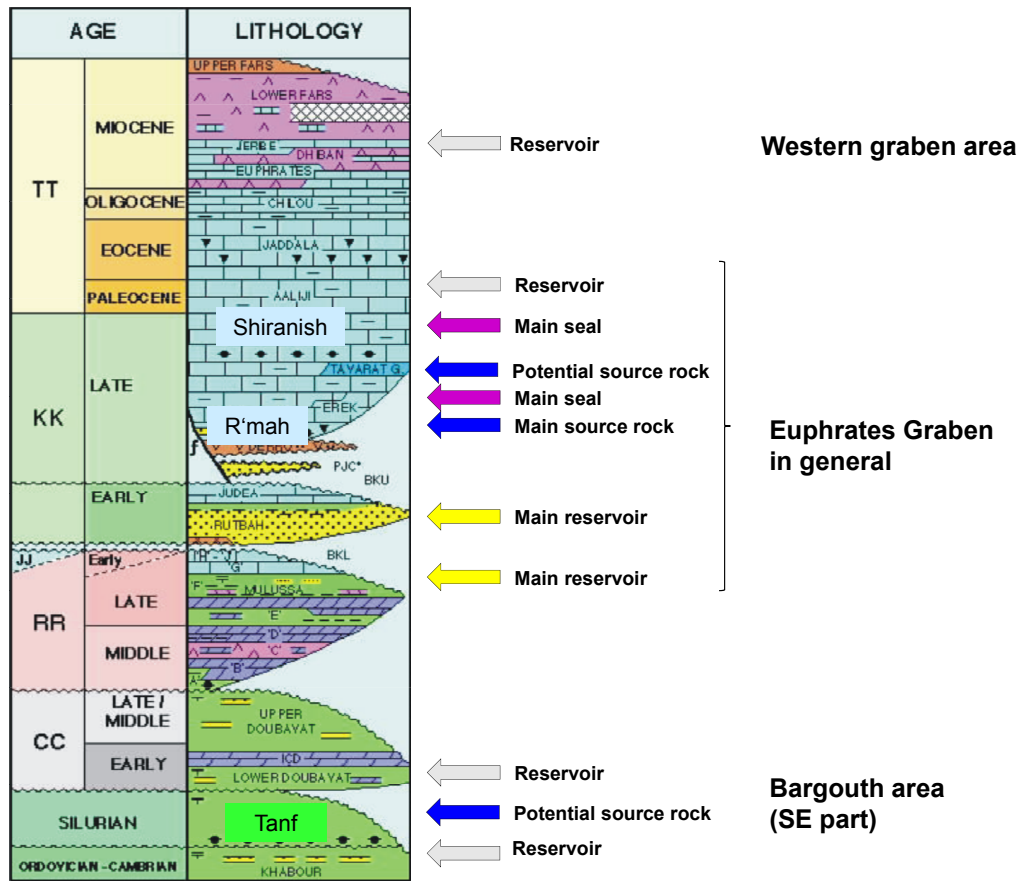


Figure 1.10: The stratigraphic column in the Euphrates Graben showing the main source rock and reservoir horizons.

neously.

- **Post-rift:** The post-rift sedimentary fill of the Euphrates Graben is the latest Maastrichtian Upper Shiranish Fm. During deposition of this younger part of the Shiranish Fm. most fault activities had ceased (de Ruiter *et al.*, 1995; Litak *et al.*, 1997). The Miocene reserves (Dhiban, Euphrates, and Jeribe formations) are located mainly in the northwestern part of the Euphrates Graben (see Fig.1.10). They are comparatively small and the production rates are low.

Chapter 2

Goals and Objectives

The Euphrates Graben is the most petroliferous province in Syria with a production capacity of about 400.000 bbd in the mid 90's. Crude oils are produced from different horizons of the stratigraphic column from Ordovician to Miocene. These oils vary in quality from light to heavy and have different geochemical signatures indicating that they might originate from various sources. Three potential source rocks can be identified in the study area; two Upper Cretaceous candidates (R'mah and Shiranish Formations) and the Silurian Tanf Formation (from the Abba group). No previous studies have been performed to assess the differences and similarities among crude oils in the study area. Additionally, there are no publications analysing the suspected sources of hydrocarbons existing in the Euphrates Graben. The current study principally utilizes "Petroleum Geochemistry" (see sec.1.1) to investigate and distinguish the main chemical features and characteristics of Syrian crude oils. The specific goals and objectives of the current study are as follows:

- Characterize the geochemical composition of crude oils in the Euphrates Graben Petroleum System (Chapter.4).
- Identify the main oil families found in the study area (sec.5.1.1).
- Evaluate the Lower Silurian Tanf Formation as a potential source rock especially in the southeastern part of the graben (sec.4.2.1).

- Try to differentiate between the two Upper Cretaceous source rocks and their related crude oils (sec.5.2).
- Assess and quantify the oil mixing potential between different sources in the reservoired oils (sec.5.3).
- Investigate the impact of secondary alteration processes (e.g. biodegradation) on the composition of crude oils trapped in shallow reservoirs (sec.5.4).
- Define the migration pathways depending on available geological data (sec.5.2.3).

To fulfill the aims of this study, various geochemical analyses have been employed (Chapter.3). Oil-oil (sec.5.1) and oil-source rock (sec.5.2) correlation tools are used to differentiate the geochemical signatures of petroleums and, consequently, to categorize crude oils into certain populations. The integration of geochemical and available geological data has been done to better understand the chemical variations of crude oils in the geological framework and to show the significant role of the very complicated tectonic settings in controlling the migration fairways and, consequently, the distribution of oil families in the study area.

Chapter 3

Experimental Methods

A total of 82 oil samples (Tab.3.1) and 37 rock samples (Tab.3.4) were made available for this study by Al Furat Petroleum Company (AFPC) and Shell International E&P B.V. Both oil- and rock-sample set were characterized by the analytical procedures described below.

3.1 Oil Samples Analysis

The oil samples were collected from reservoir zones throughout the entire stratigraphic column (Tab.3.1) and include Paleozoic, Triassic, Cretaceous and Tertiary reservoir units. In the first stage, all 82 oil samples were analysed by Whole Oil Gas Chromatography (GC-FID) to screen the main geochemical properties of crude oils. Based on these results 30 oil samples have been chosen for further detailed analyses (GC-MS, SIM-GC-MS, MRM-GC-MS).

| Number | Well code | Depth [m] | Reservoir Fm. | Age |
|------------------------|-----------|-----------------|-----------------|------------|
| G002952 | ABH101 | 330.0m | Lower Fars | Miocene |
| G002953 | ISH101 | 3219.1 - 3276.2 | Rutbah | Cretaceous |
| G002954 | AHM101 | 2735.0 - 2747.2 | Post Judea Sand | Cretaceous |
| G002955 | JID101 | 2879.0 - 2928.0 | Lower Rutbah | Cretaceous |
| G002956 | AHM102 | 2438.0 - 2465.0 | Rutbah | Cretaceous |
| G002957 | AHM102 | 2284.0 - 2290.0 | Erek | Cretaceous |
| Continued on next page | | | | |

Table 3.1 – continued from previous page

| Number | Well code | Depth [m] | Reservoir Fm. | Age |
|------------------------|-----------|-----------------|-----------------------|---------------|
| G002958 | FUR101 | 2299.0 - 2340.0 | Shiranish | Cretaceous |
| G002959 | TMM101 | 3099.5 - 3110.0 | Post Judea Sand | Cretaceous |
| G002960 | RAT102 | 1993.0 - 2017.0 | Erek | Cretaceous |
| G002961 | TMM101 | 2992.5 - 3002.5 | Derro | Cretaceous |
| G002962 | OMA102 | 3548.0 - 3624.0 | L. Rutbah / Mulussa F | Cretaceous |
| G002963 | ISB101 | 3051.0 - 3098.0 | Lower Rutbah | Cretaceous |
| G002964 | SIJ102 | 2880.0 - 2907.5 | Post Judea Sand | Cretaceous |
| G002965 | OMA107 | 3533.0 - 3620.0 | Lower Rutbah | Cretaceous |
| G002966 | SHL101 | 3706.0 - 3788.0 | Lower Rutbah | Cretaceous |
| G002967 | SIJ101 | 2781.5 - 2787.5 | Post Judea Sand | Cretaceous |
| G002968 | RAT101 | 2415.5 | Lower Doubayat | Carboniferous |
| G002969 | TAN102 | 2770.0 - 2836.0 | Mulussa F | Triassic |
| G002970 | SIJ101 | 2957.0 - 2963.0 | L. Rutbah | Cretaceous |
| G002971 | OMA102 | 3739.5 - 3844.0 | Mulussa F | Triassic |
| G002972 | ISH101 | 3289.0 - 3300.0 | Rutbah | Cretaceous |
| G002973 | TAE101 | 3017.0 - 3145.0 | Mulussa F | Triassic |
| G002974 | BRG101 | 2285.1 | Post Judea Sand | Cretaceous |
| G002975 | AKA101 | 1894.0 - 1916.0 | ICD | Carboniferous |
| G002976 | ONE101 | 3150.0 | U. Shiranish | Cretaceous |
| G002977 | AZQ101 | 2911.5 - 2922.0 | Mulussa F | Triassic |
| G002978 | SHA101 | 1750.0 - 1756.0 | Mulussa D | Triassic |
| G002979 | ABH101 | 2731.0 - 2736.0 | Mulussa F | Triassic |
| G002980 | ABH101 | 2655.0 - 2665.0 | Rutbah | Cretaceous |
| G002981 | BRS101 | 3760.0 - 3777.0 | Khabour | Ordovician |
| G002982 | BRS101 | 3026.0 - 3061.0 | U. Doubayat | Carboniferous |
| G002983 | DER44 | 581.0 - 600.0 | Jeribe | Miocene |
| G002984 | ISB120 | 3100.0 | L. Rutbah | Cretaceous |
| G002985 | JID107 | 2880.0 - 2978.0 | L. Rutbah / Mulussa F | Cret./Tri. |
| G002986 | SRT102 | 2674.0 - 2682.0 | Erek / Mulussa F | Cret./Tri. |
| G002987 | YOU103 | 2900.0 - 2972.0 | Mulussa F | Triassic |
| G002988 | DER45 | 565.0 - 593.0 | Jeribe | Miocene |
| G002989 | DER60 | 570.0 - 595.0 | Jeribe | Miocene |
| G002990 | KSR101 | 1768.0 - 1799.0 | Judea Carbonate | Cretaceous |
| G002991 | HMD101 | 2118.2 | Mulussa D | Triassic |
| G002992 | ASH001 | 558.0 - 561.5 | Jeribe | Miocene |
| Continued on next page | | | | |

Table 3.1 – continued from previous page

| Number | Well code | Depth [m] | Reservoir Fm. | Age |
|------------------------|-------------|-----------------|--------------------|---------------|
| G002993 | MAH1 | 515.0 - 527.0 | L.Fars /524 Jeribe | Miocene |
| G002994 | ASH002 | 614.0 - 618.0 | Jeribe | Miocene |
| G002995 | ASH101 | 2552.5 - 2555.5 | R'mah | Cretaceous |
| G002996 | ASH101 | 2553.0 - 2556.0 | R'mah | Cretaceous |
| G002997 | MAH3 | 516.0 - 521.0 | Jeribe | Miocene |
| G002998 | MAH3 | 616.5 - 625.0 | Euphrates | Miocene |
| G002999 | AKE101 | 2546.1 - 2561.0 | R'mah | Cretaceous |
| G003000 | THM0001 | 2944.3 - 2956.3 | Judea Carbonate | Cretaceous |
| G003001 | NIS001 | 808.0 - 815.5 | Dhiban | Miocene |
| G003002 | ISH101 | 3219.0 - 3276.2 | Rutbah | Cretaceous |
| G003003 | THM0104 | 3102.0 - 3108.0 | Rutbah | Cretaceous |
| G003004 | THM0001 | 810.1 - 826.0 | Dhiban / Euphrates | Miocene |
| G003005 | EWS101 | 2142.1 - 2157.1 | U. Shiranish | Cretaceous |
| G003006 | AKE101 | 2586.9 | Kometan | Cretaceous |
| G003007 | EWS101 | 2180.2 - 2184.2 | U. Shiranish | Cretaceous |
| G003008 | EWS101 | 2120.2 | U. Shiranish | Cretaceous |
| G003009 | EWN101 | 2819.1 - 2861.1 | Rutbah | Cretaceous |
| G003010 | WAH01 | 1781.1 - 1786.1 | Mulussa C | Triassic |
| G003011 | NIS001 | 783.1 - 808.1 | Dhiban | Miocene |
| G003012 | WAH3 | 1807.1 - 1814.1 | Mulussa B | Triassic |
| G003013 | MAD001 | 1575.1 - 1625.1 | Erek | Cretaceous |
| G003014 | THM0102 | 2374.1 | U. Shiranish | Cretaceous |
| G003015 | THM0102 | 2949.5 - 2978.0 | Rutbah | Cretaceous |
| G003016 | THM0103 | 2955.5 - 2993.0 | Rutbah | Cretaceous |
| G003017 | MNW101 | 1783.2 | Doubayat | Carboniferous |
| G003018 | WAH05 | 1778.0 - 1809.0 | Mulussa B | Triassic |
| G003019 | WAH6 | 1360.0 - 1385.0 | Mulussa H | Triassic |
| G003020 | YOS101 | 2903.0 | L. Rutbah | Cretaceous |
| G003105 | BRG-102 | | Post Judea Sand | Cretaceous |
| G003106 | BRS-101 | | Doubayat | Carboniferous |
| G003107 | BRS-104 | | Post Judea Sand | Cretaceous |
| G003108 | OMA-166 | | Lower Shiranish | Cretaceous |
| G003109 | OMA -166 St | | Rutbah | Cretaceous |
| G003110 | OMA-186 | | Rutbah | Cretaceous |
| G003111 | OMA-2011 | | Lower Shiranish | Cretaceous |
| Continued on next page | | | | |

Table 3.1 – continued from previous page

| Number | Well code | Depth [m] | Reservoir Fm. | Age |
|---------|-----------|-----------|-----------------|------------|
| G003112 | OMA-2012 | | Lower Shiranish | Cretaceous |
| G003113 | SIJ-137 | | Upper Shiranish | Cretaceous |
| G003114 | SIJ -137 | | Rutbah | Cretaceous |
| G003115 | OBM | | Oil Based Mud | |
| G003116 | THM-007 | | Euphrates | Miocene |
| G003117 | THR-110 | | Rutbah | Cretaceous |

Table 3.1: List of the analysed 82 Oil samples

3.1.1 Whole Oil Gas Chromatography (GC-FID)

The GC-FID measurements on the whole oils were carried out for the detection and quantification of saturated and aromatic compounds. Analyses were performed with a GC-FID (6890A, Agilent Technologies, USA) which was equipped with a HP-PONA fused silica capillary column (50 m x 0, 32 mm i.d., film thickness = 0, 50 μ m). The injector temperature was set to 30 °C with a rate of 700 °C/min heating up to 300 °C held for 3 minutes. The GC oven temperature was programmed from 30 °C to 60 °C at a heating rate of 2 °C/min, followed by a heating rate of 4 °C/min up to 320 °C with a final time of 35 min. The carrier gas was helium (He) with a flow rate of 1 ml/min. The split mode was set at split ratio of 1/50. Quantification of the resolved compounds (listed in Tab.3.2) was carried out using isooctane (C_8H_{18}) as internal standard. The GC-FID chromatogram of a whole oil sample is shown in Fig.3.1.

| Compound | Abbreviation | Compound | Abbreviation |
|------------------------|--------------------------|---------------------------|-----------------------------------|
| <i>iso</i> .pentane | <i>i</i> -C ₅ | <i>iso</i> -nonane | <i>i</i> -C ₉ |
| pentane | <i>n</i> -C ₅ | ethylbenzene | EBenzene |
| 2,2-dimethylbutane | 2,2-DMB | (1,3+1,4)-dimethylbenzene | <i>meta</i> + <i>para</i> -Xylene |
| cyclopentane | CP | 2+4-methyloctane | 2+4-MOct |
| 2,3-dimethylbutane | 2,3-DMB | 3-methyloctane | 3MOct |
| 2-methylpentane | 2MP | 1,2-dimethylexylene | <i>ortho</i> -Xylene |
| 3-methylpentane | 3MP | nonane | <i>n</i> -C ₉ |
| Continued on next page | | | |

Table 3.2 – continued from previous page

| Compound | Abbreviation | Compound | Abbreviation |
|---|----------------------------|-------------------------|---------------------------|
| hexane | <i>n</i> -C ₆ | decane | <i>n</i> -C ₁₀ |
| 2,2-dimethylpentane | 2,2-DMP | <i>iso</i> -undecane | <i>i</i> -C ₁₁ |
| methylecyclopentane | MCP | undecane | <i>n</i> -C ₁₁ |
| 2,4-dimethylpentane | 2,4-DMP | dodecane | <i>n</i> -C ₁₂ |
| 2,2,3-trimethylbutane | 2,2,3-TMB | <i>iso</i> -tridecane | <i>i</i> -C ₁₃ |
| benzene | Benzene | <i>iso</i> -tetradecane | <i>i</i> -C ₁₄ |
| 3,3-dimethylpentane | 3,3-DMP | tridecane | <i>n</i> -C ₁₃ |
| cyclohexane | CH | <i>iso</i> -pentadecane | <i>i</i> -C ₁₅ |
| 2-methylhexane | 2MH | tetradecane | <i>n</i> -C ₁₄ |
| 2,3-dimethylpentane | 2,3-DMP | <i>iso</i> -hexadecane | <i>i</i> -C ₁₆ |
| 1,1-dimethylpentane | 1,1-DMP | pentadecane | <i>n</i> -C ₁₅ |
| 3-methylhexane | 3MH | hexadecane | <i>n</i> -C ₁₆ |
| <i>cis</i> -1,3-dimethylcyclopentane | <i>cis</i> 1,3-DMCP | <i>iso</i> -octadecane | <i>i</i> -C ₁₈ |
| <i>trans</i> -1,3-dimethylcyclopentane | <i>trans</i> 1,3-DMCP | heptadecane | <i>n</i> -C ₁₇ |
| 3-ethylpentane | 3EP | pristane | Pr. |
| <i>cis</i> -1,2-dimethylcyclopentane | <i>cis</i> 1,2-DMCP | octadecane | <i>n</i> -C ₁₈ |
| <i>iso</i> -octane C ₈ H ₁₈ | <i>IS</i> | phytane | Ph. |
| heptane | <i>n</i> -C ₇ | nonadecane | <i>n</i> -C ₁₉ |
| methylhexane | MCH | icosane | <i>n</i> -C ₂₀ |
| 1, <i>trans</i> -1,3-trimethylcyclopentane | 1- <i>trans</i> ,1,3- TMCP | hencicosane | <i>n</i> -C ₂₁ |
| ethylcyclopentane | ECP | docosane | <i>n</i> -C ₂₂ |
| 2,5-dimethylhexan | 2,5-DMHex | tricosane | <i>n</i> -C ₂₃ |
| 1,4-dimethylhexane | 2,4-DMHex | tetracosane | <i>n</i> -C ₂₄ |
| 1, <i>trans</i> ,2,4-trimethylcyclopentane | 1- <i>trans</i> ,2,4- TMCP | pentacosane | <i>n</i> -C ₂₅ |
| 3,3-dimethylhexane | 3,3-DMHex | hexacosane | <i>n</i> -C ₂₆ |
| 1,2,3-trimethylcyclopentane | 1,2,3- TMCP | heptacosane | <i>n</i> -C ₂₇ |
| 2,3,4-trimethylcyclohexane | 2,3,4- TMCP | octacosane | <i>n</i> -C ₂₈ |
| toluene | Toluene | nonacosane | <i>n</i> -C ₂₉ |
| 2-methylheptane | 2MHep | triacontane | <i>n</i> -C ₃₀ |
| 3-methylheptane | 3MHep | hentriacontane | <i>n</i> -C ₃₁ |
| octane | <i>n</i> -C ₈ | dotriacontane | <i>n</i> -C ₃₂ |
| ethylecyclohexane | ECHex | | |
| Continued on next page | | | |

Table 3.2 – continued from previous page

| Compound | Abbreviation | Compound | Abbreviation |
|----------|--------------|----------|--------------|
|----------|--------------|----------|--------------|

Table 3.2: List of the light and saturated hydrocarbons, which were identified by gas chromatography flame ionization detection. Also given are abbreviations used in the chromatogram that is shown in Fig.3.1.

3.1.2 Single Ion Monitoring - Gas Chromatography - Mass Spectrometry (SIM-GC-MS)

The aliphatic fractions of the selected 30 oils were analysed using Single Ion Monitoring-Gas Chromatography-Mass Spectrometry (SIM-GC-MS) for diamondoids identification and quantification. The instrument and its settings is the same of GC-MS (see sec.3.3.2) except that for this analysis no full scan was carried out but the detection of some specific ions. Two groups of diamondoids were identified in the studied oils (see Fig.3.2 and Tab.3.3 for identification):

- adamantanes (including adamantane, methyladamantanes, dimethyladamantanes, trimethyladamantanes, tetramethyladamantanes, and pentamethyladamantanes using GC-MS m/z 136, 135, 149, 163, 177, and 191 fragmentograms, respectively).
- diamantanes (including diamantane, methyldiamantanes, dimethyldiamantanes, trimethyldiamantanes using GC-MS m/z 188, 187, 201, 215 fragmentograms, respectively)

3.1.3 Compound Specific Stable Isotopes

- Stable Carbon Isotopes:

The carbon isotopic composition of petroleum components was measured by GC-C-IRMS (gas chromatography-combustion-isotope-ratio mass spectrometry), Fig.3.3. The GC-C-IRMS system consisted of

| Adamantanes | Peak Nr | Assignment | Abb. | Formula | M^+ (m/z) | Base Peak (m/z) |
|-------------|---------|--|-------------------------|----------------|-----------------|---------------------|
| Adamantanes | 1 | Adamantane | A | $C_{10}H_{16}$ | 136 | 136 |
| | 2 | 1-Methyldiamantane | 1-MA | $C_{11}H_{18}$ | 150 | 135 |
| | 3 | 2-Methyldiamantane | 2-MA | $C_{11}H_{18}$ | 150 | 135 |
| | 4 | 1-Ethyladamantane | 1-EA | $C_{12}H_{20}$ | 164 | 135 |
| | 5 | 2-Ethyladamantane | 2-EA | $C_{12}H_{20}$ | 164 | 135 |
| | 6 | 1,3-dimethyldiamantane | 1,3-DMA | $C_{12}H_{20}$ | 164 | 149 |
| | 7 | 1,4-Dimethyldiamantane (<i>cis</i>) | 1,4-DMA <i>cis</i> | $C_{12}H_{20}$ | 164 | 149 |
| | 8 | 1,4-Dimethyldiamantane (<i>trans</i>) | 1,4-DMA <i>trans</i> | $C_{12}H_{20}$ | 164 | 149 |
| | 9 | 1,2-Dimethyldiamantane | 1,2-DMA | $C_{12}H_{20}$ | 164 | 149 |
| | 10 | 1-Ethyl,3-Methyldiamantane | 1-E,3-MA | $C_{13}H_{22}$ | 178 | 149 |
| | 11 | 1,3,5-Trimethyldiamantane | 1,3,5-TrMA | $C_{13}H_{22}$ | 178 | 163 |
| | 12 | 1,3,6-Trimethyldiamantane | 1,3,6-TrMA | $C_{13}H_{22}$ | 178 | 163 |
| | 13 | 1,3,4-Trimethyldiamantane (<i>cis</i>) | 1,3,4-TrMA <i>cis</i> | $C_{13}H_{22}$ | 178 | 163 |
| | 14 | 1,3,4-Trimethyldiamantane (<i>trans</i>) | 1,3,4-TrMA <i>trans</i> | $C_{13}H_{22}$ | 178 | 163 |
| | 15 | 1-Ethyl,3,5-Dimethyldiamantane | 1-E,3,5-DMA | $C_{14}H_{24}$ | 192 | 163 |
| | 16 | 1,3,5,7-Tetramethyldiamantane | 1,3,5,7-TeMA | $C_{14}H_{24}$ | 192 | 177 |
| | 17 | 1,2,5,7-Tetramethyldiamantane | 1,2,5,7-TeMA | $C_{14}H_{24}$ | 192 | 177 |
| | 18 | 1,3,5,6-Tetramethyldiamantane | 1,3,5,6-TeMA | $C_{14}H_{24}$ | 192 | 177 |
| | 19 | 1,2,3,5-Tetramethyldiamantane | 1,2,3,5-TeMA | $C_{14}H_{24}$ | 192 | 177 |
| | 20 | 1-ethyl,3,5,7-Trimethyldiamantane | 1-E,3,5,7-TrMA | $C_{15}H_{26}$ | 206 | 177 |
| | 21 | 1,2,3,5,7-Pentamethyldiamantane | 1,2,3,5,7-PMA | $C_{15}H_{26}$ | 206 | 191 |
| Diamantanes | 22 | Diamantane | D | $C_{14}H_{20}$ | 188 | 188 |
| | 23 | 4-Methyldiamantane | 4-MD | $C_{15}H_{22}$ | 202 | 187 |
| | 24 | 1-Methyldiamantane | 1-MD | $C_{15}H_{22}$ | 202 | 187 |
| | 25 | 3-Methyldiamantane | 3-MD | $C_{15}H_{22}$ | 202 | 187 |
| | 26 | 4,9-Dimethyldiamantane | 4,9-DMD | $C_{16}H_{24}$ | 216 | 201 |
| | 27 | 1,4 + 2,4-Dimethyldiamantane | 1,4 + 2,4-DMD | $C_{16}H_{24}$ | 216 | 201 |
| | 28 | 4,8-Dimethyldiamantane | 4,8-DMD | $C_{16}H_{24}$ | 216 | 201 |
| | 29 | 3,4-Dimethyldiamantane | 3,4-DMD | $C_{16}H_{24}$ | 216 | 201 |
| | 30 | 1,4,9-Trimethyldiamantane | 1,4,9-TrMD | $C_{17}H_{26}$ | 230 | 215 |
| | 31 | 3,4,9-Trimethyldiamantane | 3,4,9-TrMD | $C_{17}H_{26}$ | 230 | 215 |

Table 3.3: Adamantanes and diamantanes identified in Syrian crude oil sample. Peak series correspond to those in Fig.3.2

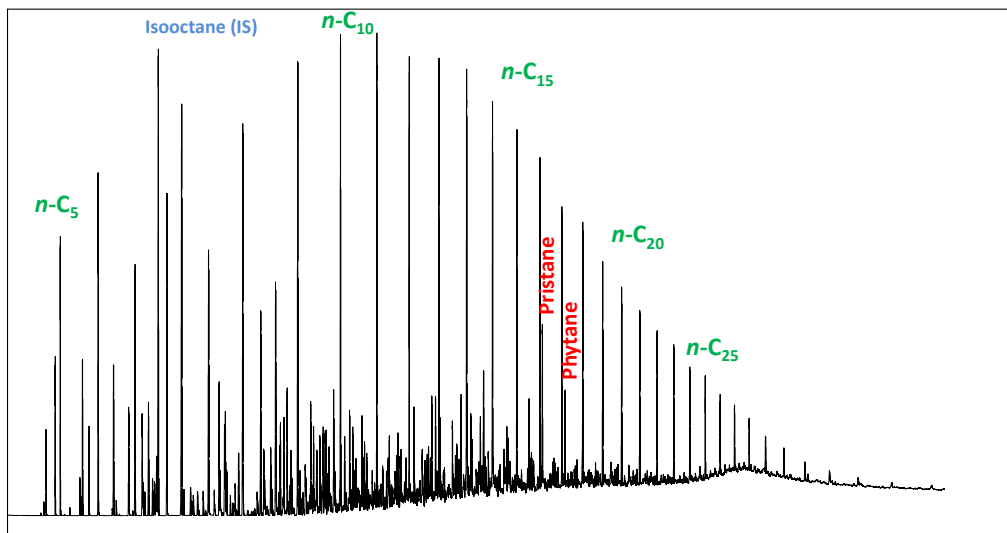


Figure 3.1: Example of a whole oil chromatogram of NSO (Norwigen Standard Oil). A full range of n -alkanes up to n -C₃₅ was observed.

a GC unit (6890N, Agilent Technology, USA) connected to a GC-C-TC III combustion device coupled via open split to a MAT 253 mass spectrometer (ThermoFisher Scientific, Germany). The organic substances of the GC effluent stream were oxidised to CO_2 in the combustion furnace held at 940 °C on a CuO/Ni/Pt catalyst. CO_2 was transferred on line to the mass spectrometer to determine carbon isotope ratios. Crude oil (0.5 μ l) was injected to the programmable temperature vaporization inlet (PTV, Agilent Technology, USA) with a septumless head, working in split/splitless mode. The injector was held at a variety of split ratios ranging from 1:20 to 1:50, depending on the compound concentrations in individual oils. The initial temperature of the injector was set to 230 °C. With injection, the injector was heated to 300 °C at a programmed rate of 700 °Cmin⁻¹ and held at this temperature for the rest of the analysis time. Petroleum components were separated on a fused silica capillary column (HP Ultra 1, 50 m x 0.32 mm ID, 0.52 μ m FT, Agilent Technology, USA). The temperature program of the GC oven was initially held at 30 °C for 10 min, followed by a 2 °Cmin⁻¹ ramp to 60 °C, then at a rate of 4 °Cmin⁻¹ to 300 °C and held there for a further 30 min. Helium, set

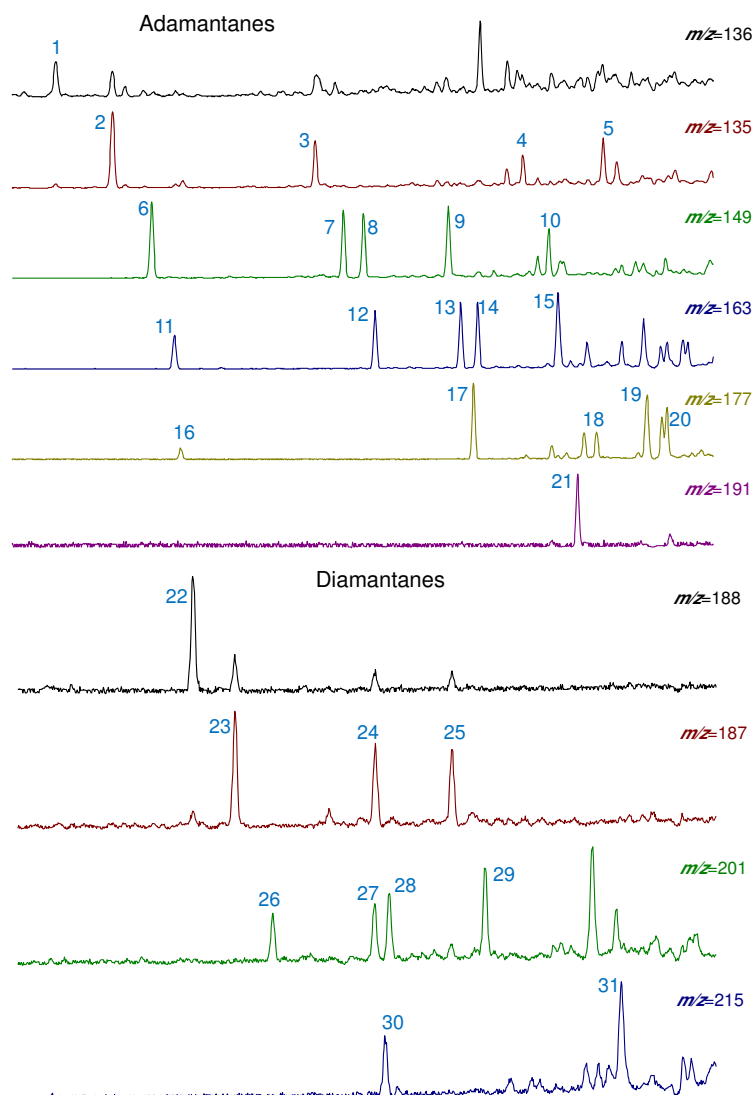


Figure 3.2: Ion chromatograms displaying the distribution of adamantanes and diamantanes in oil sample G002961 (see Tab.3.3 for peak assignments)

to a flow rate of 1.0 ml min^{-1} , was used as carrier gas. All oil samples were measured in triplicate with a standard deviation of $\lesssim 0.5 \text{ ‰}$ for most of the compounds and samples. The quality of the carbon isotope measurements was checked regularly by measuring *n*-alkane standards (*n*- C_{15} , *n*- C_{20} , and *n*- C_{25}) with known isotopic composition (provided by Campro Scientific, Germany).

- Stable Hydrogen Isotopes:

The hydrogen isotopic composition of petroleum components was measured by GC-P-IRMS (Gas Chromatography-Pyrolysis-Isotope-Ratio

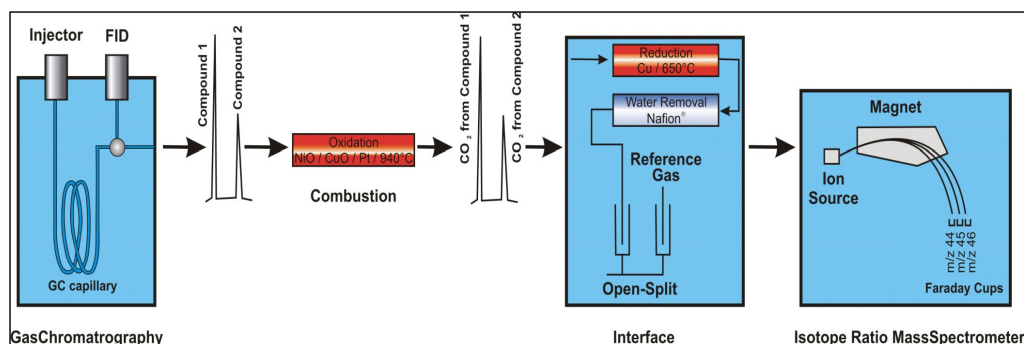


Figure 3.3: Schematic view of a GC-C-IRMS-system for compound-specific isotope analysis. The separation of complex mixtures is done by gas chromatography. At a temperature of 940 °C separated compounds are oxidized to CO_2 and H_2O catalytically. The reduction interface eliminates nitrogen oxides and the water is separated from the carrier gas by a *Nafion* membrane in the water removal device. The remaining CO_2 is ionized and detected in the mass spectrometer. From the ratio of $^{44}CO_2$ to $^{45}CO_2$ the $\delta^{13}C$ value can be calculated.

Mass Spectrometry). The GC-P-IRMS system consisted of a GC unit (6890N, Agilent Technology, USA) connected to a pyrolysis device coupled via open split to a MAT 253 mass spectrometer (ThermoFisher Scientific, Germany). After passing the GC (6890 Series, Agilent Technology, USA), hydrocarbons were reduced to H_2 and elemental carbon in the pyrolysis reactor held at 1450 °C. H_2 was transferred on line to the mass spectrometer to determine hydrogen isotope ratios. Crude oil (0.5 μ l) was injected to the programmable temperature vaporisation inlet (PTV, Agilent Technology, USA) with a septumless head, working in split/splitless mode. The injector was held at a variety of split ratios ranging from 1:10 to 1:50, depending on the compound concentrations in individual oils. The initial temperature of the injector was set to 230 °C. With injection, the injector was heated to 300 °C at a programmed rate of 700 °Cmin⁻¹ and held at this temperature for the rest of the analysis time. Petroleum components were separated on a fused silica capillary column (HP Ultra 1,50 m x 0.32 mm ID, 0.52 μ m FT, Agilent Technology, USA). The temperature program of the GC oven was initially held at 30 °C for 10 min, followed by a 2 °Cmin⁻¹ ramp to 60 °C, then at a rate of

4 °Cmin⁻¹ to 300 °C and held there for a further 30 min. Helium, set to a flow rate of 1.0 ml min⁻¹, was used as carrier gas. All oil samples were measured in triplicate with a standard deviation of $\lesssim 5$ ‰ for most of the compounds and samples. The $H_3 \pm$ factor was determined daily by measuring 10 reference gas peaks with increasing amplitude. This factor had an average value of 5.48 ± 0.13 ppm/nA. The quality of the hydrogen isotope measurements was checked regularly by measuring *n*-alkane standards (*n*-C₁₇, *n*-C₁₉, *n*-C₂₁, *n*-C₂₃, and *n*-C₂₅) with known isotopic composition (provided by A. Schimmelmann, Biogeochemical Laboratories, Indiana University).

3.2 Rock Samples Analysis

37 rock samples (Tab.3.4) from the potential source rocks in the study area have been analysed geochemically in order to assess their potentiality (sec.4.2.1) and to perform oil to source rock correlation (sec.5.2).

3.2.1 Solvent Extraction

The source rock extracts were obtained using a Soxhlet apparatus. Approximately 50 g of the whole rock sample was pulverized. An amount of the crushed samples (ca. 20g) was weighed into a cellulose extraction thimble and then placed in the extraction tube of the Soxhlet apparatus and extracted for 24 hours using approximately 350 ml of an azeotropic mixture of methanol/acetone/chloroform 30:38:32. After extraction, the solvent was removed using a turbovap device followed by a nitrogen stream. The extracts were then subjected to the following geochemical analyses: MPLC, GC-FID, GC-MS, and GC-MS-MS.

3.2.2 Gas Chromatography of Saturates GC-FID

The GC-FID measurements on the aliphatic fraction were carried out for the detection and quantification of saturated compounds in the *n*-C₁₅ to

| Sample | Code | Depth (m) | Formation | Rock Eval | Extraction | GC-FID | MPLC | GC-MS | GC-MS-MS |
|---------|---------|-------------|-------------|-----------|------------|--------|------|-------|----------|
| G005145 | OMA141 | 3626 - 3633 | R'mah | X | X | X | X | X | X |
| G005112 | OMA 165 | 3560 | R'mah | | X | X | X | X | X |
| G005113 | OMA 165 | 3565 | R'mah | | X | X | X | X | X |
| G005114 | OMA 165 | 3570 | R'mah | | X | X | X | X | X |
| G005115 | OMA 165 | 3575 | R'mah | | X | X | X | X | X |
| G005116 | OMA 165 | 3580 | R'mah | | X | X | X | X | X |
| G005117 | OMA 169 | 3745 - 3755 | R'mah | X | X | X | X | X | X |
| G005118 | OMA 180 | 3600+3605 | R'mah | | X | X | X | X | X |
| G005119 | OMA 180 | 3610+3615 | R'mah | | X | X | X | X | X |
| G005120 | BRS 101 | 3330-3345 | Abba | X | X | X | X | X | X |
| G005121 | BRS 101 | 3375-3385 | Abba | | X | X | X | X | X |
| G005122 | BRS 101 | 3415-3425 | Abba | | X | X | X | X | X |
| G005123 | BRS 101 | 3445-3455 | Abba | X | X | X | X | X | X |
| G005124 | BRS 101 | 3470-3475 | Abba | | X | X | X | X | X |
| G005125 | BRS 101 | 3485-3505 | Abba | X | X | X | X | X | X |
| G005126 | SLJ 103 | 3380+3385 | Abba | X | X | X | X | X | X |
| G005127 | SLJ 103 | 3480+3485 | Abba | | X | X | X | X | X |
| G005128 | SLJ 103 | 3530 | Abba | | X | X | X | X | X |
| G005129 | SLJ 103 | 3580+3585 | Abba | | X | X | X | X | X |
| G005130 | SLJ 103 | 3625+3630 | Abba | | X | X | X | X | X |
| G005131 | RAT 101 | 2320-2330 | Abba | X | X | X | X | X | X |
| G005132 | RAT 101 | 2435-2445 | Abba | | X | X | X | X | X |
| G005133 | RAT 101 | 2490-2500 | Abba | | X | X | X | X | X |
| G005134 | AHM 101 | 2840+2845 | Abba | X | X | X | X | X | X |
| G005135 | AHM 101 | 2925+2930 | Abba | | X | X | X | X | X |
| G005136 | AHM 101 | 2995+3000 | Abba | | X | X | X | X | X |
| G005137 | SRT 101 | 3585-3595 | Abba | X | X | X | X | X | X |
| G005138 | SRT 101 | 3670-3680 | Abba | | X | X | X | X | X |
| G005139 | SRT 101 | 3730-3740 | Abba | | X | X | X | X | X |
| G005140 | HMN 101 | 2450-2455 | Abba | X | X | X | X | X | X |
| G005141 | HMN 101 | 2610-2615 | Abba | | X | X | X | X | X |
| G005142 | HMN 101 | 2665-2675 | Abba | | X | X | X | X | X |
| G003850 | RAT 101 | 3030 | Abba | X | X | X | X | X | X |
| G003185 | OMA 102 | 2970 | U.Shiranish | X | X | X | X | X | X |
| G003188 | OMA 102 | 3050 | U.Shiranish | X | X | X | | | |
| G003200 | OMA 102 | 3300 | L.Shiranish | X | X | X | | | |
| G003211 | OMA 102 | 3520 | L.Shiranish | X | X | X | X | X | X |

Table 3.4: List of 37 rock samples analysed in the current study with different analytical methods.

n - C_{30} range. Analyses were performed with a GC-FID (6890A, Agilent Technologies, USA) which was equipped with a HP Ultra 1 capillary column (50 m x 0,32 mm i.d., film thickness = 0,50 μ m). The injector temperature was set to 40 °C with a rate of 700 °C/min heating up to 300 °C held for 3 minutes. The GC oven was programmed from 40 °C with 2 min isothermal to a final temperature of 300 °C with 65 min isothermal at a heating rate of 5 °C/min with a constant flow rate. The injected aliphatic fraction, diluted in n -hexane, was detected by a FID operating at 310 °C.

3.3 Oil and Source Rock Samples Analysis

3.3.1 Medium Pressure Liquid Chromatography MPLC

Thirty oil samples and 37 rock extracts were separated by Medium Pressure Liquid Chromatography (MPLC) (Radke et al., 1980) to obtain their three respective polarity fractions: saturates (normal, branched and cyclic alkanes), aromatic hydrocarbons, and hetero compounds, which contain nitrogen, oxygen and/or sulphur atoms. Diluted in n -hexane the sample was placed in an injector block where the sample loop starts. The MPLC was equipped with sixteen pre-columns filled with pure silica gel (Silica 100 with a grain size of 63-200 μ m), which retains the nitrogen, sulphur and oxygen (NSO) compounds of the neat crude oil or rock extract. In the downstream main column that is filled with LiChroPrep Si60, the aromatic fraction of the oil is trapped while the aliphatic compounds elute. Flow through the main column is then reserved by use of the back-flush valve and the flow rate is increased. Thus, the aromatic hydrocarbons elute during this back-flushing period into a second vial. The MPLC unit was loaded with approximately 30-40 mg of the neat crude oil or rock extract for each sample. As internal standards 5 α -androstane and 1-ethylpyrene were used for the aliphatic and aromatic fraction, respectively. The NSO compounds trapped on the pre-columns were released by using a dichloromethane/methanol (95:5) solvent mixture.

3.3.2 Gas Chromatography - Mass Spectrometry GC-MS

The aromatic hydrocarbon fractions were analysed using Gas Chromatography-Mass Spectrometry (GC-MS). Analyses were performed using a Finnigan MAT 95XL mass spectrometer that was coupled to a HP 6890A gas chromatograph. The GC was equipped with a BPX5 fused silica capillary column (50 m x 0.22 mm i.d; f.t. = 0.25 μm). The injected amount was 1 μl , and the injector temperature was set to 52°C, subsequently heated up with 720°Cmin⁻¹ to 300°C. The oven temperature started at 50°C with a 1 min isothermal stage, then heating up with 3°Cmin⁻¹ to 310°C final temperature which was held for 20 min. Helium was used as the carrier gas with a constant flow of 1 ml/min. The MS unit was operated in the EI mode at an electron energy of 70eV and a source temperature of 260°C. Full scan mass spectra were recorded from m/z 50-330 Da for the aromatic fraction at a scan rate of 2.5 scan per second. GC-MS measurements were used to evaluate several alkylated benzenes, naphthalenes, phenanthrenes and dibenzothiophenes as well as mono- and triaromatic steroids. Identification of each compound class was carried out using respective m/z values displayed in Figures (3.4 to 3.9) and Tables (3.5 to 3.10).

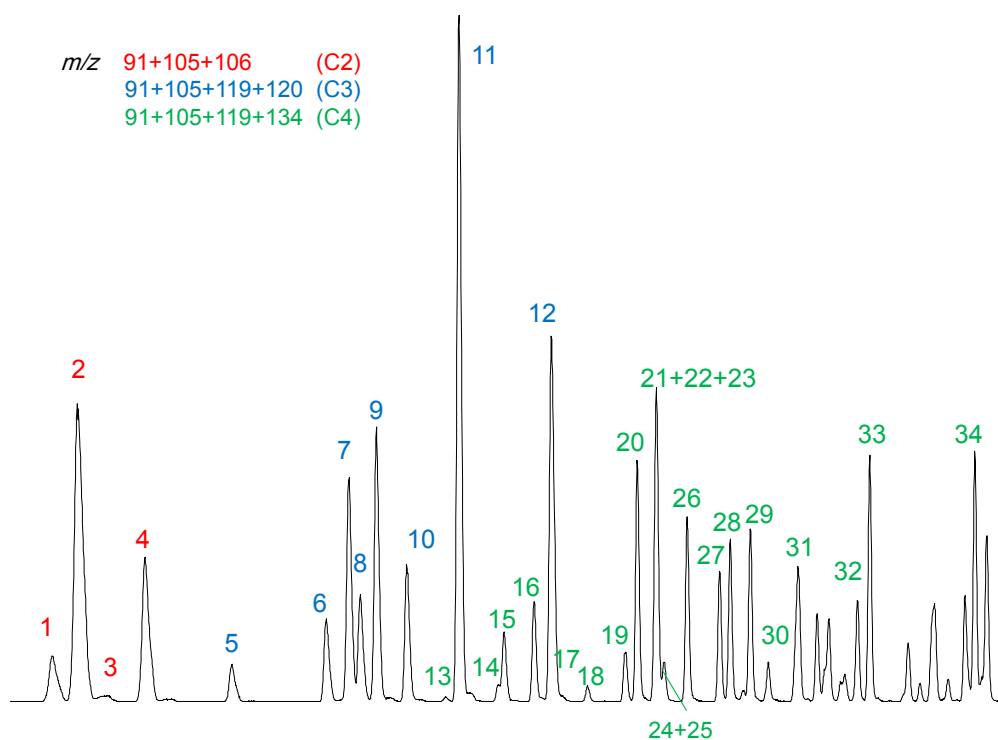


Figure 3.4: Ion chromatogram displaying the distribution of alkyl benzenes in oil sample G002963. Tab.3.5 for peak assignments.

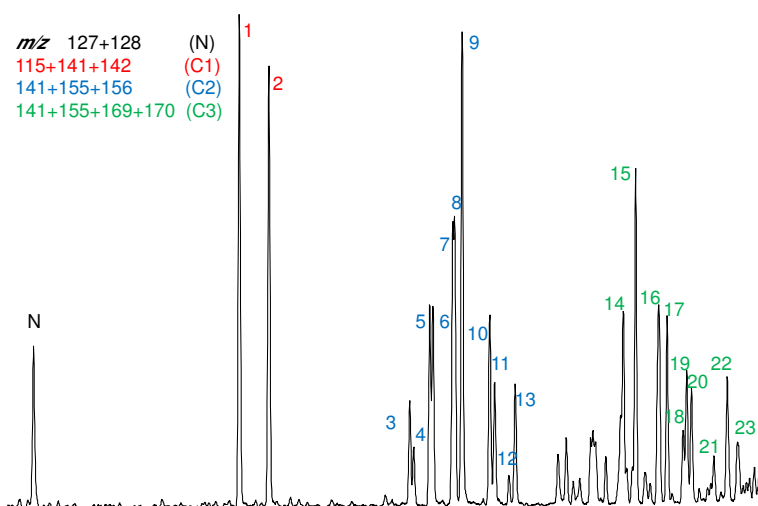


Figure 3.5: Ion chromatogram displaying the distribution of naphthalenes. Tab.3.6 for peak assignments.

| Name of Group | Number | Compound name | m/z | RT |
|---------------|--------|---|----------------|-------|
| DMB | 1 | Ethylbenzene | 91+105+106 | 12.17 |
| | 2 | 1,3-Dimethylbenzene (<i>m</i> -Xylene) | | 12.55 |
| | 3 | 1,4-Dimethylbenzene (<i>p</i> -Xylene) | | 13.00 |
| | 4 | 1,2-Dimethylbenzene (<i>o</i> -Xylene) | | 13.60 |
| TMB | 5 | Isopropylbenzene | 91+105+119+120 | 14.95 |
| | 6 | <i>n</i> -Propylbenzene | | 16.42 |
| | 7 | 1-Methyl-3-ethylbenzene | | 16.76 |
| | 8 | 1-Methyl-4-ethylbenzene | | 16.94 |
| | 9 | 1,3,5-Trimethylbenzene | | 17.19 |
| | 10 | 1-Methyl-2-ethylbenzene | | 17.67 |
| | 11 | 1,2,4-Trimethylbenzene | | 18.47 |
| | 12 | 1,2,3-Trimethylbenzene | | 19.91 |
| TeMB | 13 | <i>te.</i> -Butylbenzene | 91+105+119+134 | 18.27 |
| | 14 | Isobutylbenzene | | 19.07 |
| | 15 | <i>sec.</i> -Butylbenzene | | 19.17 |
| | 16 | 1-Methyl-3-isopropylbenzene | | 19.64 |
| | 17 | 1-Methyl-4-isopropylbenzene | | 19.94 |
| | 18 | 1-Methyl-2-isopropylbenzene | | 20.47 |
| | 19 | 1,3-Diethylbenzene | | 21.07 |
| | 20 | 1-Methyl-3-propylbenzene | | 21.24 |
| | 21 | 1,4-Diethylbenzene | | 21.54 |
| | 22 | 1-Methyl-4-propylbenzene | | |
| | 23 | <i>n</i> -Butylbenzene | | |
| | 24 | 1,3-Dimethyl-5-ethylbenzene | | 21.65 |
| | 25 | 1,2-Diethylbenzene | | |
| | 26 | 1-Methyl-2-propylbenzene | | 22.02 |
| | 27 | 1,4-Dimethyl-2-ethylbenzene | | 22.52 |
| | 28 | 1,3-Dimethyl-4-ethylbenzene | | 22.68 |
| | 29 | 1,2-Dimethyl-4-ethylbenzene | | 23.00 |
| | 30 | 1,3-Dimethyl-2-ethylbenzene | | 23.28 |
| | 31 | 1,2-Dimethyl-3-ethylbenzene | | 24.03 |
| | 32 | 1,2,4,5-Tetramethylbenzene | | 24.66 |
| | 33 | 1,2,3,5-Tetramethylbenzene | | 24.85 |
| | 34 | 1,2,3,4-Tetramethylbenzene | | 26.48 |

Table 3.5: Alkylbenzenes identified in Syrian crude oil samples. Peak series correspond to those in Fig.3.4.

| m/z | Name of Group | Number | Component | RT |
|-----------------|-----------------------------|--------|-------------------|-------|
| 127+128 | Naphthalene (N) | N | N | 28.67 |
| 115+141+142 | Methylnaphthalene (MN) | 1 | 2-MN | 33.94 |
| | | 2 | 1-MN | 34.70 |
| 141+155+156 | Di-Methylnaphthalene (DMN) | 3 | 2-Ethyl.N | 38.31 |
| | | 4 | 1-Ethyl.N | 38.41 |
| | | 5 | 2,6-DMN | 38.82 |
| | | 6 | 2,7-DMN | 38.90 |
| | | 7 | 1,3-DMN | 39.42 |
| | | 8 | 1,7-DMN | 39.45 |
| | | 9 | 1,6-DMN | 39.65 |
| | | 10 | 1,4 + 2,3-DMN | 40.36 |
| | | 11 | 1,5-DMN | 40.48 |
| | | 12 | 1,2-DMN | 41.01 |
| | | 13 | 1,8-DMN | 42.34 |
| 141+155+169+170 | Tri-Methylnaphthalene (TMN) | 14 | 1,3,7-TMN | 43.78 |
| | | 15 | 1,3,6-TMN | 44.10 |
| | | 16 | 1,4,6 + 1,3,5-TMN | 44.69 |
| | | 17 | 2,3,6-TMN | 44.90 |
| | | 18 | 1,2,7-TMN | 45.32 |
| | | 19 | 1,6,7-TMN | 45.41 |
| | | 20 | 1,2,6-TMN | 45.53 |
| | | 21 | 1,2,4-TMN | 46.10 |
| | | 22 | 1,2,5-TMN | 46.45 |
| | | 23 | 1,2,3-TMN | 47.14 |

Table 3.6: Naphthalenes identified in Syrian crude oil samples. Peak series correspond to those in Fig.3.5.

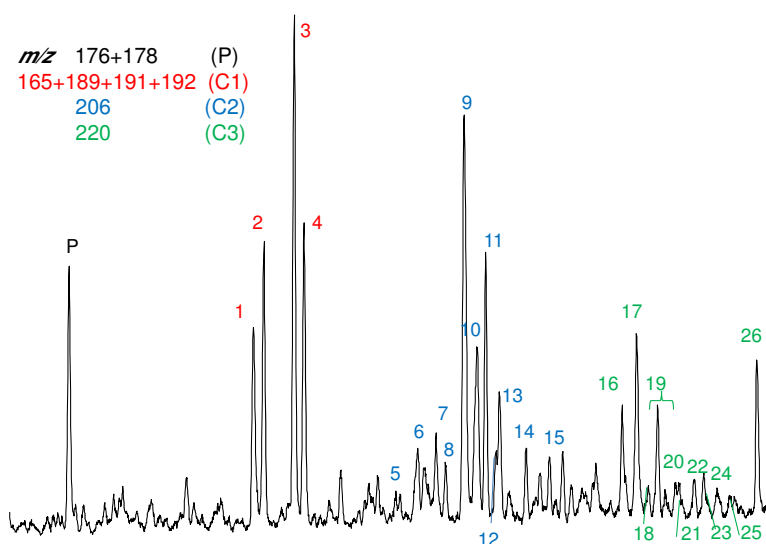


Figure 3.6: Ion chromatogram displaying the distribution of phenanthrenes. Tab.3.7 for peak assignments.

| m/z | Name of Group | Number | Compound | RT |
|-----------------|------------------------------|--|--|---|
| 176+178 | Phenanthrene (P) | P | Phenanthrene | 54,25 |
| 165+189+191+192 | Methylphenanthrene (MP) | 1 2 3 4 | 3-MP 2-MP 9-MP 1-MP | 58,10 58,32 58,95 59,16 |
| 206 | Di-Methylphenanthrene (DMP) | 5 6 7 8 9 10 11 12 13 14 15 | 3-Ethyl Phenanthrene 9-,2-,1-EP + 3,6-DMP 3,5- + 2,6-DMP 2,7-DMP 1,3- + 3,9- + 2,10- + 3,10-DMP 2,5- + 2,9- + 1,6-DMP 1,7-DMP 2,3-DMP 1,9- + 4,9- + 4,10-DMP 1,8-DMP 1,2-DMP | 61,06 61,69 61,92 62,12 62,51 62,77 62,95 63,16 63,25 63,80 64,29 |
| 220 | Tri-Methylphenanthrene (TMP) | 16 17 18 19 20 21 22 23 24 25 26 | 1,3,6- + 1,3,10- + 2,6,10-TMP 1,3,7- + 2,6,7- + 2,7,9-TMP + 7-Ethyl-1-Methyl Phenanthrene 1,3,9- + 2,3,6-TMP 1,6,9- + 1,7,9- + 2,3,7-TMP 1,3,8-TMP 2,3,10-TMP TMP (unknown) 1,6,7-TMP 1,2,6-TMP 1,2,7- + 1,2,9-TMP 1,2,8-TMP | 65,81 66,11 66,37 66,55 66,92 66,99 67,30 67,51 67,79 68,08 68,63 |

Table 3.7: Phenanthrenes identified in Syrian crude oil samples. Peak series correspond to those in Fig.3.6.

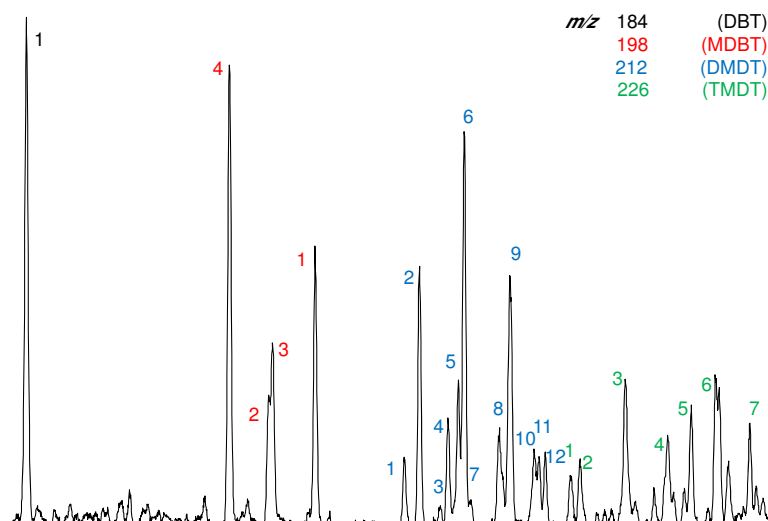


Figure 3.7: Ion chromatogram displaying the distribution of dibenzothiophenes. Tab.3.8 for peak assignments.

| m/z | Name of Group | Number | Compound | RT |
|-------|--------------------------------------|--------|------------------------|-------|
| 184 | DiBenzoThiophene (DBT) | 1 | DBT | 53.24 |
| 198 | MethylDiBenzoThiophene (MeDBT) | 4 | 4-MeDBT | 56.7 |
| | | 2 | 2-MeDBT | 57.37 |
| | | 3 | 3-MeDBT | 57.43 |
| | | 1 | 1-MeDBT | 58.16 |
| 212 | DiMethylDiBenzoThiophene (DiMeDBT) | 1 | 4-EthDBT | 59.69 |
| | | 2 | 4,6-DiMeDBT | 59.94 |
| | | 3 | 2-EthDBT | 60.3 |
| | | 4 | 2,4-DiMeDBT | 60.42 |
| | | 5 | 2,6-DiMeDBT | 60.6 |
| | | 6 | 3,6-DiMeDBT | 60.7 |
| | | 7 | 3-EthDBT | 60.81 |
| | | 8 | 2,7+3,7+2,8-DiMeDBT | 61.3 |
| | | 9 | 1,8+1,4+1,6-DiMeDBT | 61.49 |
| | | 10 | 3,4-DiMeDBT | 61.89 |
| | | 11 | 1,7-DiMeDBT | 61.98 |
| | | 12 | 1,3-DiMeDBT | 62.08 |
| 226 | TriMethylDiBenzothiophene (TriMeDBT) | 1 | 4-PropDBT | 62.5 |
| | | 2 | EthMeDBT | 62.66 |
| | | 3 | 2,4,6-TriMeDBT | 63.44 |
| | | 4 | 2,4,7 + 2,4,8-TriMeDBT | 64.17 |
| | | 5 | 1,4,6-TriMeDBT | 64.57 |
| | | 6 | 3,4,6-TriMeDBT | 64.98 |
| | | 7 | 1,3,7+3,4,7-TriMeDBT | 65.57 |

Table 3.8: Dibenzothiophenes identified in Syrian crude oil samples. Peak series correspond to those in Fig.3.7.

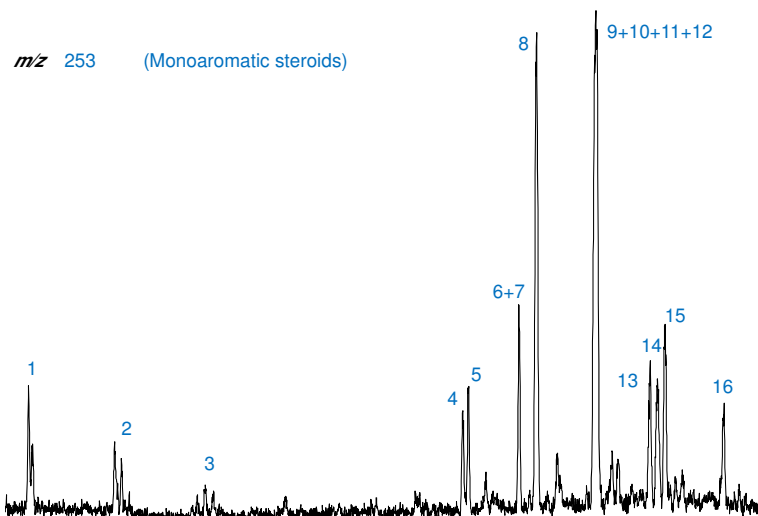


Figure 3.8: Ion chromatogram displaying the distribution of monoaromatic steroids. Tab.3.9 for peak assignments.

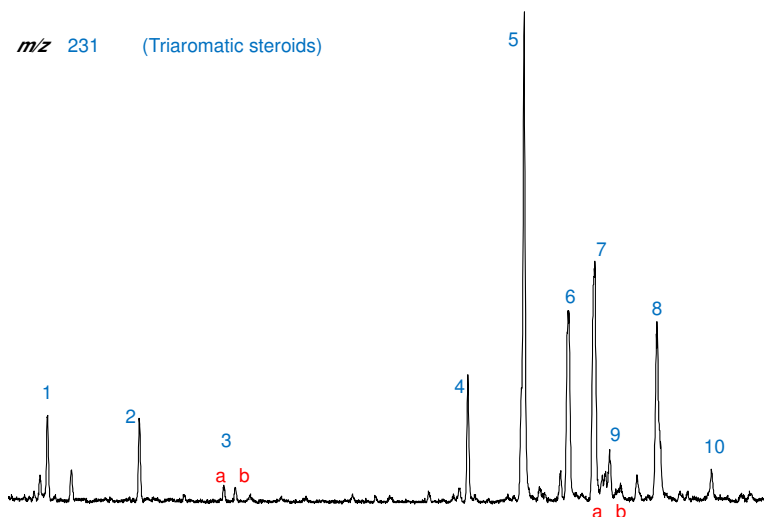


Figure 3.9: Ion chromatogram displaying the distribution of triaromatic steroids. Tab.3.10 for peak assignments.

| m/z | Name of Group | Peak | Component | Carbon Number | RT |
|-------|---------------|------|---|---------------|-------|
| 253 | Monoaromatic | 1 | Pregnane (x=ethyl) | 21 | 65,65 |
| | | 2 | 20-Methylpregnane (x=2-propyl) | 22 | 68,03 |
| | | 3 | 20-Ethylpregnane (x=2-butyl) | 23 | 70,54 |
| | | 4 | 5 β -Cholestane 20 <i>S</i> | 27 | 77,67 |
| | | 5 | Diacholestane 20 <i>S</i> | 27 | 77,83 |
| | | 6 | 5 β -Cholestane 20 <i>R</i> ; Diacholestane 20 <i>R</i> | 27 | 79,22 |
| | | 7 | 5 α -Cholestane 20 <i>S</i> | 27 | |
| | | 8 | 5 β -Ergostane 20 <i>S</i> ; Diaergostane 20 <i>S</i> | 28 | 79,71 |
| | Steroids | 9 | 5 α -Cholestane 20 <i>R</i> | 27 | 81,36 |
| | | 10 | 5 α -Ergostane 20 <i>S</i> | 28 | |
| | | 11 | 5 β -Ergostane 20 <i>R</i> ; Diaergostane 20 <i>R</i> | 28 | |
| | | 12 | 5 β -Stigmastane 20 <i>S</i> ; Diastigmastane 20 <i>S</i> | 29 | |
| | | 13 | 5 α -Stigmastane 20 <i>S</i> | 29 | 82,86 |
| | | 14 | 5 α -Ergostane 20 <i>R</i> | 28 | 83,07 |
| | | 15 | 5 β -Stigmastane 20 <i>R</i> ; Diastigmastane 20 <i>R</i> | 29 | 83,27 |
| | | 16 | 5 α -Stigmastane 20 <i>R</i> | 29 | 84,91 |

Table 3.9: Monoaromatic steroids identified in Syrian crude oil samples. Peak series correspond to those in Fig.3.8.

| m/z | Name of Group | Peak | Component | Carbon Number | RT |
|-------|---------------|------|---|---------------|-------|
| 231 | Triaromatic | 1 | Pregnane (x=ethyl) | 20 | 74.08 |
| | | 2 | 20-Methylpregnane (x=2-propyl) | 21 | 76.6 |
| | | 3 | 20-Ethylpregnanes (x=2-butyl; a and b are epimeric at C20) | 22 | 78.92 |
| | | 4 | Cholestane 20 <i>S</i> | 26 | 85.62 |
| | Steroids | 5 | Cholestane 20 <i>R</i> ; Ergostane 20 <i>S</i> | 26, 27 | 87.16 |
| | | 6 | Stigmastane 20 <i>S</i> (24-ethylcholestane 20 <i>S</i>) | 26 | 88.36 |
| | | 7 | Ergostane 20 <i>R</i> (24-methylcholestane 20 <i>R</i>) | 27 | 89.1 |
| | | 9 | 24- <i>n</i> -Propylcholastane 20 <i>S</i> (a and b are epimeric at C24) | 29 | 89.5 |
| | | 8 | Stigmastane 20 <i>R</i> | 28 | 90.8 |
| | | 10 | 24- <i>n</i> -Propylcholastane 20 <i>R</i> | 29 | 92.29 |

Table 3.10: Triaromatic steroids identified in Syrian crude oil samples. Peak series correspond to those in Fig.3.9.

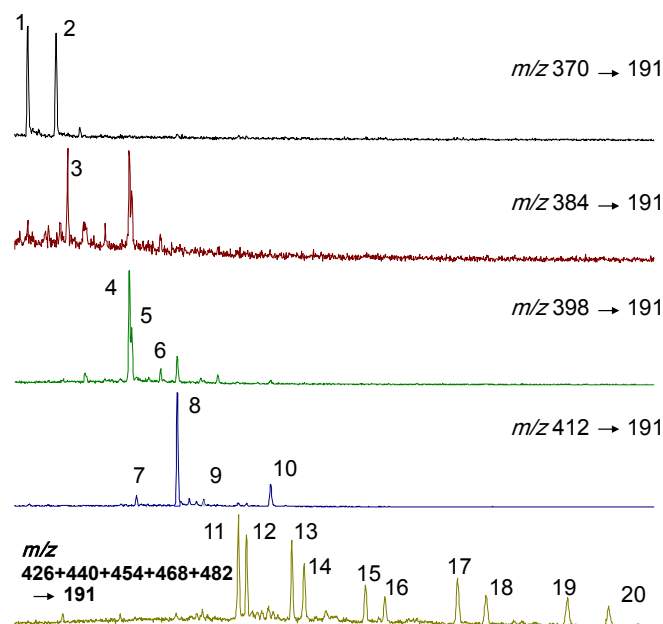


Figure 3.10: Ion chromatograms displaying the distribution of hopanes in the aliphatic fraction determined by GC-MS-MS. Tab.3.11 for peak assignments.

3.3.3 Metastable Reaction Monitoring MRM-GC-MS-MS

GC-MS-MS measurements were applied to the aliphatic fractions for evaluation of saturated biomarker compounds. The saturated hydrocarbon biomarkers were recorded in the Metastable Reaction Monitoring (MRM) mode with a dwell time of 21 ms and an inter dwell time of 20 ms per metastable transition resulting in a scan cycle time of 0.984 s for the detection of 24 metastable transitions. Evaluations of hopanes (m/z 191) and steranes (m/z 217) were carried out using these daughter fragments with corresponding parent ions m/z 370, 384, 398, 412 for hopanes, m/z 372, 386, 400, 414 for steranes, m/z 358 for norcholestanes, and m/z 414 \rightarrow 231 for C_{30} methylsteranes. The evaluation of hopane and sterane distributions of crude oils investigated in this study was carried out by relative abundances of peak areas. Contrary to the light, saturated and aromatic hydrocarbons, which were identified by GC-MS, the total concentrations in $\mu\text{g/g}$ oil were not determined. For hopane and sterane identifications please see (Figures 3.10 to ?? and Tables 3.11 to 3.14).

| Number | Name | Synonym | Mass | Formula |
|--------|---|--------------|------|----------------|
| 1 | 18 α (H)-22,29,30-Trinorneohopane | Ts | 370 | $C_{27}H_{46}$ |
| 2 | 17 α (H)-22,29,30-Trinorhopane | Tm | 370 | $C_{27}H_{46}$ |
| 3 | 17 α (H),21 β (H)-Dinorhopane | Bisnorhopane | 384 | $C_{28}H_{48}$ |
| 4 | 17 α (H),21 β (H)-30-Norhopane | | 398 | $C_{29}H_{50}$ |
| 5 | 18 α (H)-Norneohopane | C_{29} -Ts | 398 | $C_{29}H_{50}$ |
| 6 | 17 β (H),21 α (H) -30- Norhopane | Normoretane | 398 | $C_{29}H_{50}$ |
| 7 | | C_{30} -Ts | 412 | $C_{30}H_{52}$ |
| 8 | 17 α (H),21 β (H)-Hopane | Hopane | 412 | $C_{30}H_{52}$ |
| 9 | 17 β (H),21 α (H)-Hopane | Moretane | 412 | $C_{30}H_{52}$ |
| 10 | Gammacerane | | 412 | $C_{30}H_{52}$ |
| 11 | (22 <i>S</i>)-17 α (H),21 β (H)-29-Homohopane | | 426 | $C_{31}H_{54}$ |
| 12 | (22 <i>R</i>)-17 α (H),21 β (H)-29-Homohopane | | 426 | $C_{31}H_{54}$ |
| 13 | (22 <i>S</i>)-17 α (H),21 β (H)-29-Diomohopane | | 440 | $C_{32}H_{56}$ |
| 14 | (22 <i>R</i>)-17 α (H),21 β (H)-29-Diomohopane | | 440 | $C_{32}H_{56}$ |
| 15 | (22 <i>S</i>)-17 α (H),21 β (H)-29-Triomohopane | | 454 | $C_{33}H_{58}$ |
| 16 | (22 <i>R</i>)-17 α (H),21 β (H)-29-Triomohopane | | 454 | $C_{33}H_{58}$ |
| 17 | (22 <i>S</i>)-17 α (H),21 β (H)-29-Tetraomohopane | | 468 | $C_{34}H_{60}$ |
| 18 | (22 <i>R</i>)-17 α (H),21 β (H)-29-Tetraomohopane | | 468 | $C_{34}H_{60}$ |
| 19 | (22 <i>S</i>)-17 α (H),21 β (H)-29-Pentaomohopane | | 482 | $C_{35}H_{62}$ |
| 20 | (22 <i>R</i>)-17 α (H),21 β (H)-29-Pentaomohopane | | 482 | $C_{35}H_{62}$ |

Table 3.11: Individual hopanes identified in the aliphatic fraction of Syrian crude oil samples analysed by GC-MS-MS.

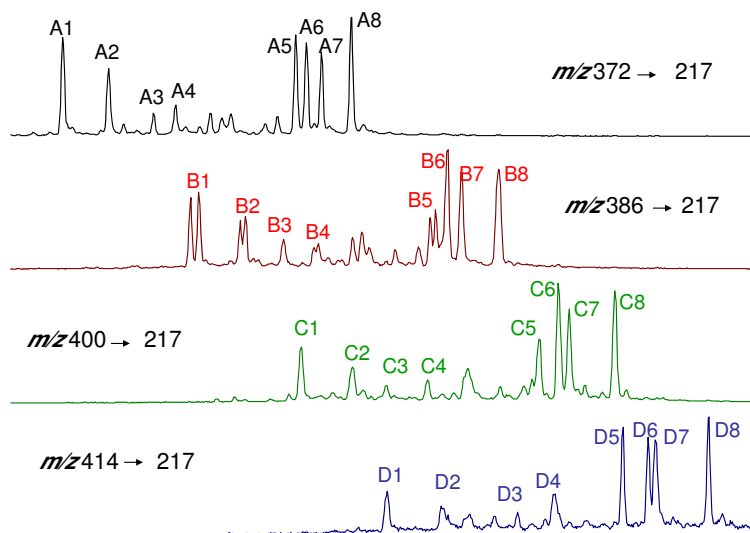


Figure 3.11: Ion chromatogram displaying the distribution of steranes in the aliphatic fraction determined by GC-MS-MS. Tab.3.12 for peak assignments.

| No. | Compound | Configuration | Mass |
|----------------------------------|--|-------------------------------|------|
| <i>C</i> ₂₇ - Sterane | 20 <i>S</i> -13 <i>β</i> (H), 17 <i>α</i> (H)-Diacholestane | <i>β</i> <i>α</i> 20 <i>S</i> | 372 |
| | 20 <i>R</i> -13 <i>β</i> (H), 17 <i>α</i> (H)-Diacholestane | <i>α</i> <i>β</i> 20 <i>R</i> | 372 |
| | 20 <i>R</i> -13 <i>α</i> (H), 17 <i>β</i> (H)-Diacholestane | <i>α</i> <i>β</i> 20 <i>R</i> | 372 |
| | 20 <i>S</i> -13 <i>α</i> (H), 17 <i>β</i> (H)-Diacholestane | <i>α</i> <i>β</i> 20 <i>R</i> | 372 |
| | 20 <i>S</i> -5 <i>α</i> (H), 14 <i>α</i> (H), 17 <i>α</i> (H)-Cholestane | <i>ααα</i> 20 <i>S</i> | 372 |
| | 20 <i>R</i> -5 <i>α</i> (H), 14 <i>β</i> (H), 17 <i>β</i> (H)-Cholestane | <i>αββ</i> 20 <i>R</i> | 372 |
| | 20 <i>S</i> -5 <i>α</i> (H), 14 <i>β</i> (H), 17 <i>β</i> (H)-Cholestane | <i>αββ</i> 20 <i>S</i> | 372 |
| | 20 <i>R</i> -5 <i>α</i> (H), 14 <i>α</i> (H), 17 <i>α</i> (H)-Cholestane | <i>ααα</i> 20 <i>R</i> | 372 |
| <i>C</i> ₂₈ - Sterane | 20 <i>S</i> -24-Methyl-13 <i>β</i> (H), 17 <i>α</i> (H)-Diacholestane | <i>ββ</i> 20 <i>S</i> | 386 |
| | 20 <i>R</i> -24-Methyl-13 <i>β</i> (H), 17 <i>α</i> (H)-Diacholestane | <i>ββ</i> 20 <i>R</i> | 386 |
| | 20 <i>R</i> -24-Methyl-13 <i>α</i> (H), 17 <i>β</i> (H)-Diacholestane | <i>αβ</i> 20 <i>R</i> | 386 |
| | 20 <i>S</i> -24-Methyl-13 <i>α</i> (H), 17 <i>β</i> (H)-Diacholestane | <i>αβ</i> 20 <i>S</i> | 386 |
| | 20 <i>S</i> -24-Methyl-5 <i>α</i> (H), 14 <i>α</i> (H), 17 <i>α</i> (H)-Cholestane | <i>ααα</i> 20 <i>S</i> | 386 |
| | 20 <i>R</i> -24-Methyl-5 <i>α</i> (H), 14 <i>β</i> (H), 17 <i>β</i> (H)-Cholestane | <i>αββ</i> 20 <i>R</i> | 386 |
| | 20 <i>S</i> -24-Methyl-5 <i>α</i> (H), 14 <i>β</i> (H), 17 <i>β</i> (H)-Cholestane | <i>αββ</i> 20 <i>S</i> | 386 |
| | 20 <i>R</i> -24-Methyl-5 <i>α</i> (H), 14 <i>α</i> (H), 17 <i>α</i> (H)-Cholestane | <i>ααα</i> 20 <i>R</i> | 386 |
| <i>C</i> ₂₉ - Sterane | 20 <i>S</i> -24-Ethyl-13 <i>β</i> (H), 17 <i>α</i> (H)-Diacholestane | <i>βα</i> 20 <i>S</i> | 400 |
| | 20 <i>R</i> -24-Ethyl-13 <i>β</i> (H), 17 <i>β</i> (H)-Diacholestane | <i>ββ</i> 20 <i>R</i> | 400 |
| | 20 <i>R</i> -24-Ethyl-13 <i>α</i> (H), 17 <i>β</i> (H)-Diacholestane | <i>αβ</i> 20 <i>R</i> | 400 |
| | 20 <i>S</i> -24-Ethyl-13 <i>α</i> (H), 17 <i>β</i> (H)-Diacholestane | <i>αβ</i> 20 <i>S</i> | 400 |
| | 20 <i>S</i> -24-Ethyl-5 <i>α</i> (H), 14 <i>α</i> (H), 17 <i>α</i> (H)-Cholestane | <i>ααα</i> 20 <i>S</i> | 400 |
| | 20 <i>R</i> -24-Ethyl-5 <i>α</i> (H), 14 <i>β</i> (H), 17 <i>β</i> (H)-Cholestane | <i>αββ</i> 20 <i>R</i> | 400 |
| | 20 <i>S</i> -24-Ethyl-5 <i>α</i> (H), 14 <i>β</i> (H), 17 <i>β</i> (H)-Cholestane | <i>αββ</i> 20 <i>S</i> | 400 |
| | 20 <i>R</i> -24-Ethyl-5 <i>α</i> (H), 14 <i>α</i> (H), 17 <i>α</i> (H)-Cholestane | <i>αα α</i> 20 <i>R</i> | 400 |
| <i>C</i> ₃₀ - Sterane | 20 <i>S</i> -24-Propyl-13 <i>β</i> (H), 17 <i>α</i> (H)-Diacholestane | <i>βα</i> 20 <i>S</i> | 414 |
| | 20 <i>R</i> -24-Propyl-13 <i>β</i> (H), 17 <i>α</i> (H)-Diacholestane | <i>βα</i> 20 <i>R</i> | 414 |
| | 20 <i>R</i> -24-Propyl-13 <i>α</i> (H), 17 <i>β</i> (H)-Diacholestane | <i>αβ</i> 20 <i>R</i> | 414 |
| | 20 <i>S</i> -24-Propyl-13 <i>α</i> (H), 17 <i>β</i> (H)-Diacholestane | <i>αβ</i> 20 <i>S</i> | 414 |
| | 20 <i>S</i> -24-Propyl-5 <i>α</i> 14 <i>α</i> (H), 17 <i>α</i> (H)-Cholestane | <i>ααα</i> 20 <i>S</i> | 414 |
| | 20 <i>R</i> -24-Propyl-5 <i>α</i> (H), 14 <i>β</i> (H), 17 <i>β</i> (H)-Cholestane | <i>αββ</i> 20 <i>R</i> | 414 |
| | 20 <i>S</i> -24-Propyl-5 <i>α</i> (H), 14 <i>β</i> (H), 17 <i>β</i> (H)-Cholestane | <i>αββ</i> 20 <i>S</i> | 414 |
| | 20 <i>R</i> -24-Propyl-5 <i>α</i> (H), 14 <i>α</i> (H), 17 <i>α</i> (H)-Cholestane | <i>ααα</i> 20 <i>R</i> | 414 |

Table 3.12: Identified steranes in the aliphatic fraction of Syrian crude oil samples analysed by GC-MS-MS.

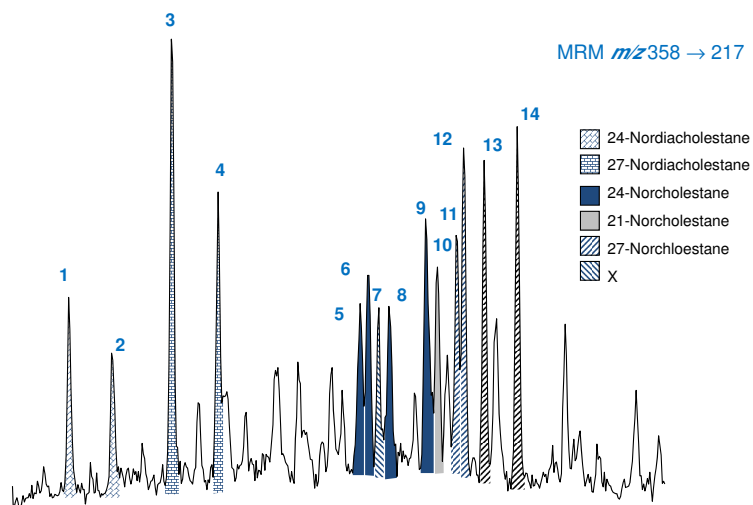


Figure 3.12: Ion chromatogram displaying the distribution of 21-, 24-, 27-norcholestanes and 24-, 27-nordiacholestanes in the aliphatic fraction analysed by GC-MS-MS. Tab.3.13 for peak assignments.

| Compound | Configuration | Peak Nr. |
|---------------------|---|----------|
| 24-Nordiacholestane | A | 1 |
| | B | 2 |
| 27-Nordiacholestane | A | 3 |
| | B | 4 |
| 24-Norcholestane | $\alpha\alpha\alpha$ -20 <i>S</i> | 5 |
| | $\alpha\beta\beta$ -20 <i>R</i> | 6 |
| | X | 7 |
| | $\alpha\beta\beta$ -20 <i>S</i> | 8 |
| 21-Norcholestane | $\alpha\alpha\alpha$ -20 <i>R</i> | 9 |
| | $\alpha\alpha\alpha$ + $\alpha\beta\beta$ | 10 |
| 27-Norcholestane | $\alpha\alpha\alpha$ -20 <i>S</i> | 11 |
| | $\alpha\beta\beta$ -20 <i>R</i> | 12 |
| | $\alpha\beta\beta$ -20 <i>S</i> | 13 |
| | $\alpha\alpha\alpha$ -20 <i>R</i> | 14 |

Table 3.13: Nor- and nordiacholestanes identified in Syrian crude oil samples.

| Peak Nr. | Compound |
|----------|--|
| 1 | 2 α -methyl-24-ethylcholestane 20 <i>S</i> |
| 2 | 3 β -methyl-24-ethylcholestane 20 <i>S</i> |
| 3 | 2 α -methyl-24-ethylcholestane 14 β ,17 α (H) 20 <i>R</i> |
| 4 | 2 α -methyl-24-ethylcholestane 14 β ,17 α (H) 20 <i>S</i> |
| 5 | 3 β -methyl-24-ethylcholestane 14 β ,17 α (H) 20 <i>R</i> |
| 6 | 3 β -methyl-24-ethylcholestane 14 β ,17 α (H) 20 <i>S</i> |
| 7 | 4 α -methyl-24-ethylcholestane 20 <i>S</i> |
| 8 | 4 α -methyl-24-ethylcholestane 14 β ,17 β (H) 20 <i>R</i> |
| 9 | 2 β -methyl-24-ethylcholestane 20 <i>R</i> + 4 α -methyl-24-ethylsterane 14 β ,17 β (H) 20 <i>S</i> |
| 10 | 3 β -methyl-24-ethylcholestane 20 <i>R</i> |

Table 3.14: C_{30} methylsteranes identified in Syrian crude oil samples by MRM GC-MS-MS.

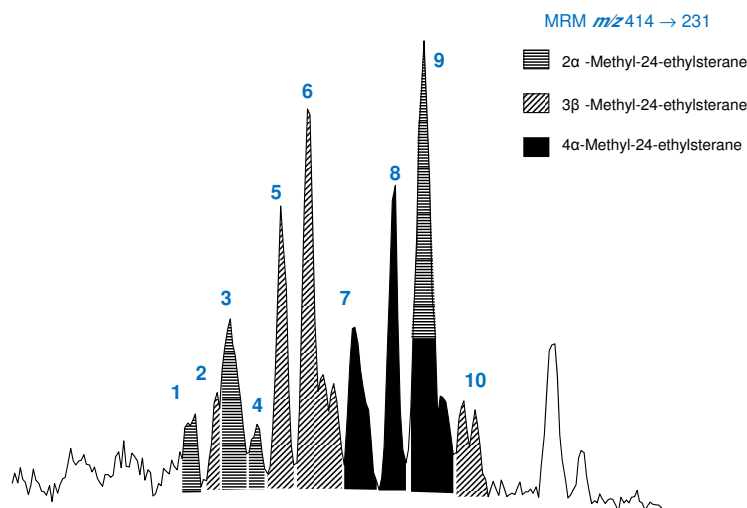


Figure 3.13: Ion chromatogram displaying the distribution of C_{30} methylsteranes. Tab.3.14 for peak assignments.

Chapter 4

Results

In this chapter, a description of the main geochemical parameters used in this study is presented. These biomarkers (i.e. aliphatic and aromatic hydrocarbons), non-biomarkers (like light hydrocarbons and diamondoids) and stable isotope signatures are obtained by performing series of geochemical analyses as described in the previous chapter (Chapter.3). Additionally, some general readings of these data in terms of depositional environment, source facies and thermal maturity will be presented to better recognize and figure out what kind of oil samples are studied.

4.1 Oil Samples

Petroleum geochemistry is an essential tool in order to understand the chemical composition of oil and gas and its variation in petroleum producing areas. The bulk geochemical and biomarker characteristics act as a "fingerprint" for oil, which may be used to characterize the oil families (oil-oil correlation) in an exploration area and to identify their possible associated source rocks.

4.1.1 Bulk Properties

The analysis of bulk properties [gross composition, API gravity, sulfur content and trace metal contents (i.e. vanadium and nickel)] of an oil yields

important information regarding the causes of oil quality variations. These data have been made available for this study by industry partners: Shell International E&P and Al Furat Petroleum Company AFPC.

- API Gravity:

API gravity is a physical property expressing the density of liquid petroleum and used to classify the crude oils into heavy or light (Tissot & Welte, 1984). API gravity values were available only for thirty oil samples and listed in Tab.4.1. Most of the samples have API gravity values above 30° and can be considered as light oils. G002980, G002982, and G002954 are the lightest samples as they have the highest values (API gravity = 58° , 49° and 43° , respectively) which might be due their high maturity level. Low API gravity (12° - 25°) of heavy oils (G002993, G002998; G003011, G003005, and G002978) could be as a result of secondary alteration processes or generation from immature source rocks (Hunt, 1996).

- Sulfur Content:

Sulfur content is another bulk property of a crude oil which reflects its quality and/or the origin (Peters *et al.*, 2005). As the average content of sulfur in crude oils is 0.65 % , low sulfur crude oils contain < 1 % of sulfur; however, oils with more than 1 % sulfur are high sulfur crude oils (Tissot & Welte, 1984). The oil samples show a range of sulfur content between 0 and 2.7 % with most of them < 1 % of weight sulfur (Tab.4.1). All oils from Miocene reservoirs have high sulfur content ranging from 1.1 % to 2.2 % which could be a result of secondary alteration processes (biodegradation). Biodegradation leads to an increase in the sulfur content in crude oils due to the preferential removal of saturated hydrocarbons (Hunt, 1996). In addition, the API gravity of oils varies inversely with the sulfur content, where crude oils greater than 1 wt.% in sulfur generally have remarkably low API gravity (12° - 20°) (see Fig.4.1). The oil sample from Cretaceous

| Number | Reservoir | API | Sat % | Arom % | NSO % | S (%) | V (ppm) | N (ppm) | sat/arom |
|---------|-----------------|-----|-------|--------|-------|-------|---------|---------|----------|
| G002953 | Rutbah | 37 | 62,90 | 26,60 | 10,50 | 0,17 | 0,09 | 0,57 | 2,36 |
| G002954 | Post Judea Sand | 43 | 77,00 | 19,00 | 4,00 | 0,60 | 0,00 | 0,00 | 4,05 |
| G002960 | Erek | 34 | 49,00 | 42,00 | 9,00 | 0,60 | 3,00 | 3,00 | 1,17 |
| G002961 | Derro | 35 | 42,00 | 46,00 | 12,00 | 1,10 | 10,00 | 7,00 | 0,91 |
| G002962 | L. Rutbah | 39 | 70,00 | 27,00 | 3,00 | 0,20 | 0,00 | 0,00 | 2,59 |
| G002964 | Post Judea Sand | 34 | 42,00 | 41,00 | 17,00 | 1,10 | 13,00 | 11,00 | 1,02 |
| G002966 | Lower Rutbah | 38 | 72,00 | 25,00 | 3,00 | 0,20 | 0,00 | 0,00 | 2,88 |
| G002967 | Post Judea Sand | 33 | 45,00 | 43,00 | 12,00 | 0,90 | 13,00 | 9,00 | 1,05 |
| G002968 | Lower Doubayat | 36 | 59,00 | 35,00 | 6,00 | 0,30 | 1,00 | 1,00 | 1,69 |
| G002969 | Mulussa F | 35 | 58,00 | 34,00 | 8,00 | 0,40 | 2,00 | 3,00 | 1,71 |
| G002970 | L. Rutbah | 33 | 53,00 | 37,00 | 10,00 | 0,60 | 11,00 | 6,00 | 1,43 |
| G002973 | L. Shiranish | 35 | 58,00 | 34,00 | 8,00 | 0,20 | 1,00 | 2,00 | 1,71 |
| G002975 | ICD | 37 | 58,00 | 35,00 | 7,00 | 0,30 | 3,00 | 2,00 | 1,66 |
| G002976 | U. Shiranish | 42 | 58,00 | 36,00 | 6,00 | 0,40 | 0,00 | 0,00 | 1,61 |
| G002978 | Mulussa D | 19 | 22,00 | 42,00 | 36,00 | 2,20 | 51,00 | 53,00 | 0,52 |
| G002979 | Mulussa F | 45 | 67,00 | 30,00 | 3,00 | 0,30 | 4,00 | 0,00 | 2,23 |
| G002980 | Rutbah | 58 | n.d | n.d | n.d | 0,10 | 0,00 | 0,00 | n.d |
| G002981 | Khabour | 30 | 57,00 | 35,00 | 8,00 | 0,60 | 1,00 | 6,00 | 1,63 |
| G002982 | U. Doubayat | 49 | 77,00 | 23,00 | 0,00 | 0,00 | 0,00 | 0,00 | 3,35 |
| G002993 | L.Fars / Jeribe | 27 | 41,80 | 37,60 | 20,60 | 1,80 | 15,00 | 54,00 | 1,11 |
| G002995 | R'mah | 35 | n.d | n.d | n.d | 0,58 | 2,90 | 4,40 | n.d |
| G002998 | Euphrates | 20 | 30,20 | 43,80 | 26,00 | 2,20 | 7,60 | 9,30 | 0,69 |
| G002999 | R'mah | 41 | n.d | n.d | n.d | n.d | n.d | n.d | n.d |
| G003001 | Dhiban | 35 | n.d | n.d | n.d | 1,40 | n.d | n.d | n.d |
| G003005 | U. Shiranish | 21 | 23,80 | 43,50 | 32,70 | 2,70 | 67,00 | 75,00 | 0,55 |
| G003006 | Kometan | 40 | n.d | n.d | n.d | 0,50 | n.d | n.d | n.d |
| G003009 | Rutbah | 37 | 62,10 | 33,70 | 4,20 | 0,61 | 0,56 | 0,48 | 1,84 |
| G003011 | Dhiban | 12 | n.d | n.d | n.d | 1,60 | n.d | n.d | n.d |
| G003013 | Erek | n.d | n.d | n.d | n.d | 0,90 | 7,30 | 8,10 | n.d |
| G003014 | U. Shiranish | n.d | 58,5 | 31,20 | 10,3 | n.d | 4,10 | 9,2 | 1,88 |

Table 4.1: Bulk geochemical composition for a suite of Syrian oil samples. where: Sat % = percent saturated hydrocarbons, Arom % = percent aromatic hydrocarbons, NSO % = percent hetero compounds (resins and asphaltenes), S % = percent sulfur content, V (ppm) = vanadium concentration [part per million], N (ppm) = nickel concentration [part per million], sat/arom = saturate to aromatic hydrocarbon ratio.

reservoirs (G003005) has the highest value of sulfur content with an API gravity value of 21°.

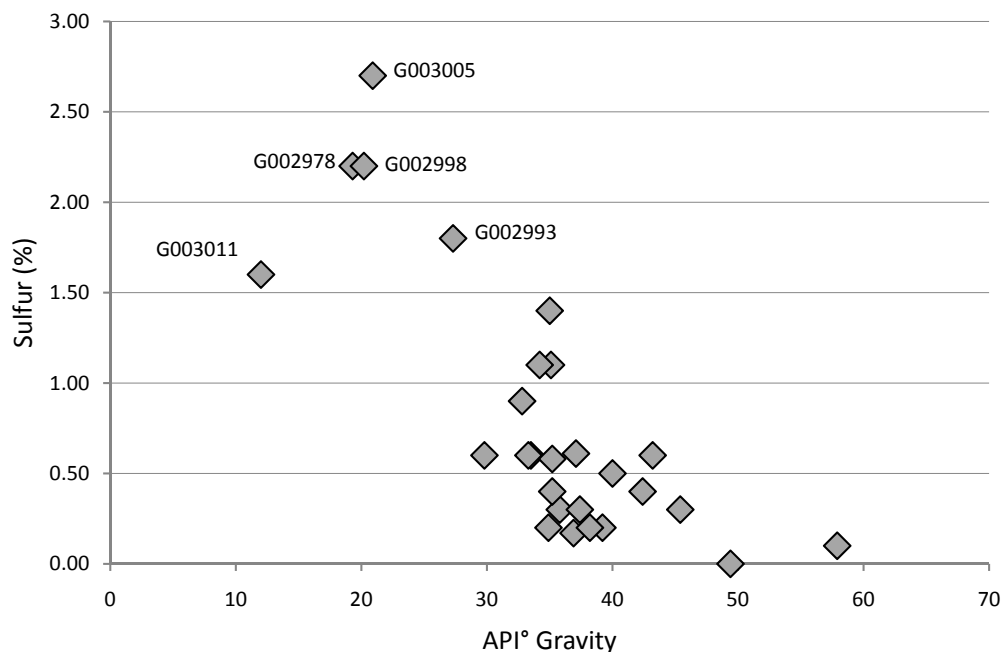


Figure 4.1: Percent of sulfur versus API gravity for selected oil samples from the study area.

- Trace Elements (vanadium and nickel content): At the time of deposition, the chlorophyll molecule loses its magnesium. Vanadium and nickel atoms are incorporated to the porphyrin in the place of magnesium during diagenesis (Tissot & Welte, 1984). These metals exist in petroleum in a wide range of concentrations from 1 to 1200 ppm. The relative stability of vanadium over nickel causes its relative dominance in marine oils (Lewan, 1984). In most cases, crude oils with high sulfur content are also enriched in vanadium and nickel metals (Hunt, 1996). Fig.4.2 shows that the oil samples with high vanadium content are also high in nickel content (G002978, G002993, and G003005). Increasing contents of these trace metals correspond with an increase in sulfur content (1.8% - 2.7%) and decrease in API gravity (19° - 27°) (see Fig.4.3) which might be interpreted as a result of a light to moderate biodegradation effect (Peters *et al.*, 2005).
- Saturated and Aromatic Hydrocarbon Composition:

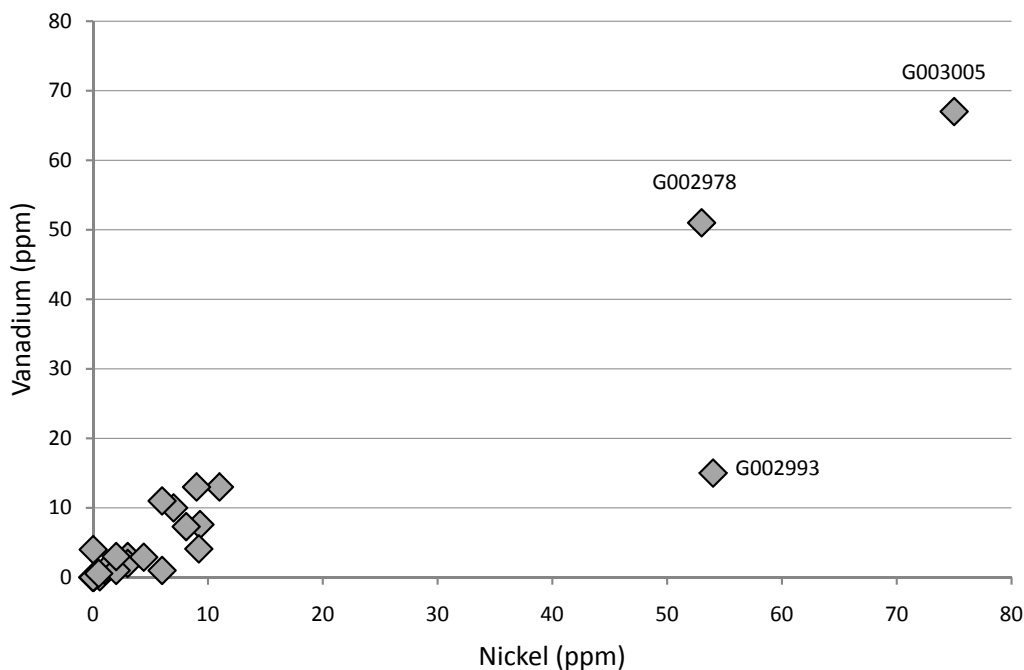


Figure 4.2: Cross plot showing nickel and vanadium concentrations for some Syrian oils. G002978, G002993, and G003005 have the highest V and N contents.

The oil samples are commonly enriched in saturated hydrocarbons. Almost all of the samples have saturated hydrocarbon contents in the range of 42% - 77% (Tab.4.1). Samples G002998, G003005, and G002978 depart significantly from the general tendency (see Fig.4.4) by having a saturate portion of only 30.2%, 23.8% and 22.0%, respectively, which can be interpreted as the influence of in reservoir biodegradation (Tissot & Welte, 1984). The aromatic hydrocarbon content of the oil samples reflects the same trend; it ranges from 19% to 46%. The ratio of saturates to aromatics is over 1 in all oil samples except three crude oils (namely G003005, G002998, and G002978). The proportion of NSO compounds is the highest (over 26.0%) for these three latter oil samples (Tab.4.1). In this context these oils are considered as the heaviest in the sample set.

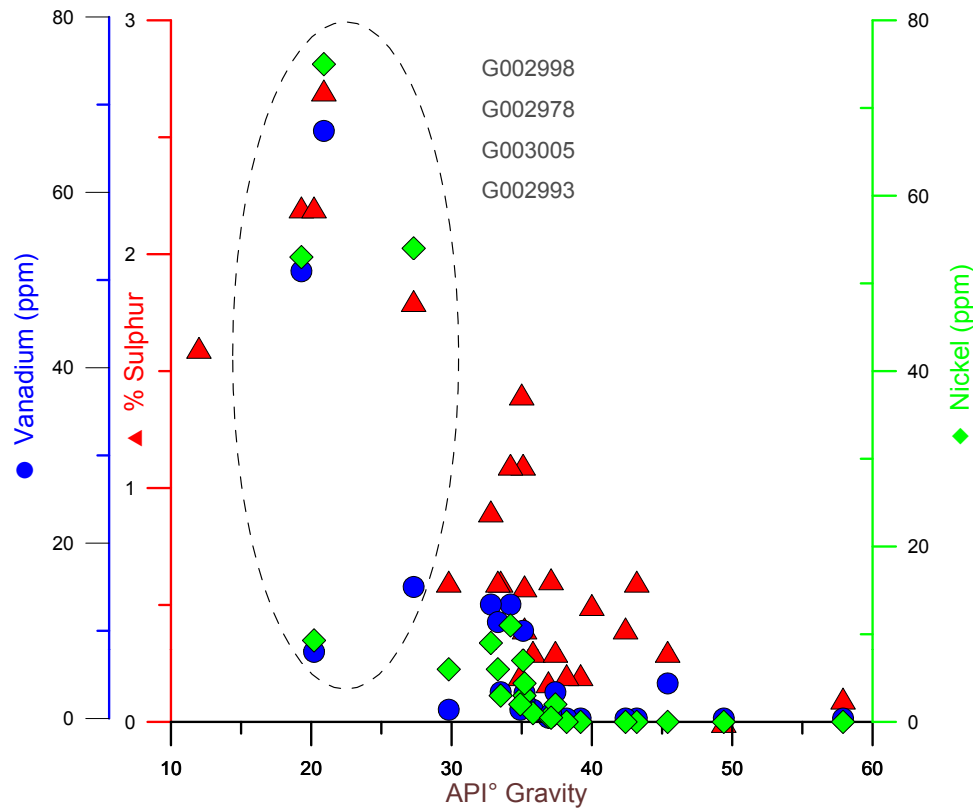


Figure 4.3: Bulk oil properties comparison for Syrian oil samples. API gravity decreases proportionally with increasing sulfur, vanadium, and nickel content.

Recap:

Bulk parameters of crude oils showed different type of crude oils found in the Euphrates Graben. G002980, G002982, and G002954 are the lightest in the available data set as they have relatively high API gravities $> 43^\circ$, which could indicate a highly mature source rock. Alteration processes could have an effect on crude oils in the northwestern part of the study area that are found in shallow Miocene reservoirs. These oils have a high content of sulfur, nickel, and vanadium and are the lowest in API gravity.

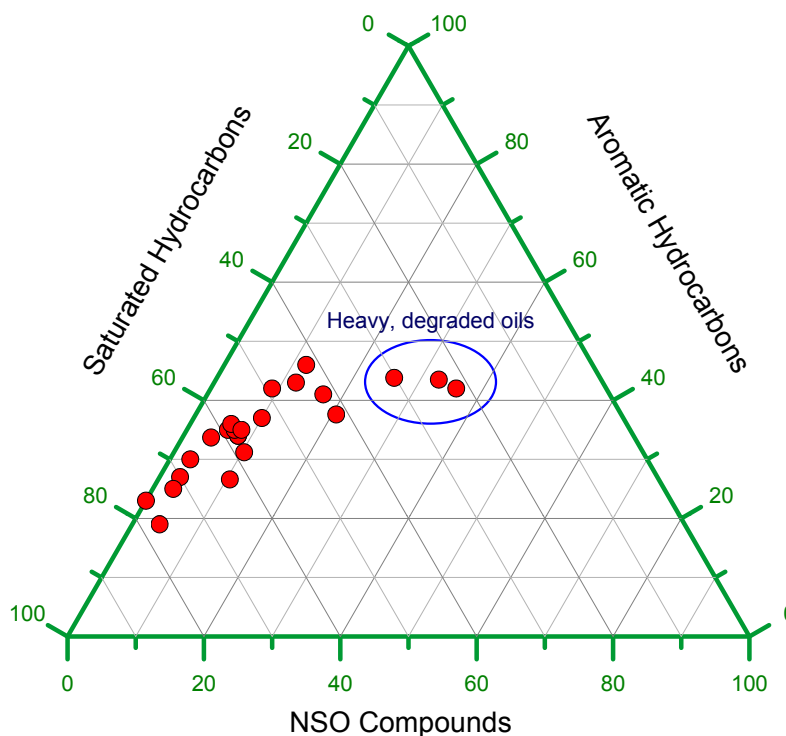


Figure 4.4: Ternary diagram showing gross composition of oil samples.

4.1.2 Molecular Composition

The molecular composition of crude oils is represented not only by light and saturated hydrocarbons but also by branched alkanes and acyclic isoprenoids which are measured by gas chromatography.

- Normal Alkanes:

The whole-oil gas chromatograms show a full range of *n*-alkanes from *n*-C₅ to *n*-C₃₇ for most of the analysed oil samples (Appendix.A).

GC fingerprints can differentiate oils because of their different origins, or because they have experienced different histories during migration and/or in the reservoir (Peters & Moldowan, 1993). Fig.4.5 shows gas chromatograms for two crude oils (G002954 and G002995) from the study area. These two oils seem to be unrelated looking at the different distribution of *n*-paraffins and isoprenoids which could be attributed to different source rocks and organic matter types. However, both non-waxy oils give the impression to be generated mainly from marine

source rocks as they do not have a dominant sequence of heavy n -alkanes.

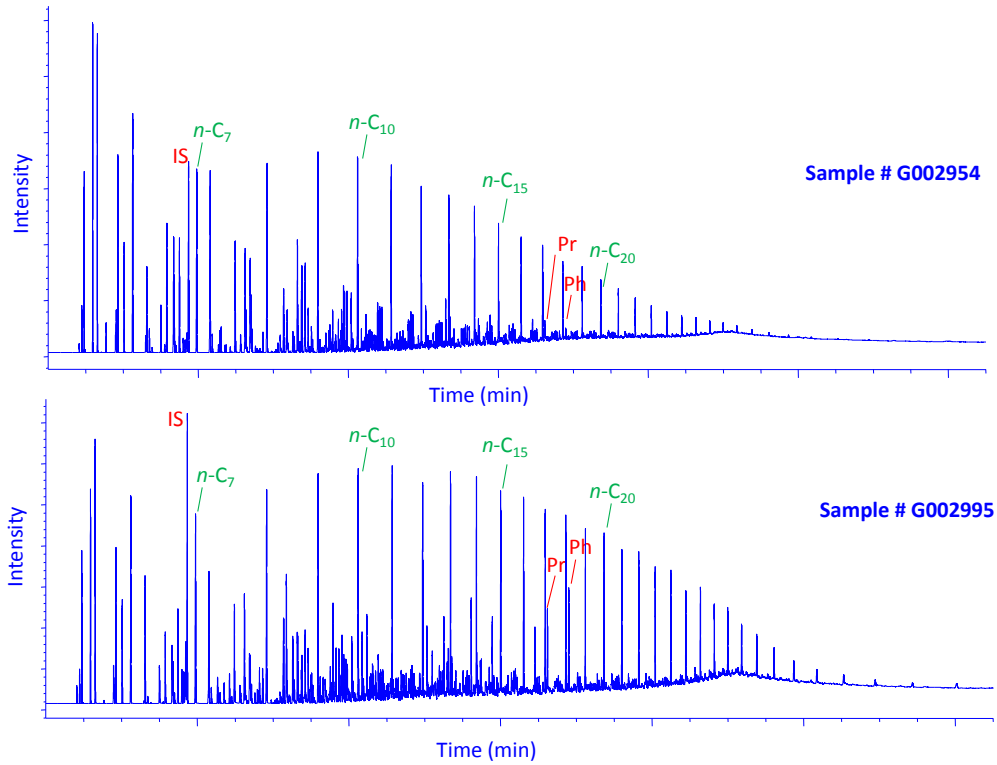


Figure 4.5: GC fingerprints for two oils from the study area. The dissimilarity can probably be attributed to different sources.

G002954 consists dominantly of low molecular weight n -alkanes ($<n-C_{20}$) with no apparent carbon number preference. Although G002995 is also dominated by light homologues, the relative amounts of higher molecular weight hydrocarbons ($>n-C_{20}$) are much higher. In addition, these n -alkanes display an even over odd carbon preference (CPI = 0.88, Tab.4.2) in the $n-C_{22}$ - $n-C_{32}$ range, a feature common to many oils originating from carbonate source rocks (Tissot & Welte, 1984).

The light hydrocarbon preference index (LHCPI) also reflects the relative dominance of short-chain over long-chain hydrocarbons as it is calculated as follows:

$$\text{LHCPI} = [n-C_{17} + n-C_{18} + n-C_{19}] / [n-C_{27} + n-C_{28} + n-C_{29}]$$

In this framework, this parameter gives an indication to the maturation level of crude oils and source rocks as well. By increasing the

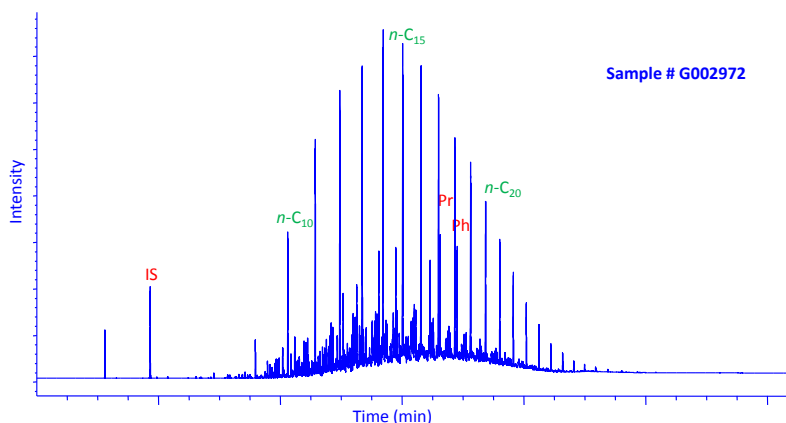


Figure 4.6: Crude oil sample (G002972) showed fewer gasoline range components, compared to the rest of the data set. This may be an indication of evaporative loss of the lighter ends during storage.

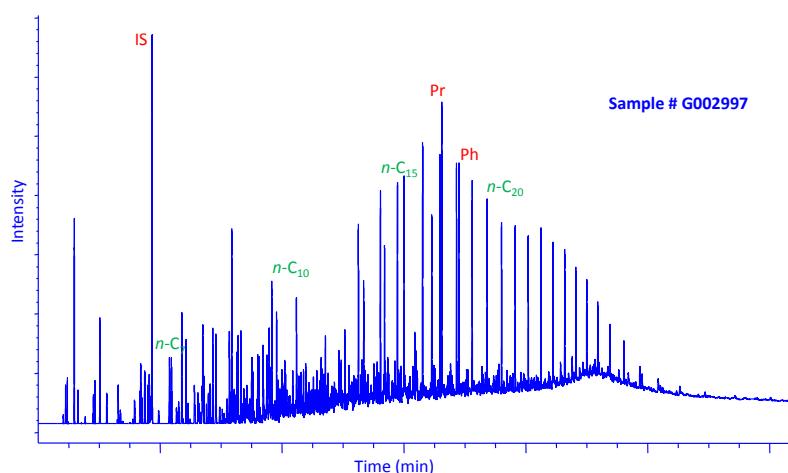


Figure 4.7: GC profile of G002997 oil sample showing loss in *n*-alkanes with a large hump of unresolved components giving them the appearance of biodegraded oils.

maturity, LHCPI values should increase as the thermal cracking of heavy compounds into smaller ones will progressively occur (Fig.4.8). For the previous two oil samples, it is obvious that the G002954 is more mature than G002995 (LHCPI=8.40 and 2.59, respectively; Tab.4.2). Some oils have lost most light compounds in front until $n\text{-C}_8$ (e.g. G002972, Fig.4.6). This deltoid *n*-alkanes distribution pattern could be attributed to evaporation processes due to storage conditions. The profiles for some samples (G002997, G002993, and G002998) are significantly different showing losses in *n*-alkanes with a large hump of

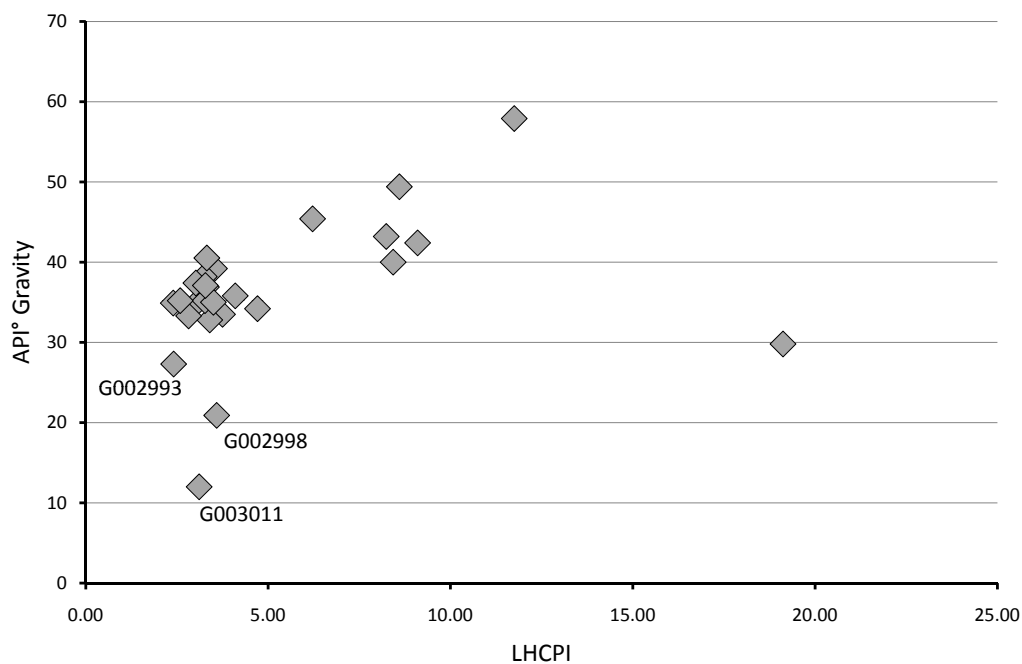


Figure 4.8: Cross plot showing that LHCPI values increase with increasing maturity.

unresolved components giving them the appearance of biodegraded oils (Fig.4.7).

| Sample | Pr/Ph | Pr/ <i>n</i> -C ₁₇ | Ph/ <i>n</i> -C ₁₈ | F | B | I | H | CPI | LHCPI |
|----------------|-------|-------------------------------|-------------------------------|------|------|------|-------|------|-------|
| G002952 | 1,56 | 0,35 | 0,27 | 1,35 | 0,27 | 4,82 | 30,58 | 0,93 | 13,80 |
| G002953 | 1,21 | 0,78 | 0,67 | 0,67 | 0,31 | 0,50 | 18,60 | 0,96 | 3,31 |
| G002954 | 1,84 | 0,30 | 0,19 | 0,97 | 0,62 | 4,69 | 24,47 | 0,97 | 8,24 |
| G002955 | 1,07 | 0,65 | 0,63 | 0,88 | 0,41 | 0,71 | 22,02 | 0,93 | 3,06 |
| G002956 | 1,10 | 0,62 | 0,62 | 1,07 | 0,42 | 0,93 | 24,41 | 0,93 | 3,07 |
| G002957 | 1,02 | 0,54 | 0,58 | 1,26 | 0,40 | 1,23 | 26,93 | 0,93 | 3,33 |
| G002958 | 1,13 | 0,81 | 0,81 | 0,82 | 0,39 | 0,37 | 18,41 | 0,96 | 2,88 |
| G002959 | 1,68 | 0,27 | 0,19 | 0,82 | 0,04 | 8,17 | 19,39 | 1,05 | 7,81 |
| G002960 | 0,90 | 0,37 | 0,45 | 1,40 | 0,50 | 2,67 | 33,49 | 0,91 | 3,75 |
| G002961 | 0,73 | 0,38 | 0,56 | 2,11 | 0,25 | 2,71 | 35,31 | 0,90 | 3,08 |
| G002962 | 1,04 | 0,55 | 0,59 | 1,11 | 0,59 | 0,85 | 26,81 | 0,95 | 3,53 |
| G002963 | 0,92 | 0,51 | 0,61 | 1,39 | 0,71 | 1,58 | 30,71 | 0,94 | 3,45 |
| G002964 | 0,75 | 0,46 | 0,66 | 1,38 | 0,21 | 2,97 | 30,98 | 0,88 | 4,71 |
| G002965 | 1,07 | 0,55 | 0,57 | 1,12 | 0,57 | 0,85 | 26,45 | 0,97 | 3,28 |
| G002966 | 0,86 | 0,54 | 0,68 | 1,37 | 0,47 | 1,08 | 29,58 | 0,95 | 3,25 |
| G002967 | 0,72 | 0,58 | 0,86 | 1,53 | 0,29 | 1,43 | 29,67 | 0,90 | 3,40 |

Continued on next page

Table 4.2 – continued from previous page

| Sample | Pr/Ph | Pr/ <i>n</i> -C ₁₇ | Ph/ <i>n</i> -C ₁₈ | F | B | I | H | CPI | LHCPI |
|---------|-------|-------------------------------|-------------------------------|------|------|------|-------|------|-------|
| G002968 | 0,97 | 0,47 | 0,55 | 1,02 | 0,21 | 1,51 | 28,80 | 0,94 | 4,10 |
| G002969 | 0,97 | 0,59 | 0,67 | 1,10 | 0,48 | 0,96 | 25,97 | 0,94 | 3,27 |
| G002970 | 0,73 | 0,62 | 0,88 | 1,47 | 0,26 | 1,17 | 28,85 | 0,87 | 2,82 |
| G002971 | 1,11 | 0,50 | 0,52 | 1,19 | 0,76 | 1,25 | 27,95 | 0,99 | 3,86 |
| G002972 | 1,05 | 0,47 | 0,55 | | | | | 0,89 | |
| G002973 | 1,24 | 0,81 | 0,72 | 0,74 | 0,36 | 0,56 | 19,21 | 0,95 | 2,40 |
| G002974 | 0,79 | 0,32 | 0,47 | 1,45 | 0,50 | 2,47 | 32,33 | 0,93 | 3,57 |
| G002975 | 0,96 | 0,43 | 0,48 | 1,24 | 0,29 | 1,87 | 31,05 | 0,93 | 3,02 |
| G002976 | 0,78 | 0,42 | 0,51 | 1,65 | 0,33 | 1,00 | 32,91 | 0,96 | 9,10 |
| G002977 | 0,81 | 0,53 | 0,71 | 1,47 | 0,39 | 2,00 | 31,55 | 0,87 | 3,00 |
| G002979 | 1,22 | 0,33 | 0,31 | 1,23 | 0,30 | 4,38 | 28,94 | 0,94 | 6,22 |
| G002980 | 1,43 | 0,35 | 0,29 | 1,30 | 0,23 | 4,87 | 28,97 | 0,94 | 11,75 |
| G002981 | 0,91 | 0,46 | 0,58 | | | | | 0,89 | 19,12 |
| G002982 | 1,70 | 0,27 | 0,19 | 1,55 | 0,38 | 3,75 | 34,06 | 0,97 | 8,60 |
| G002983 | 1,52 | 0,51 | 0,38 | 0,31 | 0,08 | 1,79 | 8,85 | 0,98 | 3,96 |
| G002984 | 1,00 | 0,52 | 0,57 | 1,18 | 0,90 | 1,43 | 29,46 | 0,94 | 3,58 |
| G002985 | 1,17 | 0,69 | 0,65 | 0,75 | 0,53 | 0,64 | 22,44 | 0,93 | 3,09 |
| G002986 | 0,93 | 0,56 | 0,64 | 1,04 | 0,52 | 1,07 | 26,14 | 0,93 | 3,25 |
| G002987 | 0,80 | 0,46 | 0,59 | 1,35 | 0,23 | 2,17 | 31,38 | 0,91 | 3,00 |
| G002988 | 1,37 | 0,51 | 0,41 | 0,25 | 0,09 | 1,77 | 7,11 | 0,98 | 3,65 |
| G002989 | 1,40 | 0,49 | 0,39 | 0,35 | 0,08 | 1,85 | 10,56 | 0,97 | 2,57 |
| G002990 | 0,70 | 0,59 | 0,87 | 1,20 | 0,32 | 1,30 | 25,16 | 0,88 | 2,34 |
| G002992 | 1,24 | 0,80 | 0,71 | 0,27 | 0,12 | 0,88 | 4,87 | 0,96 | 3,41 |
| G002993 | 1,27 | 1,40 | 1,15 | 0,25 | 0,15 | 0,59 | 6,20 | 1,04 | 2,41 |
| G002994 | 1,25 | 0,79 | 0,71 | 0,14 | 0,15 | 0,73 | 3,51 | 0,99 | 2,50 |
| G002995 | 0,83 | 0,54 | 0,72 | 1,32 | 0,56 | 1,11 | 27,62 | 0,88 | 2,59 |
| G002996 | 0,85 | 0,57 | 0,73 | 1,30 | 0,57 | 1,13 | 28,07 | 0,92 | 3,13 |
| G002997 | 1,30 | 1,57 | 1,22 | 0,15 | 0,36 | 0,70 | 3,68 | 1,03 | 2,50 |
| G002998 | 1,22 | 2,09 | 2,49 | | | | | | |
| G002999 | 1,00 | 0,63 | 0,72 | 1,26 | 0,51 | 0,78 | 25,14 | 0,96 | 3,32 |
| G003000 | 1,02 | 0,56 | 0,61 | 1,19 | 0,09 | 0,95 | 27,39 | 0,94 | 2,97 |
| G003001 | 1,10 | 0,67 | 0,69 | 0,58 | 0,38 | 0,57 | 14,84 | 0,97 | 3,50 |
| G003002 | 1,26 | 0,81 | 0,72 | 0,68 | 0,30 | 0,50 | 18,65 | 0,98 | 2,91 |
| G003003 | 1,09 | 0,52 | 0,57 | 1,09 | 0,51 | 0,93 | 27,18 | 0,90 | 6,13 |
| G003004 | 1,33 | 0,76 | 0,64 | 0,20 | 0,05 | 0,46 | 5,46 | 0,99 | 2,61 |

Continued on next page

Table 4.2 – continued from previous page

| Sample | Pr/Ph | Pr/ <i>n</i> -C ₁₇ | Ph/ <i>n</i> -C ₁₈ | F | B | I | H | CPI | LHCPI |
|---------|-------|-------------------------------|-------------------------------|------|------|------|-------|------|-------|
| G003005 | 0,93 | 0,60 | 0,73 | 1,20 | 0,57 | 0,76 | 27,49 | 0,96 | 3,59 |
| G003006 | 0,98 | 0,53 | 0,64 | 1,35 | 0,64 | 0,73 | 25,52 | 0,90 | 8,43 |
| G003007 | 0,87 | 0,62 | 0,80 | 1,33 | 0,63 | 0,71 | 25,55 | 0,93 | 5,62 |
| G003008 | 0,98 | 0,54 | 0,64 | 1,40 | 0,65 | 0,71 | 25,97 | 0,94 | 7,80 |
| G003009 | 0,78 | 0,38 | 0,52 | 1,84 | 0,22 | 2,17 | 35,35 | 0,93 | 3,28 |
| G003011 | 1,33 | 0,94 | 0,81 | 0,56 | 0,22 | 0,31 | 13,32 | 0,95 | 3,11 |
| G003013 | 0,70 | 0,38 | 0,57 | 1,25 | 0,04 | 1,31 | 32,74 | 0,93 | 2,69 |
| G003014 | 1,01 | 0,48 | 0,57 | 0,86 | 0,51 | 0,71 | 24,83 | 0,91 | 10,64 |
| G003015 | 1,04 | 0,57 | 0,61 | 0,89 | 0,40 | 0,79 | 23,16 | 0,96 | 3,15 |
| G003017 | 0,68 | 0,38 | 0,57 | 1,12 | 0,02 | 1,20 | 29,86 | 0,94 | 2,39 |
| G003020 | 0,98 | 0,40 | 0,45 | 1,14 | 0,17 | 3,15 | 27,38 | 0,93 | 7,30 |
| G003105 | 0,80 | 0,34 | 0,48 | 1,88 | 0,34 | 2,85 | 33,85 | 0,94 | 4,00 |
| G003106 | 1,74 | 0,29 | 0,20 | 1,88 | 0,21 | 3,75 | 37,01 | 0,97 | 6,37 |
| G003107 | 1,15 | 0,34 | 0,33 | 1,47 | 0,28 | 2,59 | 36,01 | 0,97 | 4,71 |
| G003108 | 1,09 | 0,56 | 0,57 | 1,02 | 0,52 | 0,86 | 25,64 | 0,96 | 3,02 |
| G003109 | 1,04 | 0,57 | 0,60 | 1,12 | 0,50 | 0,86 | 26,77 | 0,96 | 2,83 |
| G003110 | 1,07 | 0,54 | 0,57 | 1,04 | 0,71 | 0,82 | 29,58 | 0,96 | 3,35 |
| G003111 | 0,95 | 0,43 | 0,53 | | | | | 0,92 | 12,88 |
| G003112 | 1,16 | 0,64 | 0,62 | 0,77 | 0,51 | 0,65 | 21,90 | 0,96 | 3,30 |
| G003113 | 1,03 | 0,53 | 0,58 | 0,69 | 0,54 | 0,60 | 21,83 | 0,95 | 5,60 |
| G003114 | 0,86 | 0,57 | 0,73 | 1,31 | 0,32 | 0,71 | 24,95 | 0,89 | 4,58 |
| G003116 | 1,17 | 0,67 | 0,62 | 0,33 | 0,25 | 0,59 | 8,03 | 0,95 | 2,63 |
| G003117 | 1,01 | 0,56 | 0,60 | 1,07 | 0,43 | 0,81 | 25,30 | 0,91 | 3,55 |

Table 4.2: Light hydrocarbon parameters. Pr/Ph = pristane over phytane ratio; Pr/*n*-C₁₇ = pristane over heptadecane ratio; Ph/*n*-C₁₈ = phytane over octadecane ratio; F (paraffinicity) = *n*-heptane over mch ratio; B (aromaticity) = toluene over *n*-heptane ratio; I (*iso*-heptane ratio) = [(2mhex + 3mhex) / (c13dmcp + t13dmcp + t12dmcp)]; H (heptane ratio) = [(100x *n*-C₇) / ((chex + 2mhex + 23dmp + 11dmcp + 3mhex + c13dmcp + t13dmcp + t12dmcp + 3ep + 224tmp + *n*-C₇) + mchex)]; LHCPI (light hydrocarbon preference index) = [*n*-C₁₇+*n*-C₁₈+*n*-C₁₉] / [*n*-C₂₇+*n*-C₂₈+*n*-C₂₉]; see Tab.3.2 for compounds abbreviations

- Pristane and Phytane:

The phytol side chain of chlorophyll in phototrophic organisms is converted under oxic conditions mainly to pristane ($C_{19}H_{40}$) and under anoxic conditions mainly to phytane ($C_{20}H_{42}$) (Killops & Killops, 1993; Powell & McKirdy, 1973); see Fig.4.9. Therefore, Pr/Ph ratios of oils can be used to differentiate oxic from anoxic conditions (Didyk *et al.*, 1978; Peters & Moldowan, 1993).

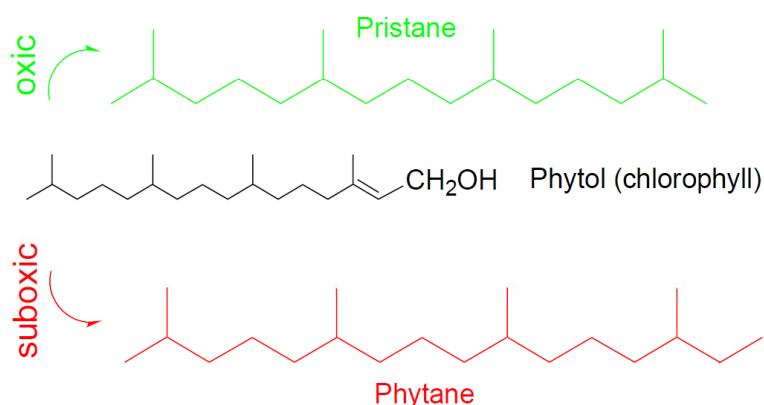


Figure 4.9: Pristane and phytane formation from phytol, which is derived from the chlorophyll side chain.

At the same time, there are evidences that pristane and phytane could have sources other than degradation of phytol (Albaiges *et al.*, 1985; Goossens *et al.*, 1984; Illich, 1983); therefore this ratio should be used with caution in interpreting paleoenvironments of oil source rocks. All the chromatograms show the presence of acyclic isoprenoids with pristane/phytane ratios ranging from 0.73 to 1.84. In this framework, the analysed crude oils were generated from marine source rocks deposited under anoxic conditions. The influence of maturity and source-facies (Hughes, 1984; Peters *et al.*, 2005) on this ratio could not be ignored as it is clear that the samples with the highest Pr/Ph ratios (e.g. G002954, G002982) (1.84 and 1.70, respectively), have the highest API gravity values ($^{\circ}43$ and $^{\circ}49$, respectively), and the highest saturated fraction at the value of 77 %. However the isoprenoid/*n*-paraffin ratios are often used to provide information not only on the deposi-

tional environment and source rock type but also on the secondary processes like biodegradation and maturation (Peters *et al.*, 1999b; Peters, 2000b). Both $\text{Pr}/n\text{-C}_{17}$ and $\text{Ph}/n\text{-C}_{18}$ ratios increase with biodegradation due to the loss of associated n -alkanes and on the other hand, decrease with increasing maturity due to the increasing dominance of these n -alkanes.

Fig.4.10 shows that most of the samples are located in the area of marine organic matter type. Three of the analysed oils (namely G002997, G002998, and G002993) are located in the upper right corner of the diagram having the highest values. At the same time, three other oils (G002982, G002959, and G002954) can be easily recognized on the left hand side of the diagram having the lowest values.

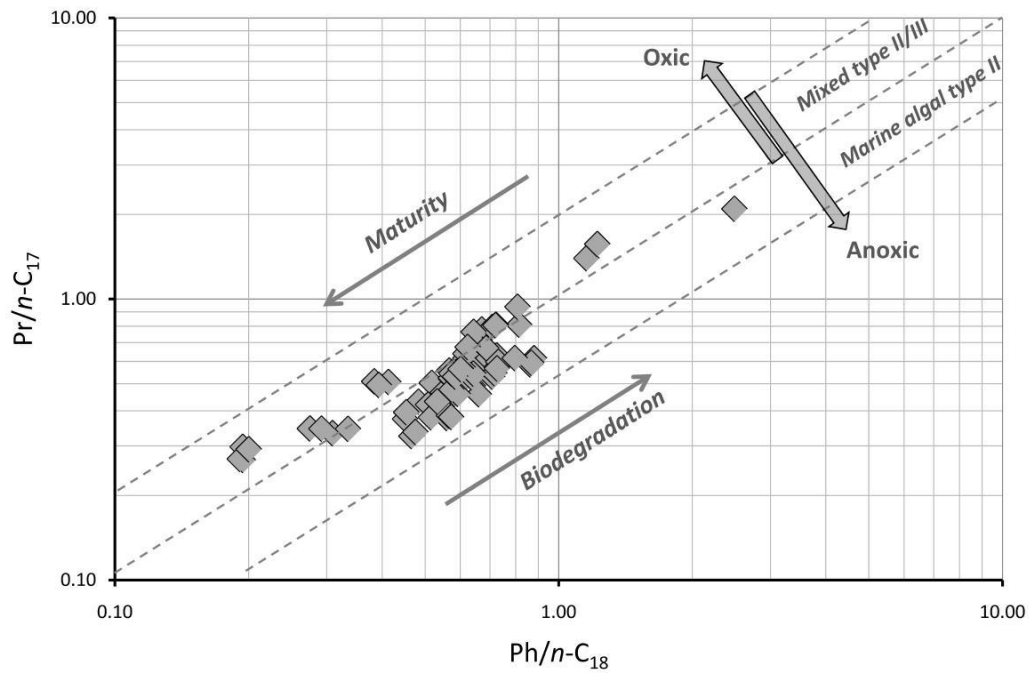


Figure 4.10: The plot of $\text{Pr}/n\text{-C}_{17}$ vs. $\text{Ph}/n\text{-C}_{18}$ can be used to infer the oxicity and the organic matter type (Peters *et al.*, 1999b).

- Gasoline Range Analysis:

A representative gasoline range gas chromatogram is presented in Fig.4.11. Gasoline range ($n\text{-C}_5$ to $n\text{-C}_8$) hydrocarbons has such a strong source and secondary alteration influence (Peters *et al.*, 2005); therefore it could give several important parameters to quantify and

| Class | Class limit % | |
|----------------|---------------|------------------|
| | Heptane ratio | Isoheptane ratio |
| normal | 18 to 22 | 0.8 to 1.2 |
| mature | 22 to 30 | 1.2 to 2.0 |
| super mature | 30 to 60 | 2.0 to 4.0 |
| biodegradation | 0 to 18 | 0 to 0.8 |

Table 4.3: Classification of oils on the basis of light hydrocarbon compositions.

assess the crude oil composition variations. Some of these parameters are suggested in Thompson's publications (Thompson, 1979 1983 1987 1988 1991). Two indices are employed, termed heptane (H) and *iso*-heptane (I) ratios (see Tab.4.2), for the classification of oils and kerogens.

These indices assess degree of paraffinicity and allow the definition of four types of oil: normal, mature, super mature, and biodegraded or immature, Tab.4.3. The values ($3.86 < H < 35.35$ and $0.56 < I < 8.17$) represent a broad range of maturities and probably different source rock types.

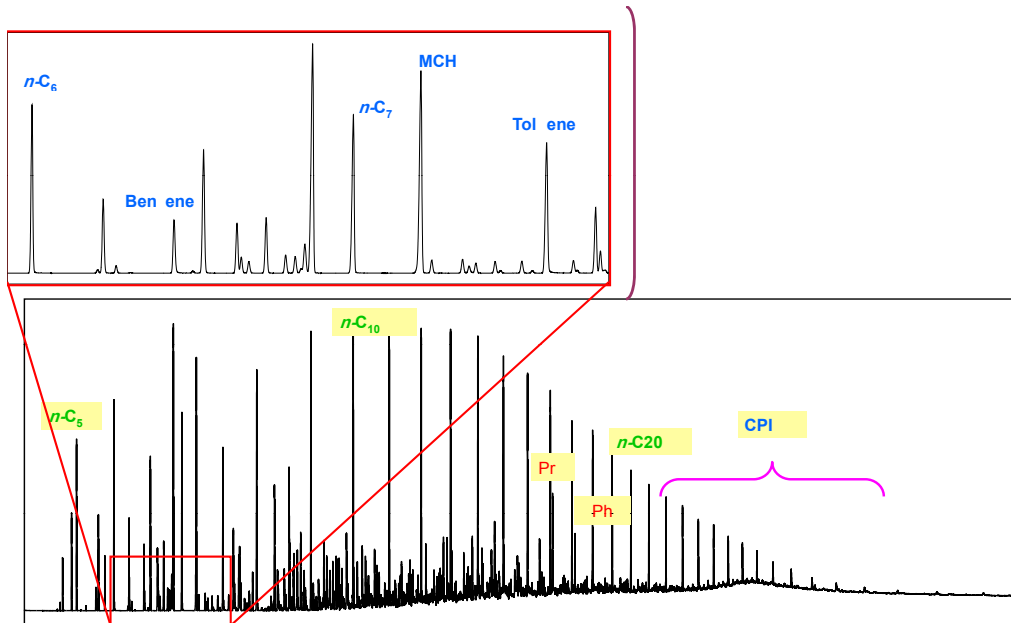


Figure 4.11: The specific components used in calculating the saturates correlation parameters: where: $n-C_5$ = *n*-pentane, $n-C_6$ = *n*-hexane, $n-C_7$ = *n*-heptane, MCH = methylcyclohexane, Pr= pristane, Ph = phytane, CPI= carbon preference index.

Paraffinicity ($F = n-C_7 / mch$) and aromaticity ($B = \text{toluene} / n-C_7$) ratios were suggested as indicators for in-reservoir evaporation processes (Thompson, 1988). Plotting both ratios against each other in one diagram could be useful to describe and illustrate the impact of several secondary alteration processes on crude oils (Talukdar *et al.*, 1990). For samples investigated in this study, it is clear that the majority of oil samples are located within the "normal oil" area, which could be defined as $F \approx 0.69 - 2.0$ and $B \approx 0.1 - 0.9$ (see Fig.4.12). Some oils have F values below 0.6 because of biodegradation effects, which reduces the heptane ratio (H) to values less than 18 (e.g. G002993, G002997, G003001, and G003011).

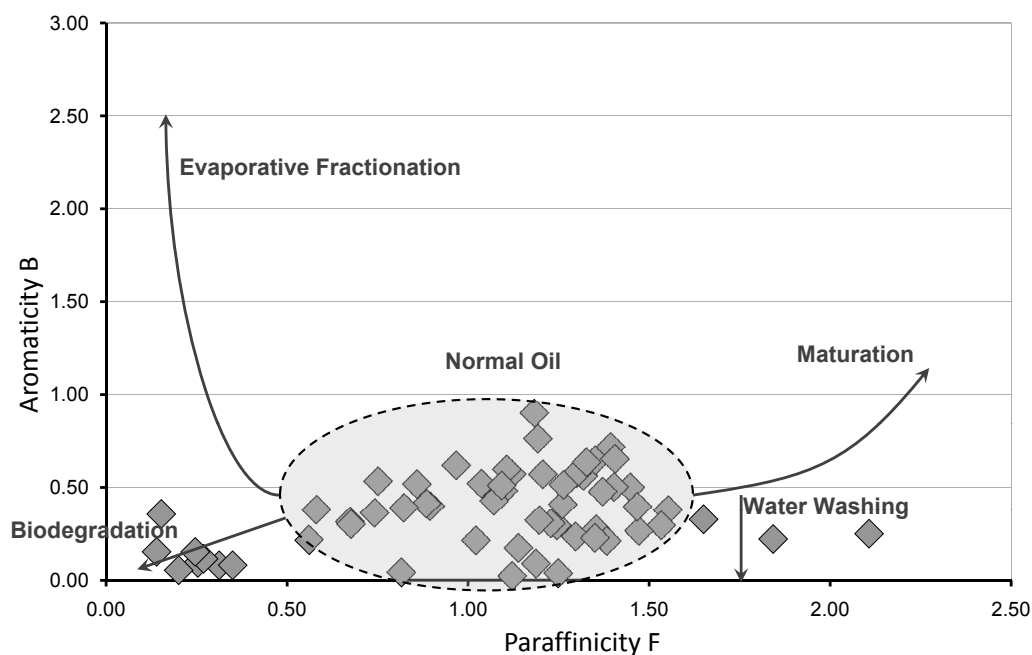


Figure 4.12: Plot of aromaticity (B) versus paraffinicity (F) ratios referring to several reservoir alteration processes after (Talukdar *et al.*, 1990).

Recap:

Normal alkane distributions of most of investigated oils show a dominance of light hydrocarbons over long-chain ones referring to mature non-waxy crude oils generated from generally marine type II, type II/III organic matter. The pristane over phytane ratio is high in oils which have the highest API gravity and saturated fraction (G002982, G002954 and G002959) which could refer to a possible impact of maturity on the Pr/Ph ratio. Although these high values might indicate a clay-rich source rock (Silurian Tanf Formation), this ratio can not be considered as a reliable source related parameter due to the maturity effect. The $\text{Pr}/n\text{-C}_{17}$ vs. $\text{Ph}/n\text{-C}_{18}$ cross plot differentiates some oils having the highest values (G002997, G002993, and G002998) due to a possible effect of biodegradation in the northwestern part of the study area where shallow Miocene reservoirs occur. On the other hand, oils having the lowest values of these two parameters (G002982, G002954, and G002959) are located in the left hand side of the plot. These latter oils are located geographically in the southeastern part of the graben where the proven occurrence of Silurian Tanf Formation exists.

4.1.3 Aliphatic Biomarkers Characteristics

GC-MS-MS analysis was used to examine the distribution of sterane and hopane chemical fossils (see Fig.4.13 for molecular structures) by monitoring the ions at m/z 217 and m/z 191, respectively (see Fig.3.10 to Fig.?? and Tab.3.11 to Tab.3.14). Biomarkers are biologically derived compounds present in crude oil and bitumen whose carbon skeleton shows a clear relationship to the structure of their assumed precursor compound (Peters & Moldowan, 1993). These compounds offer valuable information on the depositional environment, lithology, type of organic matter, and the possible age of the related source rock. Due to the detection mode (MRM) for hopanes and steranes the total concentrations (μ g/g) were not determined, therefore evaluations are based on the relative abundances.

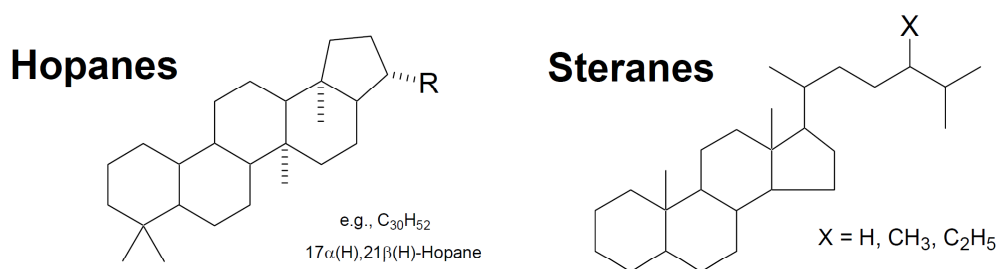


Figure 4.13: Molecular structures of hopanes and steranes.

4.1.3.1 Hopanes

The bacterial (prokaryotic) membrane lipids are the main origin of many terpanes in petroleum (Ourisson *et al.*, 1982; Ourisson & Nakatani, 1994). Terpanes include many homologous series including tricyclic, tetracyclic, and pentacyclic terpanes which have been identified in the Syrian oils (see Fig.3.10 and Tab.3.11 for the names of the compounds identified).

Visual inspection of the m/z 191 mass fragmentograms of the oil samples shows different distributions of terpane compounds which reflect different related source rocks and/or maturities (Peters *et al.*, 2005; Zumbege, 1987). Fig.4.14-a (G002997) shows a significant dominance of hopanes (C_{29} and C_{30}) over other compounds in comparison with sample (G002995) in

Fig.4.14-b which has a different pattern of the tricyclic terpanes distribution and also a dissimilar relationship between Ts and Tm biomarkers. On the other hand, it is very hard to recognize any terpanes in the biomarker profile of G002954 (Fig.4.14-c) probably because of its very high maturity level.

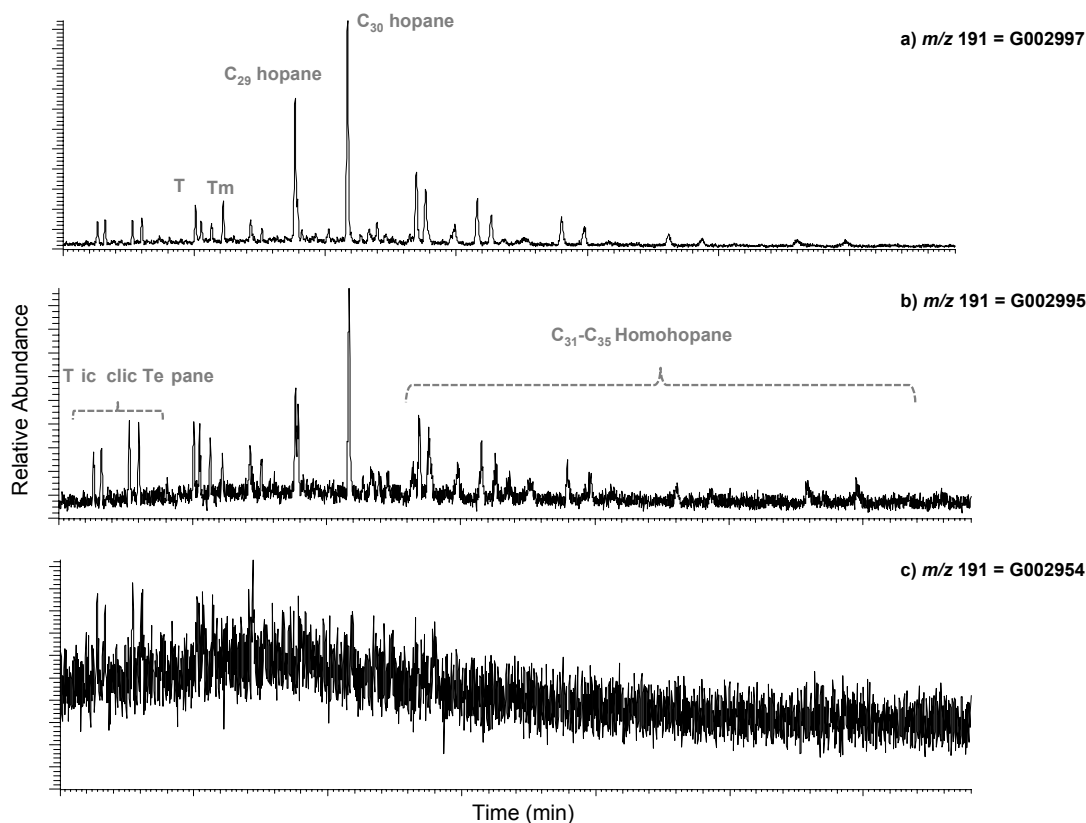


Figure 4.14: m/z 191 mass fragmentograms showing the three types (tri-, tetra-, and pentacyclic) of terpanes observed within the samples set. (a) shows a significant dominance of hopanes (C_{29} and C_{30}), (b) represents a different patterns of tricyclic and pentacyclic terpanes, (c) has no recognizable compounds to be identified.

The ratio of C_{27} 18α -trinorneohopane (18α -22,29,30-trinorneohopane *or* Ts) over C_{27} 17α -trinorhopane (17α -22,29,30-trinorhopane *or* Tm) is reported to be a maturity parameter (Seifert & Moldowan, 1978a) and also influenced by source facies as well (Bakr & Wilkes, 2002; Moldowan *et al.*, 1986b) (see Fig.4.15 for molecular structures). In the studied oil samples, the Ts/(Ts+Tm) ratio values range between 0.33 - 0.78 (see Tab.4.4). Due to the previously mentioned reasons, no considerable correlations could be

found for this biomarker against either maturity or source-related parameters as each has an influence.

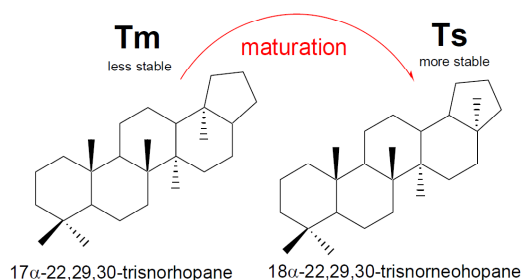


Figure 4.15: Molecular structures of C_{27} 18 α -trinorneohopane (18 α -22,29,30-trinorneohopane or Ts) and C_{27} 17 α -trinorhopane (17 α -22,29,30-trinorhopane or Tm).

The distribution of C_{31} - C_{35} 17 α ,21 β (H)-homohopanes is used to determine the homohopane index [$C_{35}/(C_{31} + C_{35})$], which provide an indication to depositional settings and maturity of the related source rocks (Hanson *et al.*, 2001; Peters & Moldowan, 1991). The homohopane index varies between 0.07 and 0.20 pointing to anoxic depositional conditions of the associated source rocks.

The relative abundance of gammacerane has widely been used as indicator of increased water salinity and water column stratification (Moldowan *et al.*, 1985; Sinninghe Damste' *et al.*, 1995; ten Haven *et al.*, 1989; Venkatesan, 1989). In this framework the high Gammacerane Index [gammacerane/(gammacerane + C_{30} hopane)] values (>1) refer to a hypersaline environment (Fu *et al.*, 1986). Gammacerane index for the studied crude oils do not exceed the value of 0.24, which reflects non-hypersaline conditions of the source strata. The 22*S*/ (22*S*+22*R*) C_{31} homohopane isomerization ratio rises from 0 to 0.6 with thermal maturation due to the conversion of *R* configuration into *S* one (Peters & Moldowan, 1993). The values of this ratio in the crude oils analysed range between 0.57 and 0.64 (see Tab.4.4). This illustrates that the ratio could not be used reliably to assess the maturation level as the equilibrium has been reached.

| Sample | Mo/(Mo+Ho) | C_{35} | HHI | GI | Ts/(Ts+Tm) | C_{35} | $S+R/C_{34}$ | $S+R$ | HH iso. |
|---------|------------|----------|-----|------|------------|----------|--------------|-------|---------|
| G002952 | 0.09 | 0.12 | | 0.11 | 0.59 | | 0.77 | | 0.62 |
| G002953 | 0.08 | 0.07 | | 0.05 | 0.70 | | 0.60 | | 0.61 |
| G002954 | 0.18 | 0.00 | | 0.00 | 0.78 | | | | 0.64 |
| G002956 | 0.05 | 0.11 | | 0.06 | 0.64 | | 1.05 | | 0.60 |
| G002959 | 0.12 | 0.00 | | 0.17 | 0.61 | | | | 0.67 |
| G002960 | 0.07 | 0.16 | | 0.11 | 0.64 | | 1.25 | | 0.61 |
| G002961 | 0.06 | 0.10 | | 0.11 | 0.48 | | 0.84 | | 0.60 |
| G002963 | 0.06 | 0.13 | | 0.24 | 0.56 | | 1.17 | | 0.62 |
| G002964 | 0.06 | 0.13 | | 0.14 | 0.45 | | 1.21 | | 0.60 |
| G002965 | 0.08 | 0.13 | | 0.13 | 0.83 | | 1.14 | | 0.67 |
| G002966 | 0.09 | 0.15 | | 0.12 | 0.73 | | 1.24 | | 0.63 |
| G002968 | 0.08 | 0.08 | | 0.08 | 0.58 | | 0.80 | | 0.61 |
| G002969 | 0.09 | 0.08 | | 0.05 | 0.66 | | 0.78 | | 0.62 |
| G002973 | 0.04 | 0.08 | | 0.07 | 0.50 | | 0.92 | | 0.59 |
| G002974 | 0.07 | 0.14 | | 0.14 | 0.76 | | 1.10 | | 0.64 |
| G002975 | 0.11 | 0.09 | | 0.04 | 0.49 | | 1.01 | | 0.57 |
| G002976 | 0.10 | 0.14 | | 0.18 | 0.57 | | 1.06 | | 0.57 |
| G002980 | 0.09 | 0.09 | | 0.09 | 0.40 | | 0.83 | | 0.57 |
| G002981 | 0.10 | 0.10 | | 0.09 | 0.43 | | 1.01 | | 0.58 |
| G002982 | 0.13 | 0.16 | | 0.00 | 0.69 | | 1.54 | | 0.62 |
| G002988 | 0.07 | 0.14 | | 0.19 | 0.52 | | 0.74 | | 0.56 |
| G002993 | 0.07 | 0.07 | | 0.07 | 0.55 | | 0.73 | | 0.60 |
| G002995 | 0.07 | 0.12 | | 0.13 | 0.72 | | 1.02 | | 0.62 |
| G002997 | 0.06 | 0.07 | | 0.07 | 0.55 | | 0.67 | | 0.60 |
| G003005 | 0.05 | 0.08 | | 0.08 | 0.78 | | 0.73 | | 0.62 |
| G003006 | 0.06 | 0.13 | | 0.11 | 0.33 | | 1.30 | | 0.60 |
| G003009 | 0.06 | 0.19 | | 0.16 | 0.64 | | 1.42 | | 0.60 |
| G003011 | 0.06 | 0.07 | | 0.05 | 0.55 | | 0.72 | | 0.60 |
| G003015 | 0.07 | 0.10 | | 0.14 | 0.67 | | 0.88 | | 0.61 |
| G003017 | 0.05 | 0.20 | | 0.16 | 0.48 | | 1.49 | | 0.59 |

Table 4.4: Hopane biomarker parameters of crude oils, where: Mo/(Mo+Ho) = moretane/(moretane+hopane); HHI = C_{35} homohopane index; GI = gammacerane index; HH iso. = homohopane isomerization ratio

4.1.3.2 Steranes

Steranes are saturated hydrocarbons bearing a tetracyclic structure which are derived from sterols present originally in eukaryotes such as higher plants and algae (Mackenzie *et al.*, 1982; Summons & Capon, 1988c).

Steranes are usually identified using the GC-MS technique by m/z 217 mass fragmentograms, but in the studied oil samples it was very hard to identify the steranes in this way because of their low concentrations. Therefore a more sensitive technique (MRM-GC-MS) was used to identify the steranes (see Fig.3.11 and Tab.3.12 for compounds identification).

Fig.4.16 shows m/z 217 mass fragmentograms for three crude oil samples. Sterane and diasterane distributions varied notably which could reveal different associated origins and/or maturities. C_{29} and C_{27} diasteranes significantly dominate over steranes in sample G002954. However, it is clear that C_{27} steranes in G002964 are more abundant in comparison to G002988, in which C_{29} steranes are the most abundant compounds. Additionally, C_{28} steranes are hard to recognize in G002954, in contrast to G0029864 for instance.

The ratio of C_{28}/C_{29} $\alpha\beta\beta$ sterane is considered as a reliable age-related parameter for marine settings as it increases from Precambrian to Tertiary due to the relative increase of C_{28} sterane and the decrease of C_{29} sterane content through geologic time (Moldowan *et al.*, 1985). Therefore, it was possible for Grantham & Wakefield (1988) to distinguish Upper Cretaceous and Tertiary oils from Palaeozoic ones. In the studied Syrian oils, this ratio ranges from 0.42 - 1.19 (Tab.4.5) with the majority of the samples having ratios >0.70 . Four samples (G002954, G002959, G002982, and G002988; see Fig.4.17) have values below 0.7 which might be an indication for a source rock Pre-Jurassic in age (probably Palaeozoic Tanf Formation).

The diasterane/sterane ratio is based on $[13\beta,17\alpha(H) 20S + 20R]/([5\alpha,14\alpha,17\alpha(H) 20S + 20R] + [5\alpha, 14\beta, 17\beta(H) 20S + 20R])$ for the C_{27} , C_{28} , and C_{29} steranes obtained from MRM-GC-MS. This parameter is considered as an indicator of the thermal maturity of the source rock (Seifert & Moldowan, 1978a;

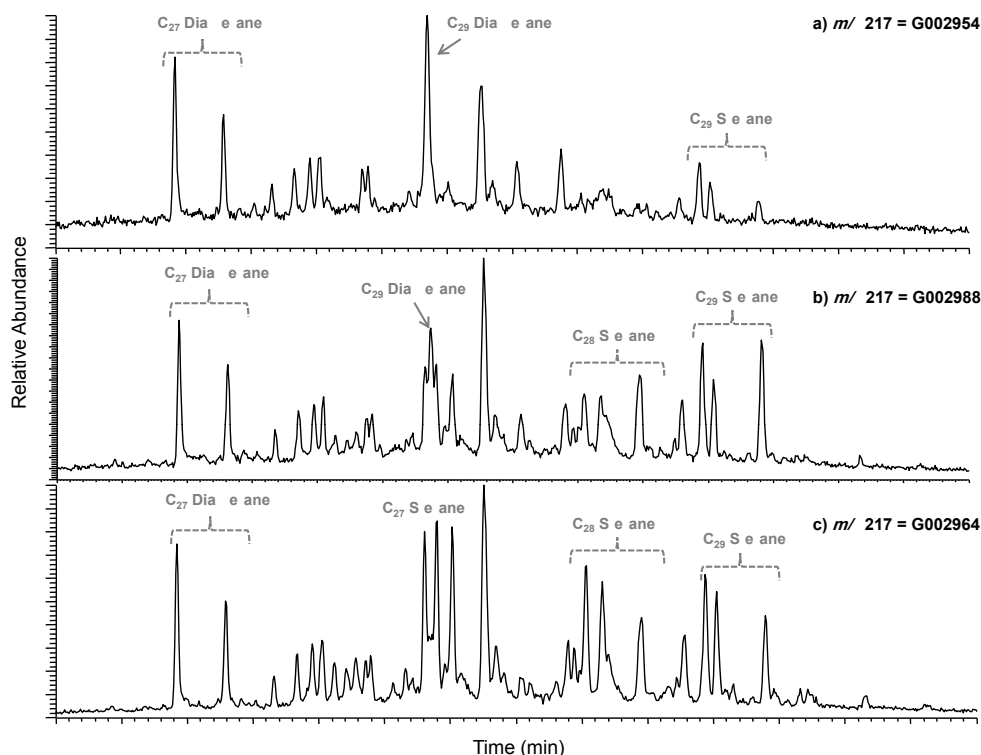


Figure 4.16: m/z 217 mass fragmentograms showing the sterane and diasterane distributions observed within the samples set. (a) shows a relative dominance of diasteranes over steranes compounds, (b) has different distribution of steranes and diasteranes, (c) represents regular steranes dominance.

van Graas, 1990). Moreover, this ratio may also indicate the mineralogy of the source rock because of the role of clay, such as illite or montmorillonite, as a catalyst for the conversion of steranes to diasteranes (Sieskind *et al.*, 1979; van Kaam-Peters *et al.*, 1998b). Therefore, the diasterane/sterane ratio is commonly used to distinguish petroleum from carbonate versus clastic source rocks (Mello *et al.*, 1988b). This ratio has a broad range in the analysed oils (between 0.15 and 2.51, see Tab.4.5), which might be an indication of different stages of thermal maturation and different type of source facies. G002954 and G002959 have the highest values (2.51 and 2.18, respectively) referring to clay-rich and highly mature source rocks.

Three series of C_{26} steranes are known, including 21-, 24-, 27-norcholestanes (Fig.4.18) (Moldowan *et al.*, 1991a). The $5\alpha,14\alpha,17\alpha(H)$ 20 S + 20 R and $5\alpha,14\beta,17\beta(H)$ 20 S + 20 R compounds were identified in the 24- and 27-norcholestanes. The lack of 20 S and 20 R isomers in the 21-norcholestanes

| Sample | Steranes% | | | Diasteranes% | | | C_{28}/C_{29} | Dia/Reg $C_{27}-C_{29}$ | $\beta\beta/(\beta\beta+\alpha\alpha)$ C_{29} | $\alpha\alpha$ 20S/(20S+20R) C_{29} | 24/(24+27) C_{29} |
|---------|-----------|-------|-------|--------------|-------|-------|-----------------|----------------------------|--|--|------------------------|
| G002952 | 45,97 | 27,72 | 26,31 | 48,07 | 27,53 | 24,39 | 1,05 | 0,77 | 0,54 | 0,46 | 0,20 |
| G002953 | 32,62 | 35,94 | 31,44 | 34,86 | 41,41 | 23,74 | 1,14 | 0,77 | 0,61 | 0,54 | 0,35 |
| G002954 | 33,47 | 19,66 | 46,88 | 30,58 | 21,08 | 48,34 | 0,42 | 2,51 | 0,63 | 0,46 | 0,21 |
| G002956 | 34,14 | 34,63 | 31,23 | 38,82 | 37,81 | 23,37 | 1,11 | 0,62 | 0,57 | 0,51 | 0,32 |
| G002959 | 44,00 | 0,00 | 56,00 | 35,96 | 27,38 | 36,66 | 0,35 | 2,18 | 0,62 | 0,50 | 0,23 |
| G002960 | 37,92 | 31,03 | 31,05 | 46,55 | 30,50 | 22,96 | 1,00 | 0,90 | 0,60 | 0,50 | 0,37 |
| G002961 | 40,61 | 29,83 | 29,56 | 47,48 | 32,45 | 20,07 | 1,01 | 0,33 | 0,59 | 0,47 | 0,35 |
| G002963 | 36,52 | 33,20 | 30,28 | 44,65 | 33,96 | 21,40 | 1,10 | 0,41 | 0,60 | 0,52 | 0,35 |
| G002964 | 38,57 | 31,62 | 29,81 | 44,74 | 33,50 | 21,76 | 1,06 | 0,37 | 0,55 | 0,51 | 0,41 |
| G002965 | 34,73 | 34,51 | 30,76 | 38,86 | 38,44 | 22,70 | 1,12 | 1,04 | 0,61 | 0,55 | 0,36 |
| G002966 | 38,47 | 31,28 | 30,25 | 45,54 | 32,33 | 22,12 | 1,03 | 1,14 | 0,59 | 0,53 | 0,38 |
| G002968 | 35,47 | 33,59 | 30,93 | 40,38 | 36,74 | 22,88 | 1,09 | 0,60 | 0,59 | 0,55 | 0,32 |
| G002969 | 33,21 | 35,33 | 31,46 | 37,49 | 40,27 | 22,23 | 1,12 | 0,69 | 0,58 | 0,54 | 0,32 |
| G002973 | 38,37 | 31,61 | 30,03 | 43,44 | 34,54 | 22,02 | 1,05 | 0,30 | 0,57 | 0,51 | 0,44 |
| G002974 | 37,64 | 32,38 | 29,97 | 45,47 | 33,15 | 21,38 | 1,08 | 1,40 | 0,60 | 0,52 | 0,37 |
| G002975 | 33,75 | 29,77 | 36,48 | 39,08 | 32,18 | 28,74 | 0,82 | 0,77 | 0,53 | 0,46 | 0,38 |
| G002976 | 44,74 | 28,50 | 26,77 | 49,82 | 26,57 | 23,61 | 1,06 | 0,78 | 0,53 | 0,58 | 0,34 |
| G002980 | 40,90 | 32,12 | 26,98 | 45,05 | 34,93 | 20,02 | 1,19 | 0,70 | 0,55 | 0,52 | 0,36 |
| G002981 | 42,36 | 30,88 | 26,77 | 47,68 | 32,48 | 19,84 | 1,15 | 0,71 | 0,52 | 0,53 | 0,43 |
| G002982 | 35,52 | 26,37 | 38,11 | 34,86 | 27,02 | 38,12 | 0,69 | 1,17 | 0,57 | 0,51 | 0,26 |
| G002988 | 31,03 | 29,13 | 39,83 | 36,78 | 27,47 | 35,75 | 0,73 | 0,60 | 0,48 | 0,42 | 0,25 |
| G002993 | 32,73 | 35,25 | 32,02 | 35,64 | 40,94 | 23,42 | 1,10 | 0,41 | 0,51 | 0,45 | 0,31 |
| G002995 | 35,19 | 33,57 | 31,24 | 41,43 | 35,20 | 23,36 | 1,07 | 0,38 | 0,54 | 0,52 | 0,37 |
| G002997 | 32,60 | 34,35 | 33,05 | 37,58 | 39,54 | 22,88 | 1,04 | 0,38 | 0,52 | 0,43 | 0,31 |
| G003005 | 33,76 | 34,66 | 31,58 | 38,47 | 39,01 | 22,52 | 1,10 | 0,54 | 0,57 | 0,55 | 0,32 |
| G003006 | 38,25 | 32,27 | 29,48 | 42,99 | 35,14 | 21,87 | 1,09 | 0,15 | 0,56 | 0,52 | 0,39 |
| G003009 | 40,18 | 28,17 | 31,65 | 48,93 | 27,81 | 23,26 | 0,89 | 0,62 | 0,58 | 0,51 | 0,35 |
| G003011 | 32,95 | 35,01 | 32,04 | 38,26 | 39,16 | 22,58 | 1,09 | 0,46 | 0,51 | 0,46 | 0,30 |
| G003015 | 34,84 | 33,38 | 31,78 | 38,09 | 38,78 | 23,12 | 1,05 | 0,57 | 0,57 | 0,50 | 0,31 |
| G003017 | 38,51 | 30,15 | 31,33 | 44,69 | 30,86 | 24,45 | 0,96 | 0,37 | 0,56 | 0,51 | 0,35 |

Table 4.5: Sterane biomarker parameters of crude oils, where: C_{28}/C_{29} = the C_{28}/C_{29} $\alpha\beta\beta$ sterane ratio; Dia/Reg $C_{27}-C_{29}$ = the ratio of diasteranes over steranes from C_{27} to C_{29} ; $\beta\beta/(\beta\beta+\alpha\alpha) = \beta\beta/(\beta\beta+\alpha\alpha)$ C_{29} steranes; $\alpha\alpha$ 20S/(20S+20R) = $\alpha\alpha$ 20S/(20S+20R) C_{29} steranes, 24/(24+27) = 24/(24+27) C_{26} nordiacholestanes.

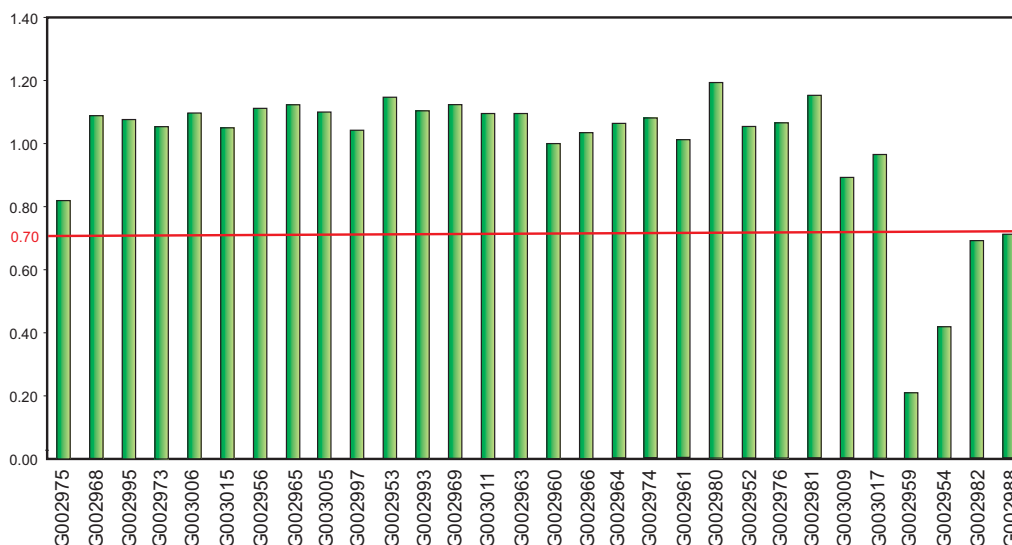


Figure 4.17: $C_{28}/C_{29} \alpha\beta\beta$ sterane ratio as an age-related biomarker. Low values (below 0.7) for G002954, G002959, G002982, and G002988 oil samples indicate probably to Palaeozoic origin.

indicates a lack of the methyl group at C-20. These C_{26} sterane compounds were identified using MRM-GCMS m/z 358 \rightarrow 217 (see Fig.3.12 and Tab.3.13 for compound identification). The 21- and 27-norcholestanes appear to have no direct sterol precursors but may originate through bacterial oxidation or thermally induced cleavage and loss of a methyl group from larger steroids ($>C_{26}$). Nordiacholestanes help to distinguish Tertiary from Cretaceous oils and Cretaceous from older oils. The 24-Nordiacholestanes probably originate from diatoms, which evolved from Jurassic to Cretaceous time and again during the Tertiary. 24/(24+27)-Nordiacholestane ratios greater than 0.25 and 0.55 typify oils from Cretaceous or younger and Tertiary source rocks, respectively (Holba *et al.*, 1998b). In the studied oils this ratio varies between 0.21-0.44 (see Tab.4.5).

Five oil samples (G002954, G002959, G002982, G002988, and G002952, Fig.4.19) have values for this ratio below 0.25 which indicates a source rock age older than Jurassic. All other oils have values not more than 0.44 asserting a source rock not younger than Upper Cretaceous in age.

Isomerization at C-20 in the C_{29} $5\alpha,14\alpha,17\alpha(H)$ -steranes causes $20S / (20S+20R)$ to rise from 0 to about 0.5 (0.52-0.55 = equilibrium) with increasing maturity (Peters *et al.*, 2005; Seifert & Moldowan, 1986). Only the

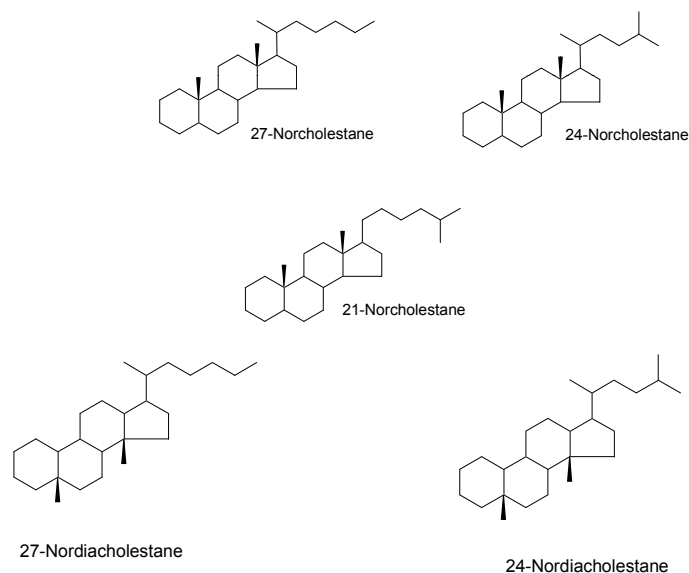


Figure 4.18: The structures of 21-, 24-, and 27-norcholestone and 24- and 27-nordiacholestone compounds identified in the crude oils.

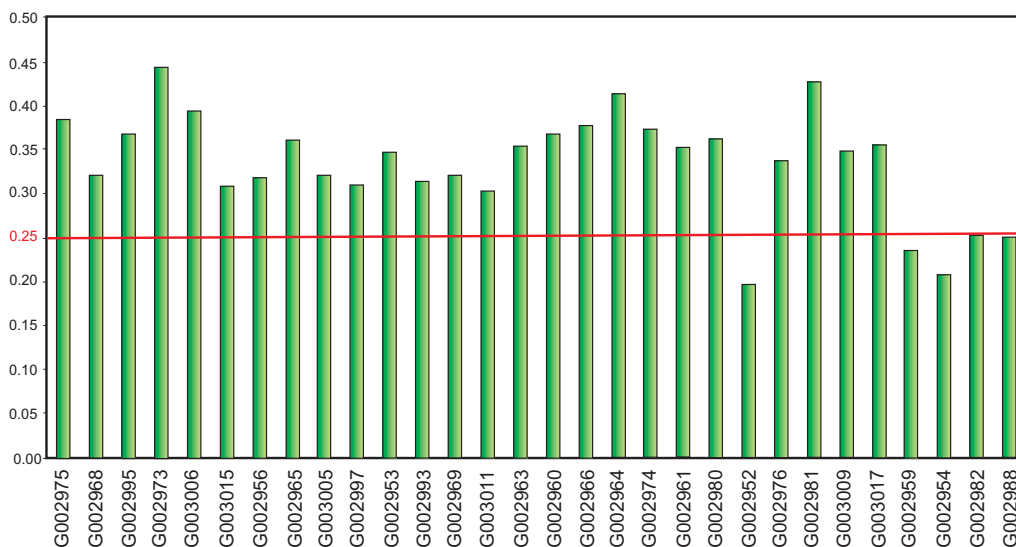


Figure 4.19: The 24/(24+27)-nordiacholestone ratio as an effective source-age parameter to distinguish oils originating from different eras.

R configuration at C-20 occurs in steroid precursors in living organisms, and is gradually converted during thermal influence into a mixture of *R* and *S* sterane configurations (see Fig.4.20). Values of this maturity parameter in the studied oils (Tab.4.5) fall in the range of 0.42-0.58 which shows that most oil samples have reached or even exceed the equilibrium limit identified above. Therefore, this parameter is not suitable to differentiate the oils

according to their maturity level.

During diagenesis and because of thermal degradation, isomerization will take place at C-20 in the *R* configuration (found only in living organisms) of the C_{29} steroid molecule (Seifert & Moldowan, 1978a). This process results in conversion of *R* into a mixture of *R* and *S* C_{29} steranes (see Fig.4.20). The equilibrium is reached at a value of about 0.52-0.55 (Peters *et al.*, 2005). Consequently, the $20S/(20S+20R)$ ratio of C_{29} $5\alpha,14\alpha,17\alpha(H)$ -steranes could provide a significant indication to the maturation degree of the associated source rock unless it reaches the equilibrium. In the studied oils, this maturity-related parameter ranges from 0.42 to 0.58 (see Tab.4.5) showing most samples have reached or even exceed the equilibrium limit identified above. Therefore, this biomarker is not very helpful to reliably assess the maturity of the oils in this sample set. Similarly, isomerization at C-14 and C-17 positions in the $20S$ and $20R$ C_{29} regular steranes due to thermal stress will lead to another maturity biomarker. $\beta\beta/(\beta\beta+\alpha\alpha)$ reaches the equilibrium at about 0.7 (Peters *et al.*, 2005) and is supposed to be independent of source organic matter input. Fig.4.21 displays a cross plot of $\beta\beta/(\beta\beta+\alpha\alpha)$ versus $20S/(20S+20R)$. There is no great benefit from this plot in evaluating the maturity of the investigated oils because both parameters are almost close to the equilibrium values. Therefore, another effective maturity-related parameters needs to be found.

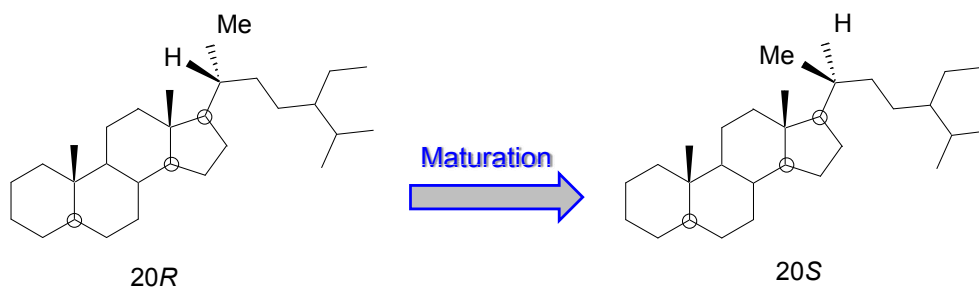


Figure 4.20: Molecular structures of $20R$ (biological epimer) and $20S$ (geological epimer) for the C_{29} $5\alpha,14\alpha,17\alpha(H)$ -steranes.

A study on recent marine and terrigenous sediments performed by (Huang & Meinschein, 1979) showed that the distribution of C_{27} , C_{28} , and C_{29} sterols

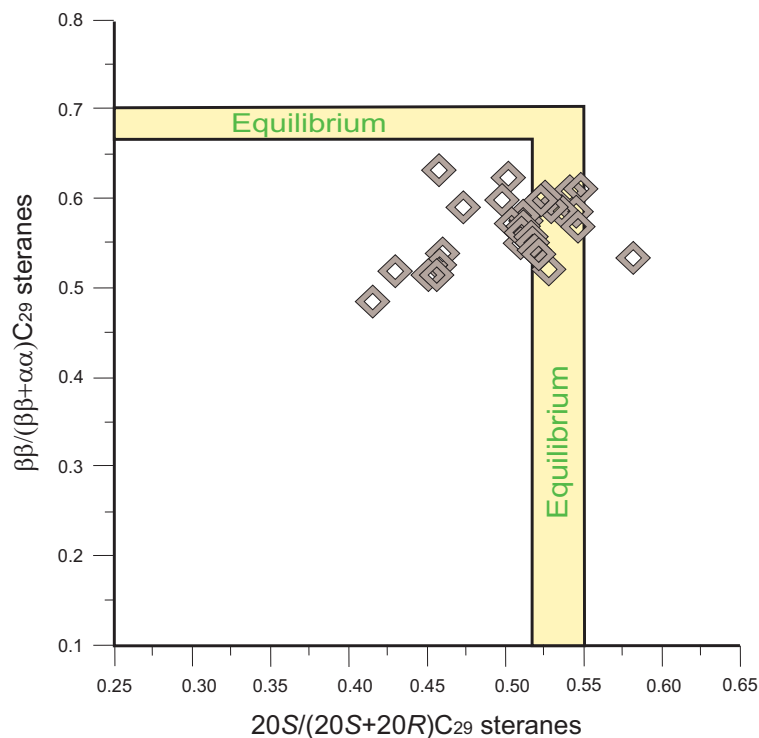


Figure 4.21: Cross plot of sterane maturity parameters based on apparent isomerization of asymmetric centers in the C_{29} steranes.

displayed on a ternary diagram can be used to differentiate depositional settings. Later, it has been stated that the corresponding sterane ternary diagrams do not change significantly throughout the oil-generative window (Peters & Moldowan, 1993). The applicability of the sterane ternary diagram for crude oils and source rocks is limited due to the broad overlaps of different depositional environments in the triangular plot (Moldowan *et al.*, 1985; Peters *et al.*, 2005). It was observed that the percentage of C_{29} steranes decreases in a broad trend through geological time (Grantham & Wakefield, 1988). Upper Jurassic and younger crude oils contain less than 40% C_{29} steranes, whilst Lower Palaeozoic and older oils contain greater than 40-50%. Fig.4.22 and Tab.4.5 illustrate that four oil samples (G002954, G002959, G002982, and G002988) have C_{29} percentage values greater than 39% which could refer to Palaeozoic source strata.

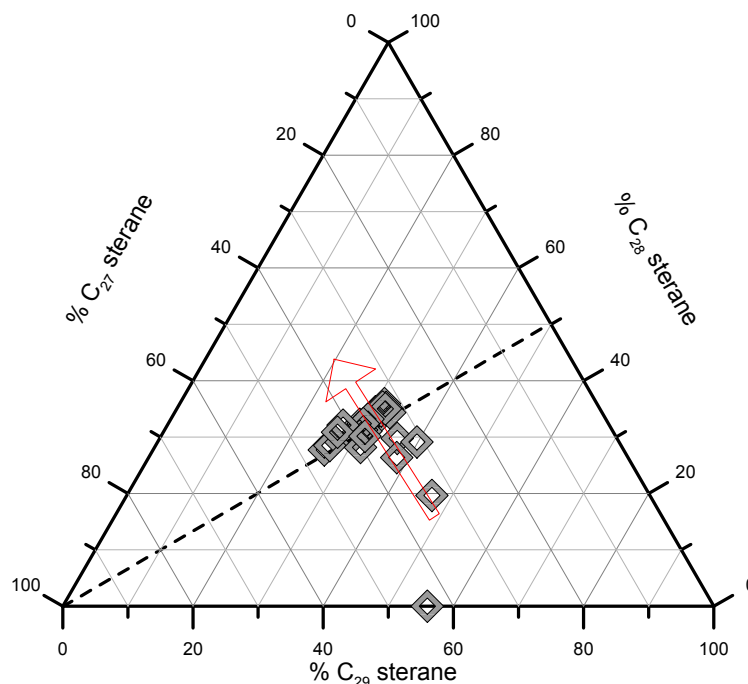


Figure 4.22: Triangular plot illustrating the relative abundance of C_{27} , C_{28} , and C_{29} regular steranes [5α , 14α , 17α (H) $20S + 20R$ and 5α , 14β , 17β (H) $20S + 20R$] in the saturate fractions of crude oils. The arrow illustrates the decreasing C_{29} concentration through geological time; after (Grantham & Wakefield, 1988).

Recap:

Hopane-based maturity parameters could not be used reliably to assess the maturation degree of crude oils investigated in this study because it is influenced by source signatures (e.g. $Ts/(Ts+Tm)$) or because it reached the equilibrium state (e.g. $22S/(22S+22R)$ C_{31} homohopane isomerization ratio).

The ratio of C_{28}/C_{29} $\alpha\beta\beta$ sterane acts as a very good clue to assess the age of associated source rock as it classifies four samples (G002959, G002954, G002982, and G002988) to be generated from source rock older than Jurassic in age which is obviously the Silurian source. The $24/(24+27)$ -nordiacholestane biomarker ratio leads to the same direction and assorts the same oils as a separate group.

The ratio of C_{27} to C_{29} diasteranes/steranes refers to clay-rich source rocks for G002959 and G002954. Sterane-based maturity biomarker ratios $\beta\beta/(\beta\beta+\alpha\alpha)$ and $20S/(20S+20R)$ are in the equilibrium range for most of oil samples and therefore, could not be used efficiently to assess the maturity of the studied crude oils.

4.1.4 Diamondoids

Diamondoids are cage-like hydrocarbons and comprised of rigid fused carbon structures that resemble tiny pieces of diamond (Mckerverey, 1980; Wingert, 1992). They naturally occur in virtually all oils and condensates in various amounts (Dahl *et al.*, 1999; Petrov *et al.*, 1973; Wei *et al.*, 2006b; Wingert, 1992). The structures (Fig.4.23) and numbering of adamantane and diamantane are shown in Fig.3.2 and Tab.3.3 .

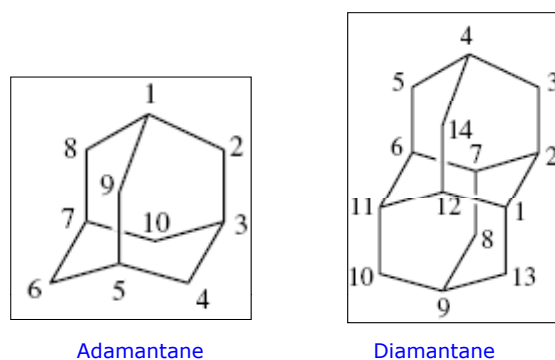


Figure 4.23: Molecular structures of diamondoids (adamantane and diamantane).

There is a kind of speculation about the real formation process of these compounds by catalytic (i.e. Lewis acids) rearrangement of polycyclic hydrocarbons during or after oil generation (Petrov *et al.*, 1973). Diamondoids are thermally more stable than most other hydrocarbons (Dahl *et al.*, 1999), and more resistant to microbial degradation than most other petroleum components (Wingert, 1992); therefore, they may be considered as an effective tool in oil correlation (Peters *et al.*, 2005). The concentrations for the diamondoid compounds were calculated based on SIM-GCFID measurements of aliphatic fraction using 5 α -androstane as an internal standard (see Appendix B.1).

The concentrations of diamondoids are observed to increase with thermal stress, simply because of cracking of the heavy hydrocarbons into smaller ones. This suggests that they can be used as a molecular proxy for thermal maturity of source rocks and crude oils. In the studied oils, the sum of

adamantane concentration ranges between 108 - 9175 ppm, that of diamantane concentrations falls in the range of 35 - 361 ppm (see Tab.4.6). Fig.4.24 shows that G002959 and G002954 crude oils have the highest amounts of diamondoids indicating to highly mature source rock which is most likely the Palaeozoic Tanf Formation. On the other hand most oils plot close to each other in the lower range of diamondoid content which could imply that they are related to source rocks lower in maturation level which are probably the Upper Cretaceous strata.

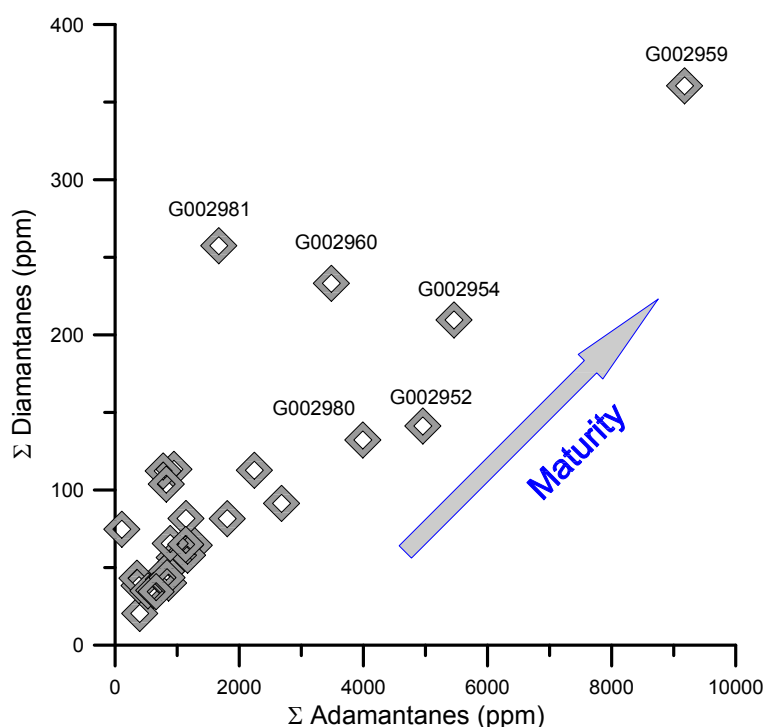


Figure 4.24: Cross plot of sum of the concentration of the entire range of diamantanes (ppm) versus the sum of the concentration of the entire range of adamantanes (ppm). Arrow refers to increasing maturity.

Basically the degree of stability differs from one diamondoid hydrocarbon to another. For instance, 1-methyladamantane (1-MA) is expected to be more stable than 2-methyladamantane (2-MA) because of the presence of the methyl group at the bridgehead position (Wingert, 1992). The same is true for 4-methyldiamantane (4-MD) which is more stable than 1- or 3-methyldiamantane (1-MD, 3-MD respectively). Therefore two ratios have been identified as maturity indicators (Chen *et al.*, 1996) as follows:

| Sample | Σ Adam.(ppm) | Σ Dia.(ppm) | 3- + 4-Mdia (ppm) | MAI | MDI | DMDI-1 | DMDI-2 |
|---------|---------------------|--------------------|-------------------|------|------|--------|--------|
| G002952 | 4958 | 141 | 36 | 0,66 | 0,41 | 0,67 | 0,57 |
| G002953 | 622 | 35 | 10 | 0,48 | 0,46 | 0,60 | 0,63 |
| G002954 | 5459 | 210 | 50 | 0,62 | 0,37 | 0,73 | 0,61 |
| G002956 | 108 | 75 | 18 | 0,56 | 0,41 | 0,66 | 0,61 |
| G002959 | 9175 | 361 | 92 | 0,69 | 0,41 | 0,64 | 0,59 |
| G002960 | 3485 | 233 | 66 | 0,60 | 0,49 | 0,65 | 0,61 |
| G002961 | 1275 | 64 | 17 | 0,63 | 0,39 | 0,65 | 0,58 |
| G002963 | 952 | 56 | 15 | 0,57 | 0,37 | 0,69 | 0,63 |
| G002964 | 948 | 113 | 31 | 0,47 | 0,43 | 0,68 | 0,62 |
| G002965 | 1167 | 58 | 17 | 0,52 | 0,37 | 0,68 | 0,67 |
| G002966 | 397 | 20 | 6 | 0,47 | 0,37 | 0,67 | 0,67 |
| G002968 | 351 | 43 | 13 | 0,52 | 0,47 | 0,58 | 0,63 |
| G002969 | 1138 | 65 | 18 | 0,58 | 0,43 | 0,63 | 0,64 |
| G002973 | 777 | 42 | 12 | 0,56 | 0,43 | 0,60 | 0,61 |
| G002974 | 1807 | 82 | 20 | 0,61 | 0,36 | 0,68 | 0,60 |
| G002975 | 981 | 54 | 15 | 0,55 | 0,44 | 0,64 | 0,62 |
| G002976 | 387 | 38 | 11 | 0,57 | 0,43 | 0,61 | 0,61 |
| G002980 | 3992 | 132 | 33 | 0,67 | 0,40 | 0,65 | 0,56 |
| G002981 | 1670 | 257 | 81 | 0,54 | 0,47 | 0,55 | 0,62 |
| G002982 | 2682 | 91 | 22 | 0,58 | 0,33 | 0,74 | 0,61 |
| G002988 | 2243 | 113 | 29 | 0,57 | 0,41 | 0,68 | 0,61 |
| G002993 | 837 | 44 | 13 | 0,50 | 0,41 | 0,61 | 0,63 |
| G002995 | 528 | 35 | 11 | 0,60 | 0,41 | 0,59 | 0,59 |
| G002997 | 862 | 40 | 12 | 0,47 | 0,44 | 0,61 | 0,65 |
| G003005 | 889 | 66 | 20 | 0,58 | 0,43 | 0,57 | 0,62 |
| G003006 | 825 | 104 | 34 | 0,55 | 0,49 | 0,55 | 0,63 |
| G003009 | 1141 | 82 | 25 | 0,60 | 0,47 | 0,56 | 0,60 |
| G003011 | 662 | 35 | 10 | 0,47 | 0,39 | 0,60 | 0,60 |
| G003015 | 828 | 48 | 14 | 0,55 | 0,39 | 0,65 | 0,66 |
| G003017 | 775 | 112 | 36 | 0,68 | 0,53 | 0,55 | 0,63 |

Table 4.6: Diamondoid-related parameters, where: Σ Adam. = sum of adamantane concentrations (ppm), Σ Dia. = sum of diamantane concentrations (ppm), 3- + 4-Mdia = sum of 3- and 4-methyldiamantane concentrations (ppm), MAI = methyladamantane index = 1-methyladamantane/(1-methyladamantane + 2-methyladamantane), MDI = 4-methyldiamantane/(4-methyldiamantane + 1-methyldiamantane + 3-methyldiamantane), DMDI-1 = dimethyldiamantane index 1 = 3-, 4-dimethyldiamantane/(3-, 4-dimethyldiamantane + 4-, 9-dimethyldiamantane), DMDI-2 = dimethyldiamantane index 2 = 4-, 8-dimethyldiamantane/(4-, 8-dimethyldiamantane + 4-, 9-dimethyldiamantane).

$$MAI \text{ (methyladamantane index)} = 1-MA/(1-MA+2-MA)$$

$$MDI \text{ (methyldiamantane index)} = 4-MD/(4-MD+1-MD+3-MD)$$

These parameters preferentially coincide with highly mature oils than with mature oils (Chen *et al.*, 1996). Since almost all of the studied oils are in the mature range, these parameters are not so useful to assess the maturity (Fig.4.25), as no significant trend could be observed in the plot of diamondoids concentrations (see Fig.4.24).

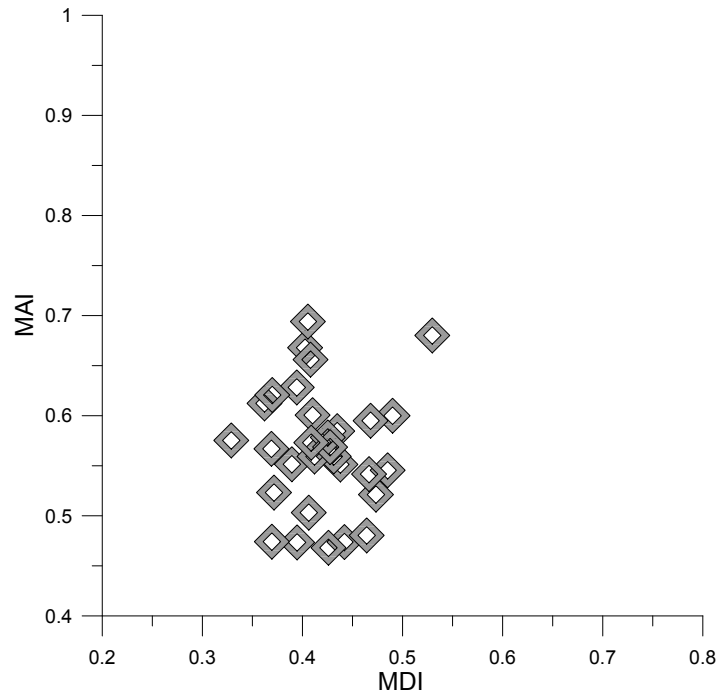


Figure 4.25: Cross plot of methyladamantane index (MAI) versus methyldiamantane index (MDI). Limits of X and Y axis are obtained from (Chen *et al.*, 1996). No significant trend could be recognized.

Diamondoid patterns are also considered as an effective source facies-related parameter according to Schulz *et al.* (2001), who have suggested the following two source-related parameters based on dimethyldiamantanes which are virtually unaffected by thermal maturation (Eq.4.1 and Eq.4.2):

$$DMDI - 1 = 3,4DMD/(3,4DMD + 4,9DMD) \quad (4.1)$$

$$DMDI - 2 = 4,8DMD/(4,8DMD + 4,9DMD) \quad (4.2)$$

From Fig.4.26, two different types of source rocks can be distinguished. The oil samples located below the dashed line show that a clastic is component dominant in the source rock which could be an indication to the Silurian shales. In contrast, oil samples plotting above the dashed line show more carbonate input which could refer to the Upper Cretaceous source rocks.

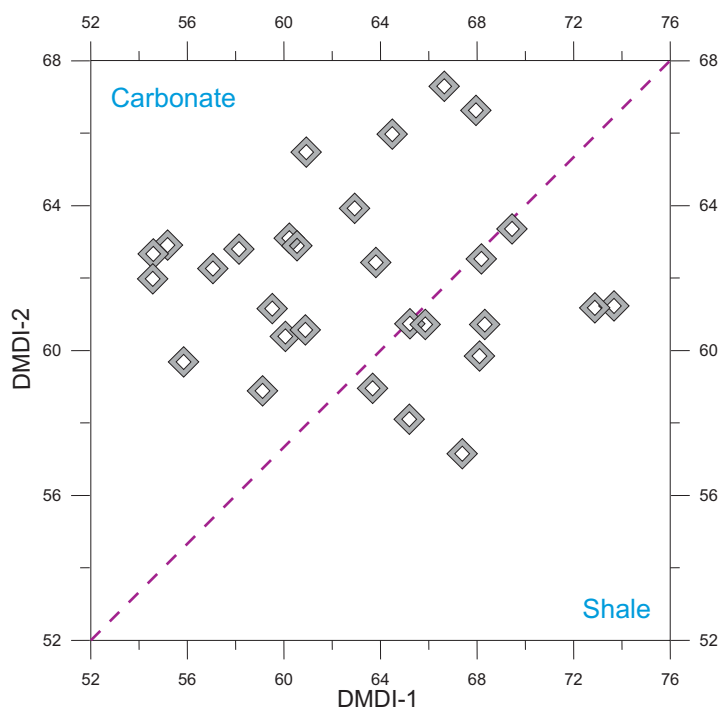


Figure 4.26: Cross plot of dimethyl diamantane index-1 (DMDI-1) versus dimethyl diamantane index-2 (DMDI-2), where DMDI-1 typifies silica type II source and DMDI-2 typifies carbonate type II source (Schulz *et al.*, 2001).

Recap:

G002959 and G002954 crude oils have the highest amount of diamondoids indicating to highly mature source rock which is most likely the Palaeozoic Tanf Formation. On the other hand most of the oils have lower diamondoid contents which could imply that they are generated from source rocks lower in maturation level which are probably the Upper Cretaceous strata. Source facies could be differentiated as well using diamondoid hydrocarbons. Some oils (like G002959, G002954 and G002982) might be generated from clay-rich Silurian source rocks, while others have been generated most likely from Upper Cretaceous carbonate source rocks.

4.1.5 Aromatic Hydrocarbons

Polycyclic Aromatic Hydrocarbons (PAHs) distribution and abundance in oils and source extracts are thought to be influenced by the origin of the organic matter, the depositional environment, source input, and maturation degree of oils and source rocks (Alexander *et al.*, 1985; Budzinski *et al.*, 1995; Huang & Pearson, 1999; Peters *et al.*, 2005). Five groups of PAHs were recognised in oil samples, alkylbenzenes (Hartgers *et al.*, 1992), naphthalenes (van Aarssen *et al.*, 1999), phenanthrenes (Budzinski *et al.*, 1995; Huang *et al.*, 2004), dibenzothiophenes (DBTs) (Chakhmakhchev *et al.*, 1997; Chakhmakhchev & Suzuki, 1995; Depauw & Froment, 1997; Mossner & Wise, 1999), and aromatic steroids (Peters *et al.*, 2005).

Two series of aromatic steroids were recognized using gas chromatography-mass spectrometry corresponding to mono- and triaromatic steroids applying the mass trace at m/z 253, m/z 231 respectively (Philp, 1985). The distribution of monoaromatic steroids in the aromatic fractions of three different oil samples as determined from their m/z 253 chromatograms are depicted in Fig.4.27.

The labeled peaks in this latter figure are identified in Tab.3.9. A visual inspection of the mass chromatograms in Fig.4.27 clearly shows a significant difference in the distribution pattern of monoaromatic steroid hydrocarbons for the investigated oils. In G002964, the compounds number 16 (20R-C₂₉ stigmastane), and number 5 (C₂₇ diacholestane) are nearly absent which could refer to a carbonate source rock. Furthermore, it can be noticed from the fragmentogram of G002954 (Fig.4.27c) that the noise is high and the concentrations of the monoaromatic steroids are low, which indicates a high level of maturity and that the monoaromatic steroids have been cracked. The triaromatic steroids were detected for three oil samples in the key mass chromatogram (m/z 231, Fig.4.28) based on the relative retention times published by Peters *et al.* (2005). There is no significant difference in triaromatic steroids distribution patterns of G002997 and G002964. However, the G002954 fragmentogram (Fig.4.28c) shows hardly recognizable

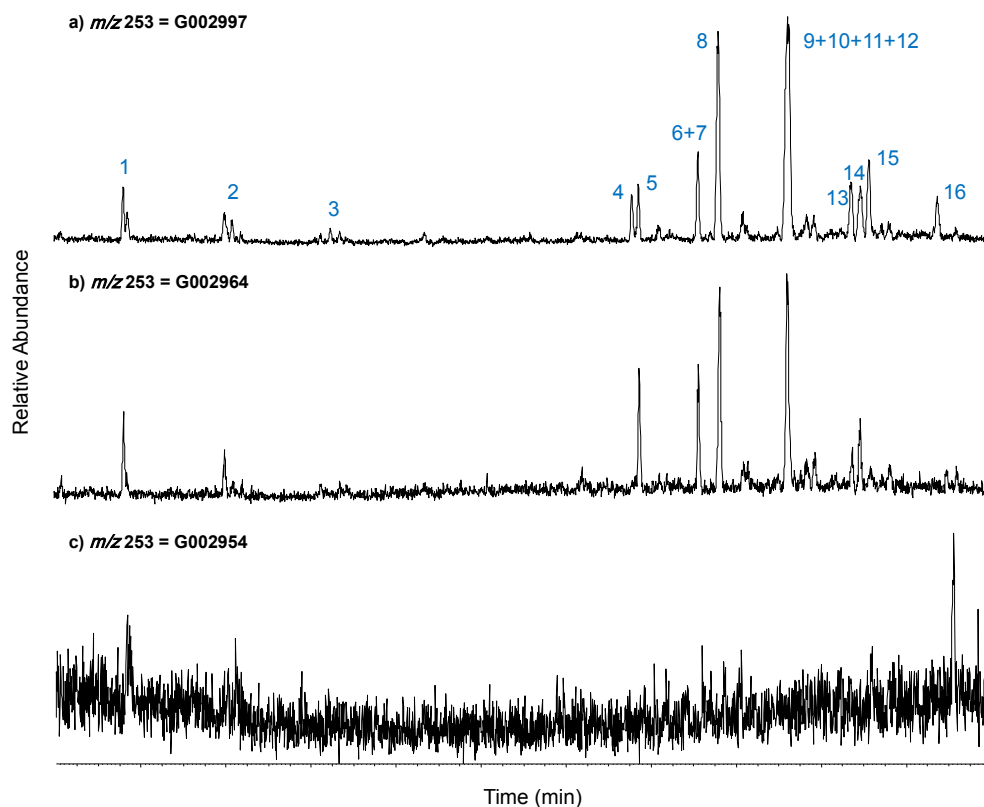


Figure 4.27: Mass chromatograms of m/z 253 showing the distribution of the monoaromatic steroid hydrocarbons in three oil samples. Labeld peaks are identified in Tab.3.9

triaromatic steroid hydrocarbons.

It has been suggested that the extent of cracking in side chains of mono- and triaromatic steroid hydrocarbons can be used to provide information regarding maturity (Seifert & Moldowan, 1978a; Mackenzie *et al.*, 1981a). The abundance ratios of the short- to long-chain components have frequently been used as maturity parameter.

The ratios MA(I)/MA(I+II) and TA(I)/TA(I+II) increase during thermal maturation from 0 to 100 % (Peters *et al.*, 2005; Seifert & Moldowan, 1978) because of (1) preferential cracking of the long-chain rather than short-chain (Beach *et al.*, 1989), or (2) conversion of long-chain to short-chain aromatic steroids or (3) both (Peters & Moldowan, 1993). The monoaromatic steroid ratio was calculated using the sum of all major C_{27} - C_{29} monoaromatic steroids as MA(II) and C_{21} plus C_{22} as MA(I) (Moldowan & Fago, 1986a) (peaks 4-16 and peaks 1-2 respectively in Fig.3.8, the monoaro-

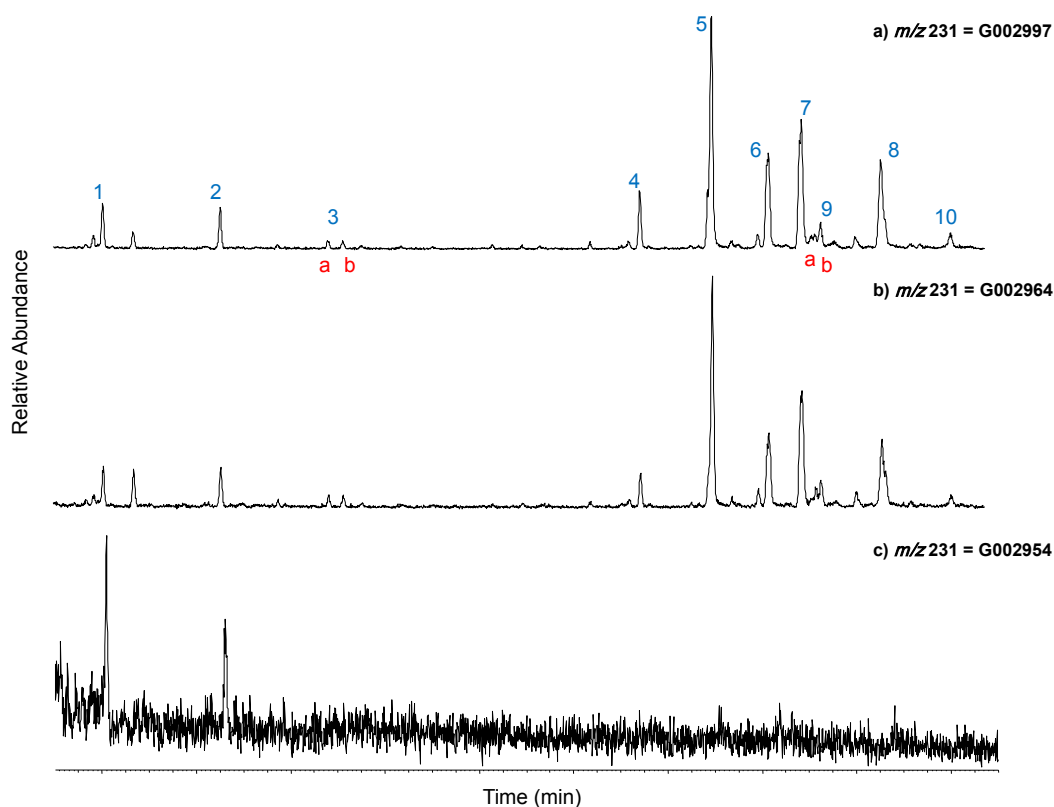


Figure 4.28: Mass chromatograms of m/z 231 showing the distribution of the triaromatic steroid hydrocarbons in three oil samples. Labeld peaks are identified in Tab.3.10

matic steroids chromatogram). The $TA(I)/TA(I+II)$ parameter is measured by concerning the sum of C_{26} - C_{28} ($20S+20R$) triaromatic steroids as $TA(II)$ and the C_{20} and C_{21} triaromatic steroids as $TA(I)$ (peaks 4-8 and peaks 1-2, respectively in Fig.3.9, the triaromatic steroids chromatogram). These aromatic steroids components could not be identified in the samples G002952, G002954, G002959, and G002982 (see Tab.4.7) due to the high levels of maturation. This coincides with investigations obtained from other maturity-related parameters which strengthen the belief of the Silurian origin of these oils.

The Methylphenanthrene Index MPI-1, which has been derived from the distribution of the phanthrene and the methylphenanthrene isomers, is widely used as a maturity indicator (Radke & Welte, 1981). MPI-1 values in crude oils increase with increasing maturity, because the thermally less stable α -isomers 1-methylphenanthrene (1-MP) and 9-methylphenanthrene

| Sample | MPI-1 | R_c | MDR | MA I/(I+II) | TA I/(I+II) |
|---------|-------|-------|------|-------------|-------------|
| G002952 | 0.85 | 1.79 | 1.28 | n.d | n.d |
| G002953 | 0.80 | 0.88 | 2.93 | 0.18 | 0.25 |
| G002954 | 0.88 | 1.77 | 4.38 | n.d | n.d |
| G002956 | 0.69 | 0.81 | 1.81 | 0.11 | 0.13 |
| G002959 | 0.68 | 1.89 | 3.78 | n.d | n.d |
| G002960 | 0.68 | 0.81 | 2.19 | 0.13 | 0.24 |
| G002961 | 0.70 | 0.82 | 1.57 | 0.13 | 0.12 |
| G002963 | 0.75 | 0.85 | 1.78 | 0.19 | 0.21 |
| G002964 | 0.84 | 0.90 | 1.27 | 0.12 | 0.10 |
| G002965 | 0.88 | 0.93 | 3.76 | n.d | 0.65 |
| G002966 | 0.77 | 0.86 | 4.29 | n.d | 0.60 |
| G002968 | 0.73 | 0.84 | 2.72 | n.d | 0.41 |
| G002969 | 0.76 | 0.85 | 2.60 | 0.14 | 0.19 |
| G002973 | 0.76 | 0.86 | 2.54 | 0.16 | 0.17 |
| G002974 | 0.79 | 0.87 | 1.61 | 0.13 | 0.13 |
| G002975 | 0.85 | 0.91 | 4.08 | n.d | 0.34 |
| G002976 | 0.75 | 0.85 | 2.01 | 0.14 | 0.13 |
| G002980 | 0.71 | 1.88 | 1.29 | n.d | 0.22 |
| G002981 | 0.92 | 0.95 | 1.95 | 0.36 | 0.58 |
| G002982 | 0.93 | 1.74 | 3.64 | n.d | n.d |
| G002988 | 0.92 | 0.95 | 2.78 | 0.09 | 0.22 |
| G002993 | 0.96 | 0.97 | 1.44 | 0.07 | 0.09 |
| G002995 | 0.69 | 0.81 | 3.13 | 0.13 | 0.20 |
| G002997 | 0.87 | 0.92 | 1.43 | 0.08 | 0.09 |
| G003005 | 0.82 | 0.89 | 3.06 | 0.13 | 0.18 |
| G003006 | 0.92 | 0.95 | 1.56 | 0.06 | 0.08 |
| G003009 | 0.70 | 0.82 | 3.12 | 0.31 | 0.42 |
| G003011 | 1.00 | 1.00 | 1.52 | 0.05 | 0.08 |
| G003015 | 0.75 | 0.85 | 2.37 | 0.14 | 0.20 |
| G003017 | 0.84 | 0.91 | 1.47 | 0.12 | 0.15 |

Table 4.7: The calculated parameters based on Polycyclic Aromatic Hydrocarbons PAHs. * where: MPI-1 = $[1.5(2\text{-MP} + 3\text{-MP}) / (P + 1\text{-MP} + 9\text{-MP})]$; % R_c = calculated Vitrenite Reflectance which is inferred from MPI-1 values by the formulas given in the text (Eq.4.4 and Eq.4.5); MDR = $4\text{-MDBT} / 1\text{-MDBT}$; MA I/(I+II) = monoaromatic steroids I/(I+II); TA I/(I+II) = triaromatic steroids I/(I+II)

(9-MP) are in the denominator, while the intermediately stable β -isomers 2-methylphenanthrene (2-MP) and 3-methylphenanthrene (3-MP) are in the numerator of the equation Eq.4.3 (Peters *et al.*, 2005).

$$MPI - 1 = [1.5(2 - MP + 3 - MP) / (P + 1 - MP + 9 - MP)] \quad (4.3)$$

The MPI-1 is also influenced by the source lithology and the organic matter type (Cassani *et al.*, 1988), as well as possible effects of migration (Radke *et al.*, 1982a). In studied oils, the MPI-1 index values range between 0.68 - 1.00 (see Tab.4.7). Using this parameter, an equivalent vitrinite

reflectance (% R_c) has been calculated from two equations (Eq.4.4 and Eq.4.5) recommended by (Radke, 1987).

$$\%R_c = 0.6 \times MPI - 1 + 0.4 \dots \dots \dots (R_m < 1.3) \quad (4.4)$$

$$\%R_c = -0.6 \times MPI - 1 + 2.3 \dots \dots \dots (R_m \geq 1.3) \quad (4.5)$$

For most of the investigated oil samples Eq.4.4 has been used for calculations as they are normal to mature oils having probably a R_m below 1.3. However, the second equation Eq.4.5 has been used to calculate the % R_c for five very light oils and condensates, where $^{\circ}\text{API} > 40$ (see Tab.4.1), (namely G002952, G002954, G002959, G002980, and G002982). For this group of oils, % R_c is in the range of 1.74-1.89.

Determination of Polycyclic Aromatic Sulphur Heterocycles PASHs resulted in recognizing dibenzothiophene and the alkyl dibenzothiophenes (DBT, MDBT, DMDBT, and TMDBT) (Mossner & Wise, 1999).

Methylbenzothiophene (MDBT) hydrocarbons distribution patterns are used commonly to differentiate the maturation level of crude oils and source rocks (Chakhmakhchev & Suzuki, 1995; Radke, 1988; Radke *et al.*, 1986; Tissot & Welte, 1984). That is based on the assumption that alkyl-DBT isomers with the methyl substituent in the 1-position have relatively low kinetic stability, whereas isomers with the methyl substituent in the 4-position are the most thermodynamically stable (Chakhmakhchev *et al.*, 1997; Radke, 1987).

Fig.4.29 shows three different alkyl-DBT distribution patterns produced from the aromatic fractions of three crude oil samples (G002954, G002995, and G002564) applying the mass trace at m/z 184+198+212+226. The relationship between DBT hydrocarbons labeled 1 and 4 (red labels) is significantly different from each other implying quite various maturation levels. G002954 illustrates the most mature sample having a clear dominance of 4-MDBT (peak number 4) relative to 1-MDBT (peak number 1) which is kinetically less stable. At the same time, DMDBTs and TMDBTs have so

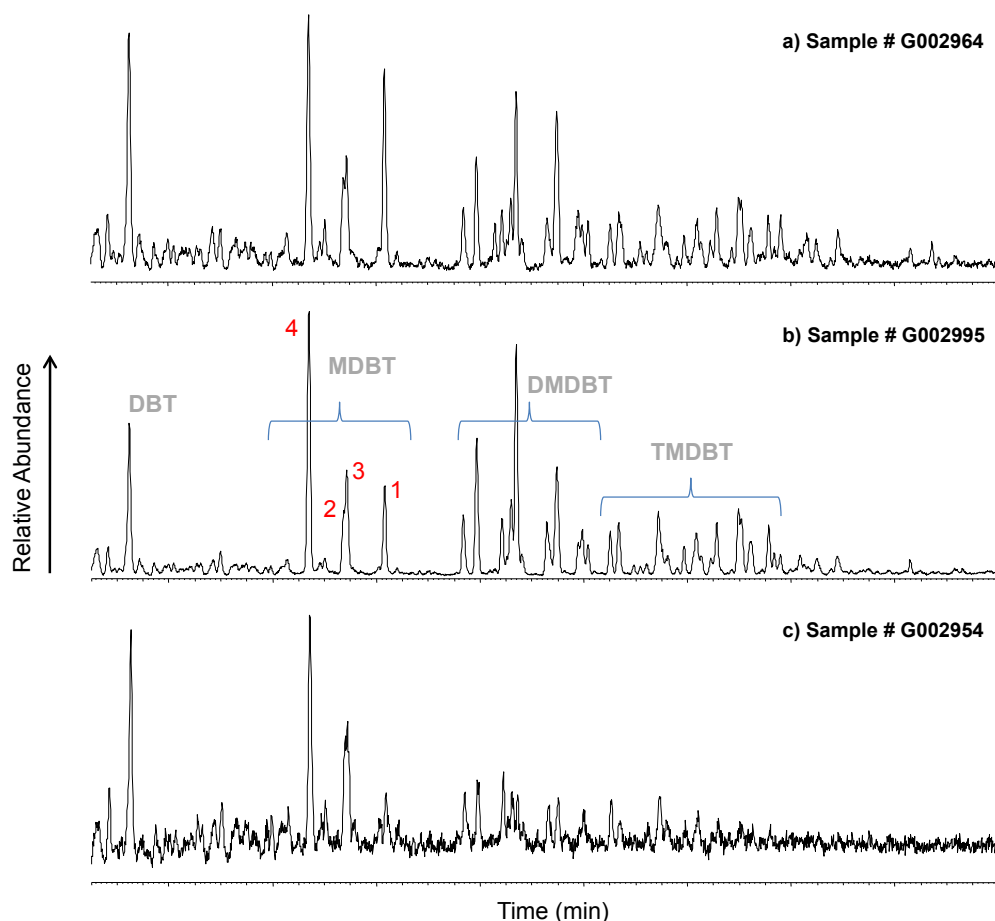


Figure 4.29: Mass chromatograms of m/z 184+198+212+226 showing the distribution of the alkyl-DBT hydrocarbons in three oil samples. Labeled peaks are identified in Fig.3.7 and Tab.3.8 for peak assignments

small peaks hardly to be recognized and identified which is another clue for the high maturity level of this oil.

Source rock lithology and type of the organic matter affect the distribution of the aromatic hydrocarbons (Peters *et al.*, 2005). Radke *et al.* (1986) distinguished Type II kerogen from the Type III one based on the significant difference of MDR (the ratio of 4-MDBT/1-MDBT) values between them. MDR values of Type III kerogen are 2.5 and above, while for Type II kerogen the values are up to 1.0. The investigated Syrian oil samples seem to be derived from a mixed organic matter type (II+III) (Fig.4.30).

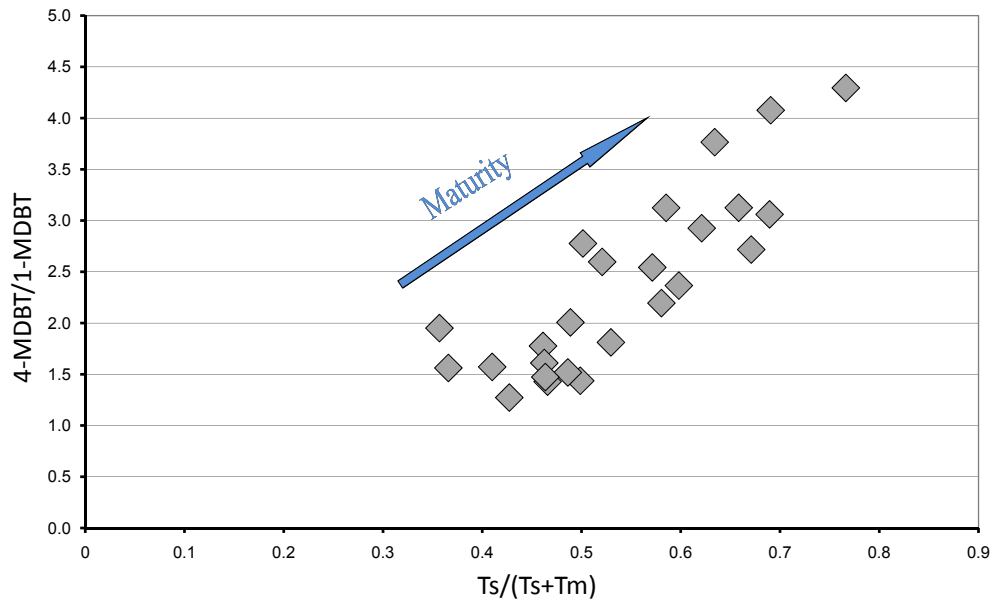


Figure 4.30: 4-MDBT/1-MDBT (MDR) versus $Ts/(Ts+Tm)$ showing a very good correlation suggesting that type (II+III) organic matter generated these oils.

Recap:

Different mono- and triaromatic steroid distribution patterns document the different source and maturity signature of source rocks generating the crude oils of the Euphrates Graben. Mono- and triaromatics in sample G002954 are hardly to recognize probably due to the high maturity. % R_c calculated from MPI-1 shows that oils in the southeastern part of the study area (which have the highest API gravity) are highly mature and could be attributed to the Silurian source rocks.

4.1.6 Stable Isotopes

Isotopes are atoms whose nuclei contain the same number of protons but different number of neutrons. The isotopes of an element have differences in chemical and physical properties "isotope effects" arising from variations in atomic mass. In contrast to the radioactive isotopes, the stable isotope quantities do not differ significantly and remain constant over geologic time. On the other hand, and as a result of chemical and physical processes taking place in nature, variations in stable isotopic signature or the so called "isotopic fractionation" will occur. Stable isotopic fractionation is a process where equilibrium isotopic effects, which are temperature-dependent equilibrium isotope-exchange reactions, and kinetic isotope effects are combined. Petroleum geochemists mostly use carbon and hydrogen isotopic compositions in geochemical studies because they are the most abundant elements in petroleum and in organic matter (Fuex, 1977; Hoefs, 1997). Determination of the stable isotopes is mostly done using mass spectrometric techniques in two different, namely bulk or compound-specific, analytical methods (Hoefs, 1997). Stable isotopic compositions are determined as ratios of heavy to light isotopes and reported in δ -notations (‰) relative to international standards. For carbon isotope ratio calculations, Vienna Pee Dee Belemnite (V-PDB) is the common international standard, as it is the Vienna Standard Mean Ocean Water (V-SMOW) for stable hydrogen isotope determination. The following two equations (Eq.4.6 and Eq.4.7) are used to calculate the carbon and hydrogen isotope ratios:

$$\delta^{13}C[\text{‰}] = \left[\frac{{}^{13}C/{}^{12}C_{\text{sample}}}{{}^{13}C/{}^{12}C_{\text{standard}}} - 1 \right] \times 1000 \quad (4.6)$$

$$\delta D[\text{‰}] = \left[\frac{D/H_{\text{sample}}}{D/H_{\text{standard}}} - 1 \right] \times 1000 \quad (4.7)$$

Compound Specific Isotope Analysis (CSIA) has been carried out to determine carbon and hydrogen isotopic composition of crude oils in this study (see sec.3.1.3).

4.1.6.1 Stable Carbon Isotopes

Carbon is the essential element of hydrocarbons and organic compounds. It has two stable isotopes, ^{13}C and ^{12}C . The lighter one (^{12}C) is favoured by photosynthetic carbon fixation resulting in ^{13}C -depleted biosynthesized organic compounds in comparison to their carbon source. Hayes (1993) has addressed a number of factors controlling the distribution of stable carbon isotopes. The most important are the $\delta^{13}\text{C}$ of carbon source and the isotopic fractionation effects of several photo- and biosynthetic processes. The advantages of determining the $\delta^{13}\text{C}$ values are quite a lot in terms of identify the geological age and depositional environment of source rocks (Andrusovich *et al.*, 1998; Bjoroy *et al.*, 1991b; Gilmour *et al.*, 1984). Moreover, it has been shown that increasing thermal exposure will result in enrichment of ^{13}C in kerogen, due to release of isotopically lighter products, and in crude oils, possibly due to mixing of isotopically light bitumen and isotopically heavier generated products (Clayton, 1991). Biodegradation may alter the short-chain light hydrocarbons (until approximately $n\text{-C}_9$) due to kinetic isotope fractionation that degrades preferentially the $\delta^{13}\text{C}$ values of light molecules (George *et al.*, 2002; Sun *et al.*, 2005). Stable carbon isotope analysis is a very useful technique applied in oil and gas exploration especially when it is used in conjunction with other geochemical and geological data (Peters *et al.*, 2005). $\delta^{13}\text{C}$ values of hydrocarbons depend on the isotopic composition of the source material and the fractionation processes during and after the petroleum formation (Schoell, 1984b). Therefore, origin type and depositional environment of the organic matter, in addition to maturation, migration, mixing and secondary alteration processes have a strong influence on the stable carbon isotopic ratios (Chung *et al.*, 1992; Clayton, 1991; Clayton & Bjoroy, 1994; Dawson *et al.*, 2007; George *et al.*, 2002; Hayes, 1993; Murray *et al.*, 1994; Schoell *et al.*, 1994; Sofer, 1984; Trindade *et al.*, 1992; Vieth & Wilkes, 2006). The stable carbon isotopic compositions of individual alkanes ($n\text{-C}_3$ to $n\text{-C}_{31}$), pristane, phytane, *iso*- and cycloalkanes were measured by the CSIA (see sec.3.1.3) technique for

29 (except for G002968 because it is contaminated with water) crude oil samples (see Appendix B.2). The $\delta^{13}\text{C}$ values of n -alkanes ($n\text{-C}_9$ to $n\text{-C}_{27}$) are plotted in Fig.4.31. This collection of hydrocarbons was chosen because all n -alkanes in this range could be identified reliably in the whole investigated sample set, whereas other components are hard to recognize and quantify out of this series. The $\delta^{13}\text{C}$ values of n -alkanes from the crude oils cover a broad range between -32 and -27 ‰. The profiles of $\delta^{13}\text{C}$ values of n -alkanes from the studied crude oils display a similar trend for the whole sample set; i.e. there is no significant variation in $\delta^{13}\text{C}$ values between lower and higher molecular weight n -alkanes.

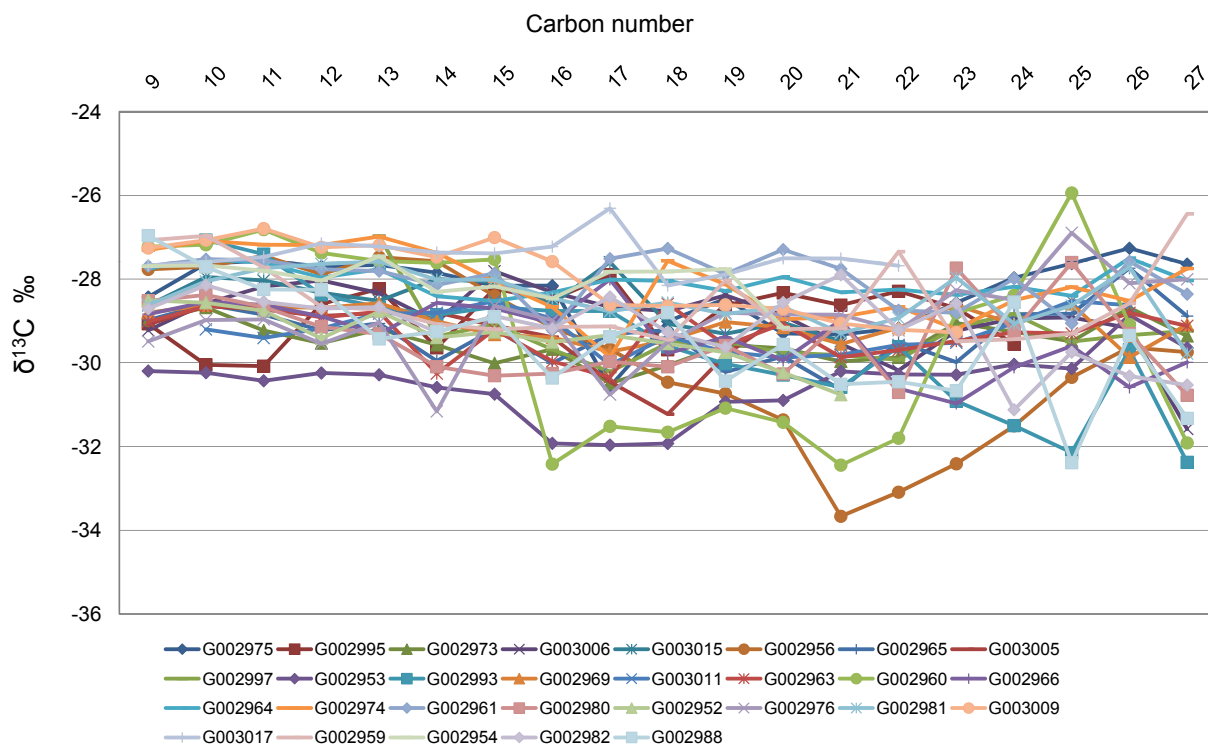


Figure 4.31: Plot of carbon number versus $\delta^{13}\text{C}$ value for n -alkanes ($n\text{-C}_9$ - $n\text{-C}_{27}$) in the Euphrates Graben crude oils. Due to contamination with water, GC-C-IRMS measurements for sample G002968 were not possible.

To assess the possible impacts of source organofacies and thermal maturity on the carbon isotopic signature of the investigated crude oils, two specific compounds were selected. Pristane and phytane (isoprenoid hydrocarbons) have been chosen because of their relative resistivity to isotopic fractionation effects caused by secondary alteration processes (like biodegra-

dation). They thus seem to be reliable indicators for effects on $\delta^{13}\text{C}$ ratios resulting from differences in source and maturity.

Therefore a plot of $\delta^{13}\text{C}$ of pristane in relation to $\delta^{13}\text{C}$ of phytane could represent the variations in source rock organofacies and maturity (Fig.4.32), which was considered as a correlation tool by Collister *et al.* (1992). In this plot it is clear that the enrichment of ^{13}C in one isoprenoid in a given sample is generally accompanied by an enrichment of ^{13}C in others in the same sample. Fig.4.32 shows that the correlation is not one to one exactly, indicating that each compound represents a different mixture from primary sources and that the relative abundances of these sources changed, which could be probably as a result of environmental factors. This could explain why it was not so efficient to rely on the ratio of pristane over phytane to reliably assess the source rock facies and depositional environment as discussed in sec.4.1.2. On the other hand the differences ($<\pm 2\text{‰}$) are not huge in comparison to the 6 ‰ depletion observed in other petroleum systems (Freeman *et al.*, 1990).

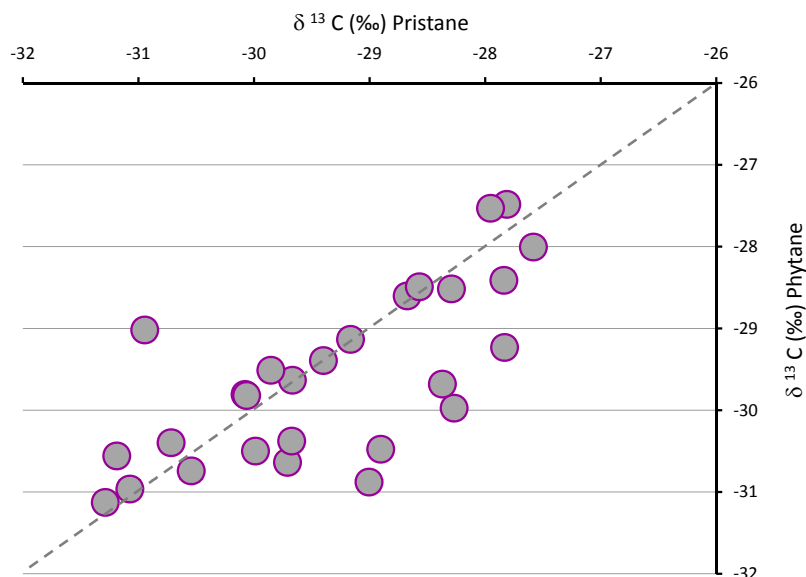


Figure 4.32: Carbon isotopic composition of pristane and phytane in individual oil samples. A linear correlation with certain deviations was recognized.

Source origin and maturation levels of the sample set have been evaluated from some biomarkers and non-biomarkers in previous sections (sec.4.1.1

through sec.4.1.5). An attempt to see how these formerly discussed source- and maturity-related parameters connect to the carbon isotopic signatures will be presented in the following lines.

As discussed in sec.4.1.3.2, the dia/reg C_{27} - C_{29} sterane ratio indicates clay-rich versus clay-poor source rocks for the investigated oils. Besides, it differentiates high mature from lower mature crude oils.

Plotting this parameter against the $\delta^{13}\text{C}$ of pristane and phytane (Fig.4.33) shows that nearly the samples have generally a slight negative trend, i.e. stable carbon isotope values are getting heavier with increasing biomarker ratio. G002954 and G002959 crude oils considered as the highest mature samples have the highest biomarker ratio and are among the isotopically heaviest samples (27.58 ‰ and 28.67 ‰ for pristane, 28.01 ‰ and 28.60 ‰ for phytane, respectively).

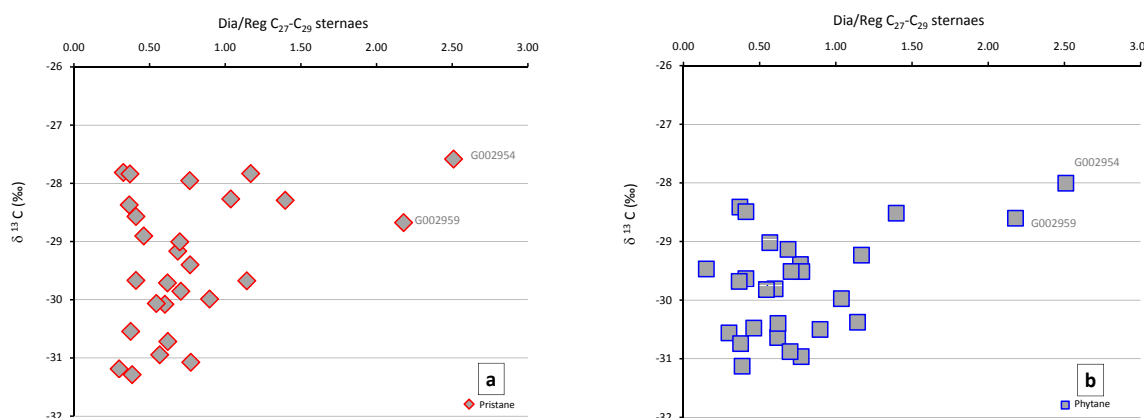


Figure 4.33: Plots of carbon isotopic signature of pristane (a) and phytane (b) versus number versus dia/reg C_{27} - C_{29} steranes. A slight negative trend could be recognized.

By increasing the maturation level of crude oil the concentrations of diamondoids (i.e. adamantenes and diamantenes) will increase due to the high stability of these compounds at high temperatures (see section. 4.1.4). G002954 and G002959 have the largest amounts of adamantanes among the investigated crude oils (5459 and 9175 ppm, respectively) (see Appendix.B.1). Plotting this parameter against the $\delta^{13}\text{C}$ of pristane and phytane (Fig.4.34) shows that nearly all samples have generally a slight negative trend, i.e. stable carbon isotope values are getting heavier with an increase

of this diamondoid-based maturity parameter.

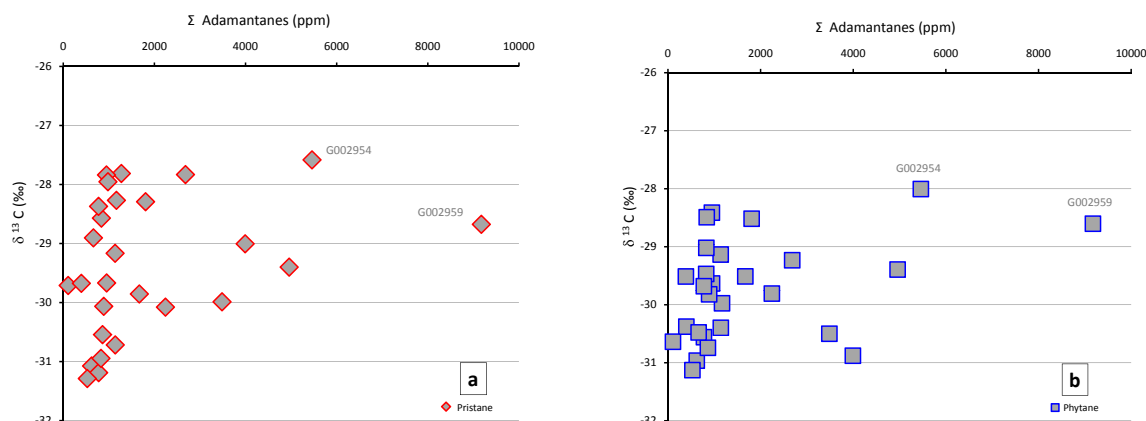


Figure 4.34: Plots of carbon isotopic signature of pristane (a) and phytane (b) versus number versus the sum of adamantene hydrocarbons concentration. A slight negative trend could be recognized especially for pristane.

4.1.6.2 Stable Hydrogen Isotopes

Hydrogen, as the most abundant element on the planet, consists of two main stable isotopes, protium (^1H , 99.985 % natural abundance) and deuterium (D, ~ 0.015 % natural abundance). It is the fundamental element in the hydrological cycle and a principle element in sedimentary organic matter and fossil fuels. Therefore, the distribution of the stable hydrogen isotopes is controlled by a number of processes occurring in the global hydrological cycle and in the biosynthesis in different organisms (Estep & Hoering, 1980; Schimmelmann *et al.*, 2006; Sessions *et al.*, 1999). Hydrogen has the largest natural variation in stable isotope ratios because it has the largest mass difference (2:1) between its two stable isotopes. Thus, stable hydrogen isotopes (δD) signatures are one of the most powerful and promising technique in petroleum geochemistry. Many geochemical studies have revealed that the stable hydrogen isotopic compositions of crude oil components are significantly influenced by physical and chemical processes accompanying or occurring after petroleum formation and accumulation such as depositional environment, organic matter type, migration, maturation, mixing and secondary alteration (Dawson *et al.*, 2005; Hassan & Spalding, 2001; Li *et al.*, 2001; Pedentchouk *et al.*, 2006; Pond *et al.*, 2002; Radke *et al.*,

2005; Rigby *et al.*, 1981; Rooney *et al.*, 1998; Schimmelmann *et al.*, 2006; Smith *et al.*, 1981; Sun *et al.*, 2005; Xiong *et al.*, 2005; Yeh & Epstein, 1981; Morasch *et al.*, 2004). The D/H compositions of individual alkanes ($n\text{-C}_3$ to $n\text{-C}_{31}$), pristane, phytane, *iso*- and cycloalkanes were measured by the CSIA technique for 29 (except for G002968 because it is contaminated with water) crude oil samples (see Appendix B.3). Missing values for compounds in individual samples are due to limited baseline separation and increased standard deviations ($>5\%$) for the three replicate measurements, and therefore are not shown.

The δD values of n -alkanes ($n\text{-C}_6$ - $n\text{-C}_{27}$), pristane and phytane are plotted in Fig.4.35. The δD values of n -alkanes from the crude oils have a broad range between -180 and -60 ‰. Pristane and phytane are clearly depleted (0 to $\sim 40\%$) in D relative to related n -alkanes ($n\text{-C}_{17}$ to $n\text{-C}_{20}$). The profiles of δD values of n -alkanes from the studied crude oils display similar trends for the whole sample set; i.e. the lower molecular weight n -alkanes ($\approx n\text{-C}_6$ to $n\text{-C}_{17}$, Fig.4.35) are depleted in D relative to the higher molecular weight n -alkanes ($\approx n\text{-C}_{19}$ to $n\text{-C}_{27}$, Fig.4.35). The amount of D-enrichment increases with increasing n -alkane carbon number, possibly as a combined result of greater thermal cracking of longer-chain n -alkanes, and the generation of isotopically lighter, short chain compounds (Tang *et al.*, 2005; Schimmelmann *et al.*, 2004). Maturation processes appear to have had a greater effect on the isotopic distribution of hydrogen than carbon.

It is believed that significant hydrogen exchange between organic hydrogen and the surrounding environment takes place during diagenetic and catagenetic effects over million of years of geological time (Alexander *et al.*, 1984; Schimmelmann *et al.*, 1999; Sessions *et al.*, 2004). Thermal stress particularly has been found to play a significant role in the alteration of indigenous δD signatures (Rigby *et al.*, 1981). Published work on maturation in natural systems provides evidence of gradual D-enrichment of organic matter with increasing thermal maturity (Rigby *et al.*, 1981; Li *et al.*, 2001; Smith *et al.*, 1981).

Similar to what has been described in sec.4.1.6.1, it is efficient to present

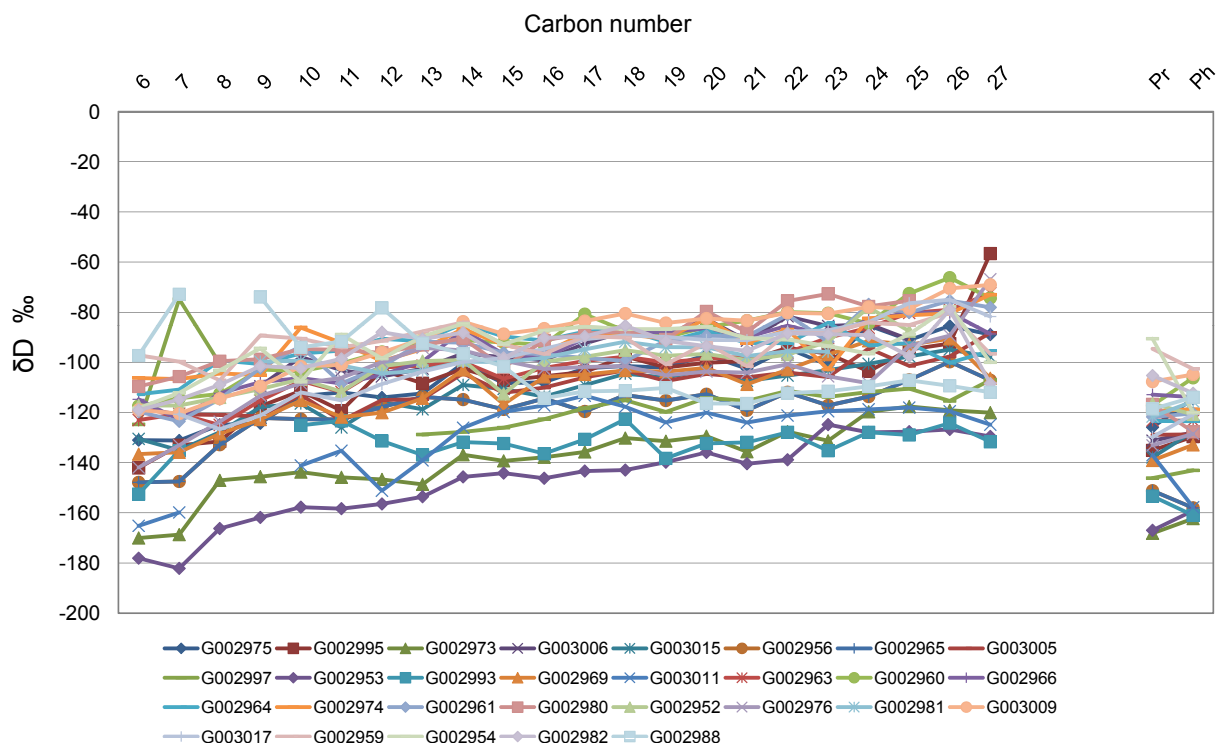


Figure 4.35: Plot of δD value versus carbon number for n -alkanes (n - C_6 - n - C_{27}), pristane and phytane in the Euphrates Graben crude oils. Due to contamination with water, GC-C-IRMS measurements for G002968 crude oil were not possible.

a plot of the hydrogen isotopic signature of pristane versus that of phytane and see how the relationship between their hydrogen isotopic composition looks like. A recognizable linear correlation close to one to one trend is seen in Fig.4.36.

One should surly not ignore the huge skeptic nowadays about the usage of hydrogen isotopic signatures in terms of assessing and evaluating the source rock characteristics and degree of maturation because this proxy needs to be understood quit well as a several factors and players have their own and different influence on. But, on the other hand, one could benefit from these isotopic values in combination with other biomarkers and non-biomarkers to better understand the different processes affecting the composition of reservoired crude oils.

In the previous paragraph sec.4.1.6.1 it was shown that the possible difference in source rock organofacies and maturity do not influenced sig-

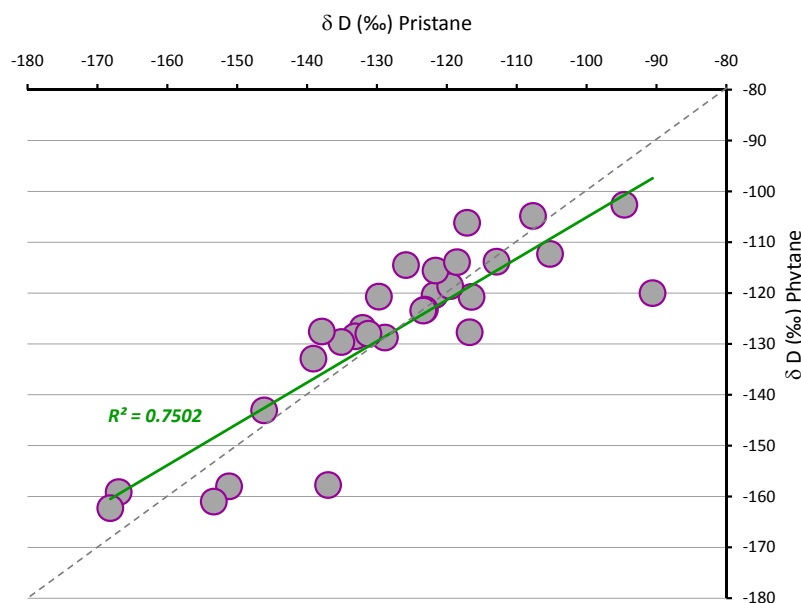


Figure 4.36: Hydrogen isotopic composition of pristane and phytane in individual oil samples. A very good linear correlation could be recognized, that is much better than that one of carbon isotope shown in Fig.4.32.

nificantly the carbon isotopic signature of individual hydrocarbons in the crude oils. Conversely, it appears likely that the hydrogen isotopic composition of these crude oil samples is affected by the source rocks. In the same way, the following section will describe the relationship between the same parameters and compound-specific hydrogen isotope ratios of pristane and phytane. Fig.4.37 illustrates the source- and maturity-related dia/reg C_{27} - C_{29} steranes ratio in relation to the δD ratios of pristane and phytane. There is quite a good correlation with the increasing biomarker ratio, indicating a gradual enrichment of D in the investigated oil samples where this trend is stronger in pristane case than it is in phytane one. The highest δD values of pristane and phytane are found for samples G002954 and G002959.

A cross plot of the average δD values of pristane and phytane versus the sum of adamantane concentrations is presented in Fig.4.38. Interestingly, the δD ratios of the isoprenoids show a systematic correlation to the thermal maturity parameter. In the investigated crude oils, there is a clear relationship linking the increase of the adamantane concentrations and the enrichment of isoprenoid constituents in deuterium as an indication of elevated maturation level. The enrichment of deuterium with increasing matu-

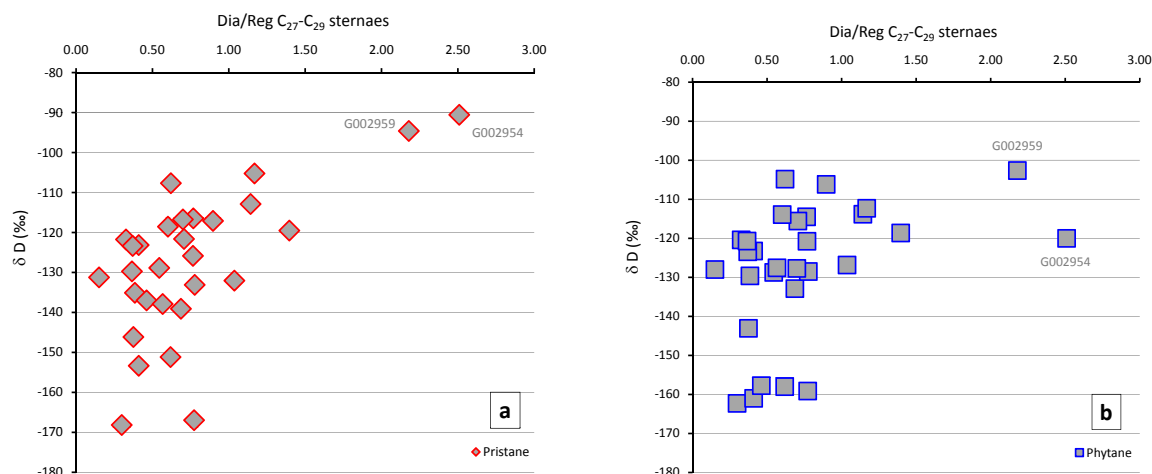


Figure 4.37: Plots of hydrogen isotopic signature of pristane (a) and phytane (b) versus dia/reg C_{27} - C_{29} steranes. Increasing biomarker ratio is in agreement to gradual elevating of D-enrichment. It could be recognised that the correlation of this biomarker is better in pristane than in phytane case.

rity possibly because: (1) water-derived hydrogen is added or (2) exchanged with organic hydrogen, or (3) both (Schimmelmann *et al.*, 1999 2001). This process continues during time until the exchangeable organic hydrogen isotopically equilibrates with the larger pool of hydrogen in water (Lis *et al.*, 2006; Alexander *et al.*, 1984). Interestingly, the compound-specific hydrogen isotopic signature of the isoprenoids have such limit which is not exceedable whatever the maturity reaches, which is -91 ‰ for pristane δD values (sample G002954) and of -103 ‰ for phytane δD values (sample G002959), Tab.4.8. This has been called as an "isotopic equilibrium" between hydrocarbons and water and lies in general in the range of -80 ‰ and -110 ‰ (Schimmelmann *et al.*, 2006; Santos Neto & Hayes, 1999).

Pedentchouk *et al.* (2006) and Dawson *et al.* (2007) have done studies on sedimentary source rocks and showed that with increasing maturity the isoprenoids (pristane and phytane) become significantly enriched in deuterium relative than n -alkanes. It was also shown that with increasing thermal stress the differences of δD ratios between n -alkanes and isoprenoids gradually decrease. Hence, the hydrogen isotopic compositions of crude oils, which are expelled during different stages of thermal maturity, may reflect the thermally promoted hydrogen exchanges by varying differences

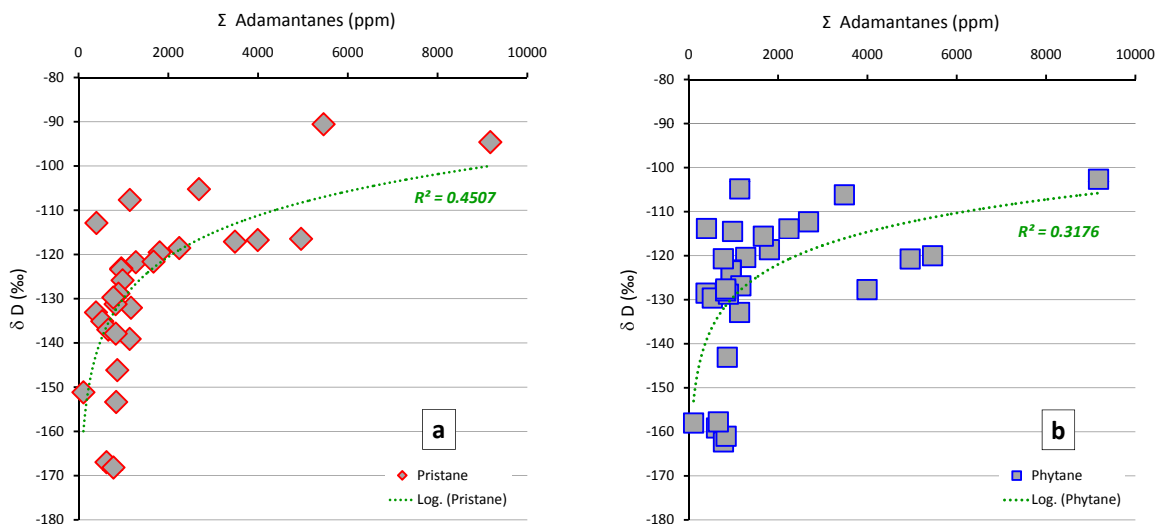


Figure 4.38: Plots of hydrogen isotopic signature of pristane (a) and phytane (b) versus the sum of adamantene concentration. Good correlation is observed as an exponential trend especially for pristane.

in δD ratios for isoprenoids and n -alkanes and, hence, denote to different levels of thermal maturity. Fig.4.39 shows the adamantane concentrations in response to the calculated difference of summed δD ratios for pristane and phytane and the summed δD ratios for n -heptadecane (n - C_{17}) and n -octadecane (n - C_{18}) (see Tab.4.8).

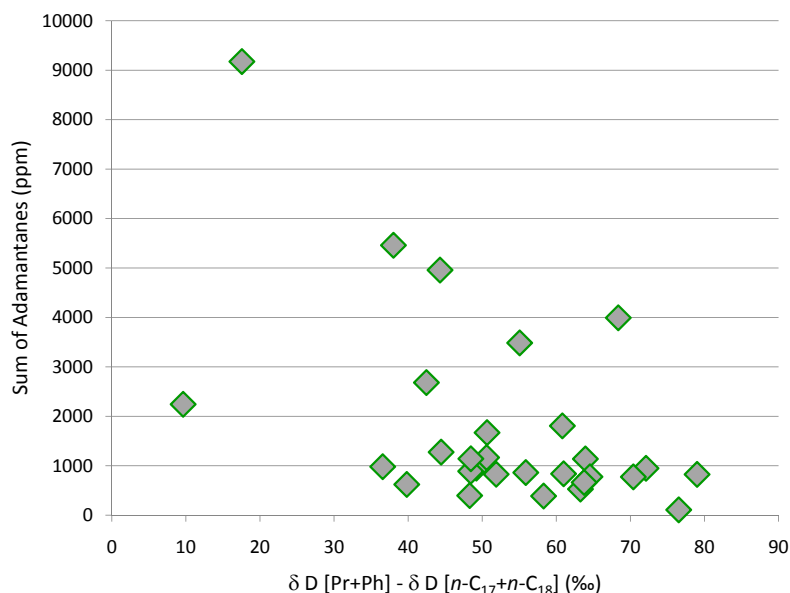


Figure 4.39: Cross plot showing the correlation of diamondoid-based maturity parameter to the calculated difference of summed δD values of pristane and phytane and the sum for δD values of n - C_{17} and n - C_{18} .

After (Dawson *et al.*, 2007; Pedentchouk *et al.*, 2006), with increasing maturity the calculated difference should decrease, which is indicated by higher concentrations of adamantane hydrocarbons. Interestingly, a systematic decrease of the calculated difference between δD ratios for isoprenoids and n -alkanes in the investigated oil samples is recognizable. This would strengthen the idea that the thermal processes have played a significant role in determining the δD composition of constituent of Syrian oils, and therefore could be a useful tool to differentiate oils from high mature source rocks (Silurian Tanf Formation) from less mature crude oils generated from Upper Cretaceous source rocks.

Dawson (2006) has investigated extracts from immature to highly mature sediments from the Perth Basin, Australia in terms of hydrogen isotope geochemistry. He has found that pristane and phytane in immature sediments were significantly depleted in deuterium by ca. 114 to 116‰ relative to n -alkanes in the sample set. This offset appears to represent the difference in isotopic signatures of their precursor (biosynthesized n -alkanes and isoprenoid lipids) (Estep & Hoering, 1980; Sessions *et al.*, 1999). In early mature strata the depletion in D of the isoprenoids was about 30 to 55‰ relative to n -alkanes. However, the difference of the δD ratio between isoprenoids and n -alkanes in mature samples had values of 6 to 23‰. In extracts from late mature sediments, where R_o is about 1.3%, the depletion in the heavy hydrogen isotope (D) of pristane and phytane was in the range of 0 to 19‰ relative to n -alkanes in the same sample. This means that the difference between δD values of isoprenoids and n -alkanes decreases gradually with increasing thermal stress, i.e. the offset between the average δD values of n -alkanes and the average δD values of isoprenoids is declining with maturation progress.

In the investigated oil samples, the offset in hydrogen isotopic signature between isoprenoids and n -alkanes ($\Delta\delta D$ ‰) ranges ca. 8 to 38‰ (see Tab.4.8). Following Dawson (2006), the analysed oil samples fall in the maturity range from early mature to high mature crude oils; with the most mature sample (G002959) has the lowest value of $\Delta\delta D$ (8‰). Fig.4.40

| Sample | Pr | Ph | Iso. Ave. | iso-alkane | Alkanes.Ave | $\Delta\delta D$ |
|---------|------|------|-----------|------------|-------------|------------------|
| G002952 | -116 | -121 | -119 | 44 | -99 | -20 |
| G002953 | -167 | -159 | -163 | 40 | -144 | -19 |
| G002954 | -91 | -120 | -105 | 38 | -91 | -14 |
| G002956 | -151 | -158 | -155 | 77 | -116 | -38 |
| G002959 | -95 | -103 | -99 | 18 | -91 | -8 |
| G002960 | -117 | -106 | -112 | 55 | -89 | -22 |
| G002961 | -122 | -120 | -121 | 44 | -93 | -28 |
| G002963 | -123 | -123 | -123 | 49 | -100 | -24 |
| G002964 | -123 | -123 | -123 | 72 | -91 | -32 |
| G002965 | -132 | -127 | -129 | 51 | -107 | -22 |
| G002966 | -113 | -114 | -113 | 48 | -94 | -20 |
| G002968 | n.d | n.d | n.d | n.d | n.d | n.d |
| G002969 | -139 | -133 | -136 | 64 | -107 | -29 |
| G002973 | -168 | -162 | -165 | 65 | -135 | -30 |
| G002974 | -120 | -119 | -119 | 61 | -91 | -28 |
| G002975 | -126 | -114 | -120 | 37 | -104 | -16 |
| G002976 | -133 | -129 | -131 | 58 | -103 | -28 |
| G002980 | -117 | -128 | -122 | 68 | -88 | -34 |
| G002981 | -122 | -116 | -119 | 51 | -98 | -21 |
| G002982 | -105 | -112 | -109 | 42 | -93 | -16 |
| G002988 | -119 | -114 | -116 | 10 | -103 | -13 |
| G002993 | -153 | -161 | -157 | 61 | -131 | -26 |
| G002995 | -135 | -130 | -132 | 63 | -104 | -28 |
| G002997 | -146 | -143 | -145 | 56 | -118 | -27 |
| G003005 | -129 | -129 | -129 | 48 | -109 | -20 |
| G003006 | -131 | -128 | -130 | 79 | -94 | -36 |
| G003009 | -108 | -105 | -106 | 48 | -88 | -19 |
| G003011 | -137 | -158 | -147 | 64 | -125 | -22 |
| G003015 | -138 | -128 | -133 | 52 | -110 | -23 |
| G003017 | -130 | -121 | -125 | 70 | -97 | -29 |

Table 4.8: δD values of parameters used in Figs.4.36-4.41, where: Iso.Ave=the average δD values of pristane and phytane, iso-alkane=the calculated difference of summed δD values of pristane and phytane and the sum for δD values of $n-C_{17}$ and $n-C_{18}$, Alkanes.Ave.=the average δD values of n -alkanes in the range from $n-C_9$ to $n-C_{25}$, $\Delta\delta D$ =the offset in hydrogen isotopic signature between the average in δD values of isoprenoids (pristane and phytane) and n -alkanes (in the range from $n-C_9$ to $n-C_{25}$).

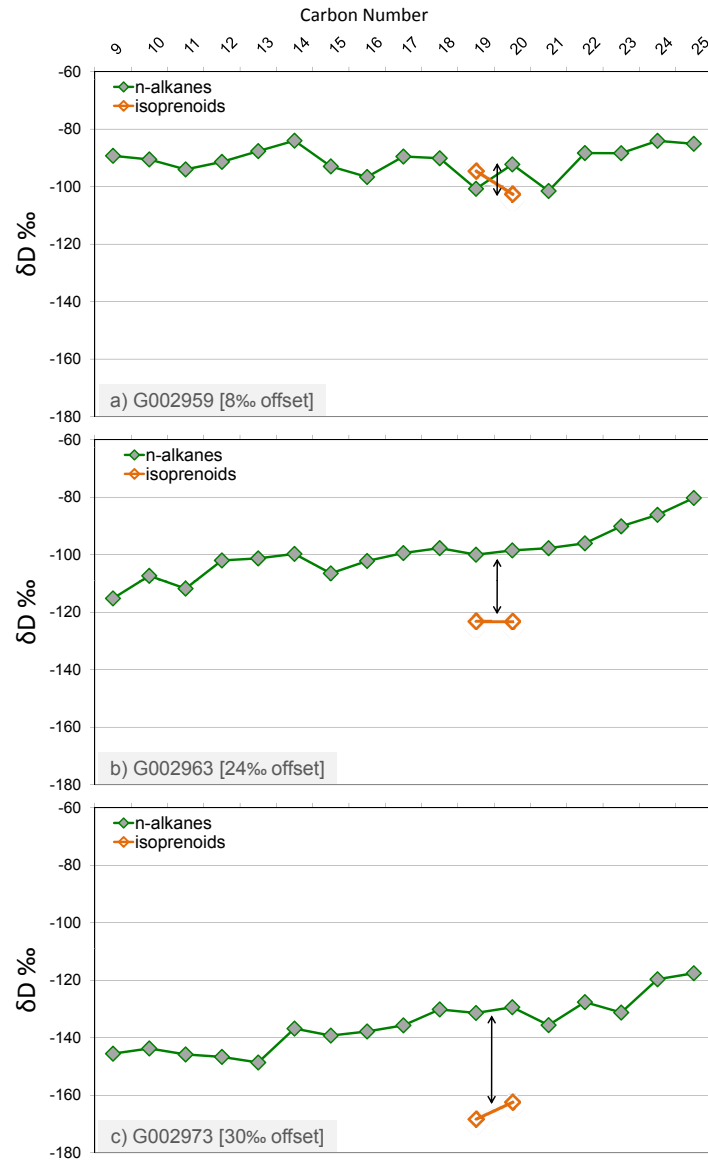


Figure 4.40: δD values of n -alkanes (n -C₉ to n -C₂₅), pristane and phytane from three crude oils. (a) G002959: offset 8‰, (b) G002963: offset 24‰, and (c) G002973: offset 30‰. Different maturation levels could be recognized looking at the different offset values (shown in parenthesis) as discussed in text.

shows three isotopically different oil samples regarding the n -alkane and isoprenoids isotopic signatures.

The n -alkane hydrogen isotopic compositions of samples G002959 and G002963 (average is -91‰ and -100‰, respectively) are significantly enriched in D relative to n -alkanes in sample G002973 (average is -135‰), which could imply a lower maturity level of the latter. This is consistent with the findings of Dawson *et al.* (2005), that mature to late mature sam-

ples have average δD values of n -alkanes heavier than -126‰ , in contrast to immature marine oils which have values about -150‰ (Santos Neto & Hayes, 1999). In this context it is noticed that almost all investigated oils have a significant level of maturity as their n -alkanes are enriched in D and have δD average values above -125‰ (see Tab.4.8). A general tendency of the D-enrichment with maturity is clearly evident in both compound classes, with the rate of enrichment being more rapid in isoprenoids relative to n -alkanes (Fig.4.41). However, similar trends for pristane and phytane are observed indicating similar rates of D-enrichment with maturity for both isoprenoids.

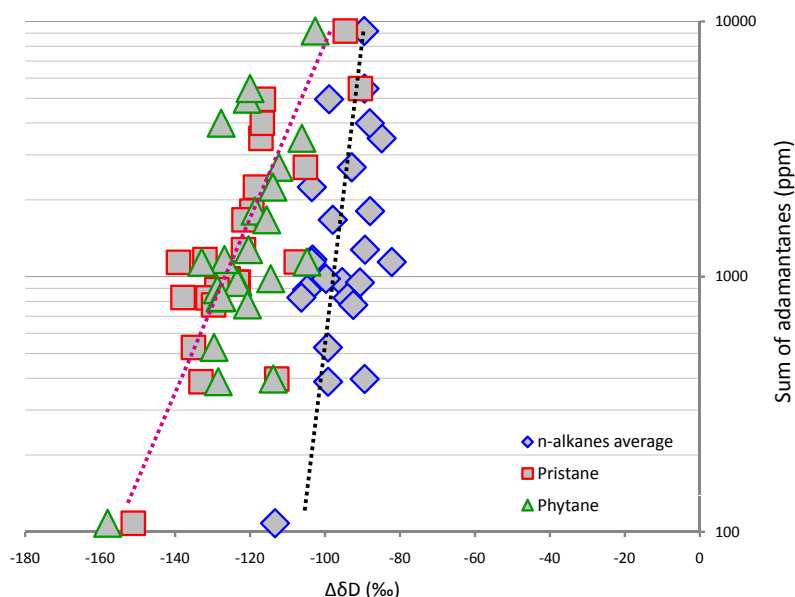


Figure 4.41: A maturity profile of the average δD values of n -alkanes, and δD values of pristane and phytane for investigated oil samples. Some samples were not plotted (e.g. G002993 and G002997) as they have possible biodegradation effect.

Average δD value of n -alkanes changes from -99 to -85‰ (ca. 14‰), while δD values of pristane and phytane change in comparable manner with maturation from -135 to -95‰ (ca. 40‰). This difference in behavior of both n -alkanes and isoprenoids, i.e isoprenoids getting isotopically enriched in D faster than n -alkanes could be attributed to the assumption that the isotopic enrichment (hydrogen isotopic exchange) occurs via a mechanism that proceeds faster with compounds containing tertiary carbon centres

(like pristane and phytane) than with compounds containing only primary or secondary carbon atoms (like *n*-alkanes) (Dawson *et al.*, 2007; Sessions *et al.*, 2004).

Recap:

The profiles of $\delta^{13}\text{C}$ values of *n*-alkanes from the studied crude oils display a similar trend for the whole sample set; i.e. there is no significant variation in $\delta^{13}\text{C}$ values between lower and higher molecular weight *n*-alkanes. $\delta^{13}\text{C}$ of pristane in relation to $\delta^{13}\text{C}$ of phytane shows a good linear correlation, the differences could be attributed to the different sources of these isoprenoids or different isotopic effects during their formation. Slight tendency was recognized for $\delta^{13}\text{C}$ with increasing maturity.

The profiles of δD values of *n*-alkanes from the studied crude oils also display similar trend for the whole sample set; i.e. the lower molecular weight *n*-alkanes ($\approx n\text{-C}_6$ to $n\text{-C}_{17}$) are depleted in D relative to the higher molecular weight *n*-alkanes ($\approx n\text{-C}_{19}$ to $n\text{-C}_{27}$). A very good correlation has been found between δD values of isoprenoids (pristane and phytane) and maturity-related biomarkers and non-biomarkers. Maturation processes appear to have had a greater effect on the isotope distribution of hydrogen than carbon. With increasing maturity pristane and phytane are getting enriched in D. The offset in hydrogen isotopic signature between isoprenoids and *n*-alkanes ($\Delta\delta\text{D}$) illustrates that G002959 has the lowest value of 8‰ and therefore can be considered as the most mature oil in the sample set.

4.2 Rock Samples

4.2.1 Source Rock Quality

Rock samples from three potential source rocks, two Upper Cretaceous (R'mah and Shiranish Formations) and one Silurian in age (Abba formation) in the study area were analysed. Rock-Eval pyrolysis (Espitalie *et al.*, 1977) has been used to identify the quality of the organic matter in the rock samples. Both R'mah samples (G005145 and G005117) have Total Organic Carbon (TOC) content below 1 % (0.9 and 0.7 %, respectively) (see Fig.4.42).

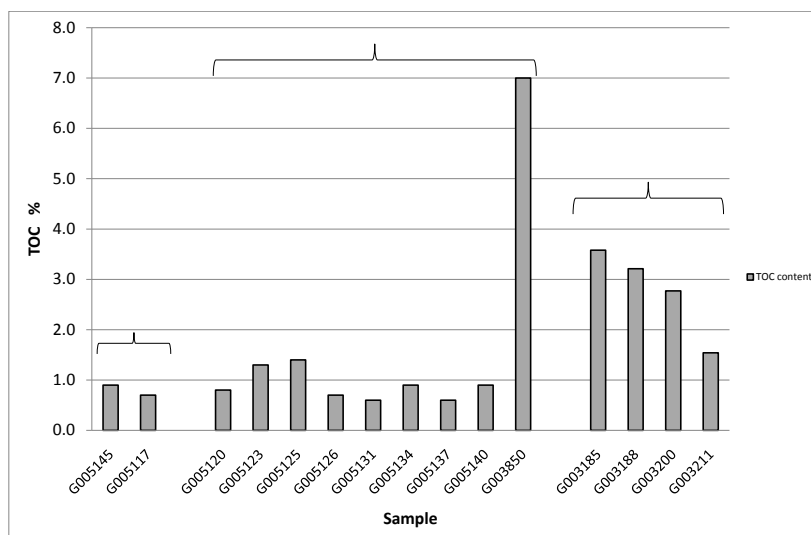


Figure 4.42: TOC content in analysed rock samples from three different potential source rocks (R'mah, Abba, and Shiranish Formations).

The TOC content of Shiranish rock samples ranges from 1.5 - 3.6 % pointing to a good to very good potential source rock. Except for the sample number G003850, which has a TOC content of 7.0 %, all other Silurian Abba samples have values between 0.6 and 1.4 % thus representing a fair to good source rock according to criteria in Peters (1986a). The Hydrogen Index (HI), and the Oxygen Index (OI) values of both R'mah (blue and pink diamonds in Fig.4.43, left) rock samples are in the range between 123 - 209 mg HC/g TOC and 68 - 87 mg CO₂/g TOC, respectively (see Tab.4.9), indicating mixed type II and III kerogen. Shiranish rock samples (red diamonds in Fig.4.43, left) plot in two separated locations

| Sample | Formation | Depth (m) | S1 | S2 | S3 | Tmax | TOC | OI | HI | PI |
|----------------|-------------|-------------|------|-------|------|------|-----|-----|-----|------|
| G005145 | R'mah | 3626 - 3633 | 0.04 | 1.11 | 0.61 | 434 | 0.9 | 68 | 123 | 0.03 |
| G005117 | R'mah | 3745 - 3755 | 0.39 | 1.46 | 0.61 | 437 | 0.7 | 87 | 209 | 0.21 |
| G005120 | Abba | 3330-3345 | 0.16 | 0.38 | 1.11 | 427 | 0.8 | 139 | 48 | 0.30 |
| G005123 | Abba | 3445-3455 | 0.04 | 1.04 | 0.09 | 435 | 1.3 | 7 | 80 | 0.04 |
| G005125 | Abba | 3485-3505 | 0.05 | 2.47 | 0.2 | 435 | 1.4 | 14 | 176 | 0.02 |
| G005126 | Abba | 3380+3385 | 0.02 | 0.5 | 1.84 | 435 | 0.7 | 263 | 71 | 0.04 |
| G005131 | Abba | 2320-2330 | 0.02 | 0.54 | 0.23 | 430 | 0.6 | 38 | 90 | 0.04 |
| G005134 | Abba | 2840+2845 | 0.05 | 1.83 | 0.3 | 432 | 0.9 | 33 | 203 | 0.03 |
| G005137 | Abba | 3585-3595 | 0.02 | 0.17 | 1.13 | 429 | 0.6 | 188 | 28 | 0.11 |
| G005140 | Abba | 2450-2455 | 0.03 | 0.85 | 0.34 | 435 | 0.9 | 38 | 94 | 0.03 |
| G003850 | Abba | 3030 | 0.2 | 5 | 0.8 | 465 | 7.0 | 11 | 71 | 0.04 |
| G003185 | U.Shiranish | 2970 | 2.78 | 16.14 | 0.41 | 437 | 3.6 | 11 | 451 | 0.15 |
| G003188 | U.Shiranish | 3030 | 2.19 | 12.96 | 0.5 | 436 | 3.2 | 16 | 404 | 0.14 |
| G003200 | L.Shiranish | 3300 | 2.03 | 7.82 | 0.28 | 439 | 2.8 | 10 | 282 | 0.21 |
| G003211 | L.Shiranish | 3520 | 1.36 | 3.31 | 0.41 | 438 | 1.5 | 27 | 215 | 0.29 |

Table 4.9: Rock-Eval data of the analysed samples of three potential source rocks plotted in Fig.4.43.

showing a remarkable difference in petroleum potential. Upper Shiranish samples (type II organic matter) are in the range between 404 - 451 mg HC/g TOC for HI and between 11 - 16 mg CO_2 /g TOC for OI, whereas the values of HI and OI for the Lower Shiranish samples (type II/III organic matter) range between 215 - 282 mg HC/g TOC, and between 10 - 27 mg CO_2 /g TOC, respectively (see Tab.4.9). Similarly, Silurian Abba samples (green and yellow diamonds in Fig.4.43, left) form two groups as well; the first one has type II/III organic matter signatures (HI >70 mg HC/g TOC and OI <38 mg CO_2 /g TOC), and the second one has kerogen type III (HI <70 mg HC/g TOC and OI >139 mg CO_2 /g TOC).

The maturity level of the source rock sample was estimated by Tmax, which is the temperature at which the maximum hydrocarbon generation rate occurs during Rock-Eval pyrolysis (Tissot & Welte, 1984). The Tmax is influenced by both kerogen type and level of organic matter maturation (Espitalie, 1986). Tmax data for R'mah and Shiranish rock samples are suggesting early mature to mature levels (Tmax between 434 - 439 °C) (see Fig.4.43,right). Tmax values of Abba rock samples reflect an immature to early mature signature of these strata. The single Abba rock sample (G003850) is located far away to the right (having a Tmax value of 465 °C)

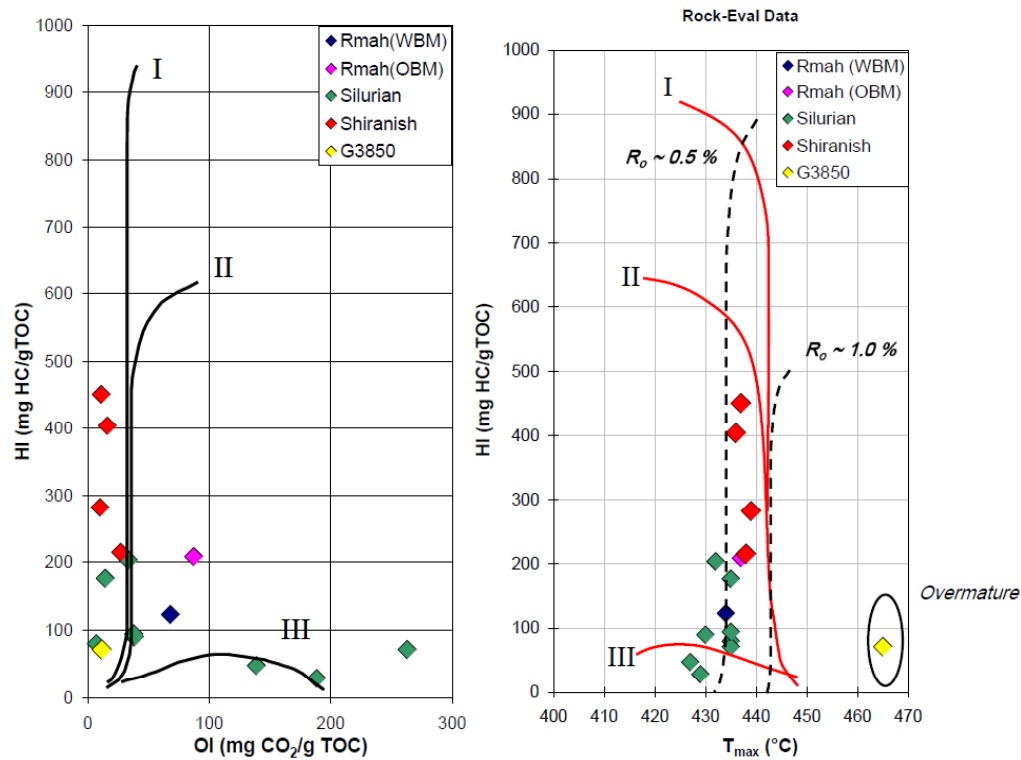


Figure 4.43: Showing: (left) hydrogen index (HI) versus oxygen index (OI) values for the analysed sample set, and (right) hydrogen index (HI) versus (Tmax) values for the analysed sample set.

referring to a super mature source rock.

It is important to point out here that the analysed Abba/Tanf rock samples are not thought to be necessarily representative for the potential Silurian source rock, because of a unsuccessful selection of rock samples to be investigated. As for other Hot Shales equivalent to it in North Africa (e.g. Tanezzuft formation in Libya) and Arabia (e.g. Qussaiba formation in Saudi Arabia), the Tanf (Abba formation) in Syria is found in the Lower Silurian in two Hot Shale zones separated by lean shale strata. Frijhoff *et al.* (2006) showed that the Hot Shales investigated from a Syrian well in the Euphrates Graben are extremely rich in organic content to be classified as oil shales. TOC contents often exceed 20% (Fig.4.44). RockEval data showed that these Hot Shales are postmature at present day (Fig.4.45). The same was shown by graptolite reflectance measurements (Frijhoff *et al.*, 2006). G003850 rock sample is the only sample which could be considered as a real Hot Shale.

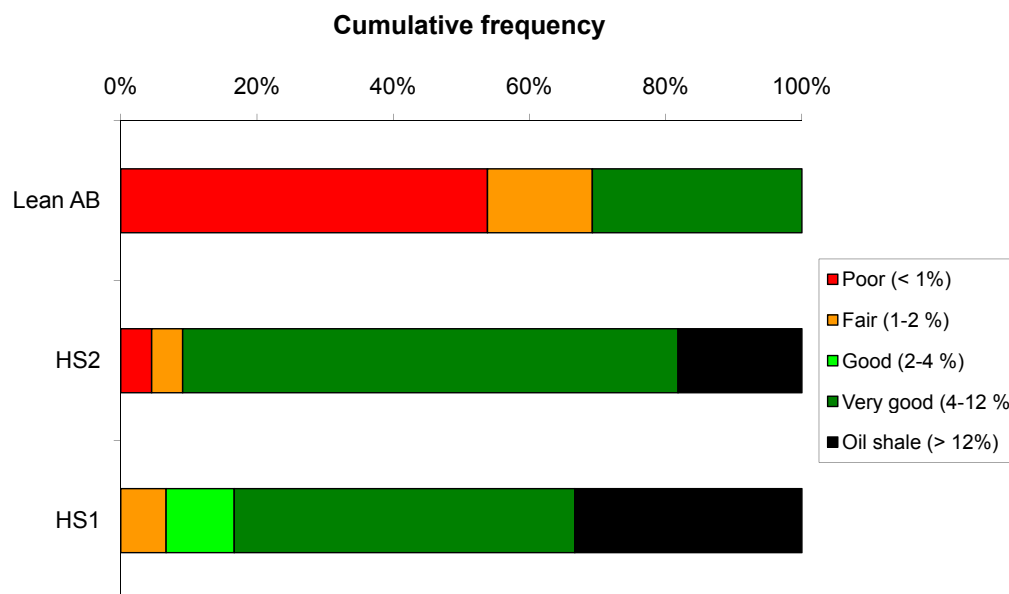


Figure 4.44: Total organic carbon content of 70 Silurian rock samples investigated in Al Furat Petroleum Company laboratory (Frijhoff *et al.*, 2006).

4.2.2 Normal Alkanes

The relative abundance of *n*-alkanes within the rock extracts show a decrease in abundance with increasing molecular weight (see Fig.4.46). Long chain hydrocarbons ($>n\text{-}C_{20}$) have low concentrations in G005136 (Silurian) relative to other Upper Cretaceous rock samples which could indicate a higher maturation level as the heavy hydrocarbons convert into light ones with increasing maturity. The pristane/phytane ratio for R'mah extracts ranges from 0.45 - 0.52 (Tab.4.10). The Shiranish extracts show slightly higher Pr/Ph values reaching 0.97 in the upper part but both members still have values below one which is typical for algal marine organic matter deposited under anoxic conditions. However, the Silurian Abba samples have the highest values up to 2.11. Since it is known that the Silurian strata have been deposited in an open marine environment and no potential supply of terrestrial organic matter existed (pre-land plant evolution); then it is expected that thermal maturity could have an effect on this relatively high Pr/Ph values. Pr/ $n\text{-}C_{17}$ vs. Ph/ $n\text{-}C_{18}$ (Fig.4.47) shows a subtle difference between both Upper Cretaceous R'mah (blue-colored symbols) and Shiranish (red-colored symbols) rock samples in terms of organic matter type.

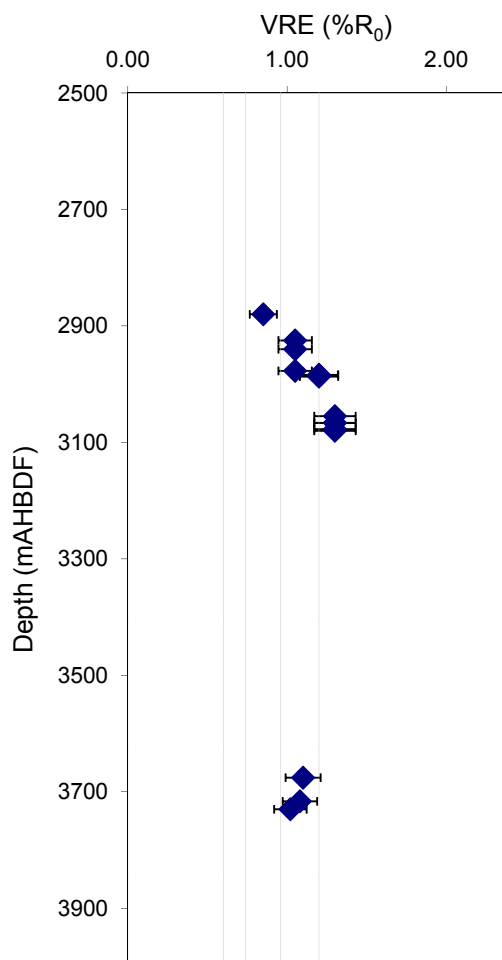


Figure 4.45: Vitritine reflectance equivalent $\% R_o$ from graptolite reflectance measurements for Silurian Tanf Formation rock samples (Frijhoff *et al.*, 2006).

Additionally, R'mah samples seem to have a relatively higher maturation level as they have lower isoprenoid over n -alkane values.

4.2.3 Biomarker Characteristics of Rock Extracts

The $Ts/(Ts+Tm)$ ratio for R'mah rock samples does not exceed 0.42 (see Tab.4.11), whereas it ranges between 0.76 - 0.79 for Shiranish rock samples which might imply a higher clay content (Bakr & Wilkes, 2002; Rullkotter *et al.*, 1985). For selected Abba rock samples the $Ts/(Ts+Tm)$ ratio varies between 0.29 - 0.66. Fig.4.48 and Fig.4.49 show triangular diagrams for C_{27} , C_{28} , and C_{29} regular and rearranged steranes. A slight difference between R'mah and Shiranish samples can be recognized. R'mah extracts

| Sample | Formation | Depth (m) | Pr/Ph | Pr/ <i>n</i> -C ₁₇ | Ph/ <i>n</i> -C ₁₈ | CPI 1 |
|---------|------------|-------------|-------|-------------------------------|-------------------------------|-------|
| G005145 | R'mah | 3626 - 3633 | 0.49 | 0.51 | 0.61 | 0.96 |
| G005112 | R'mah | 3560 | 0.45 | 0.41 | 0.53 | 0.95 |
| G005113 | R'mah | 3565 | 0.48 | 0.43 | 0.54 | 0.93 |
| G005114 | R'mah | 3570 | 0.49 | 0.42 | 0.54 | 0.94 |
| G005115 | R'mah | 3575 | 0.47 | 0.41 | 0.55 | 0.94 |
| G005116 | R'mah | 3580 | 0.50 | 0.40 | 0.52 | 0.93 |
| G005117 | R'mah | 3745 - 3755 | 0.52 | 0.34 | 0.39 | 0.89 |
| G005118 | R'mah | 3600+3605 | 0.49 | 0.27 | 0.37 | 0.96 |
| G005119 | R'mah | 3610+3615 | 0.48 | 0.27 | 0.38 | 0.92 |
| G005120 | Abba | 3330-3345 | 0.98 | 3.17 | 1.83 | 0.93 |
| G005121 | Abba | 3375-3385 | 0.84 | 3.82 | 2.10 | 0.95 |
| G005122 | Abba | 3415-3425 | 0.68 | 4.42 | 2.28 | 0.97 |
| G005123 | Abba | 3445-3455 | 0.64 | 4.81 | 2.51 | 0.94 |
| G005124 | Abba | 3470-3475 | 0.70 | 4.44 | 2.24 | 0.97 |
| G005125 | Abba | 3485-3505 | 0.72 | 4.52 | 2.20 | 0.95 |
| G005126 | Abba | 3380+3385 | 1.37 | 0.43 | 0.49 | 0.94 |
| G005127 | Abba | 3480+3485 | 1.23 | 0.39 | 0.47 | 0.83 |
| G005128 | Abba | 3530 | 1.59 | 2.21 | 1.43 | 0.90 |
| G005129 | Abba | 3580+3585 | 1.86 | 1.61 | 1.17 | 0.99 |
| G005130 | Abba | 3625+3630 | 1.80 | 1.90 | 1.15 | 1.02 |
| G005131 | Abba | 2320-2330 | 1.65 | 1.56 | 1.05 | 0.94 |
| G005132 | Abba | 2435-2445 | 1.40 | 2.10 | 1.31 | 0.92 |
| G005133 | Abba | 2490-2500 | 1.83 | 1.54 | 1.05 | 0.72 |
| G005134 | Abba | 2840+2845 | 1.35 | 1.29 | 1.06 | 0.91 |
| G005135 | Abba | 2925+2930 | 1.22 | 2.20 | 1.30 | 0.85 |
| G005136 | Abba | 2995+3000 | 2.11 | 1.46 | 0.99 | 0.87 |
| G005137 | Abba | 3585-3595 | 1.45 | 2.04 | 1.15 | 0.91 |
| G005138 | Abba | 3670-3680 | 2.09 | 1.14 | 0.81 | 0.96 |
| G005139 | Abba | 3730-3740 | 1.68 | 1.55 | 1.08 | 0.98 |
| G005140 | Abba | 2450-2455 | 1.87 | 1.34 | 0.96 | 0.88 |
| G005141 | Abba | 2610-2615 | 1.21 | 2.45 | 1.43 | 0.81 |
| G005142 | Abba | 2665-2675 | 1.65 | 1.55 | 1.09 | 0.79 |
| G003850 | Abba | 3030 | n.d | n.d | n.d | n.d |
| G003185 | U.Shranish | 2970 | 0.80 | 0.68 | 0.81 | 1.09 |
| G003188 | U.Shranish | 3050 | 0.97 | 0.70 | 0.82 | 1.18 |
| G003200 | L.Shranish | 3300 | 0.68 | 0.80 | 0.87 | 1.12 |
| G003211 | L.Shranish | 3520 | 0.70 | 0.75 | 0.79 | 1.06 |

Table 4.10: Hydrocarbon parameters obtained from analysis of rock extracts saturated fractions using GC-FID

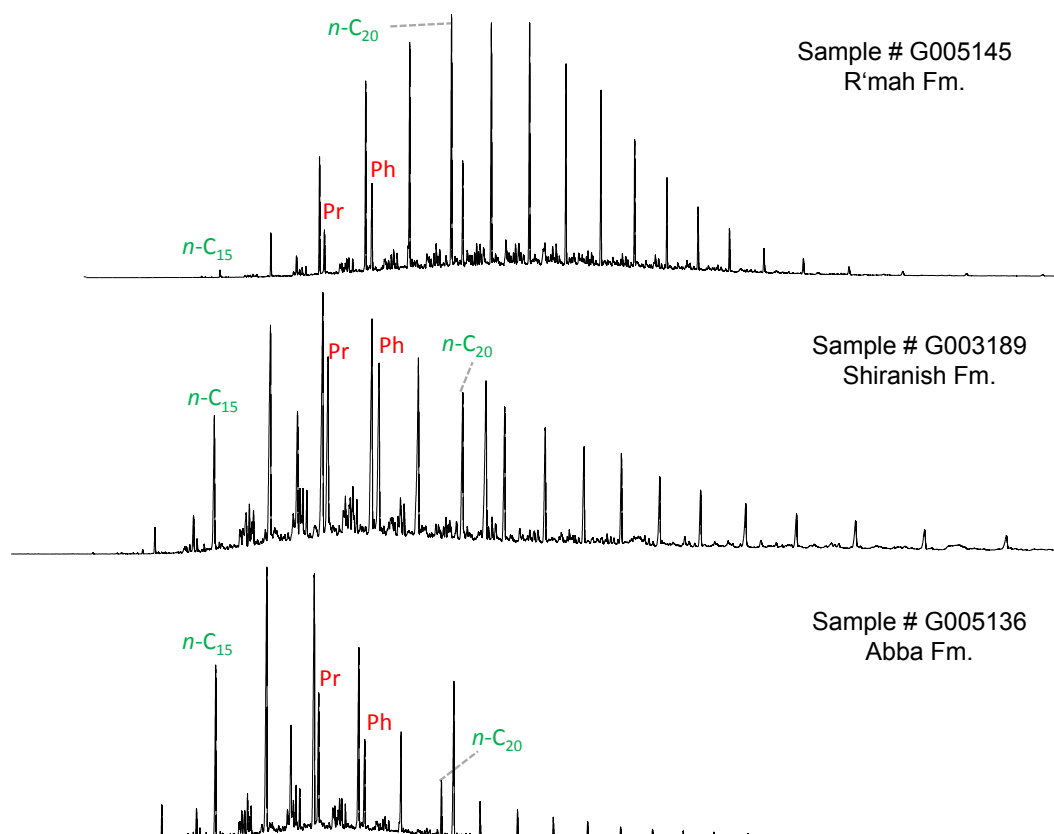


Figure 4.46: Saturate fraction gas chromatograms of the potential source rock samples.

seem to have moderately abundance C_{27} steranes and lower concentrations of C_{29} sterane compounds relative to Shiranish Formation. An implication for more algal marine organic matter and relatively higher maturation level could be considered for R'mah strata. Three Silurian Abba samples (named G005134, G005135, and G005136) coming from the same well have the highest C_{27} to C_{29} diasteranes/steranes ratio pointing to a higher maturation level for the strata in this well comparatively to the others.

| Sample | Formation | Steranes% | | | Diasteranes% | | | Dia/Reg $C_{27}-C_{29}$ | Ts/(Ts+Tm) |
|---------|-------------|-----------|----------|----------|--------------|----------|----------|----------------------------|------------|
| | | C_{27} | C_{28} | C_{29} | C_{27} | C_{28} | C_{29} | | |
| G005145 | R'mah | 47.79 | 30.36 | 21.85 | 51.26 | 32.24 | 16.50 | 1.05 | 0.40 |
| G005112 | R'mah | 45.90 | 28.53 | 25.56 | 46.95 | 33.12 | 19.93 | 1.32 | 0.40 |
| G005113 | R'mah | 46.80 | 29.04 | 24.16 | 49.61 | 33.24 | 17.16 | 1.27 | 0.39 |
| G005114 | R'mah | 46.50 | 29.64 | 23.87 | 49.35 | 33.04 | 17.60 | 1.30 | 0.37 |
| G005115 | R'mah | 48.12 | 27.30 | 24.58 | 46.60 | 32.79 | 20.61 | 1.20 | 0.40 |
| G005116 | R'mah | 45.50 | 30.44 | 24.06 | 50.34 | 32.62 | 17.04 | 1.33 | 0.42 |
| G005117 | R'mah | 46.27 | 32.17 | 21.56 | 50.78 | 31.86 | 17.37 | 1.29 | 0.35 |
| G005118 | R'mah | 48.95 | 24.91 | 26.13 | 47.52 | 32.23 | 20.24 | 1.52 | 0.33 |
| G005119 | R'mah | 48.11 | 26.49 | 25.40 | 45.94 | 34.23 | 19.83 | 1.31 | 0.35 |
| | | | | | | | | | |
| G005120 | Abba | 47.48 | 31.26 | 21.27 | 50.64 | 33.26 | 16.10 | 1.06 | 0.41 |
| G005121 | Abba | 47.00 | 32.71 | 20.29 | 50.39 | 33.68 | 15.93 | 1.09 | 0.43 |
| G005122 | Abba | 43.46 | 31.74 | 24.80 | 47.13 | 32.54 | 20.33 | 1.01 | 0.42 |
| G005123 | Abba | 45.74 | 32.49 | 21.77 | 47.79 | 33.06 | 19.15 | 0.96 | 0.42 |
| G005124 | Abba | 44.92 | 32.20 | 22.87 | 48.78 | 34.38 | 16.85 | 1.08 | 0.45 |
| G005125 | Abba | 44.87 | 32.30 | 22.82 | 47.25 | 35.53 | 17.22 | 1.09 | 0.42 |
| G005126 | Abba | 44.54 | 28.57 | 26.89 | 45.76 | 31.55 | 22.69 | 0.85 | 0.63 |
| G005127 | Abba | 40.24 | 29.77 | 29.99 | 43.71 | 34.42 | 21.87 | 0.77 | 0.66 |
| G005128 | Abba | 40.66 | 32.61 | 26.74 | 53.19 | 29.59 | 17.22 | 0.65 | 0.63 |
| G005129 | Abba | 58.54 | 41.43 | 0.03 | 62.01 | 37.97 | 0.02 | 1.01 | 0.56 |
| G005130 | Abba | 45.06 | 30.08 | 24.86 | 50.09 | 26.91 | 23.00 | 0.91 | 0.51 |
| G005131 | Abba | 36.99 | 38.03 | 24.98 | 44.16 | 37.60 | 18.23 | 1.09 | 0.43 |
| G005132 | Abba | 27.69 | 33.99 | 38.32 | 38.36 | 34.88 | 26.76 | 1.10 | 0.25 |
| G005133 | Abba | 35.76 | 30.42 | 33.82 | 42.65 | 30.98 | 26.37 | 0.73 | 0.36 |
| G005134 | Abba | 33.25 | 35.25 | 31.49 | 37.13 | 39.81 | 23.05 | 3.49 | 0.38 |
| G005135 | Abba | 31.75 | 34.89 | 33.37 | 39.50 | 36.65 | 23.85 | 2.55 | 0.40 |
| G005136 | Abba | 32.57 | 35.42 | 32.01 | 38.53 | 34.87 | 26.60 | 2.16 | 0.43 |
| G005137 | Abba | 41.64 | 30.80 | 27.57 | 50.15 | 31.31 | 18.54 | 0.82 | 0.54 |
| G005138 | Abba | 42.67 | 29.10 | 28.22 | 46.40 | 31.75 | 21.85 | 0.78 | 0.56 |
| G005139 | Abba | 41.10 | 30.62 | 28.28 | 50.41 | 29.54 | 20.05 | 0.89 | 0.54 |
| G005140 | Abba | 32.93 | 35.54 | 31.52 | 36.41 | 37.58 | 26.01 | 0.78 | 0.29 |
| G005141 | Abba | 35.95 | 31.89 | 32.16 | 41.51 | 33.46 | 25.03 | 0.70 | 0.38 |
| G005142 | Abba | 34.73 | 34.01 | 31.26 | 41.70 | 34.99 | 23.31 | 0.79 | 0.47 |
| G003850 | Abba | 32.17 | 30.05 | 37.78 | 38.67 | 31.50 | 29.83 | 1.04 | 0.44 |
| | | | | | | | | | |
| G003185 | U.Shiranish | 37.68 | 32.28 | 30.04 | 42.56 | 35.59 | 21.85 | 1.28 | 0.49 |
| G003188 | U.Shiranish | 38.17 | 30.17 | 31.66 | 42.56 | 35.03 | 22.41 | 0.86 | 0.53 |
| G003200 | L.Shiranish | 39.26 | 33.79 | 26.95 | 45.37 | 31.45 | 23.18 | 1.39 | 0.72 |
| G003211 | L.Shiranish | 35.61 | 31.32 | 33.07 | 32.59 | 40.29 | 27.12 | 0.14 | 0.76 |

Table 4.11: Saturate biomarker parameters for analysed rock extracts.

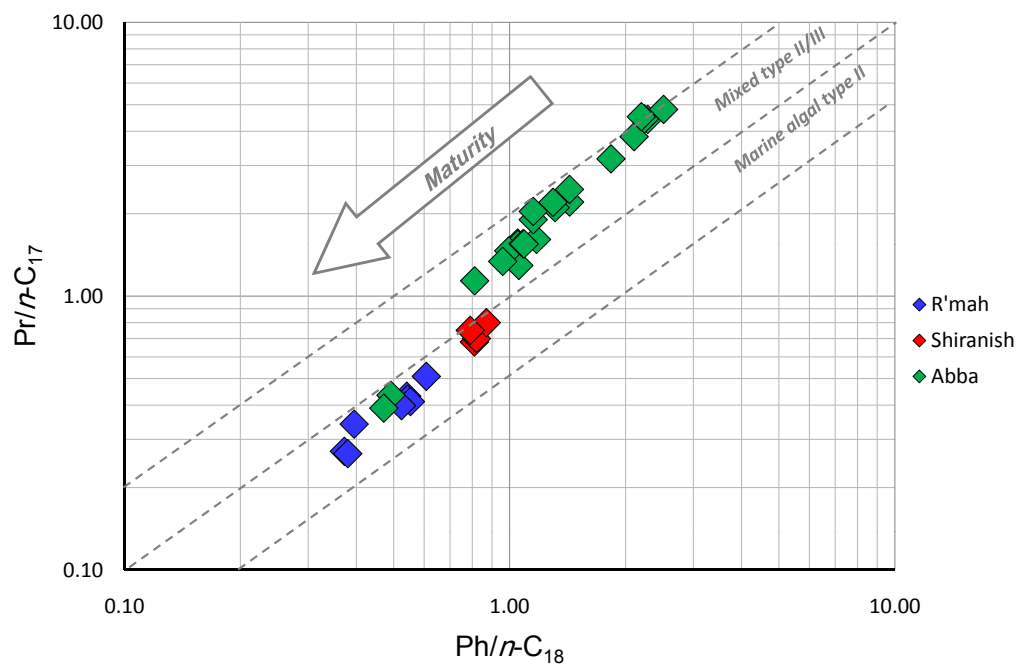


Figure 4.47: $Pr/n-C_{17}$ vs. $Ph/n-C_{18}$ cross plot of the investigated rock samples.

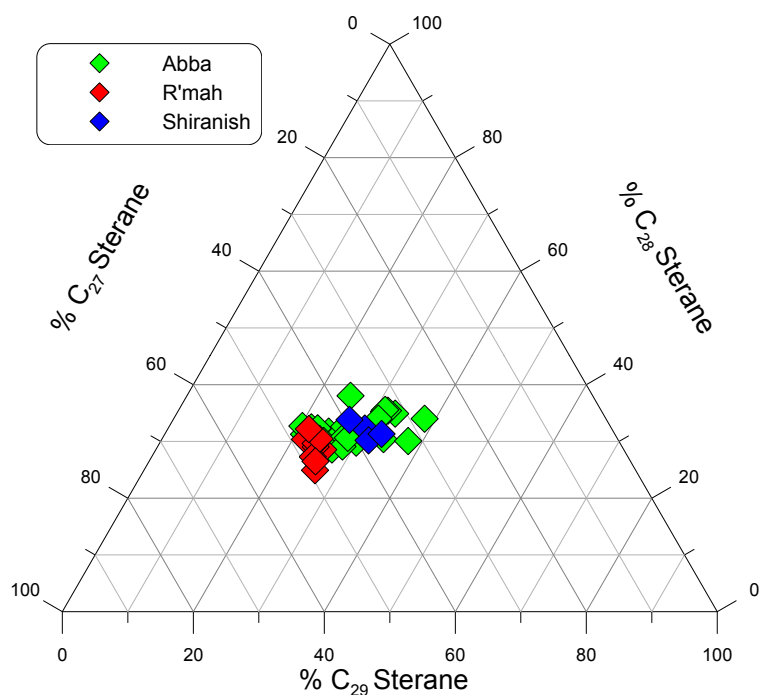


Figure 4.48: Ternary diagram showing the relative abundance of C_{27} , C_{28} and C_{29} regular steranes in saturated hydrocarbon fractions of source rock samples (R'mah in red, Shiranish in blue, and Tanf/Abba in green). A distinction between Upper Cretaceous R'mah and Shiranish source rocks is relatively obvious.

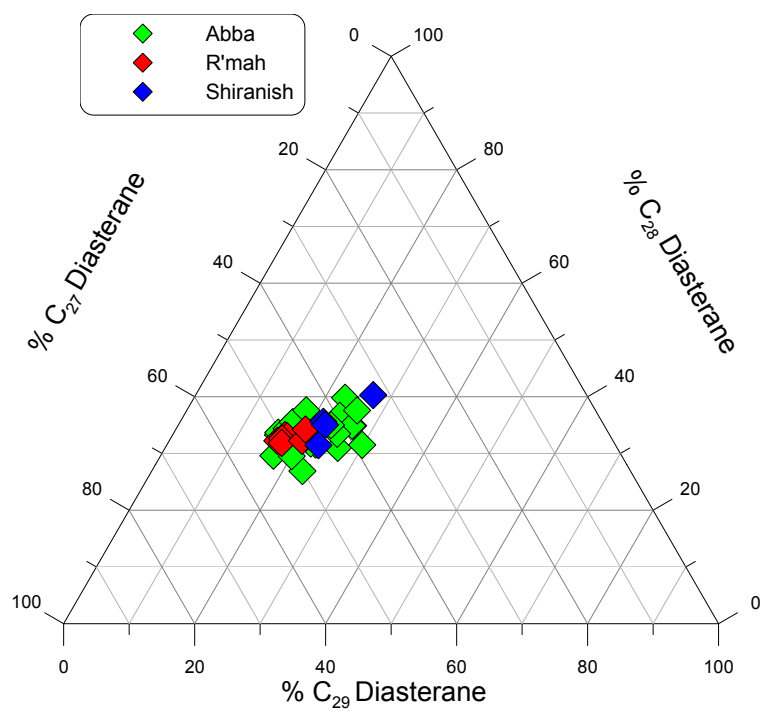


Figure 4.49: Ternary diagram showing the relative abundance of C_{27} , C_{28} and C_{29} diasteranes in saturated hydrocarbon fractions of source rock samples (R'mah in red, Shiranish in blue, and Tanf/Abba in green).

Chapter 5

Discussion and Interpretation

5.1 Oil-Oil Correlation

The correlation of crude oils with one another provides valuable tools for helping the exploration geologists answer production and exploration questions and extend existing exploratory trends. Some of the most important exploration questions are: Are these oils genetically related? Are there one or more families of oils in a particular sequence? How are these oil families distributed across the study area? What are the potential migration pathways? Are any of these oils related to potential shallower or deeper accumulations? To what degree could these oil families mix among each other?. Each family of oils represents one element of a distinct petroleum system. By identifying the source rocks of each family, the drilling can focus on prospects within the drainage areas of those sources. By using different analytical techniques, the similarity or dissimilarity among oils might be identified. In crude oil correlation, genetically related oils are differentiated from unrelated oils on the assumption that the same source material and environment of deposition produce the same oil. A biological marker compound dominant in the source rock would be expected to appear in the oils it generated. Therefore, a number of biomarker and non-biomarker parameters could be attributed to the task of differentiating the main oil families. But most difficult is the problem of interpreting how an oil may change in

moving from source to reservoir or how two crude oils of the same origin may undergo different physical and chemical changes after accumulation. The accumulated oils can be altered by secondary processes, such as maturation, gravity segregation, water washing, biodegradation, and secondary migration. In this study, a series of parameters are chosen to group oils that are little affected by secondary factors. Depending on the sophistication of analyses and statistical analysis methods, the oils fall into relatively distinct groups. Then, correlating these groups with available geological data has been performed to derive the genetic relationships within the petroleum system in the study area.

- Statistical Method Description:

Chemometric exploratory data analysis (EDA) is a statistical method that employs many variables from many samples for elucidation and interpretation purposes. It is a valuable technique in identifying hydrocarbon systems because the multivariate statistical analysis is dealing with large numbers of variables all at once resembling each sample as a point in space that has a number of axes equals to the numbers of variables (Christensen *et al.*, 2005a 2004; Peters *et al.*, 2005). Fig.5.1 shows, for instance, a point in a three dimensional system. There are several statistical techniques applied in order to classify crude oils to genetic groups. Hierarchical Cluster Analysis (HCA) has been applied for this study using **Sirius Pro.7** software that has been developed by *Pattern Recognition Systems (PRS®)*.

HCA depends on the principle of grouping the samples into distinct subsets (called clusters) by calculating the distances between samples for each variable. HCA displays the results graphically in a dendrogram structure. The dendrogram reveals the dissimilarity among the objects in the subsets and the information can be used in the classification/discrimination analysis. The dendrogram consists of many U-shaped lines connecting objects in a hierarchical tree. The height of each U represents the distance between the two objects being con-

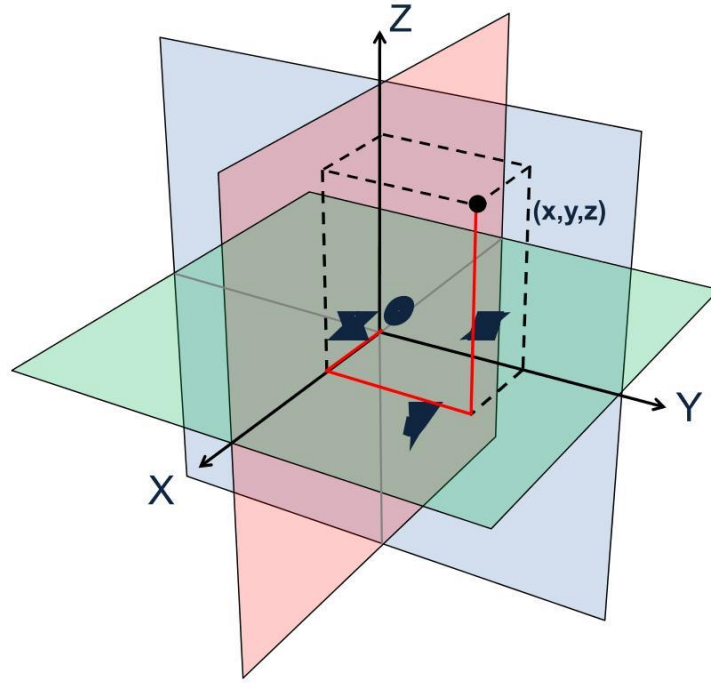


Figure 5.1: Three-dimensional Euclidean space. The point (x,y,z) is determined; like every point in such system, by three coordinates X , Y , Z .

nected; therefore, the smallest U legs are the closest these two samples (genetically) will be. The distance between each two samples is calculated in a Euclidean space, which has as many dimensions (n) as variables. In one dimension, the distance between two points on the real line is the absolute value of their numerical difference. Thus if x and y are two points on the real line, then the distance between them is calculated in Eq.5.1:

$$\sqrt{(x - y)^2} = |x - y| \quad (5.1)$$

The Euclidean distance between points \mathbf{a} and \mathbf{b} is the length of the line segment $\overline{\mathbf{ab}}$. In Cartesian coordinates, if $\mathbf{a}=(a_1, a_2, \dots, a_n)$ and $\mathbf{b}=(b_1, b_2, \dots, b_n)$ are two points in Euclidean n -space (where n is the number of variables), then the distance from \mathbf{a} to \mathbf{b} is given by Eq.5.2:

$$d(\mathbf{a}, \mathbf{b}) = \sqrt{(a_1 - b_1)^2 + (a_2 - b_2)^2 + \dots + (a_n - b_n)^2} = \sqrt{\sum_{i=1}^n (a_i - b_i)^2} \quad (5.2)$$

At the first stage of the study, 69 crude oils were available for geochemical analysis. Seven samples were too viscous to inject them into the GC-FID apparatus, therefore, light hydrocarbons parameters were obtained only for 62 oil samples (the top 62 samples in Tab.4.2). It was the aim to reduce the number of oils to be analyzed further using more specific techniques (GC-MS, GC-MS-MS, and CSIA), therefore a clustering approach was used to group the oils into main populations. Eight parameters based on acyclic isoprenoids and light hydrocarbons (Pr/Ph , $\text{Pr}/n\text{-C}_{17}$, $\text{Ph}/n\text{-C}_{18}$, heptanes value, isoheptane value, paraffinity, aromaticity, and carbon preference index) have been used for this basic classification. It is clear that not all of the parameters within the dataset are specific for only one kind of the process that affect the crude oil composition (depositional environment, maturity, biodegradation). The constructed HCA dendrogram is presented in Fig.5.2. Principally, seven clusters could be identified in this tree structure.

Two or three of these clusters which are more or less compatible with the geographical distribution could easily be recognized. For instance, oils of cluster 1, which includes what is thought to be biodegraded oils (G002997, G002998, and G002993), are distributed mainly on the northwestern part of the graben (yellow diamonds in Fig.5.3). On the other hand the group 5 contains the most mature oils (G002982, G002980, and G002952), which are located generally in the southeastern part of the study area (black diamonds in Fig.5.3). The loss of the light hydrocarbons like $n\text{-C}_7$, MCH, and toluene because of the storing conditions or other unknown circumstances in samples G002972 & G002981 forced them to fall in the biodegraded oils group which is not strictly correct because their gas chromatographic fingerprints indicate a light hydrocarbon evaporation and not biodegradation effect.

The sample G002959 (as a unique sample) is a strange case among the rest as it has the lowest values of $\text{Pr}/n\text{-C}_{17}$, $\text{Ph}/n\text{-C}_{18}$ and the highest value of the isoheptane ratio of 8.17 which indicates a very high maturity level, but on the other hand it has the highest value of Pr/Ph . Therefore this sample should be taken into account for further analyses. Nevertheless, this

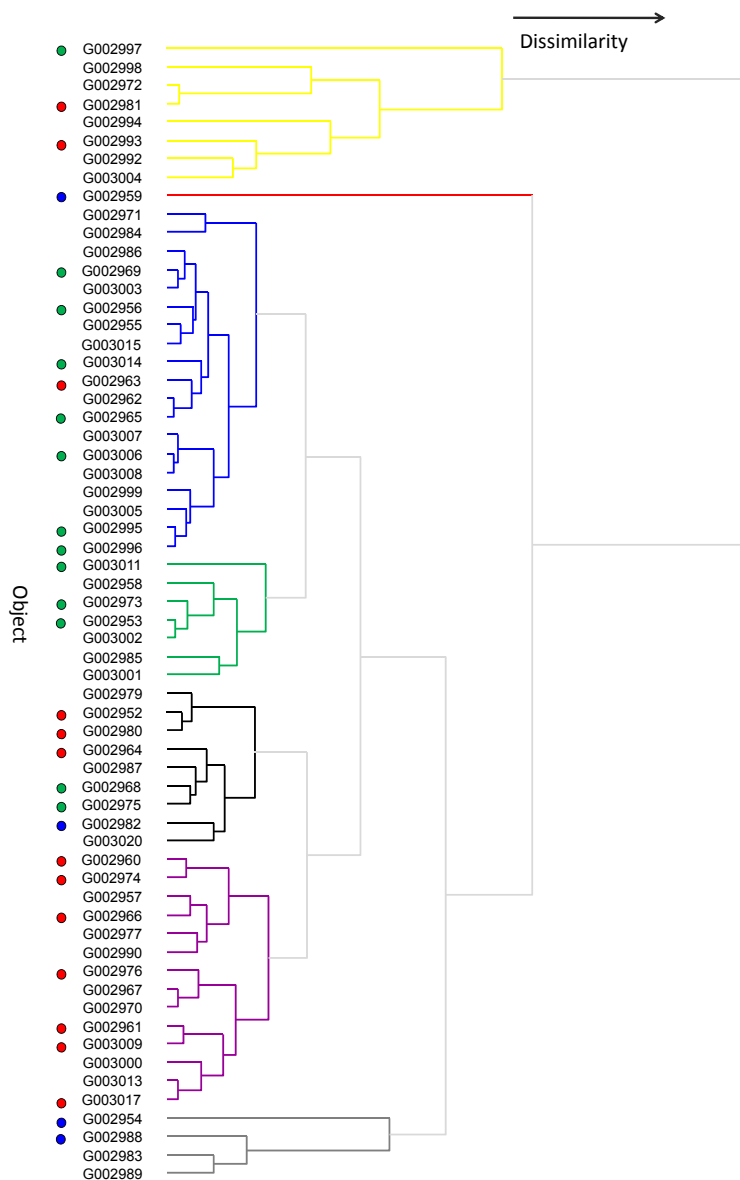


Figure 5.2: Dendrogram of light hydrocarbon parameters listed in Tab.4.2 for 62 investigated oil samples from the Euphrates Graben. Hierarchical clustering distinguishes seven different groups of crude oils. Colored dots represent the oil samples selected for further geochemical analysis.

classification is useful as a starting point to select a restricted set of oils for biomarker and other geochemical analyses. Depending on the previous results and clusters, thirty samples were chosen for further analyses. These samples represent the noticed oil clusters concerning their geographical distribution across the Euphrates Graben area (see Fig.5.4).

Two samples (G002954, G002988) were selected from the group 7 because they belong to two different wells with very long distance between

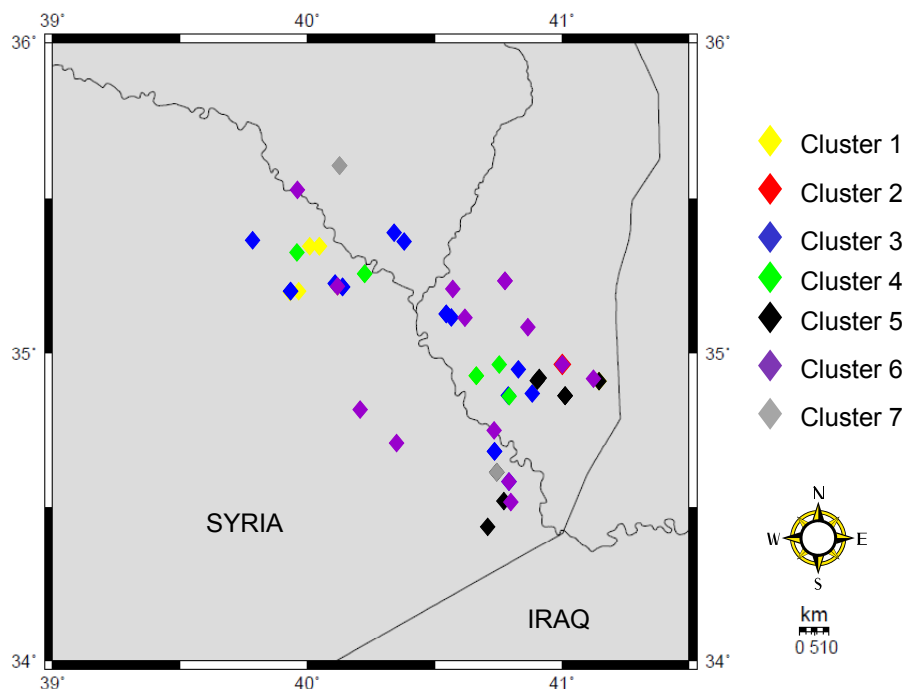


Figure 5.3: Geographic distribution of 62 oil samples representing the seven general crude oil groups identified in the study area. Symbol colors coincide with cluster colors illustrated in previous Fig.5.2.

them. Two samples (G002980, G002952) were selected from the same well because the big difference in signature between them. Oils of clusters 3 and 6 are scattered along the main axis of the graben extended from southeast towards northwest; samples from the middle and from the two edges of each distribution band have been chosen to make sure about the signatures of these subsets. The single G002959 sample was chosen as well. The last three samples chosen were the proposed biodegraded samples (G002997, G002993, G003011) from cluster 1 to be sure about them and to determine if they are biodegraded or if they were generated from immature source rocks. The distribution of the selected samples is shown in Fig.5.4.

5.1.1 Oil Families: Classification and Identification

Several geochemical analyses have been performed for these representative 30 oil samples. These analyses include GC-MS, GC-MS-MS, SIM-GC-MS, and CSIA (see Chapter.3) in order to determine biomarkers, aromatic hydrocarbons, diamondoids and compound specific stable carbon and hydro-

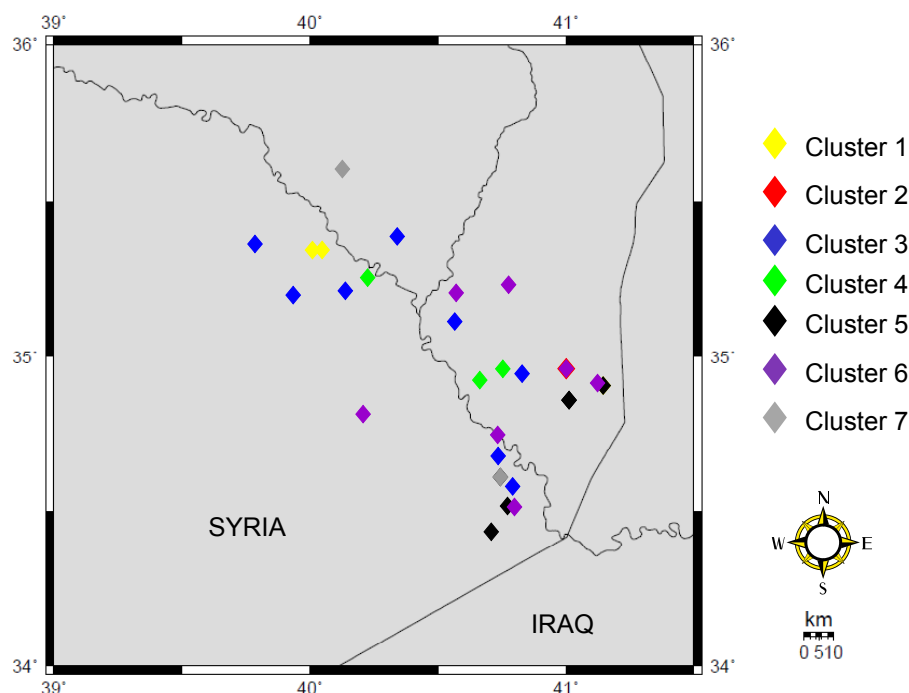


Figure 5.4: Geographic distribution of 30 oil samples which have been selected for biomarker and stable isotope analyses. It is obvious that this sub set of samples is very well representing the whole sample set not only from the geochemical signature point of view but also from geographical distribution pattern in the study area.

gen isotopes. Recapping the explanations made in the previous chapter (Chapter.4), the oils are sourced mainly from marine organic matter and range in maturity from early to late oil window. The highest maturity oils are found in Post Judea Sand (Cretaceous), Doubayat and Khabour (Palaeozoic) reservoirs. The lower maturity oils are located in Cretaceous and Triassic reservoirs (Rutbah and Mulussa). Oils with biodegradation appearance are found in shallow Miocene reservoirs (Dhiban, Euphrates, and Jeribe). The oils appear to be derived from two different source rocks; one, a clastic and the other, a carbonate based on information from the bulk properties, gasoline range, diamondoids, and biomarker data. The classification of oils into families is based on relationships apparent in their bulk and molecular composition. Cross plots of various parameters are usually of great use in revealing homologous suits of oils.

Moreover, chemometric analysis of source-related light hydrocarbons, biomarkers and non-biomarkers data was based on 23 source- and age-

related parameters for the 30 oils selected out of the whole sample set (see Appendix.C).

It may be worthy to mention that the pristane to phytane ratio has been avoided to be used as a pure source-related parameter because of the possible multiple sources of these isoprenoids, in addition to the effect of maturity on this ratio and the ratios of isoprenoids over n -alkanes discussed in sec.4.1.2. Distinct geochemical characteristics and Hierarchical Cluster Analysis HCA resulted in three genetic families and subfamilies (see Fig.5.5). The families have been termed; Family 1, Family 2A, and Family 2B. Geochemical properties of these oil families are listed in Appendix.C.

Geochemical features of Family 1 (blue in Fig.5.5) imply that its oil samples are generated from clay-rich, high mature Silurian Tanf Formation which contains hot shale beds equivalent to others found elsewhere in Middle East and North Africa. Family 1 consists of four oils G002959, G002954, G002982, and G002988. These very light oils (API gravity $>43^\circ$) have a high pristane/phytane ratio ($\text{Pr/Ph} > 1.37$) and their plot locations in Fig.5.6 indicate that their source rock was deposited under reducing conditions in marine environment. Relatively low values of $\text{Pr}/n\text{-C}_{17}$ and $\text{Ph}/n\text{-C}_{18}$ are attributed probably to the high maturity level of the source rock.

Age-diagnostic biomarkers (Fig.4.17 and Fig.4.19) are distinctive, signifying that oil samples of this family were derived obviously from a different source rock than the other oil samples. The C_{28}/C_{29} $\alpha\beta\beta$ sterane ratio is below 0.7 for Family 1 oils pointing to the Palaeozoic source rock (Grantham & Wakefield, 1988; Moldowan *et al.*, 1985). The same conclusion is obtained from 24/(24+27)-nordiacholestane ratio which has values less than 0.25 (Holba *et al.*, 1998b). Although steranes and diasteranes are low, the relatively high diasterane/regular sterane ratio for C_{27} to C_{29} sterane implies that these oils originated from a clay-rich clastic rock (see sec.4.1.3.2). Fig.5.7 shows that Family 1 oil samples (blue triangles) are apparently discrete from in the sample set being more rich in C_{29} sterane and diasterane relative to other samples and located in a range of Palaeozoic sourced-oils defined after (Grantham & Wakefield, 1988). This distinguishing sterane

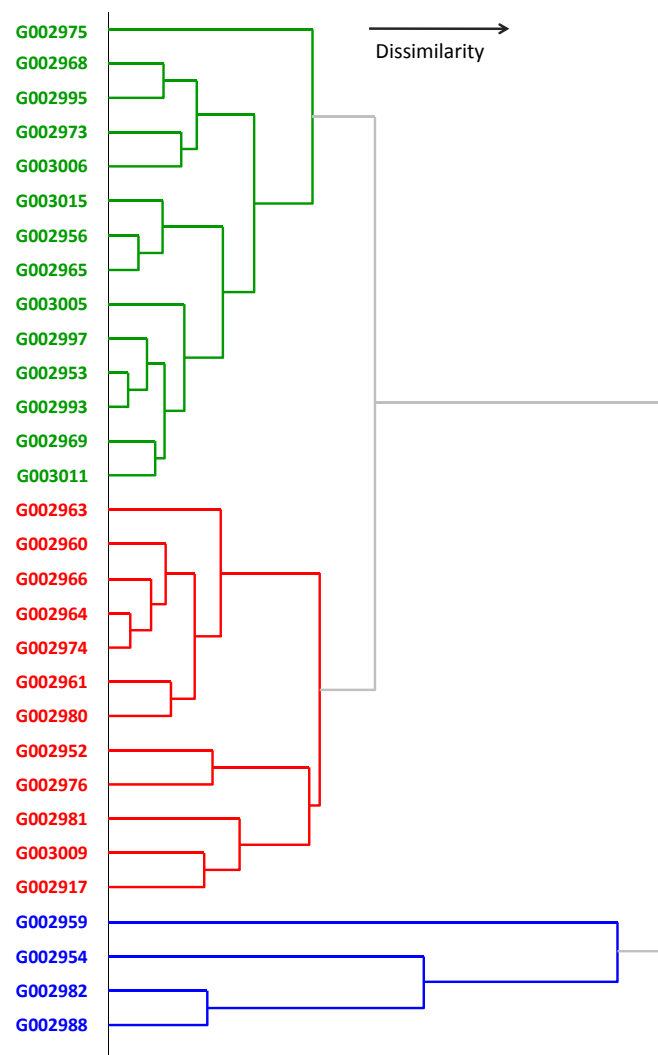


Figure 5.5: Dendrogram shows genetic relationships among oils based on chemometric analysis of 23 source-related geochemical parameters (Appendix.C). Cluster distance is measure of genetic similarity indicated by the vertical distance from any two samples on the bottom to their branch point on the top. Family 1 (in blue) is probably generated from the Silurian Tanf Formation. Oils from Family 2A (in green) are most likely attributed to Upper Cretaceous source rocks.

signature of Silurian oils is also clear looking at the m/z 217 fragmentogram presented in Fig.4.16, sample G002954 (Appendix.A contains all other gas chromatograms).

As diamondoid-based source facies parameters, a cross plot of DMDI-1 versus DMDI-2 (Fig.5.8) distinguishes Family 1 oil samples (blue triangles) as they plotted in the area of clay-rich source rocks, in contrast to other oil samples which are probably derived from Upper Cretaceous carbonate

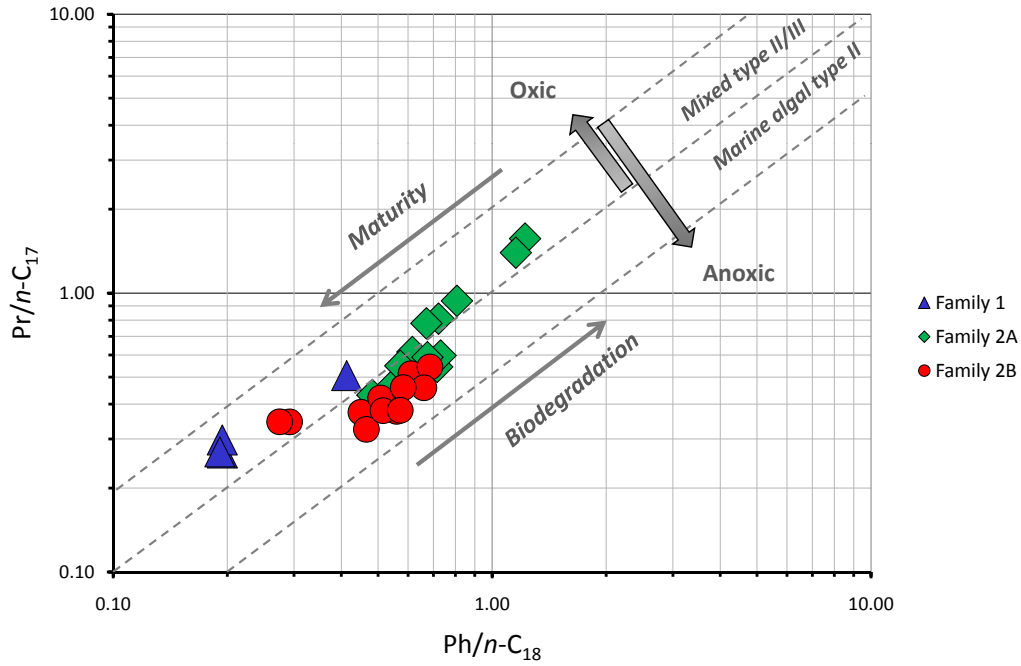


Figure 5.6: Cross-plot shows $\text{Pr}/n\text{-C}_{17}$ against $\text{Ph}/n\text{-C}_{18}$ for the different families. Family 1 crude oils (blue triangles) have relatively low values of $\text{Pr}/n\text{-C}_{17}$ and $\text{Ph}/n\text{-C}_{18}$ which are attributed probably to the high maturity level of the source rock.

strata (Schulz *et al.*, 2001).

Fig.5.9 shows a C_7 oil correlation star diagram ($C_7\text{OCSD}$) which is a multivariate plot in polar coordinates used to correlate both transformed and primary oils based on source-related chemical differences (Halpern, 1995).

This diagram is used normally to differentiate types of oils because the compounds used to calculate these parameters (C_1 through C_5) are proved to be invariant within a family of oils (oils derived from the same source rock), but have enough variance between oils from different families (Halpern, 1995). These multi-branched heptanes are very resistant to the effects of transformation. C_1 through C_5 parameters are calculated from the following equations based on the multi-branched heptanes (together are known as P3) are very resistant to the effects of transformation (Mango, 1990b):

$$C1 = 2,2 - \text{dimethylpentane} / P3 \quad (5.3)$$

$$C2 = 2,3 - \text{dimethylpentane} / P3 \quad (5.4)$$

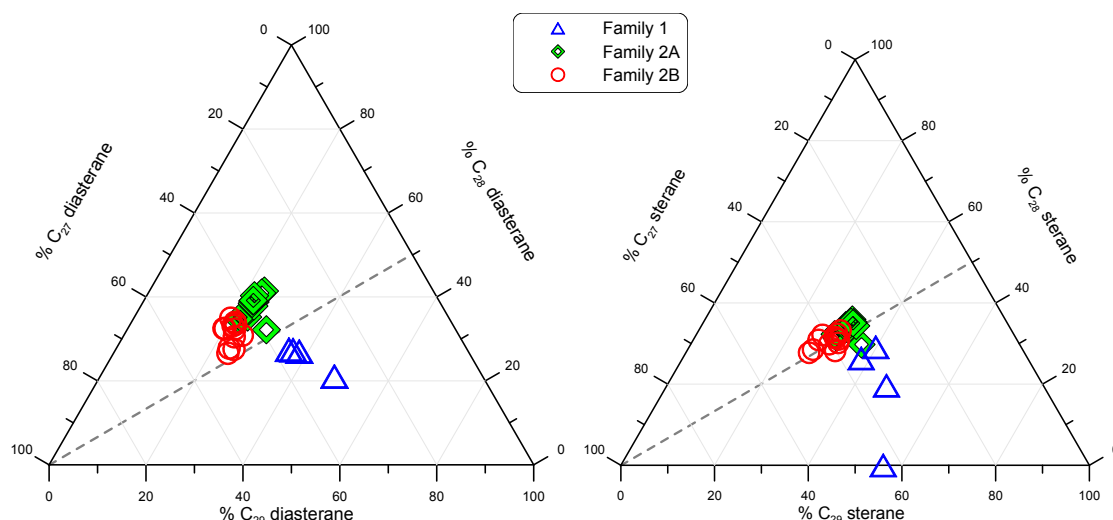


Figure 5.7: Ternary diagrams of C_{27} , C_{28} , and C_{29} sterane and diasterane composition for analysed oils based on MRM-GC-MS-MS. The identified three oil families are clearly distinguished. Dashed lines are only for visual reference.

$$C3 = 2,4 - \text{dimethylpentane}/P3 \quad (5.5)$$

$$C4 = 3,3 - \text{dimethylpentane}/P3 \quad (5.6)$$

$$C5 = 3 - \text{ethylpentane}/P3 \quad (5.7)$$

where $P3 = 2,2 - \text{dimethylpentane} + 2,3 - \text{dimethylpentane} + 2,4 - \text{dimethylpentane} + 3,3 - \text{dimethylpentane} + 3 - \text{ethylpentane}$. Silurian-originated crude oils (blue lines) are found to be clearly different from Cretaceous crude oils (green lines). Halpern (1995) could differentiate Silurian from Jurassic oils in one petroleum system of Saudi Arabia.

In contrast to Family 1, all other oil samples (family 2 generally) are characterized to be generated from Upper Cretaceous source rocks (R'mah and Shiranish). Crude oil samples of this family have C_{28}/C_{29} sterane age-diagnostic biomarker values above 0.7 (Fig.4.17) referring to Cretaceous and younger source rocks. Similarly, $24/(24+27)$ -nordiacholestane ratio for family 2 oils (Fig.4.19) also in the range of Cretaceous origin. In terms of source rock lithofacies and maturity, oils of family 2 could be subdivided into two sub-families 2A and 2B (green and red samples in Fig.5.5; respectively). Small variations could be observed between both families 2A and 2B as both Upper Cretaceous source rocks (R'mah and Shiranish) are mainly carbonate

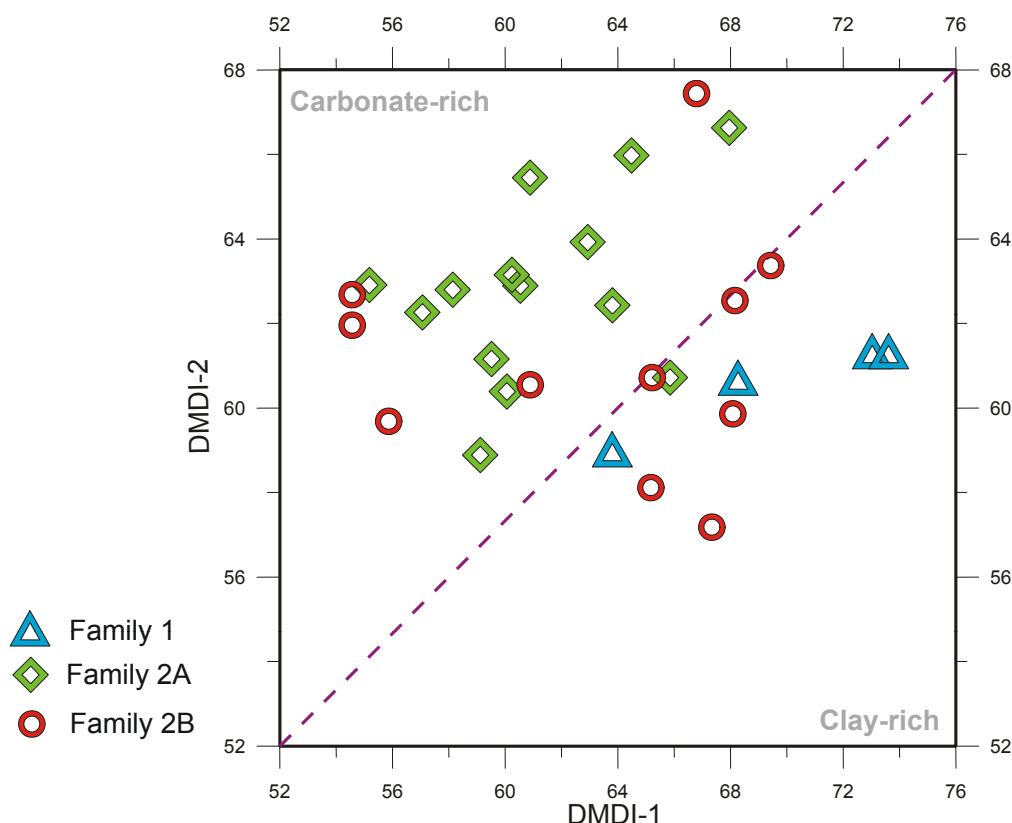


Figure 5.8: Cross-plot of dimethyldiamantene index DMDI-1 versus DMDI-2 (see equations Eq.4.1 and Eq.4.2 for identification) illustrates that Silurian oils (blue triangles) are identified to originate from a clay-rich source. Some oils from Family 2B (red circles) are located below the dashed line referring to a clear input of clay-rich source to these basically calcareous oils.

and have very similar features. Fig.5.6 shows that Family 2B oils (red dots) originate principally from marine type II organic matter while Family 2A oils (green diamonds) have both II and mixed II/III organic matter which could be in agreement to Upper Shiranish Formation as it contains a small terrestrial organic matter contribution. Two of the red dots on the most left hand side (G002952 and G002980) have the lowest values of $\text{Pr}/n\text{-C}_{17}$ (0.35 for both) and $\text{Ph}/n\text{-C}_{18}$ (0.27 and 0.29, respectively) in family 2 oils coming close to the Silurian oils maturity range. Sterane and diasterane ternary diagrams (Fig.5.7) illustrate a nice separation between two Upper Cretaceous subfamilies as the oil samples of Family 2A have more C_{28} steranes relative to Family 2B oils which are more affluent in C_{27} steranes (see Appendix.C). Diasterane over sterane ratio ranges from 0.15 and 1.04 for Family 2A oils and it is in the range of 0.33 - 1.40 for oils of Family 2B indicating to a

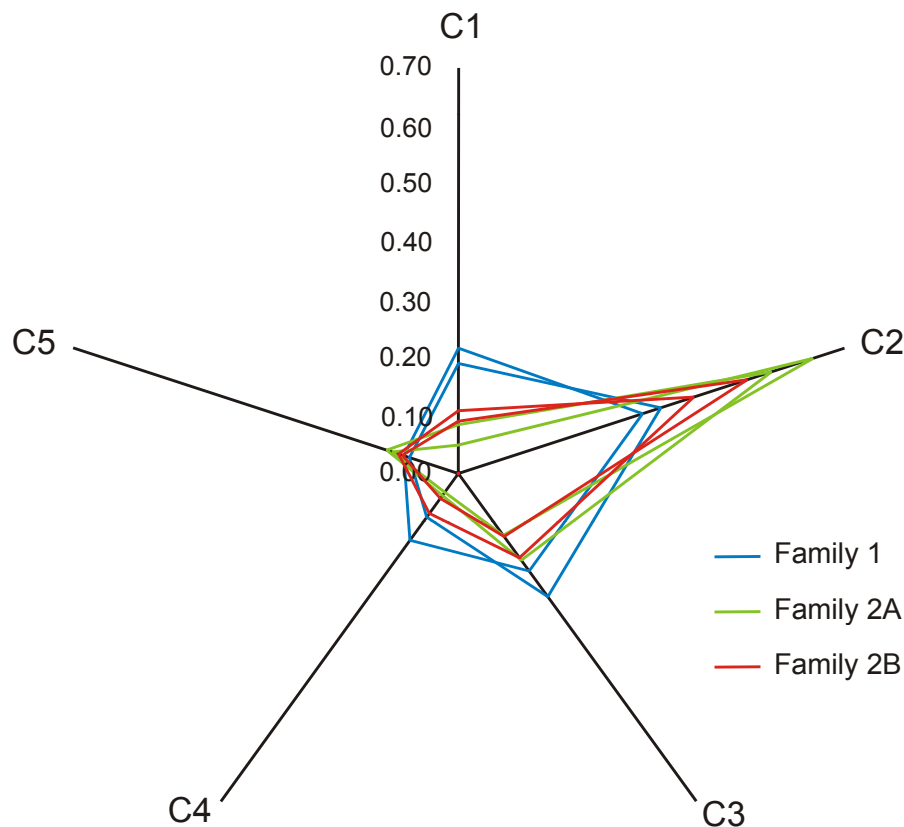


Figure 5.9: C_7 oil correlation star diagram (C_7 OCSD) clarifies the distinguishable signature of Family 1 crude oils (blue lines) from the Family 2A (green lines) and Family 2B (red lines) oils. It can be recognized that red lines are in an intermediate state between blue and green ones implying the assumption for red-colored oils to be a mixture from Silurian and Upper Cretaceous source rocks.

slight variation in maturation degree (see Appendix.C). Fig.5.8 shows that all members of Family 2A (green diamonds) are in the area of carbonate-rich source rock as defined from the facies-related diamondoids parameters. At the same time some oils from Family 2B are located near to Silurian oils in the clay-rich part raising the point about their real origin if it is pure Cretaceous or has contribution of Palaeozoic shale to some extent. Red and green polygons in Fig.5.9 are almost identical regarding the general frames which imply principally similar origin of the Upper Cretaceous source beds in contrast to Silurian one for blue shapes (Family 1). But, on the other hand, a small shift could be observed pointing to different signatures with respect to source-facies or maturity.

5.1.2 Oil Families: Maturity Variations

In terms of thermal maturity, it is obvious that Silurian source rocks should be highly mature relative to mature Upper Cretaceous source rocks as they are buried deeper. In this framework, oils originating from the Silurian Tanf Formation are signifying the signature of high maturity in several biomarker and non-biomarker maturity parameters. One plot of the very good examples of these parameters is shown in Fig.5.10. Diamondoids, as discussed in sec.4.1.4, are light hydrocarbons which are very sensitive to thermal maturation and therefore could be used as a very good molecular proxy for evaluation the maturity extent of crude oils. It is believed that the concentration of these cage-like compounds increases with increasing the thermal stress easily because of the cracking of heavy compounds into lighter ones. Fig.5.10 illustrates that oils of the Silurian family (blue triangles) have the highest amounts of diamondoids indicating high maturity. On the other hand, green diamonds representing the Family 2A oil samples are located in the lower left corner as they originate from source rocks lower in maturity. Interestingly, some oils (G002980, G002952, G002960, and G002981) from Family 2B plot close to the Silurian oils referring to a maturation degree higher than other members of the family. This observation is in agreement with other parameters (such as $\text{Pr}/n\text{-C}_{17}$ vs. $\text{Ph}/n\text{-C}_{18}$ in Fig.5.6, dia/reg steranes, C_7OCSD in Fig.5.9, facies-related diamondoids in Fig.5.8) regarding the idea of a co-sourcing possibility for these oils from Silurian and Cretaceous source rocks. Additionally, as discussed later on, the geographical locations of these oils near to the distribution of crude oils of Family 1 could support the hypothesis of mixed oils presence in the study area.

5.1.3 Oil Families: Stable Isotopic Composition

The molecular composition of crude oils shows that three subsets of samples differ clearly regarding source rock organofacies, lithofacies and thermal maturity. Determination of stable carbon and hydrogen isotopic compositions of oils at the molecular level is rapidly becoming a powerful tool for

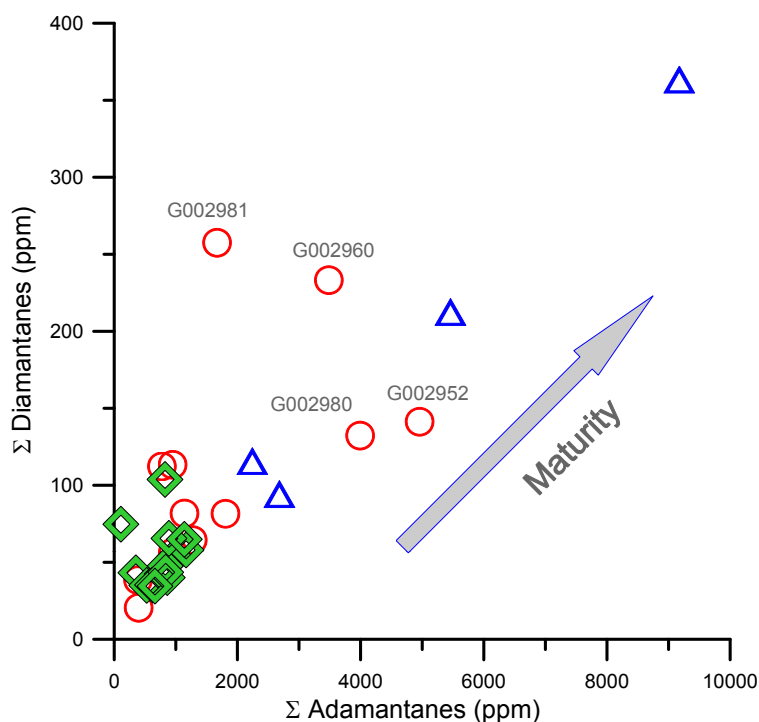


Figure 5.10: Cross plot based on diamondoids concentration illustrating the maturity variation of identified oil families.

the accurate definition of petroleum systems through better constrained oil-oil and oil-source correlation. The discussion below is to see to which extent the isotopic composition of crude oils is compatible with the observations obtained from the molecular composition. As illustrated earlier in sec.4.1.6, carbon and hydrogen isotopic signatures are variable within the studied samples. The carbon isotopic composition of light hydrocarbons and acyclic isoprenoids seem to be not so distinguishing to be a valuable tool for discrimination of the oils. In contrast, hydrogen isotopes could give distinctive information for oil families classification purpose. *Li et al. (2001)* have investigated isotopically crude oils from western Canada sedimentary basin WCSB. They have observed that a special depositional settings and/or minor contribution of terrestrial organic matter are responsible for a shift towards a lighter hydrogen isotopic composition from Palaeozoic to Upper Cretaceous oils. Besides, thermal maturity does have significant effects on δD values of *n*-alkanes causing an enrichment of D in more mature crude oils, because of isotopic exchange of D-depleted organic matter with forma-

tion waters that are relatively D-enriched (Li *et al.*, 2001). Fig.5.11 shows the hydrogen isotopic composition of *n*-alkanes for identified oil families. One can easily detect that oils of Family 1 are less negative in δD values relative to Family 2A which could imply a high maturity of the associated source rock (Silurian Tanf Formation). At the same time it seems to show that Family 2A originates from a source rock with a slight terrestrial input (Upper Cretaceous Shiranish Formation). Some oils from Family 2B have relatively same maturation degree as the Silurian oils.

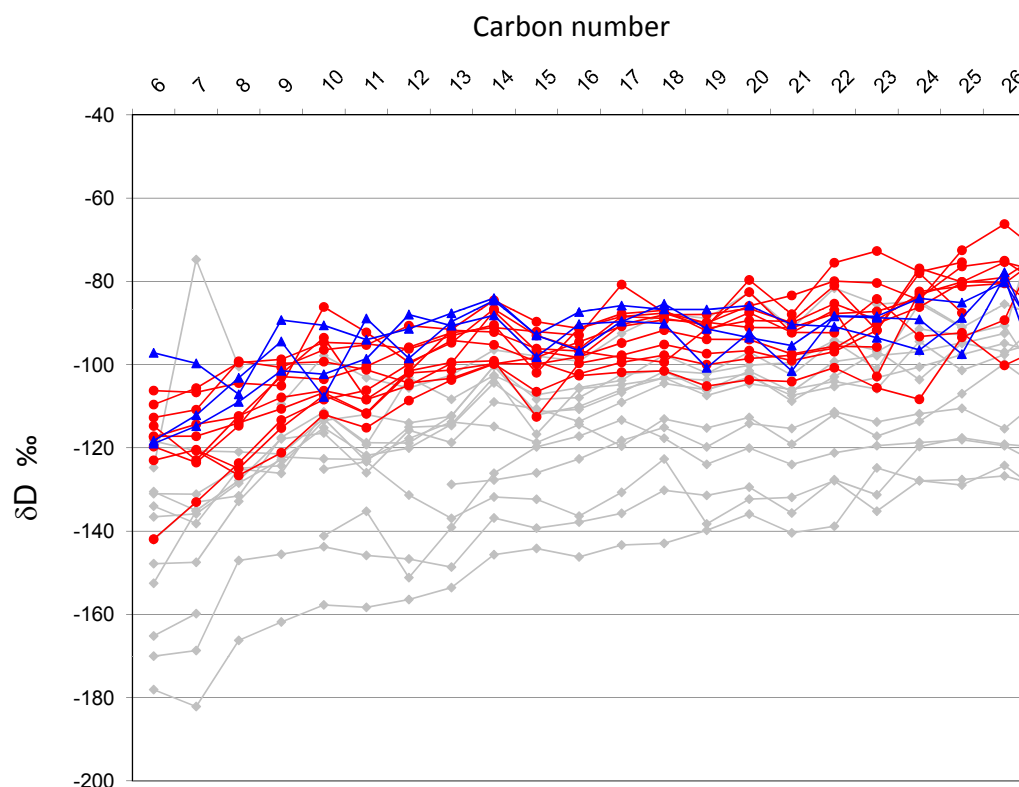


Figure 5.11: Hydrogen isotopic profiles of *n*-alkanes from *n*-C₆ to *n*-C₂₆ for different oil families, where Family 1 in blue, Family 2B in red, and Family 2A in gray.

Fig.5.12 illustrates the plotting of δD against $\delta^{13}C$ values of different compounds (*n*-C₇, *n*-C₁₀, *n*-C₁₅, *n*-C₂₀, Pristane, and Phytane). The discrimination between Family 1 (blue triangles) and Family 2A (green diamonds) is more significant and recognizable for heptane (*n*-C₇) than for other aliphatic hydrocarbons which could be attributed to the considerable effect of thermal maturity on short chain hydrocarbons in comparison to longer chain hydrocarbons. It has been observed that secondary oil mi-

gration does not appear to have any significant impact on hydrogen isotopic signature of light hydrocarbons in contrast to thermal maturity do (Li *et al.*, 2001). This could imply that oils derived from Silurian and Upper Cretaceous ages still keep valuable signatures of the hydrogen isotopic compositions of source organic matter.

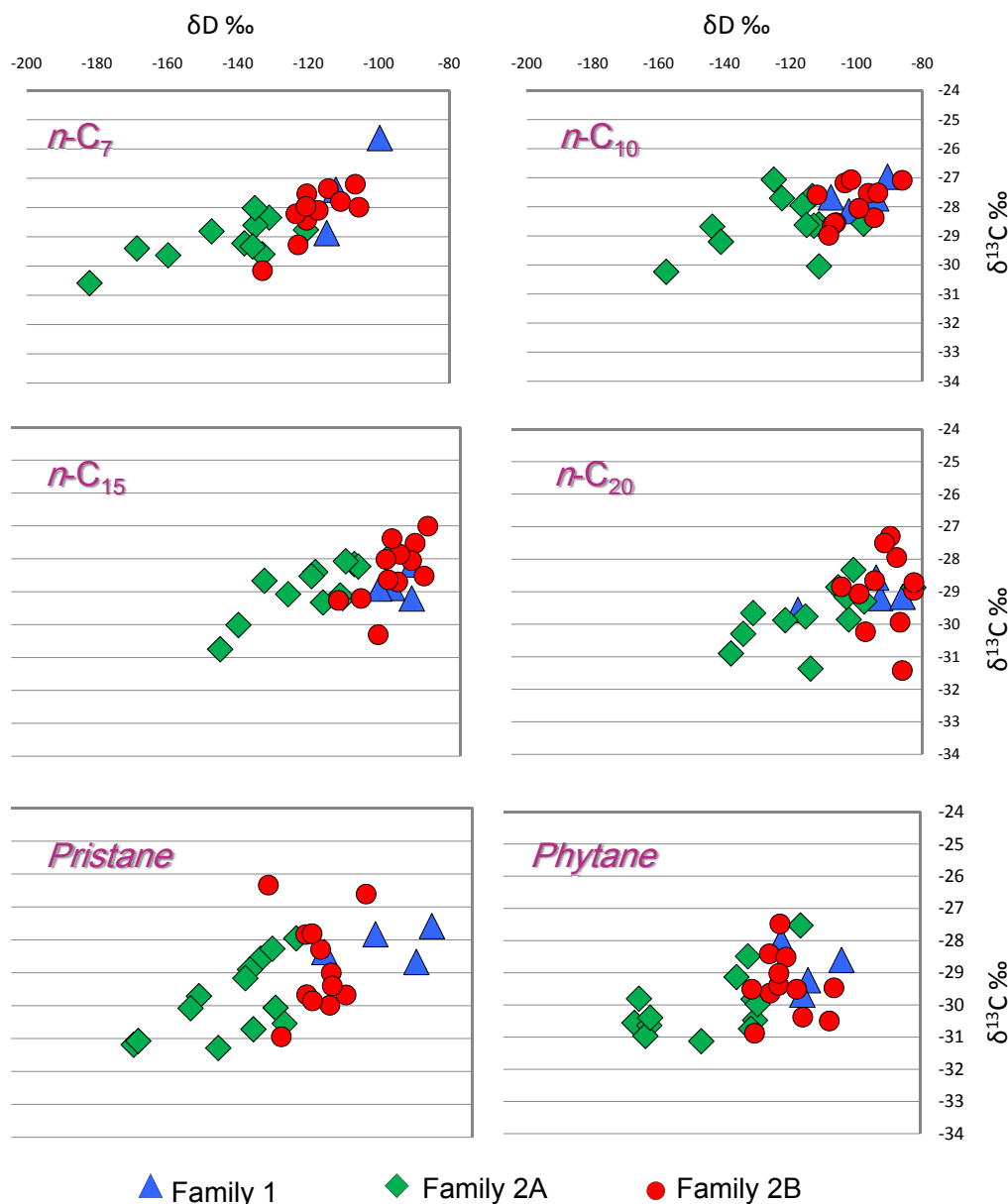


Figure 5.12: Cross plots of δD versus $\delta^{13}C$ values for different hydrocarbons $n-C_7$, $n-C_{10}$, $n-C_{15}$, $n-C_{20}$, Pristane, and Phytane.

Interestingly, Family 2B oils (red circles) are always located between Family 1 and Family 2A which strengthens the interpretation that these oils are more mature than Family 2A members. This maturity variation

is one of the key elements to subdivide the family 2 into two subfamilies. Different maturity of the oil families is also observed from calculating the offset in δD values between acyclic isoprenoids (pristane and phytane) and n -alkanes in Fig.4.40 where G002959 sample represents Family 1, G002963 oil represents Family 2B, and G002973 represents Family 2A.

Two isoprenoid hydrocarbons (pristane and phytane) have been chosen to assess the impact of source and maturity on hydrogen isotopic signature of identified oil families as these compounds are relatively resistive to isotopic fractionation effect caused by secondary alteration processes. Fig.5.13 shows the plot of pristane versus phytane δD values for the identified oil families. Family 1 oil samples are obviously separated from Family 2A by having heavier hydrogen isotopic values pointing to different source rock features. Crude oils of Family 1 originate probably from more D-enriched organic matter relative to Family 2A. In other words, Family 1 oils were generated from a source rock (Silurian strata) more mature than that of Family 2A (Upper Cretaceous strata). The interpretation of this variation in pristane and phytane δD values as more influenced by maturity should be proved by another way.

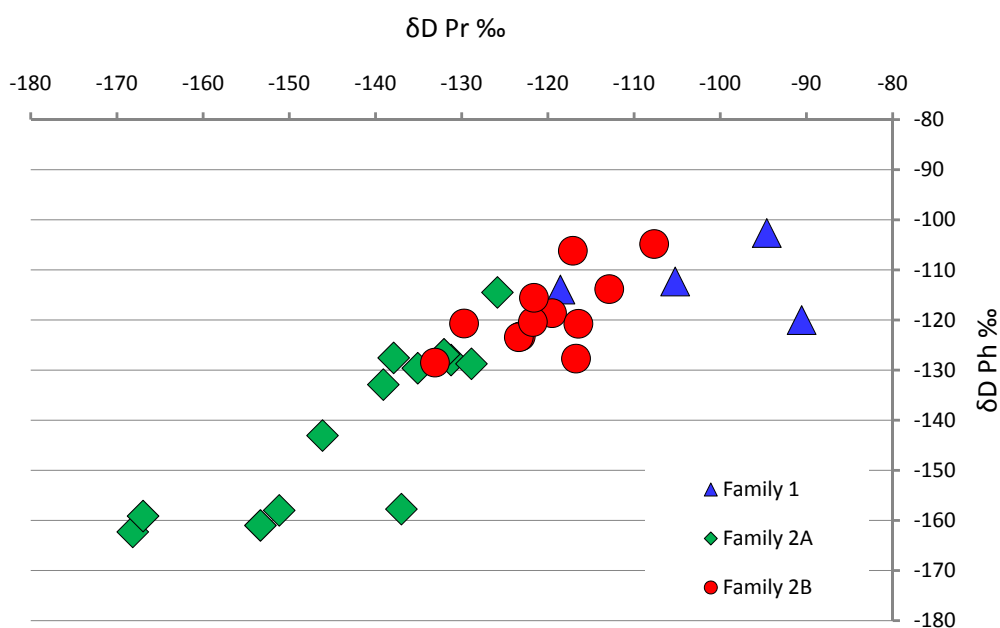


Figure 5.13: Cross plots of pristane versus phytane δD values.

Fig.5.14 shows a cross plot of pristane δD values versus the sum of adamantanes as a good indicator to maturation level. Family 2A crude oils show a very good linear correlation close to a horizontal line indicating that there is no difference in maturation level for the members of this family, as no significant difference is present in diamondoids concentration. Therefore, the variation in hydrogen isotopic compositions is attributed to different organofacies within the source rock. On the other hand, crude oils of Family 1 and Family 2B are showing nice exponential trends due to heavier δD values with increasing maturity.

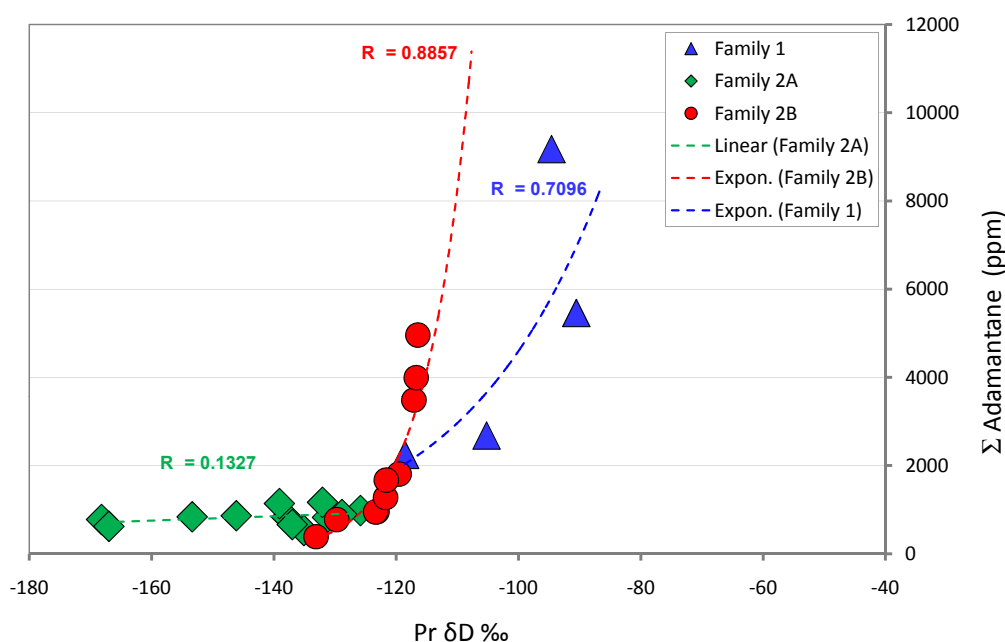


Figure 5.14: Cross plots of pristane δD values versus sum of adamantane concentration.

Interestingly to signify that both Silurian and Upper Cretaceous families have such limits for hydrogen isotopic signatures would not be exceeded whatever the maturity reaches. These values could be called as "equilibrium limits". This recognized onset is about -80 ‰ for Silurian oil family and about -115 ‰ for Upper Cretaceous oil families (see Fig.5.14). A possible explanation for this is the influence of equilibrium isotope-exchange reactions between organic matter and the formation water associated with source rocks.

5.1.4 Oil Families: Geographic and Stratigraphic Distribution

The geographic occurrence of oil families identified in the study area is demonstrated in Fig.5.15. The Silurian crude oils of Family 1 (blue dots) concentrated mainly in the southeastern part of the Euphrates Graben. Oils represented by samples G002959 and G002954 are produced from the Cretaceous Post Judea Sand (PJS) reservoir and G002982 from the Palaeozoic Upper Doubayat reservoir (see Appendix.C). One oil sample (G002988) in the northwestern part is attributed to the shallow Miocene Jeribe reservoir. Family 2A, which is thought to originate from Upper Cretaceous source rocks (possibly Shiranish Formation), is distributed in the central part along the graben axes from southeast to northwest (green dots). Reservoirs with Family 2A oils are found in different stratigraphic horizons. Two oils samples (G002968 and G002975) in the south are produced from Palaeozoic reservoirs (Lower Doubayat and ICD, respectively). In contrast, three other oil samples (G002993, G002997, and G003011) in the north are produced from shallow Miocene Lower Fares, Jeribe, and Dhiban reservoirs (see Appendix.C). All other crude oils in the central element are produced from Cretaceous reservoirs (Rutbah, Mulussa F, and Lower Shiranish). Interestingly, the younger age and shallower depth of the reservoirs towards northwest gives a hint about the migration pathways of oils in this specific family.

Family 2B oil samples, which are probably generated from the Upper Cretaceous R'mah Formation, are located mainly in the northeastern margin of the graben and produced from Cretaceous sediments (Lower Rutbah and PJS). Three crude oils are situated, however, in the southern part namely G003017 (Palaeozoic Doubayat reservoir), G003009 (Cretaceous Rutbah pool) and G002960 (Cretaceous Ereka accumulation). It is interesting to see that some oils (G002981, G002952, and G002980) are produced from the same wells or wells close to those which produce oils from Silurian source rocks. These oils have significantly higher maturation

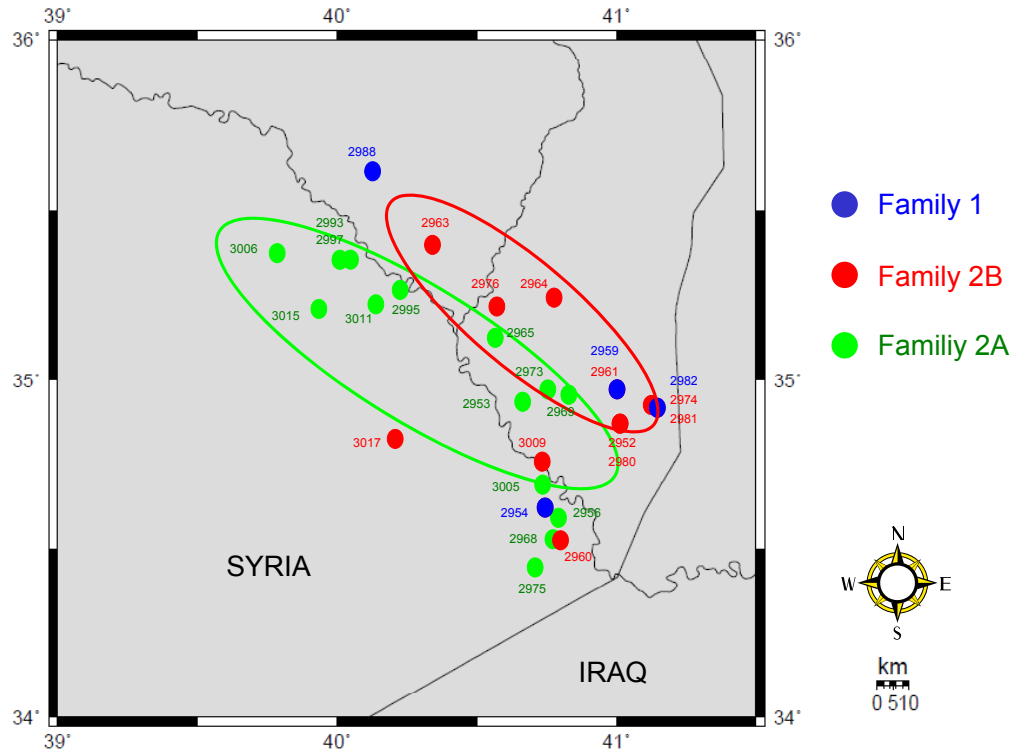


Figure 5.15: Geographic distribution of the main genetic oil families in the Euphrates Graben. Numbers near dots represents the oil samples code G00xxxx (e.g. 3017 is G003017)

levels than other oils in Family 2B (see Fig.5.10 for instance). Moreover, these oils have signatures of clay-rich source rocks (see Fig.5.8) which are not so common in Upper Cretaceous source rocks. This might raise a question mark about the possibility of oil mixing between Silurian and Upper Cretaceous sources for these crude oils. In this context it is also remarkable that two oils (G002959 and G002961) produced from the same well but having totally different oil signatures and fall in two different oil families. Other examples are samples G002974 and G002982 which are produced from two wells in the same area but which have different oil compositions.

This highlights the key role of the very complicated tectonic and geologic structures of the Euphrates Graben in controlling the locality of the reservoirs and oil families distribution across, but also migration pathways in the study area.

5.2 Oil-Source Rock Correlation

In the previous sec.5.1 evidence has been provided indicating that there are two distinct families of oils in the study area. Both have been sourced by separate and relatively unique source rock intervals. The potential source rock suggested for Family 1 oils is the Silurian Tanf Formation. Upper Cretaceous source rocks are the main source of oils of the main family 2. The subdivision of this family into two subfamilies 2A and 2B was due to slight differences in source rock facies and some variations in the maturation level of oils. Therefore, it is supposed that the Shiranish Formation could be the main source rock of Family 2A, and that the R'mah Formation is the main contributor to Family 2B.

5.2.1 Source Rock Distribution

Before making the routine oil-source rock geochemical correlation, it is worthy to have a look at the regional distribution of the potential source rocks across the study area and see to which extent this distribution fits to the occurrence of the oil families shown in Fig.5.15. A compilation of the oil families distribution as have been expected from oil-oil correlation and the possible distribution of possible source rocks in the study area is provided in Fig.5.16.

The probable distribution of the Silurian Tanf Formation has been obtained from the literature (Luning *et al.*, 2000; Serryea, 1990). Here one should keep in mind that the real distribution of Lower Silurian Hot Shales is still controversial and that there is no ultimate definition about the accurate spread of this formation. But, as the equivalent Hot Shales found elsewhere in the Middle East and in North Africa, these organic-rich shales are not found everywhere in the study area even if the Lower Silurian strata are present. At the same time, it is generally accepted that there is no presence of the Silurian Tanf Formation in the central part of the graben. The confirmed existence of this formation is the southeast and northwest of the Euphrates Graben. In this context, it is interesting to see that the Family

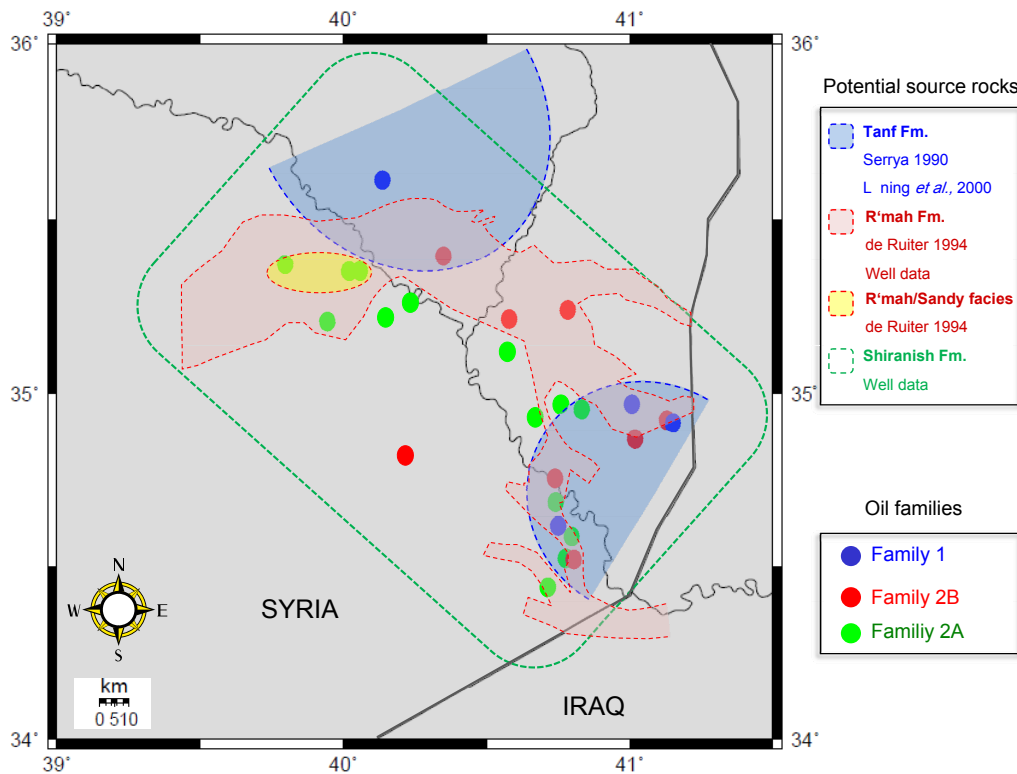


Figure 5.16: Figure shows a combination of the distribution of identified oil families and the probable spread of potential source rocks across the study area. Very good correlation is obvious between the oil families and the probable associated source rocks.

1 oil samples are found exclusively in these two marginal parts fitting to the possible distribution of the associated potential source rock. Family 2A crude oils are supposed geochemically to be generated from the Upper Cretaceous Shiranish Formation. This potential source rock distributes over the study area and reaches the highest thickness and depth in the central part along the graben axes. The rifting process during the Upper Cretaceous ceased in the late Maastrichtian period during the deposition of the Upper Shiranish Formation. This caused a maximum burial of the Shiranish Formation in the central part of the graben and resulted in a thermal maturity to generate oil. This coincides to the presence of Family 2A crude oils in the central part of the graben. The Upper Cretaceous R'mah Formation is not present in the whole region, but is preserved mainly in the northeastern margin and in some areas in the southern sector (see Fig. 5.16). The distribution pattern matches the distribution of Family 2B crude oils.

5.2.2 Geochemical Oil-Source Rock Correlation

Based on geochemical characteristics of the crude oils analysed (sec.5.1), it has been inferred that Family 1 oils were generated from a high mature clastic Palaeozoic source rock which is the Silurian Tanf Formation as a unique strata fitting these source features. Oil samples of families 2A and 2B were proven to be generated from mature carbonate rocks Upper Cretaceous in age. The two potential source rocks R'mah and Shiranish Formations, have relatively similar source traits and thermal maturity level. Therefore, uncertainties remain whether the oil was derived from the R'mah or Shiranish Formation. An attempt to use some geochemical parameters to correlate between oils and the potential source rocks is offered in the following lines. As discussed in sec.4.2 the Silurian rock samples are unfortunately not representative for the whole organic matter-rich Silurian sequence. Therefore the following oil-source correlation will exclusively compare Upper Cretaceous R'mah and Shiranish rock samples with crude oils of Family 2A and 2B. Geochemical correlation between source rock extracts and crude oils relies upon establishing similarities in the composition or properties of the crude oil and extracts which indicate common points in the genesis of the samples. The major difficulty of the correlation task is that the majority of parameters used for correlation purposes are influenced by maturity. Some biomarker parameters have been selected to establish the oil-source rock correlation in this study. Fig.5.17 shows a cross plot of $\text{Pr}/n\text{-C}_{17}$ versus $\text{Ph}/n\text{-C}_{18}$ which is typically used to predict the nature of the original organic material and the stage of diagenesis of the system.

There is a quite good correlation between, on the one hand, Shiranish source extracts and Family 2A oil samples and, on the other hand, between R'mah extracts and Family 2B oil samples. There is an overlay between oil families which could be expected as the potentially associated source rocks having similar features. But a slight difference can be really observed between Shiranish- and R'mah-sourced oils. R'mah source extracts have lower values of the isoprenoid over n -alkane ratio which could give the im-

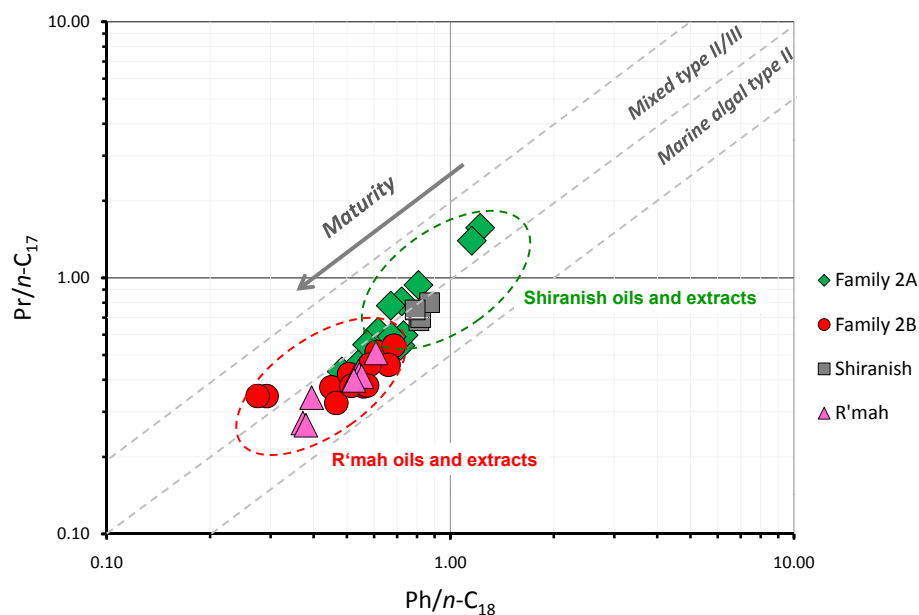


Figure 5.17: Plot of pristane/ n -C₁₇ vs. phytane/ n -C₁₈ for oil samples of Family 2A and Family 2B and associated potential source rocks (Upper Cretaceous Shiranish and R'mah).

pression being slightly more mature than Shiranish rock samples, but this is not confirmed from Rock-Eval analysis data (see Tab.4.9).

Biomarker-based correlation plots are shown in Fig.5.18 and Fig.5.19 where triangles of C_{27} , C_{28} and C_{29} regular sterane and diasteranes are shown. The crude oils of Family 2A show C_{27} , C_{28} and C_{29} regular sterane and diasterane distributions similar to those of the Shiranish rock extracts. Similarly, R'mah source rock extracts correlate very well to Family 2B crude oils (red circles). This could imply that the Family 2A oils are derived from Shiranish Formation and R'mah source rocks are probably responsible for generating crude oils of Family 2B. These implications are in agreement with what has been observed previously.

5.2.3 Possible Oil Migration Pathways

The determination of migration fairways in the study area is based on the integration of the geochemical data with regional stratigraphic and structural features in this area. At this point one should signify that the Euphrates Graben is a complex tectonic structure with numerous fault systems

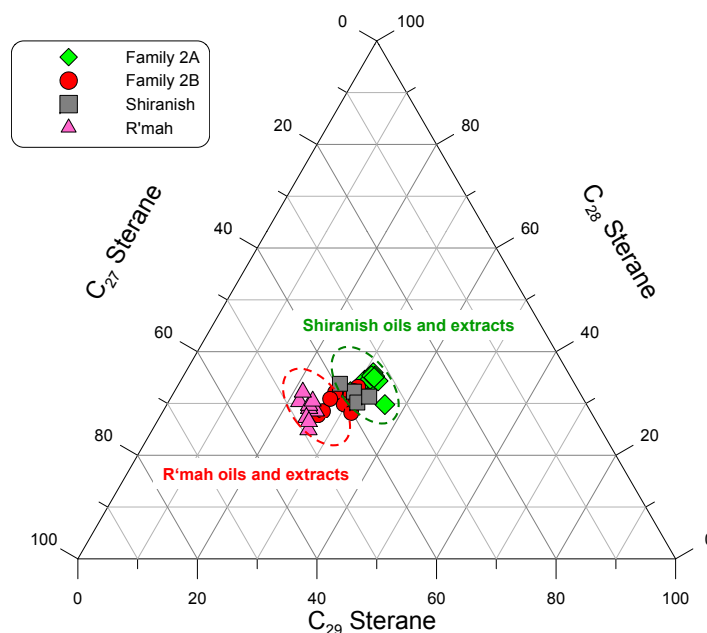


Figure 5.18: Ternary diagram showing the relative abundance of C_{27} , C_{28} and C_{29} regular steranes in saturated hydrocarbon fractions of oils (families 2A and 2B) and extracted source rocks (R'mah and Shiranish).

in different directions. The main families of fault trends in the Euphrates Graben contain the following directions (Anton Koopman, personal communication):

- N - S to NNE - SSW
- WSW - ENE (Palmyride trend)
- W - E
- WNW - ESE to NW - SE (basic Euphrates trend)
- NW - SE to NNW - SSE (Mesopotamian trend)

This numerous tectonic directions and related features complicate the analysis of the primary migration and/or the secondary oil migration pathways from the source to the reservoirs and even the tertiary migration from main to secondary reservoirs. In this framework, a simple and modest attempt to investigate the potential migration fairways is presented in this study. As there are three oil families identified in the Euphrates Graben,

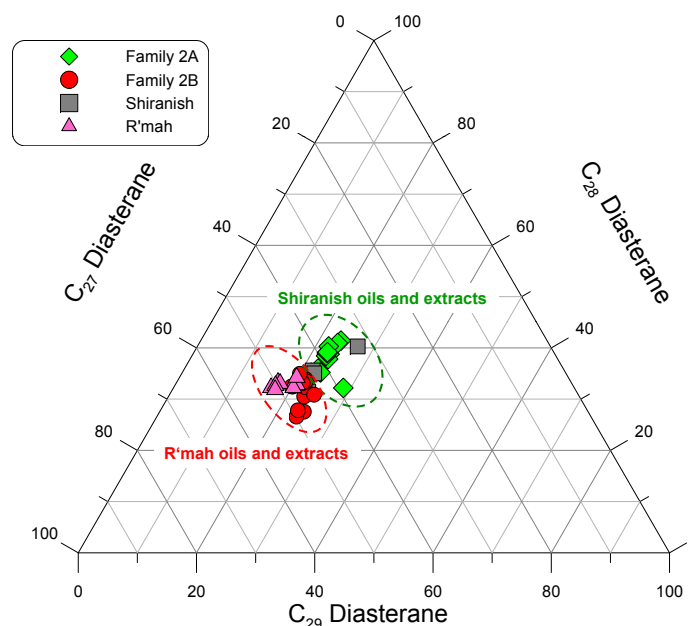


Figure 5.19: Ternary diagram showing the relative abundance of C_{27} , C_{28} and C_{29} diasteranes in saturated hydrocarbon fractions of oils (families 2A and 2B) and extracted source rocks (R'mah and Shiranish).

models of potential migration pathways for each identified oil family are presented.

Fig. 5.20 shows one kind of trap configuration in the Euphrates Graben when the syn-rift R'mah Formation is the main source rock and the reservoirs are attributed to the top of pre-rift Early Cretaceous deposits. In the northeastern margin of the graben where the R'mah Formation is most likely the main source rock, the generated oils (Family 2B members) migrate laterally into the Lower Cretaceous reservoirs (e.g. Rutbah, L. Shiranish, and Ereka).

The accumulations of Family 2A crude oils are attributed to different horizons from the Mesozoic (G002969, G003973 and G002965) in the central section into Miocene reservoirs (e.g. G002993, G002997 and G003011) in the northwestern element. This could also imply lateral migration from the southeast towards the northwest as the reservoirs are becoming shallower in this direction. Moreover, tar sands and oil seeps occur in the Bishri block just on the northwest of the western-most oil field in the study area (where G002993 and G002997 oil samples are coming from). Additionally,

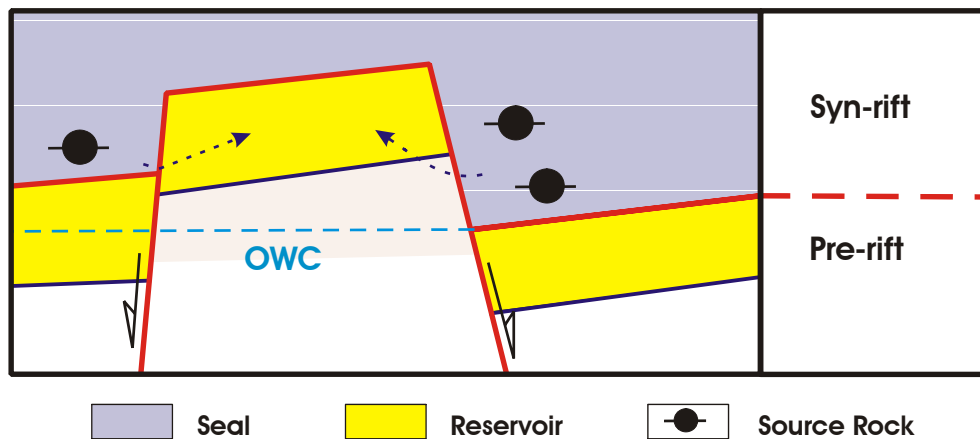


Figure 5.20: Schematic sketch shows the possible migration routes of Family 2B from R'mah source rock to the accumulations.

some changes in the molecular composition of the crude oils found in the Miocene reservoirs might be an indication to re-migration of crude oils from deeper reservoirs (see Fig.5.21). These changes include the loss of light hydrocarbons and relatively big hump (or unresolved complex mixture UCM) as seen in whole oil gas chromatograms e.g. Fig.4.7

G002997 and G002993 oil samples, for instance, are produced from the Miocene Jeribe reservoir and have the same genetic properties as other oils found in the Cretaceous reservoirs (e.g. G002995 and G02969). The possible explanation is due to the Tertiary inversion of this area which is in close relation to the formation of Palmyride Foldbelt. As a consequence the seal and the carbonates above the Cretaceous accumulations have been fractured and led to re-migration of oil from the Cretaceous reservoirs into the Miocene ones through the near-vertical, north-east trending faults (Litak *et al.*, 1997).

G002975 and G002968 oil samples are produced from Palaeozoic reservoirs (Infra Carboniferous Dolomite ICD and Lower Dabayat, respectively), and have Cretaceous source signatures. Migration pathways are probably due to tectonic forces which resulted in a juxtaposition between the Upper Cretaceous source rock and the Palaeozoic reservoirs (Litak *et al.*, 1997).

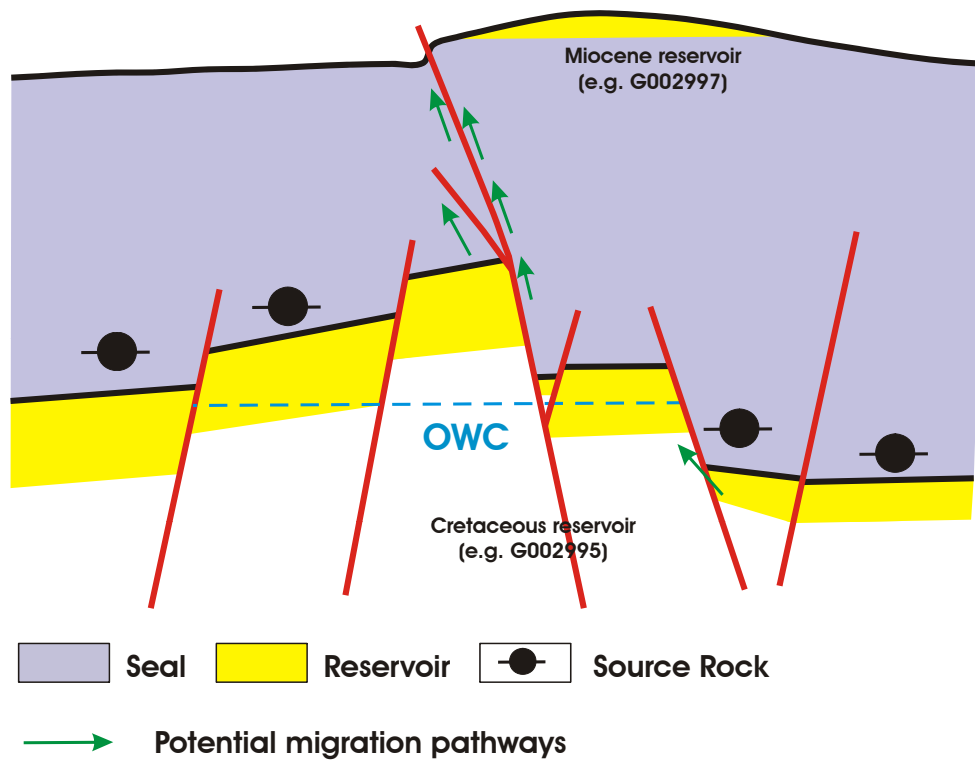


Figure 5.21: Schematic sketch illustrates the potential secondary migration pathways of Family 2A crude oils from the source rocks into the main reservoirs and the re-migration from Cretaceous into the Miocene accumulations.

As shown earlier (see sec.5.1), there are some oil samples attributed to Family 2B which have a clear signature of a Upper Cretaceous source, but that are significantly higher mature than their counterparts. Additionally, these oils (namely G002981, G002952, and G002980) are located in the southeastern part where the Silurian oils are found. This could imply a mixing potential between Silurian and Upper Cretaceous oils to form some Family 2B crude oils.

5.3 Oil Mixing Potential

Based on numerous molecular geochemical parameters and stable isotopes, oil-oil correlation (sec.5.1) in the Euphrates Graben Petroleum System has shown that there are primarily three oil families in the study area. The Family 1 oil samples originate from the Silurian Tanf Formation source rock and its oil samples are found principally in the southeastern part of the study area (Fig.5.15). The remaining oil samples are belonging to Family 2 which are derived from Upper Cretaceous source rocks. Oil-source rock correlation (sec.5.2) between the oils of Family 2 and the known Upper Cretaceous source rocks (R'mah and Shiranish Formation) has supported the assumption that this family can be subdivided into two subfamilies. Family 2A, which is concentrated in the graben centre, has signatures attributed to the Shiranish Formation and Family 2B is most likely generated from the R'mah Formation and its oils occur mainly on the northeastern margin (Fig.5.16). Some source- and maturity-related parameters showed that a number of oil samples from Family 2B do not fit totally to the source rock signatures of Upper Cretaceous. G002952, for instance, has a value below 0.25 for the $24/(24+27)$ -nordiacholestane ratio (Fig.4.19) which points to contribution from a source rock older than Jurassic in age. Diamondoid-based facies related parameters (Fig.5.8) show that certain oil samples (G002952, G002980, G002960, G002961 and G002974) have a clay-rich source rock signature which does not fit totally to Upper Cretaceous carbonate source rocks. From the maturity point of view, some oil samples (e.g. G002952, G002960 and G002980) identified as Upper Cretaceous oils have clearly a higher maturity level than the others (Fig.5.10) raising the question about the reasons behind that. One could explain it as these oils have been generated from different source rock horizons (which could be rich in clay) and during different stages of maturation of Upper Cretaceous source rocks. But this explanation leaves open questions as the Upper Cretaceous source rocks did not reach that high level of maturation during oil expulsion and, additionally, the localities of these oils are in certain parts (southeastern

section) , but not all over the study area. The assumption, which might be more reliable and truthful, is that these oils are mixtures between Silurian and Upper Cretaceous oils. To proof the validity of this hypothesis, one should first be aware about the petroleum mixing in general and what has been done previously in this field. All petroleum are essentially mixtures of compositionally different pooled oils derived from the source rock(s) at different temperatures (Wilhelms & Larter, 2004). Consequently, when there are multiple source rocks in a sedimentary basin charging traps, then two regimes of mixed oils could be found: (1) in-reservoir mixed oils derived from the same source rock but at different maturity stages and (2) in-reservoir mixed oils originated from different source rocks (Wilhelms & Larter, 2004). Several studies have attempted to analyze and identify the mixing problems in different approaches. First studies applied the "oil fingerprinting" to predict the mixing and commingled features between oils (Hwang *et al.*, 1994 2000; Kaufman & Ahmed, 1990). Peters *et al.* (1989) have used the carbon isotopic composition of the oil and source rock extracts to evaluate the mixing between Jurassic and Devonian hydrocarbons in Beatric Basin, UK. Source-, age- and biodegradation-related biomarkers have been applied to distinguish and recognize oil mixing in some Scottish (Peters *et al.*, 1999b), Colombian (Dzou *et al.*, 1999), Liaohe Basin (Koopmans *et al.*, 2002) and Williston Basin (Jiang & Li, 2002) oil fields. Others used the aromatic hydrocarbons in order to determine the oil mixing potential (Aroui & McKirdy, 2005; van Aarssen *et al.*, 1999). The artificial mixing of typical end-member oils is used by several researchers to solve the potential oil mixing issue employing the mixing curves to assess the contribution of each source rock to the mixed oil (Chen *et al.*, 2003b; Zhang *et al.*, 2003). Mathematical calculations based on whole-oil carbon isotopic compositions and absolute concentrations of selected alkanes and biomarkers were also applied to solve oil mixing and commingled problems (McCaffrey *et al.*, 1996; Peters, 1986a; Zhang *et al.*, 2003). In this study, as already presented, there are three oil families indicating three source rocks in the study area. The proposed petroleum mixing matter is

involved with oils found especially in the southeastern part where signatures of different source horizons have been observed. These oil samples are: G002952, G002960, G002961, G002974, G002980 and G002981 (see Fig.5.15 for locations). The most critical and important step in dealing with the oil mixing subject is the reasonable and logical identification of the end-members which will be the key elements of the mixing evaluation processes. The end-members are representing oils generated from the main source rocks in the study area. As no well-representing source samples (especially for Silurian source) are available for the main source rocks, another approach will be considered in defining the end-members. Since three main oil families were identified, it is acceptable and sufficient to pick-up three oils which reflect their sources very well. Some oils have been avoided to be selected as end-members as those supposed to be influenced by biodegradation or evaporation. The selected end-members are G002954 for the Silurian (Family 1) oils, G002973 for the Shiranish oils (Family 2A) and G002964 for the R'mah oils (Family 2B). Mathematical calculations based on absolute concentrations, specific hydrogen and carbon isotopic composition of selected alkanes and isoprenoids are applied. It has been concluded from several studies that the interpretation of source and maturity of mixed oils with biomarker ratios does not accurately reflect the mixtures due to the varying component concentrations in the end-members (Jiang & Li, 2002; Wang & Stout, 2007; Wilhelms & Larter, 2004). Therefore, the use of the concentrations of light hydrocarbons and isoprenoids, which will have similar order of magnitude concentrations in most oils, is the most reliable mean of detecting the compositional differences in reservoir geochemical settings in many petroleum systems (Wang & Stout, 2007; Wilhelms & Larter, 2004). To build the mathematical matrix used to calculate the proportion of each end-member to the mixed oil, absolute concentrations and compound specific isotope data for end-members (Tab.5.1) and proposed mixed oils (Tab.5.2) have been used.

| | End-members | | | | | |
|---------------------------|-------------|-------------------|-----------|-------------------|---------|-------------------|
| Source | Tanf | | Shiranish | | R'mah | |
| Sample | G002954 | | G002973 | | G002964 | |
| Compound | ppm | ‰ | ppm | ‰ | ppm | ‰ |
| <i>n</i> -C ₁₅ | 5267.95 | -92.81 -28.18 | 6716.10 | -139.28 -30.01 | 7032.22 | -89.69 -28.52 |
| <i>n</i> -C ₁₆ | 4594.02 | -87.35 -28.47 | 6287.83 | -137.84 -29.68 | 6795.63 | -91.31 -28.32 |
| <i>n</i> -C ₁₇ | 4042.74 | -85.82 -27.83 | 5908.16 | -135.73 -30.49 | 6054.74 | -87.76 -28.01 |
| Pr. | 1203.06 | -90.56 -27.58 | 4785.31 | -168.16 -31.19 | 2772.21 | -123.37 -27.84 |
| <i>n</i> -C ₁₈ | 3361.70 | -86.74 -27.82 | 5325.88 | -130.19 -30.06 | 5585.36 | -86.95 -28.05 |
| Ph. | 652.07 | -120.01 -28.01 | 3844.83 | -162.29 -30.56 | 3689.92 | -123.44 -28.41 |
| <i>n</i> -C ₁₉ | 3188.86 | -86.75 -27.76 | 5707.77 | -131.42 -29.57 | 5454.98 | -91.91 -28.28 |
| <i>n</i> -C ₂₀ | 2399.53 | -85.80 -29.16 | 4689.86 | -129.42 -29.66 | 4584.79 | -87.52 -27.95 |
| <i>n</i> -C ₂₁ | 2040.77 | -90.33 | 4395.46 | -135.65 | 3961.52 | -92.25 |
| <i>n</i> -C ₂₂ | 1628.20 | -90.88 | 4536.44 | -127.64 | 3480.62 | -92.33 |
| <i>n</i> -C ₂₃ | 1382.90 | -93.55 | 4024.89 | -131.27 | 2656.72 | -84.23 |

Table 5.1: The concentration (ppm), carbon and hydrogen isotopic values (‰) for each compound in the three end-members.

The concentrations of *n*-alkanes in the range from *n*-C₁₅ through *n*-C₂₃ and pristane and phytane were used after the normalization to the minimum concentration values. The normalized concentration values are obtained by dividing the concentration of each compound by the lowest concentration of that compound in the sample set. Using a multivariate linear method, the fitting matrix can be expressed as follows (Fig.5.22):

In which X_{nm} refers to the normalized concentration value multiplying by the isotopic composition of each compound in the different end members, Y_n refers to the normalized concentration value multiplied by the isotopic composition of each compound in the mixed oils, and f_m refers to the contribution factor of each class of crude oil. If the mixed oil came only from some combination from the three sources, then the relative contributions from the three end-members could be readily determined (matrix M in Fig.5.22) because

$$M = [GG^T]^{-1}G^T d \quad (5.8)$$

| Sample Compound | Mixed oils | | | | | | | | | | | |
|---------------------------|------------|----------------|---------|----------------|---------|----------------|---------|----------------|---------|----------------|----------|----------------|
| | G002952 | | G002960 | | G002961 | | G002974 | | G002980 | | G002981 | |
| | ppm | % _o | ppm | % _o | ppm | % _o | ppm | % _o | ppm | % _o | ppm | % _o |
| <i>n</i> -C ₁₅ | 6679.57 | -112.55 | 9101.12 | -92.08 | 6331.21 | -96.17 | 7757.89 | -93.02 | 7528.55 | -101.95 | 42417.24 | -99.88 |
| | | -29.26 | | -27.53 | | -27.86 | | -28.06 | | -30.31 | | -28.02 |
| <i>n</i> -C ₁₆ | 5755.51 | -99.68 | 8730.15 | -92.94 | 6010.20 | -96.72 | 7291.45 | -96.20 | 6487.28 | -91.23 | 36641.06 | -98.13 |
| | | -29.50 | | -32.42 | | -29.22 | | -28.67 | | -30.26 | | -28.46 |
| <i>n</i> -C ₁₇ | 4620.43 | -97.75 | 7803.79 | -80.78 | 5468.03 | -98.28 | 6789.10 | -88.44 | 5407.73 | -88.46 | 32009.28 | -94.81 |
| | | -29.34 | | -31.52 | | -27.51 | | -29.87 | | -29.97 | | -28.77 |
| Pr. | 1597.93 | -116.47 | 2919.39 | -117.11 | 2060.91 | -121.75 | 2205.94 | -119.52 | 1867.71 | -116.74 | 14677.38 | -121.62 |
| | | -29.40 | | -29.99 | | -27.81 | | -28.29 | | -29.01 | | -29.85 |
| <i>n</i> -C ₁₈ | 3716.64 | -95.16 | 7212.70 | -87.45 | 5078.69 | -99.41 | 6004.69 | -88.90 | 4465.24 | -87.62 | 27561.04 | -91.73 |
| | | -29.54 | | -31.66 | | -27.27 | | -27.56 | | -30.10 | | -28.56 |
| Ph. | 1021.87 | -120.75 | 3249.69 | -106.18 | 2840.67 | -120.40 | 2796.86 | -118.63 | 1303.69 | -127.70 | 16056.95 | -115.57 |
| | | -29.39 | | -30.50 | | -27.48 | | -28.52 | | -30.88 | | -29.51 |
| <i>n</i> -C ₁₉ | 2981.82 | -97.36 | 6859.78 | -90.02 | 5017.61 | -91.36 | 5846.11 | -90.44 | 3842.13 | -90.87 | 26628.73 | -93.93 |
| | | -29.75 | | -31.08 | | -27.88 | | -28.13 | | -29.59 | | -28.84 |
| <i>n</i> -C ₂₀ | 2181.27 | -96.63 | 5740.79 | -85.90 | 4651.42 | -89.40 | 4872.31 | -82.57 | 2888.10 | -79.66 | 20423.06 | -93.98 |
| | | -30.23 | | -31.42 | | -27.30 | | -28.96 | | -30.27 | | -28.66 |
| <i>n</i> -C ₂₁ | 1766.78 | -99.06 | 5056.20 | -83.38 | 4026.51 | -89.62 | 4265.77 | -92.32 | 2300.50 | -87.92 | 16581.09 | -97.46 |
| <i>n</i> -C ₂₂ | 1390.49 | -96.90 | 4650.37 | -79.94 | 3776.45 | -81.04 | 4038.19 | -86.90 | 1896.59 | -75.52 | 12884.74 | -95.58 |
| <i>n</i> -C ₂₃ | 1067.91 | -91.75 | 3926.31 | -80.39 | 3117.13 | -91.76 | 3368.72 | -102.84 | 1427.69 | -72.70 | 9389.45 | -95.76 |
| | | | | | | | | | | | 2430.90 | -88.74 |

Table 5.2: The concentration (ppm), carbon and hydrogen isotopic values (‰) for each compound in the proposed mixed oils.

$$\underbrace{\begin{bmatrix} X_{11} & X_{12} & X_{13} & \cdots & X_{1n} \\ X_{21} & X_{22} & X_{23} & \cdots & X_{2n} \\ X_{31} & X_{32} & X_{33} & \cdots & X_{3n} \\ \cdots & \cdots & \cdots & \cdots & \cdots \\ X_{m1} & X_{m2} & X_{m3} & \cdots & X_{mn} \end{bmatrix}}_{\mathbf{G}} \times \underbrace{\begin{bmatrix} f_1 \\ f_2 \\ f_3 \\ \vdots \\ f_m \end{bmatrix}}_{\mathbf{M}} = \underbrace{\begin{bmatrix} Y_1 \\ Y_2 \\ Y_3 \\ \vdots \\ Y_n \end{bmatrix}}_{\mathbf{d}}$$

Figure 5.22: The theoretical structure of matrices used for mixing calculations, where \mathbf{G} resembles the main matrix includes data of the end-members, \mathbf{d} refers to the data of proposed mixed oil, and f is the proportion of each end-member in the mixed oil.

where the G^T is the transpose of matrix \mathbf{G} . However, it should be controlled by the following conditions: the number of potentially certain sources cannot exceed the number of compounds used to construct the fingerprint of each oil, in other words, the number of variables (end-members) must be less than or equal to the number of equations (compounds). If the number of rows (compounds) is less than the number of columns (end-members), then no solution can be identified. However, the form in which the equation (Eq.5.8) is written does not allow the number of end-members to exceed the number of compounds. Tab.5.3 shows the matrices used for theoretical calculations. Eq.5.8 can be readily solved using the built-in functions in Microsoft EXCEL, as described in Appendix.D.

To test the validity of this approach, a test has been made for an oil sample attributed to Silurian oil family (G002982). Fig.5.23 shows that the Silurian portion in this oil is almost 99% (blue track) which is fully in agreement with the geochemical observations.

Results of the theoretical calculations of six proposed mixed oils are illustrated in Fig.5.24, most of the mixed-proposed oils have proportion from Silurian source of about 50% and more (except G002981 which has a value of 38%). This supports the hypothesis of the mixing potential of these oils between Silurian and Upper Cretaceous origins.

| Source | End-members | | | Mixed oils | | | | | | | |
|------------|-------------|-----------|---------|------------|---------|---------|---------|---------|----------|---------|--|
| | Tanf | Shiranish | R'mah | | | | | | | | |
| Sample | G002954 | G002973 | G002964 | G002952 | G002960 | G002961 | G002974 | G002980 | G002981 | G002982 | |
| $n-C_{15}$ | -92.81 | -177.57 | -119.73 | -142.71 | -159.07 | -115.58 | -136.98 | -145.70 | -804.23 | -176.31 | |
| | -28.18 | -38.26 | -38.08 | -37.11 | -47.56 | -33.49 | -41.32 | -43.31 | -225.60 | -51.86 | |
| $n-C_{16}$ | -87.35 | -188.66 | -135.07 | -124.89 | -176.62 | -126.54 | -152.68 | -128.83 | -782.65 | -175.81 | |
| | -28.47 | -40.62 | -41.89 | -36.96 | -61.61 | -38.22 | -45.50 | -42.73 | -226.97 | -56.84 | |
| $n-C_{17}$ | -85.82 | -198.36 | -131.44 | -111.72 | -155.92 | -132.93 | -148.51 | -118.32 | -750.68 | -172.23 | |
| | -27.83 | -44.56 | -41.96 | -33.53 | -60.84 | -37.21 | -50.16 | -40.09 | -227.80 | -54.60 | |
| Pr. | -90.56 | -668.89 | -284.29 | -154.69 | -284.17 | -208.56 | -219.16 | -181.23 | -1483.78 | -183.09 | |
| | -27.58 | -124.05 | -64.15 | -39.05 | -72.77 | -47.65 | -51.88 | -45.03 | -364.22 | -48.42 | |
| $n-C_{18}$ | -86.74 | -206.25 | -144.46 | -105.21 | -187.63 | -150.18 | -158.80 | -116.38 | -752.06 | -163.73 | |
| | -27.82 | -47.63 | -46.60 | -32.66 | -67.93 | -41.20 | -49.23 | -39.98 | -234.14 | -56.12 | |
| Ph. | -120.01 | -956.92 | -698.52 | -189.23 | -529.17 | -524.51 | -508.84 | -255.32 | -2845.86 | -212.16 | |
| | -28.01 | -180.19 | -160.78 | -46.06 | -152.00 | -119.73 | -122.31 | -61.74 | -726.71 | -55.22 | |
| $n-C_{19}$ | -86.75 | -235.22 | -157.23 | -91.04 | -193.65 | -143.75 | -165.80 | -109.48 | -784.35 | -170.56 | |
| | -27.76 | -52.93 | -48.38 | -27.82 | -66.86 | -43.87 | -51.57 | -35.65 | -240.81 | -55.29 | |
| $n-C_{20}$ | -85.80 | -252.95 | -167.23 | -87.84 | -205.51 | -173.31 | -167.67 | -95.88 | -799.85 | -174.22 | |
| | -29.16 | -57.96 | -53.40 | -27.48 | -75.18 | -52.91 | -58.80 | -36.43 | -243.92 | -53.21 | |
| $n-C_{21}$ | -90.33 | -292.16 | -179.08 | -85.76 | -206.59 | -176.83 | -192.98 | -99.11 | -791.87 | -171.07 | |
| $n-C_{22}$ | -90.88 | -355.62 | -197.38 | -82.75 | -228.33 | -187.96 | -215.53 | -87.97 | -756.35 | -162.92 | |
| $n-C_{23}$ | -93.55 | -382.07 | -161.82 | -70.85 | -228.25 | -206.83 | -250.51 | -75.06 | -650.20 | -155.99 | |

Calculation results

| | | | | | | | |
|-----------|------|------|------|------|------|------|-------|
| Tanf | 0.99 | 1.16 | 0.61 | 0.96 | 0.91 | 2.26 | 1.97 |
| Shiranish | 0.01 | 0.07 | 0.00 | 0.04 | 0.00 | 0.16 | -0.01 |
| R'mah | 0.09 | 0.48 | 0.64 | 0.50 | 0.22 | 3.50 | -0.02 |

Table 5.3: No units for these data because they result from multiplying the hydrogen isotopic value with the normalized concentration value. The normalized concentration values result from dividing the concentration of each compound by the lowest concentration of that compound in the sample set.

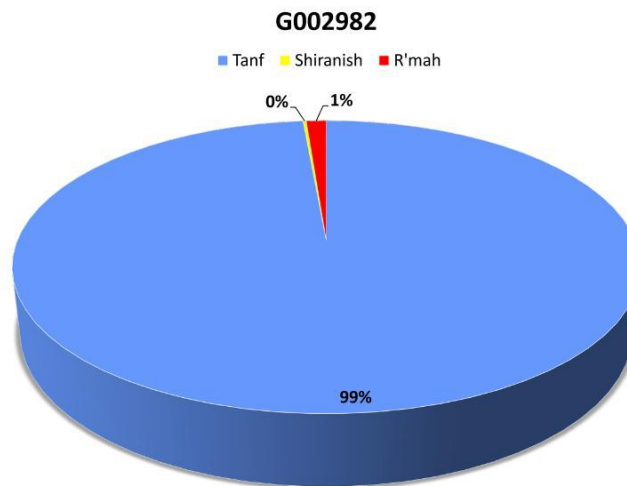


Figure 5.23: Calculation result when applied for a (pure) Silurian oil.

G002952 and G002980 have the highest calculated Silurian contribution 91 % and 81% , respectively. Both oil samples are attributed to the same producing well but from two different reservoirs. The calculated Silurian contributions to G002960, G002974, G002961 are also significant (68 %, 64 %, and 49%, respectively). G002961 is coming from the same well as G002959, which is considered as a Silurian-sourced sample, but from another accumulation. Interestingly, the calculation results show that the proportion of Shiranish Formation into mixed oils (yellow sectors in Fig.5.24) is very low ranging from 0-4% which is fully logical and in agreement with previous conclusions that Family 2B oil samples are most likely generated from Upper Cretaceous R'mah Formation. From what has been presented in this section one could conclude that the petroleum mixing can play a significant role in defining the hydrocarbon composition of oils produced in the Euphrates Graben especially in parts where both source rocks occur (e.g. in the southeastern sector). Therefore, it is strongly recommended to perform an artificial mixing experiment to get a better assessment of the petroleum mixing. These observations could imply an important hint to the exploration efforts in the study area. Today target of new drilled production wells are the well-known Cretaceous and Triassic accumulations as most of the oils produced in the area are trapped in these reservoirs. But considering the possible migration from the Silurian Tanf Formation

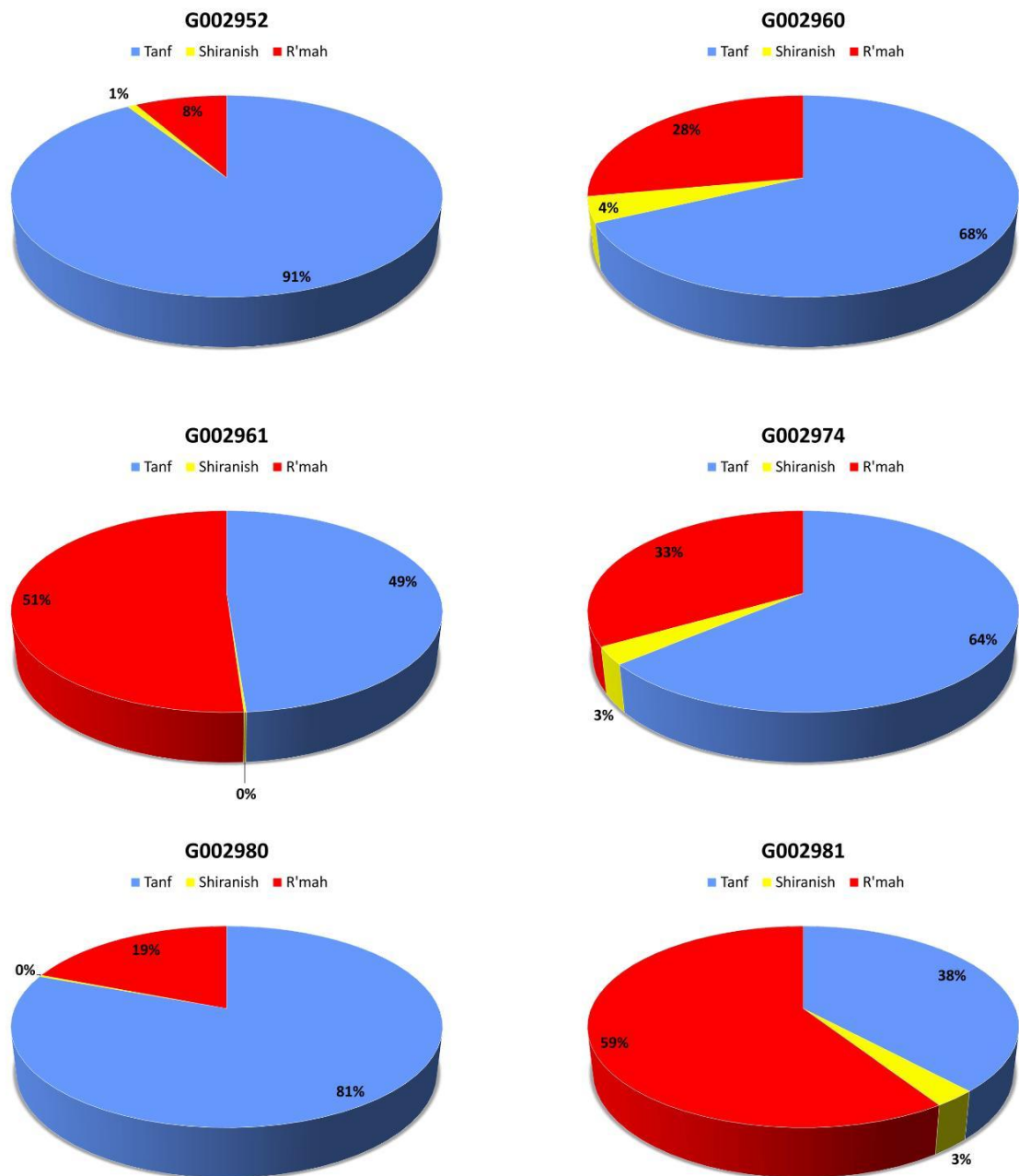


Figure 5.24: Mixing calculation results for proposed mixed oil samples (for oil sample locations see Fig.5.15).

upwards especially where mixing oils are found, one could expect new oil reserves in horizons older than Triassic or eventually younger with mixing background.

The apparently successful application of this new approach in defining oil mixing potential in study area can have promised implications in oil industry and research. In more general sense this approach can be applied

in different petroleum systems to identify the petroleum mixing between two or more source rocks. The advantage of this approach that there is no need to have samples from the associated source rocks to get reliable results about the mixing potential among several oil families. But at the same time the logical and reliable determination of oil families plays a key role in building up the petroleum mixing model. Additionally, the careful selection of end-members is very important and basic step in oil mixing model calculations.

5.4 Petroleum Biodegradation

The alteration of crude oils by living organisms is called "Petroleum Biodegradation", (Milner *et al.*, 1977; Connan, 1984; Palmer, 1993; Blanc & Connan, 1994). Biological degradation of crude oils in reservoirs is a kind of hydrocarbon oxidation by anaerobic (Davis & Yarbrough, 1966; Wilkes *et al.*, 2000 2002) or aerobic microorganisms (Bailey *et al.*, 1973; Goodwin *et al.*, 1981). Such organisms use specific hydrocarbons as energy and/or carbon sources for their metabolic processes and to build up biomass. Petroleum biodegradation, as a hydrocarbon oxidation process, leads to the formation of carbon dioxide CO_2 and potentially oxidized residues, such as organic acids (Peters *et al.*, 2005). The alteration of the crude oil compositions caused by biological activity predominantly occurs within the reservoir and is accompanied by a decrease in the net volume of petroleum and a significant deterioration of the crude oil quality (Peters *et al.*, 2005; Wenger *et al.*, 2001). The petroleum biodegradation takes place in the subsurface when specific geological and geochemical conditions are found that enable and enhance microbial life.

In the so-called water leg is that located beneath the oil column microbes are thought to live and utilize the hydrocarbons of the petroleum within the water phase or near the oil-water contact in the reservoir (Larter *et al.*, 2006). It is assumed that the diffusion of hydrocarbons from the oil column to the oil-water contact zone may control and limit the degradation processes (Huang *et al.*, 2004). Another requirement for microbial activity in the deep biosphere is a sufficient porosity and permeability in the rock fabric which enables the diffusion of nutrients and sufficient bacterial mobility (Peters *et al.*, 2005). Petroleum biodegradation can occur up to a reservoir temperature of $\sim 80^\circ\text{C}$ (corresponding $\sim 2\text{-}3$ km in normal geothermal gradient). It is believed that biodegradation can not be found in petroleum reservoirs with formation water salinity more than 100-150 parts per thousand (Peters *et al.*, 2005; Head *et al.*, 2003). The schematic mechanisms within a biodegrading petroleum accumulation are summarized

in Fig.5.25.

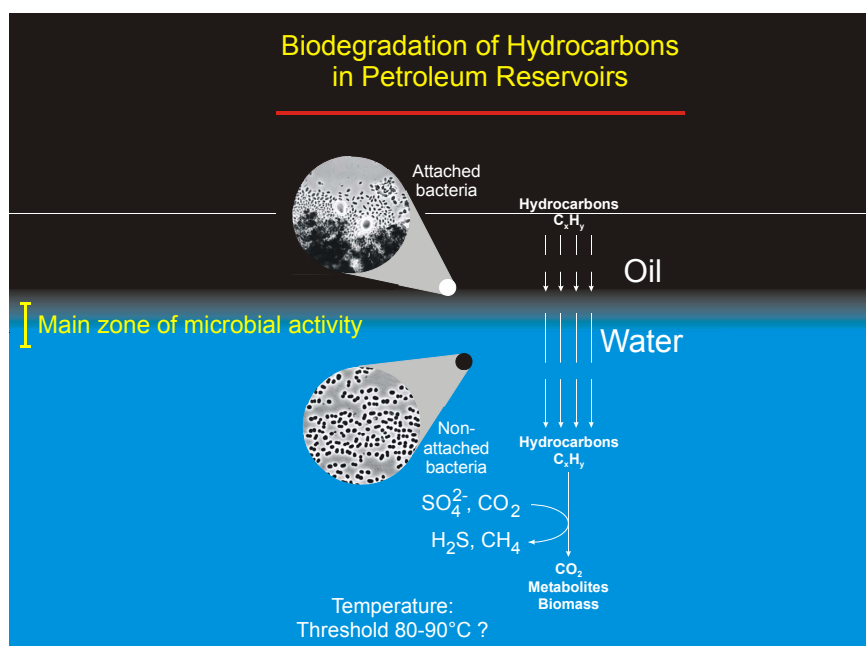


Figure 5.25: Schematic mechanisms of biodegradation within a petroleum reservoir.

It is assumed that biodegradation leads to a selective removal of specific types of crude oil constituents as it proceeds (Peters & Moldowan, 1993; Wenger *et al.*, 2001), with saturated hydrocarbons being degraded first. Peters & Moldowan (1993) have suggested a classification scheme for the degradation stages called PM scale. This model proposes a systematic and sequential removal of individual compound classes with proceeding biodegradation. The authors suggest that biodegradation should be ranked on a scale from 1-10, with rank 1 indicating a slight extent of biodegradation while rank 10 denotes to severe effects on composition of crude oils. A modified biodegradation scheme that is based on the PM scale, was published by Wenger *et al.* (2001) and modified by Head *et al.* (2003), and is shown in Fig.5.26

This scheme describes a quasi-sequential removal of compound groups as follows: *n*-alkanes > *i*-alkanes > alkylbenzenes > alkylnaphthalenes > alkylcyclohexanes, alkylphenanthrenes and alkyl dibenzothiophenes > isoprenoids > regular steranes > hopanes > aromatic steranes (Wenger *et al.*, 2001; Peters & Moldowan, 1993). Due to the microbial degradation of specific oil

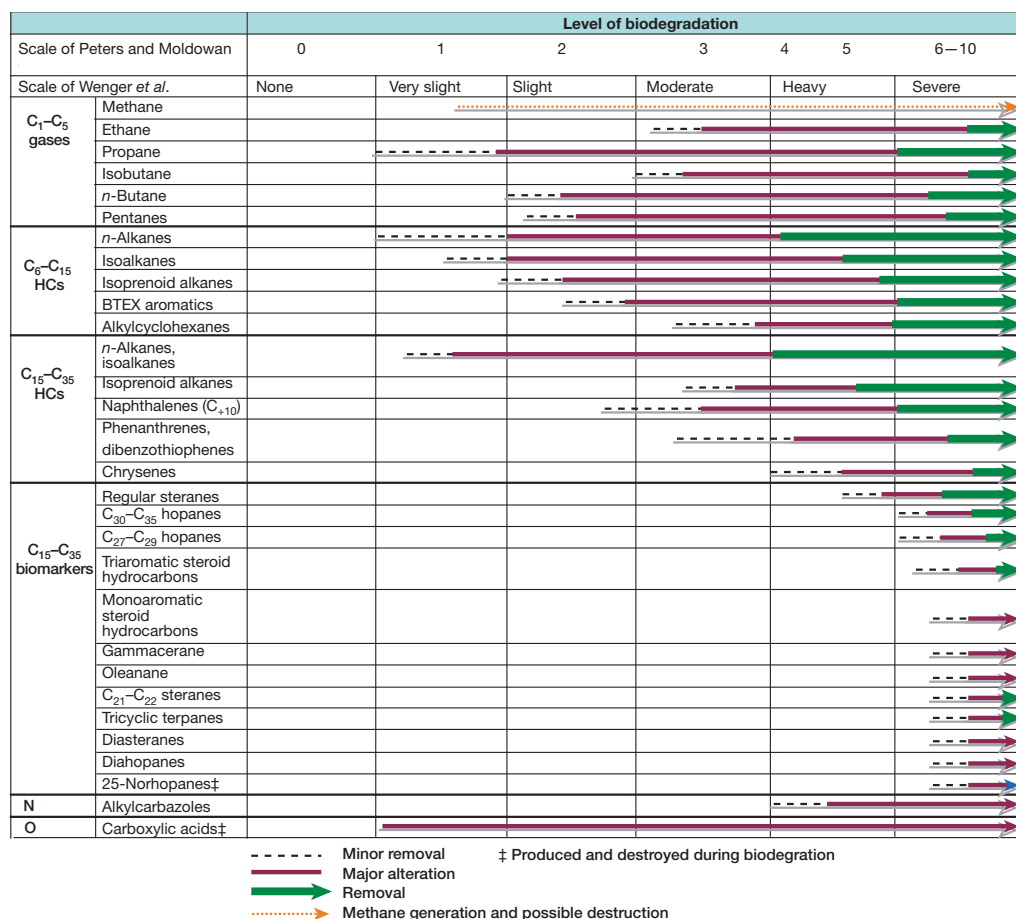


Figure 5.26: Generalized sequence of the removal of selected molecular groups at increasing levels of biodegradation, modified from (Wenger *et al.*, 2001).

constituents major changes in the bulk chemical and physical properties of petroleum occur. Biodegradation leads to relative enrichment in NSO compounds increase in oil viscosity, and relative enrichment of metal contents (e.g. Ni, V, and S) (Peters & Moldowan, 1993; Tissot & Welte, 1984). However, a very important indicator for the oil recovery is the API gravity, which is significantly reduced by proceeding biodegradation making the oils pastier Fig.5.27 (Tissot & Welte, 1984; Elias *et al.*, 2007).

It is shown in this study that some oils produced in the northeastern part of the Euphrates Graben from relatively shallow reservoirs (500-800 m depth) are might be affected by microbial biodegradation. These oils (G002993, G002997, G002998, G003001, and G003011, see Fig.5.15 for locations) presumably originate from the Upper Cretaceous Shiranish For-

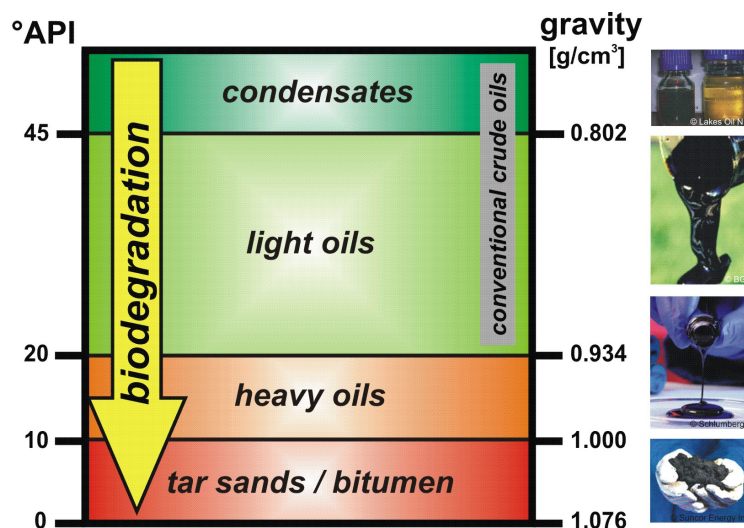


Figure 5.27: Biodegradation leads to the deterioration of crude oil quality as indicated by API gravity.

mation based on oil-oil (sec.5.1) and oil-source rock (sec.5.2) correlation. To verify these observations, geochemical correlation between the proposed biodegraded and non-biodegraded oils has been carried out. The oil samples involved in this correlation have been selected to be genetically-related (i.e. belong to the same oil family) to get a reliable assessment of the biodegradation effect on studied crude oils. Fig.5.28 shows that the proposed biodegraded oils have API gravity lower than other oil samples (about 12° at lowest) and have high concentrations of the metals nickel (Ni) and vanadium (V) and also of sulfur (S) Tab.4.1.

Fig.5.29 shows the whole-oil gas chromatograms of Shiranish-sourced conventional oils (pink) and potentially biodegraded heavy oils (blue). Light hydrocarbons (yellow circles) are preferentially and partially removed in samples G002993, G002997, G002998 and G003011 in comparison to branched alkanes (red triangles) and isoprenoids (pristane and phytane).

Toluene has an enhanced water solubility relative to saturated hydrocarbons and hence the low toluene content (see Appendix.E) could be a result of solubilisation by water washing process (Thompson, 1987). As *n*-alkanes are removed, the elevated chromatographic baseline consisting of the unresolved complex mixture (UCM) becomes more prominent. But these GC profiles give an indication to very slight to slight biodegradation effects as

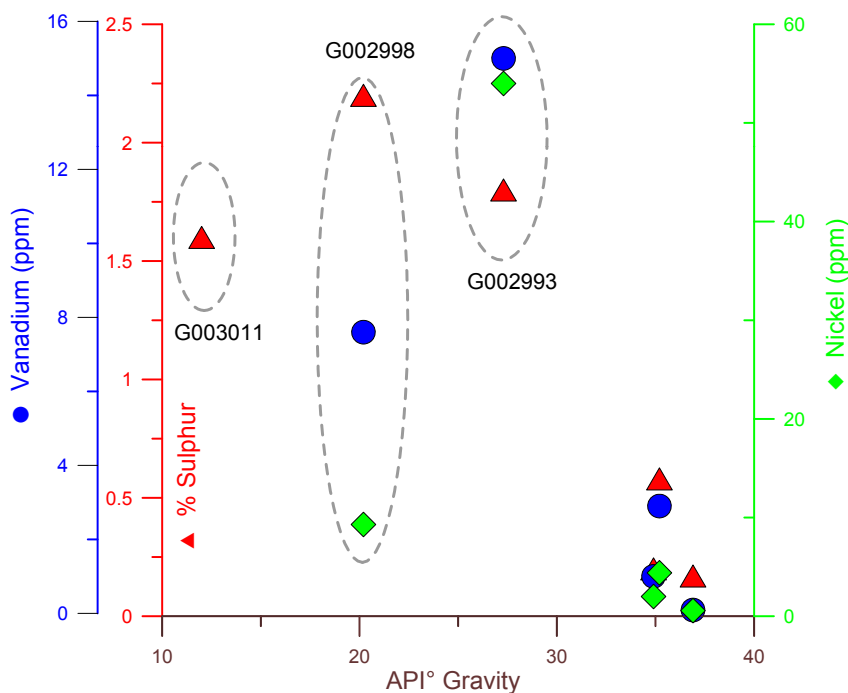


Figure 5.28: Sulfur, nickel, and vanadium contents increase with decreasing API gravity as an indication of the biodegradation effect.

the low molecular *n*-alkanes are not removed totally and, additionally, pristane and phytane are not affected as there is no remarkable difference in isoprenoids concentration between biodegraded and non-degraded oils (see Appendix.E). This is not in agreement with the findings made by Elias *et al.* (2007), where pristane and phytane are affected even in slight biodegradation level.

The concentration ratios of *iso*-alkanes and branched alkanes over *n*-alkanes are also decreasing with increasing biodegradation since the *n*-alkanes are more sensitive to alteration effects (Welte *et al.*, 1982). Fig.5.30 shows a plot of the conventional biodegradation parameters $i-C_5/(i-C_5+n-C_5)$ versus $3MP/(3MP+n-C_6)$ illustrating that blue-colored samples have been affected by in-reservoir alteration processes.

The cross plot of $Pr/n-C_{17}$ vs. $Ph/n-C_{18}$ is the most commonly used biodegradation indicator based on this assumption for initial to moderate alteration levels (Peters *et al.*, 1999a). Fig.5.31 illustrates that what are proposed to be biodegraded oils have relatively high isoprenoid over *n*-alkane ratios which can be an indication of microbial effects.

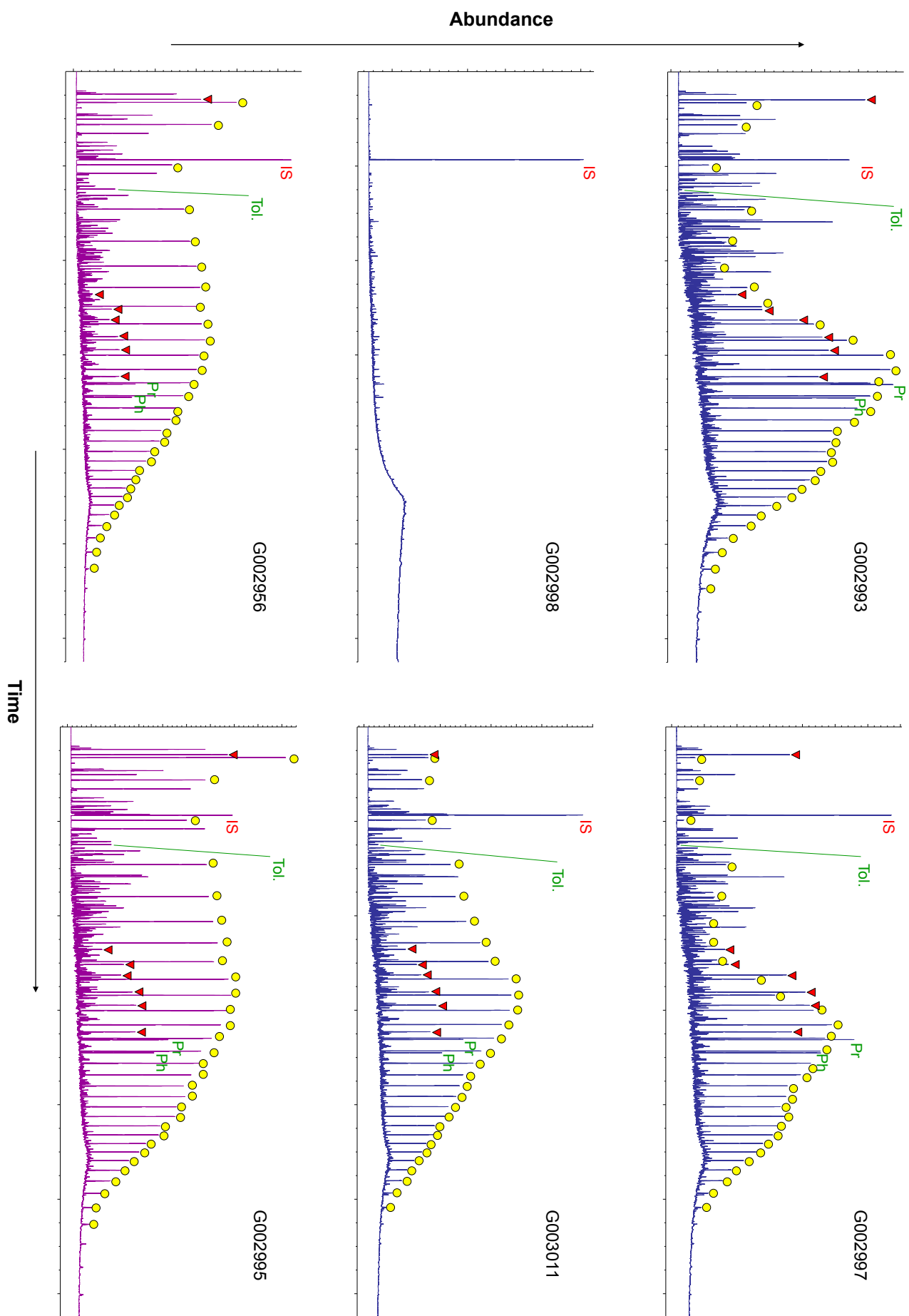


Figure 5.29: Whole oil GC-FID chromatograms for selected non-biodegraded (pink) and biodegraded (blue) oil samples. Different distribution of saturated hydrocarbons can easily be recognized.

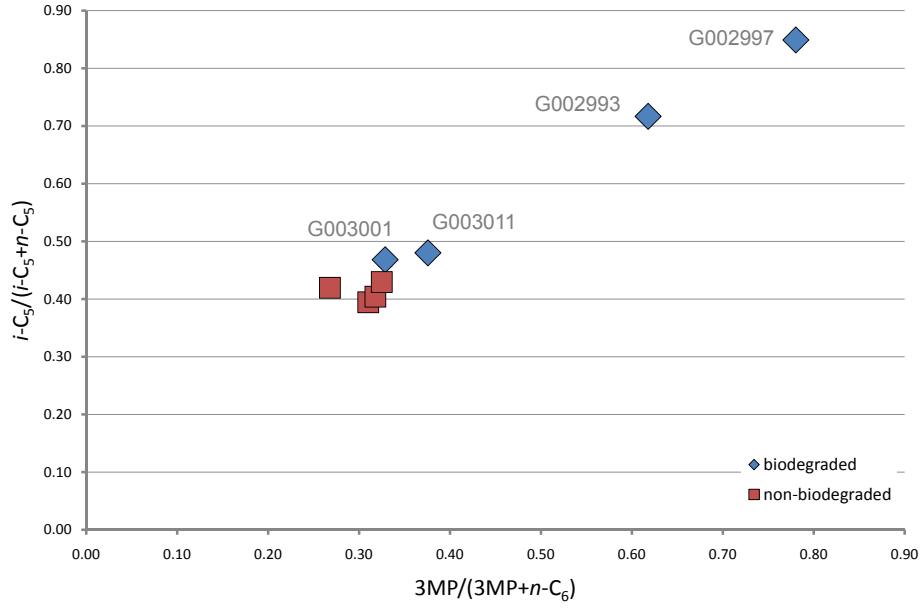


Figure 5.30: Plot of conventional biodegradation parameters $i-C_5/(i-C_5+n-C_5)$ vs. $3MP/(3MP+n-C_6)$ showing different signatures of the proposed biodegraded oils (in blue).

G002998 (API = 20°) seems to be severely biodegraded since almost no n -alkanes can be reliably identified Fig.5.32. But unfortunately no more data are available for this sample to better assess the extent of biodegradation.

Halpern (1995) suggested that 1,1-dimethylcyclopentane (1,1-DMCP) is the most resistant of all C_7 hydrocarbons and used this hydrocarbon in the denominator of 7 transformation ratios (Tr1 to Tr7; see Tab.5.4).

Transformation parameters are calculated from the following series of equations:

$$Tr1 = Toluene/1,1 - DMCP \quad (5.9)$$

$$Tr2 = n-C_7/1,1 - DMCP \quad (5.10)$$

$$Tr3 = 3MH/1,1 - DMCP \quad (5.11)$$

$$Tr4 = 2MH/1,1 - DMCP \quad (5.12)$$

$$Tr5 = P2/1,1 - DMCP \quad (5.13)$$

| Sample | Pr/ <i>n</i> -C ₁₇ | Ph/ <i>n</i> -C ₁₈ | iso-/ <i>n</i> -alkane | br-/ <i>n</i> -alkane | Tr1 | Tr2 | Tr3 | Tr4 | Tr5 | Tr6 | Tr7 | Tr8 | MDL% |
|---------|-------------------------------|-------------------------------|------------------------|-----------------------|-------|-------|------|------|-------|------|------|------|-------|
| G002993 | 1.40 | 1.15 | 0.72 | 0.62 | 0.18 | 1.19 | 2.45 | 1.55 | 4.00 | 2.32 | 2.33 | 1.29 | 45.90 |
| G002997 | 1.57 | 1.22 | 0.85 | 0.78 | 0.18 | 0.50 | 2.03 | 1.24 | 3.26 | 1.19 | 1.98 | 0.90 | 50.37 |
| G002998 | 2.09 | 2.49 | nd | nd | nd | nd | nd | nd | nd | nd | nd | nd | nd |
| G003001 | | | 0.47 | 0.33 | 2.20 | 5.84 | 4.12 | 2.89 | 7.01 | 6.21 | 2.91 | 2.66 | 2.34 |
| G003011 | 0.94 | 0.81 | 0.48 | 0.38 | 0.87 | 4.03 | 2.34 | 1.47 | 3.81 | 6.53 | 2.85 | 1.94 | 39.52 |
| G002953 | 0.78 | 0.67 | 0.39 | 0.31 | 2.34 | 7.48 | 3.22 | 2.26 | 5.48 | 5.62 | 2.62 | 2.33 | N-D |
| G002956 | 0.62 | 0.62 | 0.42 | 0.27 | 6.50 | 15.33 | 7.03 | 5.55 | 12.58 | 7.05 | 3.18 | 2.95 | N-D |
| G002973 | 0.81 | 0.72 | 0.40 | 0.32 | 3.33 | 9.25 | 4.35 | 3.04 | 7.39 | 6.81 | 3.11 | 2.52 | N-D |
| G002995 | 0.54 | 0.72 | 0.43 | 0.32 | 10.46 | 18.72 | 8.88 | 5.44 | 14.32 | 6.62 | 3.04 | 2.54 | N-D |

Table 5.4: Mean degradative loss (MDL %) values and molecular parameters used to assess the biodegradation extent for some crude oil samples in the study area, where *iso*-/*n*-alkane = *i*-C₅/(*i*-C₅+*n*-C₅), *br*-/*n*-alkane = **3MP**/(**3MP**+*n*-C₆). N-D is non-degraded oil. nd = no data.

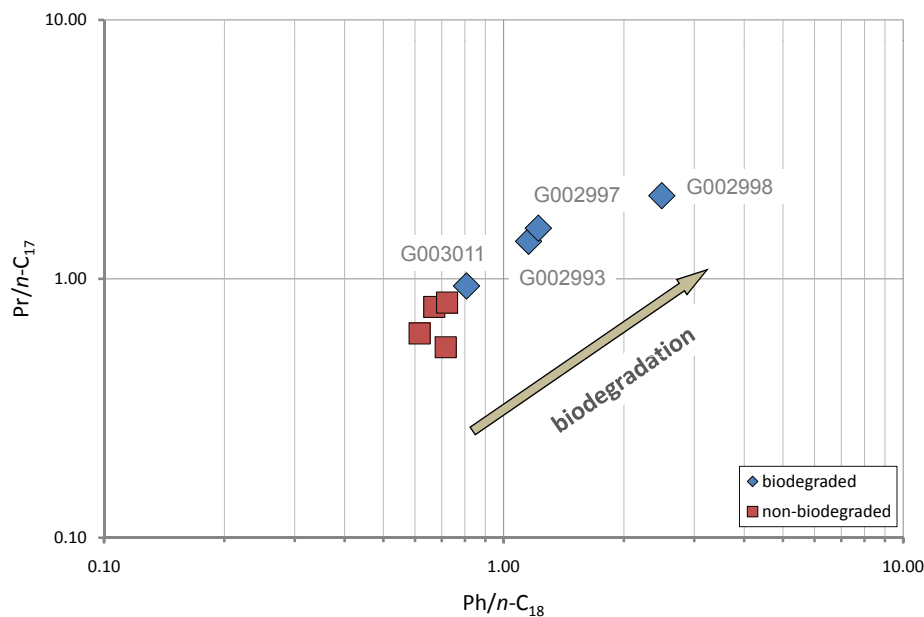


Figure 5.31: Cross plot of the ratios $\text{Pr}/n\text{-C}_{17}$ vs. $\text{Ph}/n\text{-C}_{18}$. The increased values of the blue samples can be interpreted as a result of biodegradation effects.

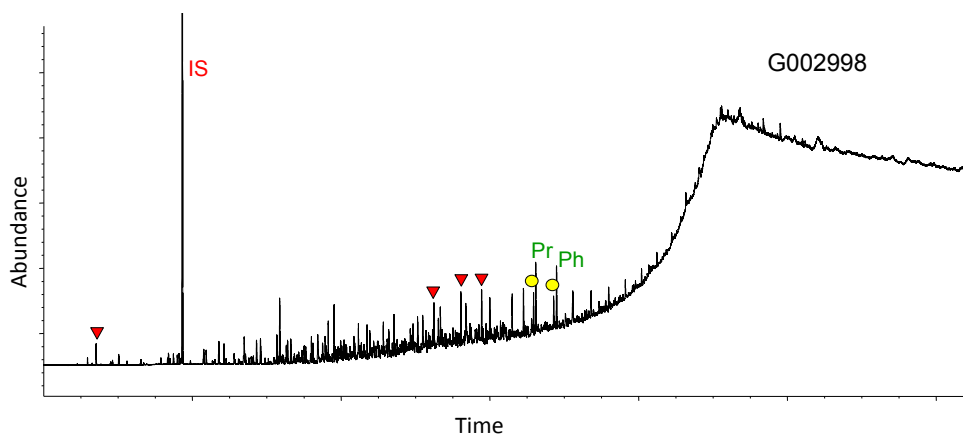


Figure 5.32: Whole-oil chromatogram of G002998 sample shows higher biodegradation degree in comparison with other biodegraded oil samples.

$$Tr6 = 1 - cis - 2 - DMCP/1, 1 - DMCP \quad (5.14)$$

$$Tr7 = 1 - trans - 3 - DMCP/1, 1 - DMCP \quad (5.15)$$

$$Tr8 = P2/P3 \quad (5.16)$$

where: $P2 = 2MH + 3MH$ and $P3 = 2,2\text{-DMP} + 2,3\text{-DMP} + 2,4\text{-DMP} + 3,3\text{-DMP} + 3\text{-EP}$, (Mango, 1990b) (see Tab.3.2 for abbreviations).

These ratios were used by Halpern (1995) in the C_7 oil transformation star diagram ($C_7\text{OTSD}$) to differentiate water washing, biodegradation and

evaporation for oils from Saudi Arabia. Fig.5.33 shows the C_7 OTSD of the studied oils illustrating different compositions of altered oils (G002993, G002997, and G003011) compared to non-affected oils (G002956, G002973, and G002995).

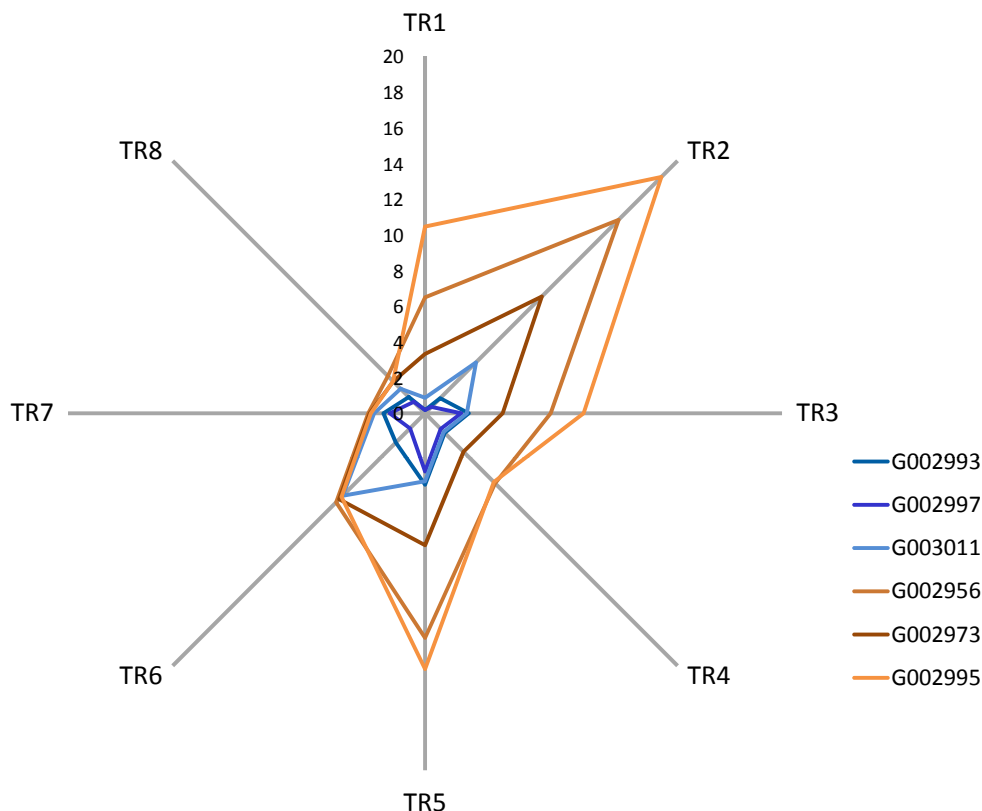


Figure 5.33: C_7 oil transformation star diagram (C_7 OTSD) shows that G002997, G002993, and G003011 oil samples have suffered from alteration processes as having relatively low values of Tr's as interpreted according to (Halpern, 1995).

Elias *et al.* (2007) have suggested a new molecular biodegradation parameter, the degradative loss, which can be used to quantify depletion in individual crude oil constituents. Low to moderate biodegradation extent in crude oil samples has been analysed by means of the *mean degradative loss* (MDL) calculated from the following equation:

$$MDL(\%) = 100 - [(\sum conc.(i-C_5 - n-C_{30})_{sample} \times 100) \div (\sum conc.(i-C_5 - n-C_{30})_{end-member})] \quad (5.17)$$

In this equation (Eq.5.17) the summed concentrations ($\mu\text{g/g}$ oil) for 66 quantitatively important crude oil constituents (Appendix.E) were used to calculate the MDL for a single crude oil relative to the end-member of the respective sample set. Crude oils with a MDL of 100% have already reached alteration levels above moderate biodegradation (Elias *et al.*, 2007). MDL values (Tab.5.4) have been calculated for the proposed biodegraded oil samples using G002973 oil sample as an end-member (which is used as well in oil mixing calculations in sec.5.3). G002997 has the highest value of MDL (50.37 %) and is considered as the (relatively) most biodegraded oil in the sample set. G002993 and G003011 have lower values of MDL (45.90 and 39.52 %; respectively) indicating a lower extent of secondary alteration. G003001 has a very low degradative loss (MDL=2.34 %) and may be considered as a non-biodegraded oil sample. These observations are in agreement with other conventional biodegradation parameters presented previously (see Fig.5.34).

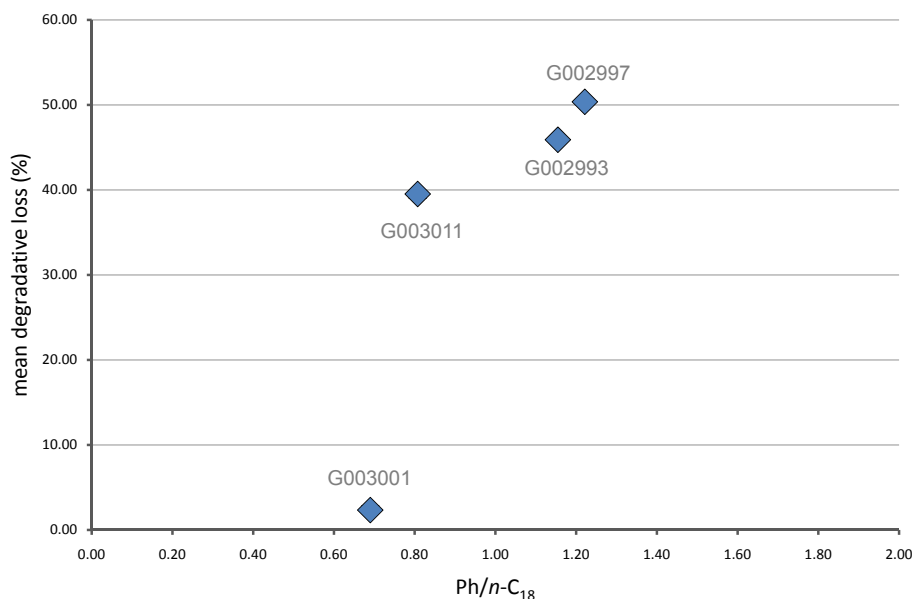


Figure 5.34: Plot of the conventional biodegradation parameter $\text{Ph}/n\text{-C}_{18}$ vs. the *mean degradative loss* (MDL) for biodegraded oil samples.

In Fig.4.3, two oil samples (G0022978 and G003005) are characterized to have higher metal content and lower API gravity relatively to other oil samples. G002978 (API = 19°) was too viscous for injection into the GC-FID apparatus and therefore no data are available for this sample. G003005

(API = 21°) is generated from Upper Shiranish Formation (~2150 m deep) from the southern part of the study area. The whole-oil GC profile of this sample (Fig. 5.35) does not show a significant appearance of biodegraded oils as no big hump is present and almost no absence of light hydrocarbons except some very light hydrocarbons (e.g. *i*-C₅ and *n*-C₅) probably due to evaporation effect. Additionally, the mean degradative value (MDL = 0.51 %) is too low to consider this crude oil as biodegraded. Therefore, two possible explanations can interpret these observations, one is that this oil is immature, or this oil is a mixed oil between biodegraded and non-biodegraded oils.

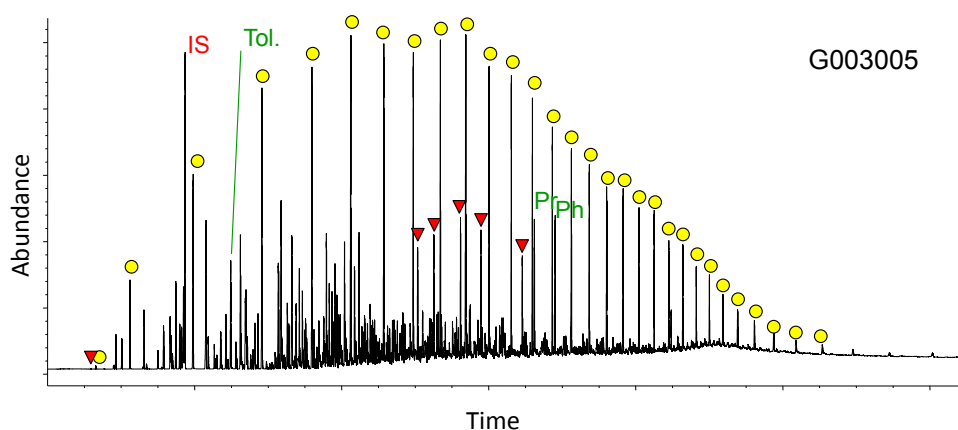


Figure 5.35: Whole-oil chromatogram of G003005 sample shows no significant appearance of biodegradation effect.

Recent studies have reported a remarkable effect of microbial degradation on carbon and hydrogen isotopic signatures for *n*-alkanes (Santos Neto & Hayes, 1999; Vieth & Wilkes, 2006; Wilkes *et al.*, 2008). It is concluded that biodegradation causes an enrichment in ¹³C and D of certain petroleum hydrocarbons in reservoir oils as bacteria consume favorably the light isotopes (George *et al.*, 2002; Masterson *et al.*, 2001; Rooney *et al.*, 1998). On the other hand, other researchers proved that light to moderate biodegradation will not have a noticeable effect on hydrogen and carbon isotopic composition of light hydrocarbons, but severe biodegradation seems to have a significant impact on the carbon isotopic fractionation of low molecular weight *n*-alkanes (*n*-C₁₅-*n*-C₁₈) (Sun *et al.*, 2005). In the studied oils, no changes can be observed in δ¹³C and δD values for *n*-alkanes of biodegraded

oils (G002997, G002993, and G003011) in comparison to non-biodegraded oils (Fig.5.36 and Fig.5.37). This supports the conclusion of very slight to slight biodegradation effects for the studied crude oils. But on the other hand other light hydrocarbon groups like branched alkanes and aromatic hydrocarbons have been affected by biodegradation. Carbon isotopic value of methyl-cyclopentane (MCP) is getting heavier in biodegraded oils (-25.72 ‰ for G002997) relative to non-biodegraded ones (-26.21 ‰ for G002973). The same can be observed for aromatic hydrocarbons (e.g toluene and benzene) where their carbon isotopic values in biodegraded oils (-27.80 and -24.21 ‰ ; respectively for G002997) are relatively heavier than in non-biodegraded oils (-29.20 and 27.66 ‰ ; respectively for G002973).

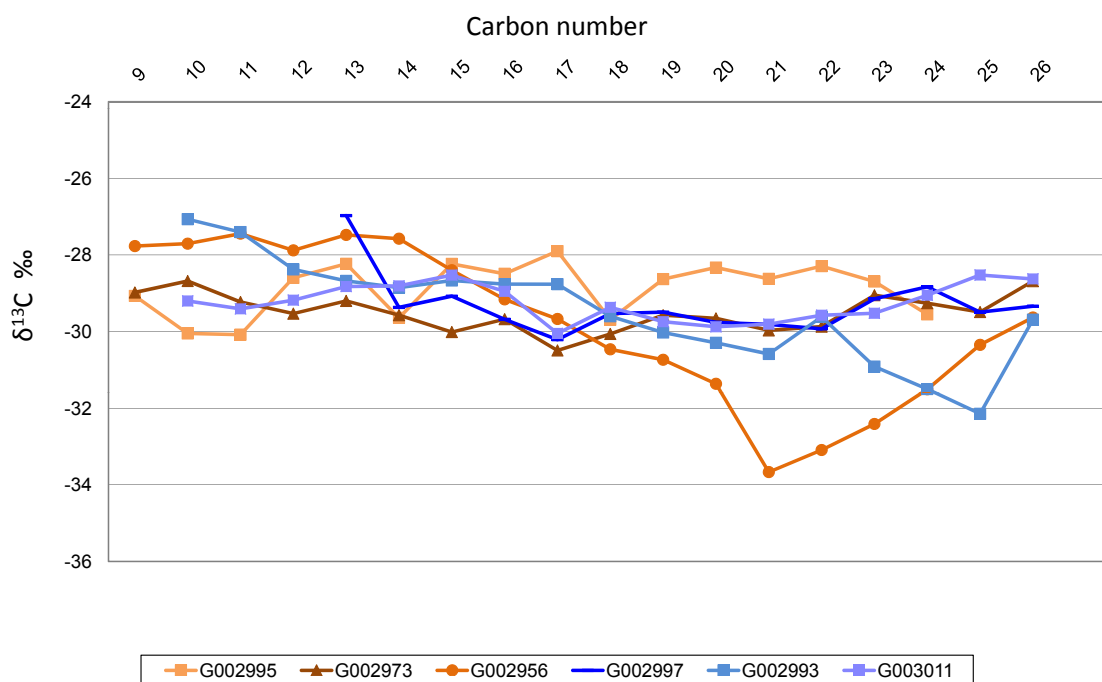


Figure 5.36: Stable carbon isotopic profiles of n -alkanes (n -C₉- n -C₂₆) for biodegraded (blue) and non-biodegraded (orange) oil samples.

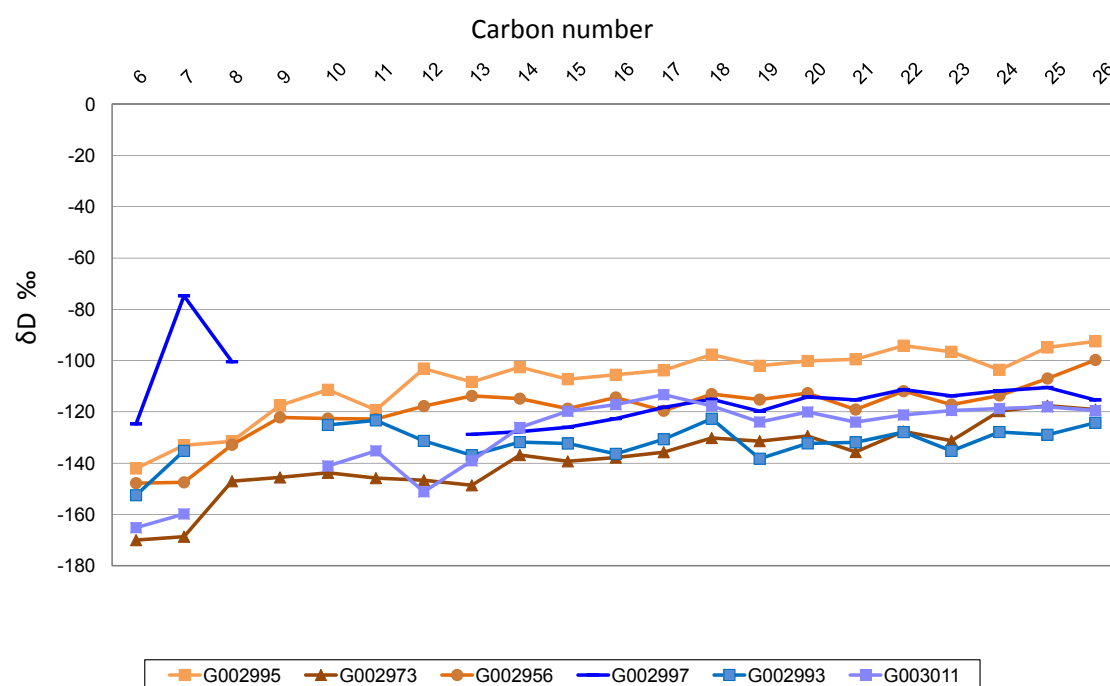


Figure 5.37: Stable hydrogen isotopic profiles of n -alkanes (n -C₆- n -C₂₆) for biodegraded (blue) and non-biodegraded (orange) oil samples.

Chapter 6

Summary and Conclusions

The Euphrates Graben is the most petroliferous province in Syria with a production capacity of about 400.000 bbd in the mid 90's (Alsharhan & Nairn, 1997; de Ruiter *et al.*, 1995). A total of 82 oil samples and 37 rock samples from the study area, provided by our industry partners Shell E&P and AFPC, were analysed geochemically. The oil samples are attributed to different reservoir horizons from Ordovician to Miocene. The studied oils showed different geochemical signatures referring to different origins and maturities. Normal alkane distribution of most of the investigated oils had a dominance of light hydrocarbons over long-chain ones referring to non-waxy crude oils generated from marine type II, type II/III organic matter deposited under anoxic conditions (sec.4.1.2). Most of oil samples have carbonate-source signature as shown by a number of biomarkers and non-biomarkers (e.g. CPI (sec.4.1.2) and diamondoids (sec.4.1.4)). The investigated samples varied from very heavy (API = 12°) to very light (API = 59°) crude oils due to different maturation and/or secondary alteration effects. The maturation level of the studied oil samples ranged from early to high mature as revealed by various maturity-related geochemical parameters (Thompson parameters (sec.4.1.2), diamondoids (sec.4.1.4), and stable carbon and hydrogen isotopic composition (sec.4.1.6). Hopane- and sterane-based maturity parameters (sec.4.1.3)) could not be used reliably to assess the maturity of crude oils as some are affected by source lithology

(e.g. $Ts/(Ts+Tm)$) and others have already reached their respective equilibrium values (e.g. $22S/(22S+22R)$ C_{31} homohopane isomerization ratio, $\beta\beta/(\beta\beta+\alpha\alpha)$ and $20S/(20S+20R)$ C_{30} sterane ratios). Different mono- and triaromatic steroid distribution patterns documented different source and maturity level of the related source rocks. % Rc values calculated from the MPI-1 showed a high maturation level of the oils in the southeastern part of the Euphrates Graben. Stratigraphically, the oils of highest maturity were found in the PJS (Cretaceous), Doubayat and Khabour (Palaeozoic) reservoirs (sec.4.1.5). Oils of lower maturity were located in Cretaceous and Triassic reservoirs (Rutbah and Molossa Formations), respectively. Based on bulk properties, gasoline range hydrocarbons, diamondoids, and biomarker data, the studied crude oils appeared to be derived from two different source rocks; one, a clastic and the other, a carbonate.

The $\delta^{13}C$ profiles of n -alkanes displayed no significant variation in carbon isotopic values between lower and higher molecular weight n -alkanes. $\delta^{13}C$ of pristane in relation to $\delta^{13}C$ of phytane showed a good linear correlation, where the differences in values could be attributed to different sources of these isoprenoids or different isotopic effects during their formation (sec.4.1.6). The profiles of δD values of n -alkanes showed a similar trend for all studied oil samples where the lower molecular weight n -alkanes ($n-C_6$ - $n-C_{17}$) were depleted in D relative to the high molecular weight n -alkanes ($n-C_{19}$ - $n-C_{27}$). A very good correlation has been found between the maturity-related parameters (e.g. diamondoids) and the δD values of pristane and phytane which reflects the effect of thermal maturity on hydrogen isotopic composition.

Oil-oil geochemical correlation and statistical data analysis identified three oil families within the Euphrates Graben Petroleum System. These have been termed Families 1, 2A and 2B (Fig.5.5). Chemometric analysis of source-related hydrocarbons, biomarker and non-biomarker data was based on 23 source- and age-related parameters for 30 oil samples selected out of the whole sample set. Family 1 oils (G002954, G002959, G002982 and

G002988) exhibited properties characteristics of a marine, clastic, and high mature source rock and, in this frame, were correlated to the Silurian Tanf Formation. These very light oils (API gravity $>43^\circ$) have a high Pr/Ph ratio (>1.37). Age-diagnostic biomarkers (C_{28}/C_{29} sterane and $24/(24+27)$ nordiacholestane) indicated that Family 1 crude oils derived from a source rock older than Jurassic in age. Although steranes and diasteranes were low, due to high maturity, the relatively high diasterane over sterane ratio for C_{27} to C_{29} implied clay-rich source rock. The relative abundance of C_{27} , C_{28} and C_{29} steranes and diasteranes showed that these four oil samples are different from the rest and located in a range of Palaeozoic-sourced oils defined after (Grantham & Wakefield, 1988). The diamondoid-based facies parameters distinguished Family 1 oil samples which plotted them in the area of clay-rich source rocks, in contrast to other oil samples which probably derive from Upper Cretaceous strata (Schulz *et al.*, 2001). Family 2A and 2B oils exhibited characteristics associated with marine, carbonate, and low mature source rocks and have been linked to the Upper Cretaceous R'mah and Shiranish Formations. Age-diagnostic biomarkers (C_{28}/C_{29} sterane and $24/(24+27)$ nordiacholestane) revealed that oils of both oil families have Cretaceous source rocks. Family 2B oils originated principally from marine type II organic matter (probably R'mah Formation) while Family 2A oils were generated from both type II and type II/III kerogen which is in agreement with the Upper Shiranish Formation as it contains a small terrestrial organic matter contribution. The distinction between oil samples originating from the R'mah and Shiranish Formations was not possible with the available data as both source rocks have very similar features and characteristics. However, oil-source rock geochemical correlation confirmed that oils of Family 2A were generated from the Upper Cretaceous Shiranish Formation, while R'mah Formation was the origin of the Family 2B crude oils (sec.5.2). Considering maturity, Family 1 oil samples have a high level of maturation in comparison to oil samples of families 2A and 2B (sec.5.1.2). The carbon isotopic composition of light hydrocarbons and acyclic isoprenoids was not a valuable tool for discrimination of the oils.

In contrast, hydrogen isotopes gave distinctive information supporting the classification of oil families in the study area. Crude oils of Family 1 are less negative in δD values for *n*-alkanes relative to other oil families due to the high maturation level of the associated source rock (Silurian Tanf Formation). The impact of increasing maturation on δD values of *n*-alkanes was obvious looking at the relationship between the hydrogen isotopic values of pristane and the concentration of adamantanes as a reliable indicator to oil maturity (Fig.5.14). However, it appears that the hydrogen isotopic values have certain upper limits for each oil family (about -80 ‰ for oils of Family 1 and -115‰ for oils of Family 2A) which could be the result of different isotopic-exchange reactions between organic matter and formation water.

Based on geological information, the known distribution of source rocks across the study area demonstrated the reliable classification of oil families (sec.5.1.4). It was interesting to see that the Family 1 oil samples were found exclusively in the southeastern and northwestern parts of the graben, fitting very well to the distribution of the Silurian Tanf Formation as described in the literature (Fig.5.16). The R'mah Formation is preserved mainly on the northeastern margin and in some areas in the southern sector, which was in agreement with the distribution of Family 2B oils. The Shiranish Formation is distributed over the whole study area but is in the oil generation window just in the central part as a result of the rifting event in the Late Cretaceous. Family 2A oil samples were located also in the central part of the graben. The agreement between the distribution of oil families and their related potential source rocks led to the conclusion that vertical migration is more important and significant than lateral migration in the study area. Moreover, tertiary migration from Cretaceous reservoirs upwards was probably responsible for the findings in the Miocene plays in northeastern part of the graben (sec.5.2.3).

This study has shown that petroleum mixing played an important role in the Euphrates Graben petroleum system. A theoretical mixing model has been applied for some oil samples which have different geochemical signatures

related to their origin from different source rocks. These oils were located in the area where three potential source rocks are present. Calculation results showed that some oils from Family 2B (R'mah-sourced oil family) in the southeastern part of the graben contain a significant contribution from the Silurian Tanf Formation (sec.5.3). It was also interesting to see that the contribution of the Shiranish Formation to these oils was very low (0-4%) which totally supported the finding that Family 2B oils were generated from the R'mah Formation. This new approach could be applied in other petroleum systems to analyse petroleum mixtures from various source rocks. The advantage of this approach is that there is no need for the availability of source rock samples to obtain reliable results about the mixing potential among several oil families.

Furthermore, this study showed that the oils produced in the north-western part of the graben from relatively shallow reservoirs (e.g. G002998, G002997, G002993, and G003011) have been affected by secondary alteration processes like biodegradation. These heavy oils (API \sim 12-26°) have relatively high metal contents (Ni, V, and S). The GC fingerprints of these oils showed a low abundance of light hydrocarbons relative to isoprenoids in addition to a remarkable hump. The calculated mean degradative loss (Elias *et al.*, 2007) ranged between 40-50 %. According to the PM scale of biodegradation degree the studied oils underwent very slight to slight biodegradation as they have 1 to 2 level of biodegradation Fig.5.26.

For future work in this area, it is recommended to consider the following:

- Analyse representative source rock samples especially from the Tanf Formation to make oil-source rock correlation with Family 1 oils.
- Perform experimental mixing of end member oils in different ratios to ensure about the results of mathematical calculations. This would be also helpful to investigate the petroleum composition.
- The complex geological frame of the graben needs to be understood

well by getting more geological information to better define the migration pathways of petroleum.

- Perform hydrogen isotopic analysis for formations water to investigate its effect on the isotopic values of reservoired hydrocarbons.

Bibliography

- Abboud, M., Philp, R. P., & Allen, J. 2005. Geochemical Correlation of Oils and Source Rocks from Central and NE Syria. *Journal of Petroleum Geology*, 28(2), 203–218. [cited at p. 9, 15]
- Abu-Ali, M. A., & Littke, Ralf. 2005. Paleozoic petroleum systems of Saudi Arabia: a basin modeling approach. *GeoArabia*, 10(3), 131–168. [cited at p. 9]
- Abu-Ali, M. A., Rudkiewicz, J. L., McGillivray, J. G., & Behar, F. 1999. Paleozoic Petroleum System of Central Saudi Arabia. *GeoArabia*, 4(3), 321–336. [cited at p. 9, 12]
- Abu-Ali, M.A., Franz, U.A., Shen, J., Monnier, F., Mahmoud, M.D., & Chambers, T.M. 1991. Hydrocarbon generation and migration in Paleozoic sequence of Saudi Arabia. *Society of Petroleum Engineers (SPE), INC. (7th Middle East Oil Show)*, November, 345–356. [cited at p. 12]
- Ahlbrandt, Thomas S., Pollastro, Richard M., Klett, Timothy R., Schenk, Christopher J., Lindquist, Sandra J., & James E, Fox. 2000. *Region 2 - Assessment Summer-Middle East and North Africa*. Tech. rept. [cited at p. 10, 11, 12]
- Al-Habba, Y., & Abdullah, M. 1989. Geochemical study of the hydrocarbon source rocks from north east of Iraq (in Arabic). *Oil and Arab Cooperation*, 15(57), 11–50. [cited at p. 12]
- Al-Husseini, M.I. 1991. Potential petroleum resources of the Paleozoic rocks of Saudi Arabia. *Proceeding of the World Petroleum Congress, Buenos Aires, Argentina*, 3–13. [cited at p. 12]

- Al-Saad, Damen, Sawaf, Tarif, Gebran, Ali, Barazangi, Muawia, Best, John A., & Chaimov, Thomas A. 1992. Crustal structure of central Syria: The intra-continental Palmyride mountain belt. *Tectonophysics*, 207(3-4), 345–358. TY - JOUR. [cited at p. 14]
- Ala, M. A., & Moss, B.J. 1979. Comparative Petroleum Geology of Southeast Turkey and Northeast Syria. *Journal of Petroleum Geology*, 1(4), 3–27. [cited at p. 18]
- Ala, M.A., Kinghorn, R.R.F., & Rahman, M. 1980. Organic geochemistry and source rock characteristics of the Zagros petroleum provience, southwest Iran. *Journal of Petroleum Geology*, 3(1), 61–89. [cited at p. 12]
- Albaiges, J., Borb?n, J., & Walker, W. 1985. Petroleum isoprenoid hydrocarbons derived from catagenetic degradation of archaebacterial lipids. *Organic Geochemistry*, 8(4), 293–297. [cited at p. 67]
- Aldahik, Ahmad. 2001. *Oil Production Optimizing Using Acidizing Process. Case Study: Massive Formation in Suwaidiyah Oil Field, NE Syria (in Arabic)*. Bachelor thesis, Al-Baath University. [cited at p. 15]
- Aldahik, Ahmad. 2003. *Hydraulic Evaluation of the Syrian Crude Oil Pipeline (in Arabic)*. Diploma Thesis, Al-Baath University. [cited at p. 13]
- Alexander, R., Kagi, R. I., Rowland, S. J., Sheppard, P. N., & Chirila, T. V. 1985. The effects of thermal maturity on distributions of dimethylnaphthalenes and trimethylnaphthalenes in some Ancient sediments and petroleums. *Geochimica et Cosmochimica Acta*, 49(2), 385–395. [cited at p. 93]
- Alexander, Robert, Kagi, Robert Ian, & Larcher, Alfons V. 1984. Clay catalysis of alkyl hydrogen exchange reactions–reaction mechanisms. *Organic Geochemistry*, 6, 755–760. [cited at p. 108, 111]
- Alsdorf, Douglas, Barazangi, Muawia, Litak, Robert, Dogan, Seber., Sawaf, Tarif, & Al-Saad, Damen. 1995. The interplate Euphrates sault system-Palmyrides mountain belt junction and relationship to Arabian olate boundray tectonics. *Annali di Geofisica*, 38(3-4), 385–397. [cited at p. 15]

- Alsharhan, A. S. 2003. Petroleum geology and potential hydrocarbon plays in the Gulf of Suez rift basin, Egypt. *AAPG Bulletin*, 87(1), 143–180. [cited at p. 16]
- Alsharhan, A. S., & Nairn, A. E. M. 1997. *Sedimentary Basins and Petroleum Geology of the Middle East*. Elsevier Science B.V. [cited at p. 10, 11, 12, 13, 14, 15, 18, 191]
- Andrusevich, V. E., Engel, M. H., Zumberge, J. E., & Brothers, L. A. 1998. Secular, episodic changes in stable carbon isotope composition of crude oils. *Chemical Geology*, 152(1-2), 59–72. TY - JOUR. [cited at p. 102]
- Aqrawi, Adnan A.M. 1998. Paleozoic stratigraphy and petroleum systems of the western and south western deserts of Iraq. *GeoArabia*, 3, 229–248. [cited at p. 9]
- Arouri, Khaled R., & McKirdy, David M. 2005. The behaviour of aromatic hydrocarbons in artificial mixtures of Permian and Jurassic end-member oils: application to in-reservoir mixing in the Eromanga Basin, Australia. *Organic Geochemistry*, 36(1), 105–115. [cited at p. 166]
- Bailey, N. J. L., Jobson, A. M., & Rogers, M. A. 1973. Bacterial degradation of crude oil: Comparison of field and experimental data. *Chemical Geology*, 11(3), 203–221. [cited at p. 175]
- Bakr, Mohamed M. Y., & Wilkes, Heinz. 2002. The influence of facies and depositional environment on the occurrence and distribution of carbazoles and benzocarbazoles in crude oils: a case study from the Gulf of Suez, Egypt. *Organic Geochemistry*, 33(5), 561–580. [cited at p. 76, 119]
- Barazangi, Muawia, Seber, D, Chaimov, Thomas A., Best, John A., Litak, Robert K., Al-Saad, Damen, & Sawaf, Tarif. 1993. Tectonic evolution of the northern Arabian plate in western Syria. in: *E. Mantovani, A. Morelli, and E. Boschi, eds., Recent evolution and seismic of the Mediterranean region: Netherlands. Kluwer Academic, NATO ASI Series*, 117–140. [cited at p. 14]
- Baskin, D. K., & Jones, R. W. 1993. Prediction of oil gravity prior to drill-stem testing in Monterey Formation reservoirs, offshore California. *AAPG Bulletin*, 77(9), 1479–1487. [cited at p. 3]

- Baskin, David K., Hwang, Rong J., & Purdy, R. Kirk. 1995. Predicting gas, oil, and water intervals in Niger Delta reservoirs using gas chromatography. *AAPG Bulletin*, 79(3), 337–350. [cited at p. 3]
- Beach, F., Peakman, T. M., Abbott, G. D., Sleeman, R., & Maxwell, J. R. 1989. Laboratory thermal alteration of triaromatic steroid hydrocarbons. *Organic Geochemistry*, 14(1), 109–111. [cited at p. 95]
- Behar, F., Vandenbroucke, M., Tang, Y., Marquis, F., & Espitalie, J. 1997. Thermal cracking of kerogen in open and closed systems: determination of kinetic parameters and stoichiometric coefficients for oil and gas generation. *Organic Geochemistry*, 26(5-6), 321–339. TY - JOUR. [cited at p. 2]
- Bement, W. O., Mcneil, R. I., & Lippincott, R. G. 1996. Predicting oil quality from sidewall cores using PFID, TEC, and NIR analytical techniques in sandstone reservoirs, Rio Del Rey Basin, Cameroon. *Organic Geochemistry*, 24(12), 1173–1178. TY - JOUR. [cited at p. 3]
- Best, John A., Barazangi, Muawia, Al-Saad, Damen, Sawaf, Tarif, & Gebran, Ali. 1993. Continental margin Evolution of the Northern Arabian Platform in Syria. *AAPG Bulletin*, 77(2), 173–193. [cited at p. 14]
- Beydoun, Z. R. 1986. The Petroleum Resources of the Middle East: A Review. *Journal of Petroleum Geology*, 9(1), 5–28. [cited at p. 20]
- Beydoun, Z. R. 1991. Arabian plate hydrocarbon geology and potentiala plate tectonic approach. *AAPG Bulletin Studies in Geology*, 33, 77p. [cited at p. 18]
- Beydoun, Z. R., & Dunnington, H. V. 1975. *The petroleum geology and resources of the Middle East*. Beaconsfield: Scientific Press Ltd. [cited at p. 10]
- Beydoun, Ziad.R. 1998. Arabian Plate oil and gas; why so rich and so prolific? *Episodes*, 21(2), 74–81. [cited at p. 10]
- Bjoroy, M., Hall, K., Gillyon, P., & Jumeau, J. 1991b. Carbon isotope variations in n-alkanes and isoprenoids of whole oils. *Chemical Geology*, 93(1-2), 13–20. TY - JOUR. [cited at p. 102]
- Blanc, Ph., & Connan, J. 1994. Crude oils in reservoirs: the factors influencing their composition. *AAPG Memoir*, 60, 237–247. [cited at p. 175]

- Bordenave, M.L. 1993. *Applied Petroleum Geochemistry*. Paris: Edition Technip.
[cited at p. 6, 7]
- BP, p.l.c. June 2008. *BP Statistical Review of World Energy June 2008*. Tech. rept. [cited at p. 10]
- Brew, Graham, Litak, Robert K., Seber, D, Barazangi, Muawia, Al-Imam, Anwar, & Sawaf, Tarif. 1997a. Basement Depth and Sedimentary Velocity Structure in the Northern Arabian Platform, Eastern Syria. *Geophys. J. Int.*, 128, 617–631. [cited at p. 14, 15]
- Brew, Graham, Litak, Robert K., Seber, Dogan, Barazangi, Muawia, Sawaf, Tarif, & Al-Imam, Anwar. 1997b. Summary of the geological evolution of Syria through geophysical interpretation: Implications for hydrocarbon exploration. *The Leading Edge*, October, p. 9. [cited at p. x, 14, 16, 18]
- Brew, Graham, Barazangi, Muawia, Litak, Robert K., & Sawaf, Tarif. 1999. Tectonic Evolution of Northeast Syria: Regional Implications and Hydrocarbon Prospects. *GeoArabia*, 4(3), 289–318. [cited at p. 14, 18]
- Brew, Graham, Barazangi, Muawia, Al-Maleh, Khaled, & Sawaf, Tarif. 2001a. Tectonic and geologic Evolution of Syria. *GeoArabia*, 6(4), 573–616. [cited at p. x, 13]
- Budzinski, H., Garrigues, Ph., Connan, J., Devillers, J., Domine, D., Radke, M., & Oudins, J. L. 1995. Alkylated phenanthrene distributions as maturity and origin indicators in crude oils and rock extracts. *Geochimica et Cosmochimica Acta*, 59(10), 2043–2056. [cited at p. 93]
- Caron-Cecile, & Jamal-Maher. 2000. Basin development and tectonic history of the Euphrates Graben (eastern Syria), a stratigraphic and seismic approach. *Memories du Museum National d'Histoire Naturelle*, 182, 169–201. [cited at p. 17]
- Cassani, Fernando, Gallango, Oswaldo, Talukdar, Suhas, Vallejos, Carlos, & Ehrmann, Ursula. 1988. Methylphenanthrene maturity index of marine source rock extracts and crude oils from the Maracaibo Basin. *Organic Geochemistry*, 13(1-3), 73–80. [cited at p. 97]

- Chaimov, Thomas A., Barazangi, Muawia, Al-Saad, Damen, Sawaf, Tarif, & Khaddour, Mohammed. 1993. Seismic fabric and 3-D structure of the southwestern intracontinental Palmyride fold belt, Syria. *AAPG Bulletin*, 77(12), 2032–2047. [cited at p. 14]
- Chakhmakhchev, Alexander, & Suzuki, Noriyuki. 1995. Aromatic sulfur compounds as maturity indicators for petroleum from the Buzuluk depression, Russia. *Organic Geochemistry*, 23(7), 617–625. [cited at p. 93, 97]
- Chakhmakhchev, Alexander, Suzuki, Masaru, & Takayama, Kuniaki. 1997. Distribution of alkylated dibenzothiophenes in petroleum as a tool for maturity assessments. *Organic Geochemistry*, 26(7-8), 483–489. [cited at p. 93, 98]
- Chen, Jianping, Deng, Chunping, Liang, Digang, Wang, Xulong, Zhong, Ningning, Song, Fuqing, Shi, Xinpu, Jin, Tao, & Xiang, Shuzheng. 2003b. Mixed oils derived from multiple source rocks in the Cainan oilfield, Junggar Basin, Northwest China. Part II: artificial mixing experiments on typical crude oils and quantitative oil-source correlation. *Organic Geochemistry Chinese 2001 Symposium on Research and Technological Advances of Reservoir Geochemistry*, 34(7), 911–930. TY - JOUR. [cited at p. 3, 166]
- Chen, Junhong, Fu, Jiamo, Sheng, Guoying, Liu, Dehan, & Zhang, Jianjun. 1996. Diamondoid hydrocarbon ratios: novel maturity indices for highly mature crude oils. *Organic Geochemistry*, 25(3-4), 179–190. [cited at p. xi, 90, 91]
- Christensen, Jan H., Hansen, Asger B., Karlson, Ulrich, Mortensen, John, & Andersen, Ole. 2005a. Multivariate statistical methods for evaluating biodegradation of mineral oil. *Journal of Chromatography A*, 1090(1-2), 133–145. TY - JOUR. [cited at p. 134]
- Christensen, J.H., Hansen, A.B., Tomasi, G., Mortensen, J., & Andersen, O. 2004. Integrated Methodology for Forensic Oil Spill Identification. *Environ. Sci. Technol.*, 38(10), 2912–2918. [cited at p. 134]
- Christian, Louis. 1997. Cretaceous Subsurface Geology of the Middle East Region. *GeoArabia*, 2(3), 239–256. [cited at p. 11]

- Chung, H. M., Rooney, M. A., Toon, M. B., & Claypool, George E. 1992. Carbon isotope composition of marine crude oils. *AAPG Bulletin*, 76(7), 1000–1007. [cited at p. 102]
- Clayton, C. J. 1991. Effect of maturity on carbon isotope ratios of oils and condensates. *Organic Geochemistry*, 17(6), 887–899. [cited at p. 102]
- Clayton, C. J., & Bjoroy, M. 1994. Effect of maturity on $^{13}\text{C}/^{12}\text{C}$ ratios of individual compounds in North Sea oils. *Organic Geochemistry*, 21(6-7), 737–750. [cited at p. 102]
- Cole, G. A., Abu-Ali, M. A., Aoudeh, S. M., Carrigan, W. J., Chen, H. H., Colling, E. L., Gwathney, W. J., Al-Hajji, A. A., & Halpern, H. I. 1994a. Organic Geochemistry of the Paleozoic Petroleum System of Saudi Arabia. *Energy Fuels*, 8(6), 1425 – 1442. [cited at p. 9]
- Cole, G. A., Carrigan, W. J., Colling, E.L., Halpern, H. I., AlKhadhrawi, M.R, & Jones, P.J. 1994b. The organic geochemistry of the Jurassic petroleum system in eastern Saudi Arabia. *Memoir-Canadian Society of Petroleum Geologists*, 413–438. [cited at p. 9]
- Collister, James W., Summons, Roger E., Lichtfouse, Eric, & Hayes, J. M. 1992. An isotopic biogeochemical study of the Green River oil shale. *Organic Geochemistry*, 19(1-3), 265–276. [cited at p. 103]
- Connan, J. 1984. Biodegradation of crude oils in reservoirs. In: J. Brooks, D.H. Welte (Eds.), *Advances in Petroleum Geochemistry*. Academic Press, London, 299–330. [cited at p. 2, 175]
- Dahl, J E, Moldowan, J M, Peters, K E, Claypool, G E, Rooney, M A, Michael, G E, Mello, M R, & Kohnen, M L. 1999. Diamondoid hydrocarbons as indicators of natural oil cracking. *Nature*, 399(6731), 54–57. [cited at p. 87]
- Dahl, Jeremy, Michael Moldowan, J., & Sundararaman, Padmanabhan. 1993. Relationship of biomarker distribution to depositional environment: Phosphoria Formation, Montana, U.S.A. *Organic Geochemistry*, 20(7), 1001–1017. TY - JOUR. [cited at p. 1]

- Davis, J.B., & Yarbrough, H.F. 1966. Anaerobic oxidation of hydrocarbons by *Desulfovibrio desulfuricans*. *Chemical Geology*, 1, 137–144. [cited at p. 175]
- Dawson, Daniel. 2006. Stable hydrogen isotope ratios of individual hydrocarbons in sediments and petroleum. *PhD Thesis*, pp.175. [cited at p. 112, 115]
- Dawson, Daniel, Grice, Kliti, & Alexander, Robert. 2005. Effect of maturation on the indigenous δD signatures of individual hydrocarbons in sediments and crude oils from the Perth Basin (Western Australia). *Organic Geochemistry*, 36(1), 95–104. [cited at p. 107, 115]
- Dawson, Daniel, Grice, Kliti, Alexander, Robert, & Edwards, Dianne. 2007. The effect of source and maturity on the stable isotopic compositions of individual hydrocarbons in sediments and crude oils from the Vulcan Sub-basin, Timor Sea, Northern Australia. *Organic Geochemistry Australian Special Issue*, 38(7), 1015–1038. [cited at p. 102, 111, 112, 115]
- de Ruiter, Rudolf S.C, Lovelock, Philip E.R., & Nabulsi, Nader. 1995. The Euphrates Graben, Eastern Syria,: a new petroleum provience in the northern Middle East. *Geo-94, Middle East Petroleum, Gulf PetroLink*, 1, 357–368. [cited at p. x, 9, 17, 18, 19, 20, 191]
- Demaison, Gerard, & Huizinga, Bradley J. 1991. Genetic classification of petroleum systems. *AAPG Bulletin*, 75(10), 1626–1643. [cited at p. 9]
- Demirel, I .H., & Guneri, S. 2000. Cretaceous carbonates in the Adiyaman region, SE Turkey: An assessment of burial history and source-rock potential,. *Journal of petroleum geology*, 23, 91–106. [cited at p. 9]
- Demirel, I. H., Yurtsever, T. S., & Guneri, S. 2001. Petroleum systems of the Adiyaman region, Southeastern Anatolia, Turkey. *Marine and Petroleum Geology*, 18(3), 391–410. TY - JOUR. [cited at p. 9]
- Demirel, Ismail Hakki. 2004. Petroleum systems in the eastern and central Taurus region, Turkey. *Marine and Petroleum Geology*, 21(8), 1061–1071. TY - JOUR. [cited at p. 9]
- Depauw, Guy A., & Froment, Gilbert F. 1997. Molecular analysis of the sulphur components in a light cycle oil of a catalytic cracking unit by gas chromatog-

- raphy with mass spectrometric and atomic emission detection. *Journal of Chromatography A*, 761(1-2), 231–247. [cited at p. 93]
- di Primio, R., & Horsfield, B. 1996. Predicting the generation of heavy oils in carbonate/evaporitic environments using pyrolysis methods. *Organic Geochemistry Proceedings of the 17th International Meeting on Organic Geochemistry*, 24(10-11), 999–1016. TY - JOUR. [cited at p. 7]
- Didyk, B., Simoneit, B.R.T., Brassell, S.C., & Eglinton, G. 1978. Organic geochemical indicators of palaeoenvironmental conditions of sedimentation. *Nature*, 272, 216–222. [cited at p. 67]
- Dieckmann, V., Schenk, H. J., Horsfield, B., & Welte, D. H. 1998. Kinetics of Petroleum generation and cracking by programmed-temperature closed-system pyrolysis of Toarcian Shales. *Fuel*, 77(1/2), 23–31. [cited at p. 7]
- Dieckmann, V., Schenk, H. J., & Horsfield, B. 2000. Assessing the overlap of primary and secondary reactions by closed- versus open-system pyrolysis of marine kerogens. *Journal of Analytical and Applied Pyrolysis*, 56(1), 33–46. TY - JOUR. [cited at p. 7]
- Droste, Henk H.J. 1997. Stratigraphy of the Lower Paleozoic Haima Supergroup of Oman. *GeoArabia*, 2(4), 419–472. [cited at p. 12]
- Dzou, Leon I., Holba, Albert G., Ramon, Juan C., Moldowan, J. Michael, & Zinniker, David. 1999. Application of new diterpane biomarkers to source, biodegradation and mixing effects on Central Llanos Basin oils, Colombia. *Organic Geochemistry*, 30(7), 515–534. [cited at p. 166]
- EIA. 2010. *International Energy Statistics*. Tech. rept. U.S. Energy Information Administration, www.eia.doe.gov. [cited at p. 10]
- Elias, Rouven, Vieth, Andrea, Riva, Angelo, Horsfield, Brian, & Wilkes, Heinz. 2007. Improved assessment of biodegradation extent and prediction of petroleum quality. *Organic Geochemistry*, 38(12), 2111–2130. [cited at p. xv, 177, 179, 185, 186, 195, 263]
- Espitalie, J. 1986. Use of Tmax as a Maturation Index for Different Types of Organic Matter Comparison with Vitrinite Reflectance. In: *Thermal Modeling*

- in Sedimentary Basins, J. Burrus (ed.), Editions Technip, Paris, 475–495.*
[cited at p. 118]
- Espitalie, J., Laporte, J., Madec, M., & Marquis, F. 1977. Rapid method for source rock characterization and for evaluating their petroleum potential and their degree of evolution. *Institut Francais du Petrole, Paris.*, pp.19.
[cited at p. 5, 117]
- Estep, Marilyn F., & Hoering, Thomas C. 1980. Biogeochemistry of the stable hydrogen isotopes. *Geochimica et Cosmochimica Acta*, 44(8), 1197–1206.
[cited at p. 107, 114]
- Fox, James E., & Ahlbrandt, Thomas S. 2002. *Petroleum geology and total petroleum systems of the Widyan Basin and interior platform of Saudi Arabia and Iraq.* Denver, Colo. :: U.S. Dept. of the Interior, U.S. Geological Survey. TY - BOOK Version 1.0. Title from title screen (viewed on Jan. 14, 2004). Includes bibliographical references. [cited at p. 9]
- Freeman, Katherine H., Hayes, J. M., Trendel, Jean-Michel, & Albrecht, Pierre. 1990. Evidence from carbon isotope measurements for diverse origins of sedimentary hydrocarbons. 343(6255), 254–256. [cited at p. 103]
- Frijhoff, Ren, Lechner, Maarten, Wassouf, Nada, Pimentel, Robert, Kabbesh, Fahed, Mahmoud, Bahaa, & Ahmad, Mokhles. 2006. Evaluating the Palaeozoic Gas Potential of the Euphrates Graben, Syria. *GEO 2006 Middle East Conference and Exhibition, Manama, Bahrain.* [cited at p. xii, 18, 118, 119, 127]
- Fu, Jiamo, Guoying, Sheng, Pingan, Peng, Brassell, Simon C., Eglinton, Geoffrey, & Jigang, Jiang. 1986. Peculiarities of salt lake sediments as potential source rocks in China. *Organic Geochemistry*, 10(1-3), 119–126. [cited at p. 77]
- Fuex, A. N. 1977. The use of stable carbon isotopes in hydrocarbon exploration. *Journal of Geochemical Exploration*, 7, 155–188. [cited at p. 101]
- George, Simon C., Boreham, Christopher J., Minifie, Sandra A., & Teerman, Stan C. 2002. The effect of minor to moderate biodegradation on C5 to C9 hydrocarbons in crude oils. *Organic Geochemistry*, 33(12), 1293–1317.
[cited at p. 102, 187]

- Gilmour, I., Swart, P. K., & Pillinger, C. T. 1984. The carbon isotopic composition of individual petroleum lipids. *Organic Geochemistry*, 6, 665–670. TY - JOUR. [cited at p. 102]
- Goodwin, N., Park, P., & Rawlinston, A. 1981. Crude oil biodegradation under simulated and natural conditions. *Advances in Organic Geochemistry*, 650–658. [cited at p. 175]
- Goossens, H., de Leeuw, J. W., Schenck, P. A., & Brassell, S. C. 1984. Tocopherols as likely precursors of pristane in ancient sediments and crude oils. *Nature*, 312(5993), 440–442. [cited at p. 67]
- Grantham, P. J., & Wakefield, L. L. 1988. Variations in the sterane carbon number distributions of marine source rock derived crude oils through geological time. *Organic Geochemistry*, 12(1), 61–73. TY - JOUR. [cited at p. xi, 77, 85, 87, 140, 141, 193]
- Grantham, P. J., Lijmbach, G.W.M., Posthuma, J., Hughes Clarke, M.W., & Willink, R.J. 1987. Origin of Crude Oils in Oman. *Journal of Petroleum Geology*, 11(1), 61–80. [cited at p. 9, 12]
- Greene, Todd J., Zinniker, David, Moldowan, J. Michael, Keming, Cheng, & Aiguo, Su. 2004. Controls of oil family distribution and composition in nonmarine petroleum systems: A case study from the Turpan-Hami basin, northwestern China 10.1306/10270303015. *AAPG Bulletin*, 88(4), 447–481. [cited at p. 10]
- Guyot, Claude, & Zeinab, Hassan. 2000. Euphrates Graben, East Syria, basin evolution and petroleum Habitat. *GeoArabia*, 5(1), 100–101. [cited at p. 16]
- Halpern, Henry I. 1995. Development and Application of Light-Hydrocarbon-Based Star Diagrams. *AAPG Bulletin*, 79(6), 801–815. [cited at p. xiii, 2, 142, 144, 182, 184, 185]
- Hanson, Andrew D., Ritts, Bradley D., Zinniker, David, Moldowan, J. Michael, & Biffi, Ulderico. 2001. Upper Oligocene Lacustrine Source Rocks and Petroleum Systems of the Northern Qaidam Basin, Northwest China. *AAPG Bulletin*, 85(4), 601–619. [cited at p. 76]

- Hartgers, W. A., Sinninghe Damste, J. S., & de Leeuw, J. W. 1992. Identification of C₂—C₄ alkylated benzenes in flash pyrolysates of kerogens, coals and asphaltenes. *Journal of Chromatography A*, 606(2), 211–220. [cited at p. 93]
- Hassan, Kamaleldin M., & Spalding, Roy F. 2001. Hydrogen isotope values in lacustrine kerogen. *Chemical Geology*, 175(3-4), 713–721. [cited at p. 107]
- Hayes, J.M. 1993. Factors controlling ¹³C contents of sedimentary organic compounds: Principles and evidence. *Marine Geology Marine Sediments, Burial, Pore Water Chemistry, Microbiology and Diagenesis*, 113(1-2), 111–125. [cited at p. 102]
- Head, Ian M., Jones, D. Martin, & Larter, Steve R. 2003. Biological activity in the deep subsurface and the origin of heavy oil. 426(6964), 344–352. [cited at p. 175, 176]
- Hoefs, Jochen. 1997. Stable Isotope Geochemistry. *Springer Verlag Berlin Heidelberg*, 4. Edition, 201.p. [cited at p. 101]
- Holba, A. G., Dzou, L. I. P., Masterson, W. D., Hughes, W. B., Huizinga, B. J., Singletary, M. S., Moldowan, J. M., Mello, M. R., & Tegelaar, E. 1998b. Application of 24-norcholestanes for constraining source age of petroleum. *Organic Geochemistry*, 29(5-7), 1269–1283. [cited at p. 82, 140]
- Horsfield, B., & Dueppenbecker, S. J. 1991. The decomposition of posidonia shale and green river shale kerogens using microscale sealed vessel (MSSV) pyrolysis. *Journal of Analytical and Applied Pyrolysis*, 20, 107–123. TY - JOUR. [cited at p. 7]
- Horsfield, B., & Rullkotter, J. 1994a. Diagenesis, catagenesis and metagenesis of organic matter. *Pages 189–199 of: Magoon, LB, & Dow, WG (eds), The petroleum system - from source to trap*. Tulsa: American Association of Petroleum Geologists Memoir 60. [cited at p. x, 3, 4, 5, 6]
- Horsfield, B., Schenk, H. J., Mills, N., & Welte, D. H. 1992. An investigation of the in-reservoir conversion of oil to gas: compositional and kinetic findings from closed-system programmed-temperature pyrolysis. *Organic Geochemistry*, 19(1-3), 191–204. TY - JOUR. [cited at p. 2]

- Huang, Haiping, & Pearson, Michael J. 1999. Source rock palaeoenvironments and controls on the distribution of dibenzothiophenes in lacustrine crude oils, Bohai Bay Basin, eastern China. *Organic Geochemistry*, 30(11), 1455–1470. [cited at p. 93]
- Huang, Haiping, Bowler, Bernard F.J., Oldenburg, Thomas B.P., & Larter, Steve R. 2004. The effect of biodegradation on polycyclic aromatic hydrocarbons in reservoired oils from the Liaohe basin, NE China. *Organic Geochemistry Advances in Organic Geochemistry 2003. Proceedings of the 21st International Meeting on Organic Geochemistry*, 35(11-12), 1619–1634. [cited at p. 93, 175]
- Huang, Wen-Yen, & Meinschein, W. G. 1979. Sterols as ecological indicators. *Geochimica et Cosmochimica Acta*, 43(5), 739–745. TY - JOUR. [cited at p. 84]
- Hughes, G.W. 1984. Use of thiophenic organosulfur compounds in characterizing crude oils derived from carbonate versus siliciclastic sources. *In: Petroleum Geochemistry and Source Rock Potential of Carbonate Rocks (ed. J. G. Palacas)*, 181–196. [cited at p. 67]
- Hunt, J.M. 1996. Petroleum Geochemistry and Geology. *Freeman, New York*. [cited at p. 1, 3, 5, 7, 56, 58]
- Huvaz, Ozkan. 2009. Comparative petroleum systems analysis of the interior basins of Turkey: Implications for petroleum potential. *Marine and Petroleum Geology*, 26(8), 1656–1676. TY - JOUR. [cited at p. 9]
- Hwang, R. J., Ahmed, A. S., & Moldowan, J. M. 1994. Oil composition variation and reservoir continuity: Unity field, Sudan. *Organic Geochemistry*, 21(2), 171–188. [cited at p. 166]
- Hwang, R. J., Baskin, D. K., & Teerman, S. C. 2000. Allocation of commingled pipeline oils to field production. *Organic Geochemistry*, 31(12), 1463–1474. TY - JOUR. [cited at p. 3, 166]
- Illich, Harold A. 1983. Pristane, phytane, and lower molecular weight isoprenoid distributions in oils. *AAPG Bulletin*, 67(3), 385–393. [cited at p. 67]

- Illiffe, James, Blackstock, Carl, & Bulley, Ian. 1998. The Hydrocarbon Charge to the Bishri Block, Palmyrides, Syria: An Integrated Multi-disciplinary Study. *GeoArabia (Book of Abstracts for GEO98)*, 3, 103. [cited at p. 15]
- Jamal, Maher, Bizra, Yousef, & Caron, Cecile. 2000. Palaeogeography and hydrocarbon habitat of the Triassic series in Syria. *Comptes Rendus de l'Academie des Sciences - Series IIA - Earth and Planetary Science*, 331(2), 133–139. TY - JOUR. [cited at p. 14, 15]
- Jiang, Chunqing, & Li, Maowen. 2002. Bakken/Madison petroleum systems in the Canadian Williston Basin. Part 3: geochemical evidence for significant Bakken-derived oils in Madison Group reservoirs. *Organic Geochemistry*, 33(7), 761–787. [cited at p. 166, 167]
- Kaufman, R.L., & Ahmed, A.S. 1990. Gas Chromatography as a Development and Production Tool for Fingerprinting Oils from Individual Reservoirs: Applications in The Gulf of Mexico. *Proceedings of the 9th Annual Research Conference of the Society of Economic Paleontologists and Mineralogists. (D. Schumaker and B.F. Perkins, Ed.)*, 263–282. [cited at p. 3, 166]
- Kent, W. Norman, & Hickman, Robert G. 1997. Structural Development of Jebel Abd Al Aziz, Northeast Syria. *GeoArabia*, 2(3), 307–330. [cited at p. 9, 14, 15]
- Killops, S.D., & Killops, V.J. 1993. An introduction to organic geochemistry. *Longman Scientific and Technical Publishers, Harlow, UK*. [cited at p. 3, 4, 6, 67]
- Konert, Geert, Afifi, Abdulkader M., Al-Hhajri, Sa'id A., & Dorste, Henk J. 2001. Paleozoic Stratigraphy and Hydrocarbon Habitat of the Arabian Plate. *GeoArabia*, 6(3), 407–442. [cited at p. x, 11, 18]
- Koopmans, Martin P., Larter, Steve R., Zhang, Chunming, Mei, Bowen, Wu, Tiesun, & Chen, Yixian. 2002. Biodegradation and Mixing of Crude Oils in Eocene Es3 Reservoirs of the Liaohe Basin, Northeastern China. *AAPG Bulletin*, 86(10), 1833–1843. [cited at p. 166]
- Lababidi, M.M., & Hamdan, A.N. 1985. Preliminary lithostratigraphic correlation study in OAPEC member countries. *OAPEC*, 1–87. [cited at p. 18]

- Larter, Steve, Huang, Haiping, Adams, Jennifer, Bennett, Barry, Jokanola, Olufemi, Oldenburg, Thomas, Jones, Martin, Head, Ian, Riediger, Cindy, & Fowler, Martin. 2006. The controls on the composition of biodegraded oils in the deep subsurface: Part II—Geological controls on subsurface biodegradation fluxes and constraints on reservoir-fluid property prediction: Part I of this study was published in *Organic Chemistry* in 2003 (Larter et al., 2003). *AAPG Bulletin*, 90(6), 921–938. [cited at p. 175]
- Lewan, M.D. 1984. Factors controlling the proportionality of vanadium to nickel in crude oils. *Geochimica et Cosmochimica Acta*, 48(11), 2231–2238. [cited at p. 58]
- Li, Maowen, Huang, Yongsong, Obermajer, Mark, Jiang, Chunqing, Snowdon, Lloyd R., & Fowler, Martin G. 2001. Hydrogen isotopic compositions of individual alkanes as a new approach to petroleum correlation: case studies from the Western Canada Sedimentary Basin. *Organic Geochemistry*, 32(12), 1387–1399. [cited at p. 107, 108, 148, 149]
- Lis, Grzegorz P., Schimmelmann, Arndt, & Mastalerz, Maria. 2006. D/H ratios and hydrogen exchangeability of type-II kerogens with increasing thermal maturity. *Organic Geochemistry*, 37(3), 342–353. TY - JOUR. [cited at p. 111]
- Litak, Robert K., Barazangi, Muawia, Beauchamp, Weldon, Dogan, Seber., Brew, Graham, Sawaf, Tarif, & Al-Youssef, Wasif. 1997. Mesozoic-Cenozoic evolution of the intraplate fault system, Syria: implications for regional tectonics. *Journal of Geological Society*, 154, 653–666. [cited at p. 16, 20, 164]
- Litak, Robert K., Barazangi, Muawia, Brew, Graham, Sawaf, Tarif, Al-Imam, Anwar, & Al-Youssef, Wasif. 1998. Structure and Evolution of the Petroliferous Euphrates Graben System, Southeast Syria. *AAPG Bulletin*, 82(6), 1173–1190. [cited at p. 15, 16, 17, 18]
- Luning, S., Craig, J., Loydell, D. K., Storch, P., & Fitches, B. 2000. Lower Silurian ‘hot shales’ in North Africa and Arabia: regional distribution and depositional model. *Earth-Science Reviews*, 49(1-4), 121–200. [cited at p. 18, 156]

- Luning, S., Shahin, Y. M., Loydell, D., Al-Rabi, H. T., Masri, A., Taraneh, B., & Kolonic, S. 2005. Anatomy of the world-class source rock: Distribution and depositional model of Silurian organic-rich shales in Jordan and implications for hydrocarbon potential. *AAPG Bulletin*, 89(10), 1397–1427. [cited at p. 18]
- Mackenzie, A. S., Hoffmann, C. F., & Maxwell, J. R. 1981a. Molecular parameters of maturation in the Toarcian shales, Paris Basin, France—III. Changes in aromatic steroid hydrocarbons. *Geochimica et Cosmochimica Acta*, 45(8), 1345–1355. [cited at p. 94]
- Mackenzie, A. S., Brassell, S. C., Eglinton, G., & Maxwell, J. R. 1982. Chemical Fossils: The Geological Fate of Steroids 10.1126/science.217.4559.491. *Science*, 217(4559), 491–504. [cited at p. 77]
- Mackenzie, A. S., Maxwell, J-R, & Coleman, M.L. 1983. Biological Marker and Isotope Studies of North Sea Crude Oils and Sediments. *In: Proceedings of the 11th World Petroleum Congress, London*, 45–56. [cited at p. 1]
- MacKenzie, Andrew-S. 1984. Applications of biological markers in petroleum geochemistry. *Advances in petroleum geochemistry; Volume 1*, 115–214. [cited at p. 1]
- Magoon, Leslie B., & Dow, Wallace G. 1994. The Petroleum System. *Pages 3–24 of: Magoon, LB, & Dow, WG (eds), The petroleum system - from source to trap*. Tulsa: American Association of Petroleum Geologists Memoir 60. [cited at p. x, 8]
- Mango, Frank D. 1990b. The origin of light hydrocarbons in petroleum: A kinetic test of the steady-state catalytic hypothesis. *Geochimica et Cosmochimica Acta*, 54(5), 1315–1323. [cited at p. 143, 184]
- Masterson, W. Dallam, Dzou, Leon I. P., Holba, Albert G., Fincannon, Ann L., & Ellis, Leroy. 2001. Evidence for biodegradation and evaporative fractionation in West Sak, Kuparuk and Prudhoe Bay field areas, North Slope, Alaska. *Organic Geochemistry*, 32(3), 411–441. [cited at p. 187]
- May, Paul R. 1991. The Eastern Mediterranean Mesozoic Basin: Evolution and Oil Habitat. *AAPG Bulletin*, 75(7), 1215–1232. [cited at p. 14]

- McCaffrey, Mark A., Legarre, Henry A., & Johnson, Scott J. 1996. Using biomarkers to improve heavy oil reservoir management; an example from the Cymric Field, Kern County, California. *AAPG Bulletin*, 80(6), 898–913. [cited at p. 3, 166]
- Mckervery, M. Anthony. 1980. Synthetic approaches to large diamondoid hydrocarbons. *Tetrahedron*, 36(8), 971–992. [cited at p. 87]
- Mello, M. R., Telnaes, N., Gaglianone, P. C., Chicarelli, M. I., Brassell, S. C., & Maxwell, J. R. 1988b. Organic geochemical characterisation of depositional palaeoenvironments of source rocks and oils in Brazilian marginal basins. *Organic Geochemistry*, 13(1-3), 31–45. [cited at p. 80]
- Metwalli, M. Hamed, Philip, G., & Moussly, M. M. 1974. Petroleum-Bearing formations in Northeastern Syria and Northern Iraq. *AAPG Bulletin*, 58(9), 1781–1796. [cited at p. 12]
- Milner, C.W.D, Rogers, M.A, & Evans, C.R. 1977. Petroleum transformations in reservoirs. *Journal of Geochemical Exploration*, 7, 101–153. [cited at p. 175]
- Moldowan, J. Michael, & Fago, Frederick J. 1986a. Structure and significance of a novel rearranged monoaromatic steroid hydrocarbon in petroleum. *Geochimica et Cosmochimica Acta*, 50(3), 343–351. [cited at p. 95]
- Moldowan, J. Michael, Seifert, Wolfgang K., & Gallegos, Emilio J. 1985. Relationship between petroleum composition and depositional environment of petroleum source rocks. *AAPG Bulletin*, 69(8), 1255–1268. [cited at p. 76, 77, 84, 140]
- Moldowan, J. Michael, Sundararaman, Padmanabhan, & Schoell, Martin. 1986b. Sensitivity of biomarker properties to depositional environment and/or source input in the Lower Toarcian of SW-Germany. *Organic Geochemistry*, 10(4-6), 915–926. [cited at p. 76]
- Moldowan, J. Michael, Lee, Cathy Y., Watt, David S., Jeganathan, Alwarsamy, Slougui, Nacer-Eddine, & Gallegos, Emilio J. 1991a. Analysis and occurrence of C26-steranes in petroleum and source rocks. *Geochimica et Cosmochimica Acta*, 55(4), 1065–1081. [cited at p. 82]

- Morasch, Barbara, Richnow, Hans H., Vieth, Andrea, Schink, Bernhard, & Meckenstock, Rainer U. 2004. Stable Isotope Fractionation Caused by Glycyl Radical Enzymes during Bacterial Degradation of Aromatic Compounds. *Appl. Environ. Microbiol.*, 70(5), 2935–2940. [cited at p. 107]
- Mossner, S.G., & Wise, S.A. 1999. Determination of Polycyclic Aromatic Sulfur Heterocycles in Fossil Fuel-Related Samples. *Anal. Chem.*, 71(1), 58–69. [cited at p. 93, 97]
- Murray, Andrew P., Summons, Roger E., Boreham, Christopher J., & Dowling, Lesley M. 1994. Biomarker and n-alkane isotope profiles for Tertiary oils: relationship to source rock depositional setting. *Organic Geochemistry*, 22(3–5), 521–542. [cited at p. 102]
- Murris, R. J. 1980. Middle East: Stratigraphic Evolution and Oil Habitat. *AAPG Bulletin*, 64(5), 597–618. [cited at p. 11]
- Murris, R. J. 1984. Introduction. *Pages x – xii of: Demaison, G. J. (ed), Petroleum Geochemistry and Basin Evaluation*. Tulsa: American Association of Petroleum Geologists: AAPG Memoir 35. [cited at p. x, 1, 2]
- Nederlof, Peter J.R., Gijzen, Mary A., & Doyle, Mark A. 1994. Application of Reservoir Geochemistry to Field Appraisal. *Geo-94, Middle East Petroleum, Gulf PetroLink*, 2, 709–722. [cited at p. 2]
- Newell, K.D., & Hennington, R.D. 1983. Potential Petroleum Source Rock Deposition in the Middle Cretaceous Wadia Formation, Rub’Al Khali, Saudi Arabia. *In: 3rd Middle East oil show, proceedings.*, 151–160. [cited at p. 11]
- OAPEC. 2010. *Organization of Arab Petroleum Exporting Countries (OAPEC) Statistical Annual Report 2009 (in Arabic)*. Tech. rept. [cited at p. 12]
- Osadetz, Kirk G., Brooks, Paul W., & Snowdon, Lloyd R. 1992. Oil families and their sources in Canadian Williston Basin, (southeastern Saskatchewan and southwestern Manitoba). *Bulletin of Canadian Petroleum Geology*, 40(3), 254–273. [cited at p. 10]
- Ourisson, Guy, & Nakatani, Yoichi. 1994. The terpenoid theory of the origin of cellular life: the evolution of terpenoids to cholesterol. *Chemistry & Biology*, 1(1), 11–23. [cited at p. 74]

- Ourisson, Guy, Albrecht, Pierre, & Rohmer, Michel. 1982. Predictive microbial biochemistry – from molecular fossils to procaryotic membranes. *Trends in Biochemical Sciences*, 7(7), 236–239. [cited at p. 74]
- Palmer, Suzan E. 1993. Effect of biodegradation and water washing on crude oil composition. In: Engel, M.H., Macko, S.A. (Eds.), *Organic Geochemistry*, Plenum Press, New York, 511–533. [cited at p. 175]
- Pedentchouk, Nikolai, Freeman, Katherine H., & Harris, Nicholas B. 2006. Different response of δ D values of n-alkanes, isoprenoids, and kerogen during thermal maturation. *Geochimica et Cosmochimica Acta*, 70(8), 2063–2072. [cited at p. 107, 111, 112]
- Peters, K. E., & Moldowan, J. M. 1991. Effects of source, thermal maturity, and biodegradation on the distribution and isomerization of homohopanes in petroleum. *Organic Geochemistry*, 17(1), 47–61. [cited at p. 76]
- Peters, K. E., Moldowan, J. Michael, Driscoll, A. R., & Demaison, G. J. 1989. Origin of Beatrice oil by co-sourcing from Devonian and Middle Jurassic source rocks, inner Moray Firth, United Kingdom. *AAPG Bulletin*, 73(4), 454–471. [cited at p. 166]
- Peters, K. E., Snedden, J. W., Sulaeman, A., Sarg, J. F., & Enrico, R. J. 2000a. A New Geochemical-Sequence Stratigraphic Model for the Mahakam Delta and Makassar Slope, Kalimantan, Indonesia. *AAPG Bulletin*, 84(1), 12–44. [cited at p. 2]
- Peters, K.E., Moldowan, J.M., Schoell, M., & Hemphkins, W.B. 1986b. Petroleum isotopic and biomarker composition related to source rock organic matter and depositional environment. *Organic Geochemistry*, 10(1-3), 17–27. TY - JOUR. [cited at p. 1]
- Peters, K.E., Kontorovich, A.E., Huizinga, B.J., Moldowan, J.M., & Lee, C.Y. 1994. Multiple oil families in the West Siberian Basin. *American Association of Petroleum Geologists Bulletin*, 78(6), 893–909. [cited at p. 1, 10]
- Peters, Ken E. 1986a. Guidelines for Evaluating Petroleum Source Rock Using Programmed Pyrolysis. *AAPG Bulletin*, 70(3), 318–329. [cited at p. 117, 166]

- Peters, Ken E., Fraser, Tom H., Armis, Welly, Rustanto, Budi, & Hermanto, Eddy. 1999a. Geochemistry of crude Oils from Eastern Indonesia. *AAPG Bulletin*, 83(12), 1927–1942. [cited at p. 181]
- Peters, Ken E., Clutson, Mike J., & Robertson, Gary. 1999b. Mixed marine and lacustrine input to an oil-cemented sandstone breccia from Brora, Scotland. *Organic Geochemistry*, 30(4), 237–248. [cited at p. xi, 68, 71, 166]
- Peters, Kenneth E. 2000b. Petroleum tricyclic terpanes: predicted physicochemical behavior from molecular mechanics calculations. *Organic Geochemistry*, 31(6), 497–507. [cited at p. 68]
- Peters, Kenneth E., & Moldowan, J. Michael. 1993. The Biomarker Guide: Interpreting Molecular Fossils in Petroleum and Ancient Sediments. *Prentice Hall, Englewood Cliffs. New Jersey 07632*, pp.363. [cited at p. 1, 6, 62, 67, 73, 77, 84, 95, 176, 177]
- Peters, Kenneth E., Walters, Clifford C., & Moldowan, J. Michael. 2005. The Biomarker Guide. *Cambridge University Press*, Volumes 1+2. [cited at p. 3, 6, 9, 56, 59, 67, 69, 74, 82, 83, 84, 88, 93, 94, 97, 99, 102, 134, 175]
- Petrov, Al.A., Arefjev, O.A., & Yakubson, Z.V. 1973. Hydrocarons of Adamantane Series as Indices of Petroleum Catagenesis Process. *In: Advances of Organic Geochemistry 1973, Paris, Edition Technip.*, 517–522. [cited at p. 87]
- Philippi, G. T. 1965. On the depth, time and mechanism of petroleum generation. *Geochimica et Cosmochimica Acta*, 29(9), 1021–1049. TY - JOUR. [cited at p. 3]
- Philp, R. Paul. 1985. Biological markers in fossil fuel production. *Mass Spectrometry Reviews*, 4(1), 1–54. [cited at p. 1, 93]
- Pitman, Janet K., Steinshouser, Douglas, & Lewan, Michael D. 2004. Petroleum generation and migration in the Mesopotamian Basin and Zagros Fold Belt of Iraq: results from a basin-modeling study. *GeoArabia*, 9(4), 41–72. [cited at p. 12]
- Pond, K.L., Huang, Y., Wang, Y., & Kulpa, C.F. 2002. Hydrogen Isotopic Composition of Individual n-Alkanes as an Intrinsic Tracer for Bioremediation

- and Source Identification of Petroleum Contamination. *Environ. Sci. Technol.*, 36(4), 724–728. [cited at p. 107]
- Powell, T.G., & McKirdy, D.M. 1973. Relationship between ratio of pristane to phytane, crude oil composition and geological environment in Australia. *Nature*, 243, 37–39. [cited at p. 67]
- Radke, Jens, Bechtel, Achim, Gaupp, Reinhard, Pttmann, Wilhelm, Schwark, Lorenz, Sachse, Dirk, & Gleixner, Gerd. 2005. Correlation between hydrogen isotope ratios of lipid biomarkers and sediment maturity. *Geochimica et Cosmochimica Acta*, 69(23), 5517–5530. [cited at p. 107]
- Radke, M. 1987. Organic Geochemistry of Aromatic Hydrocarbons. *In: Advances in Organic Geochemistry 1987, Academic Press INC. (London) LTD.*, 140–208. [cited at p. 97, 98]
- Radke, M., & Welte, D H. 1981. The methylphenanthrene index (MP1): a maturity parameter based on aromatic hydrocarbons. *In: Bjoray, M. et al. ed. Advances in organic geochemistry 1981. Chichester, John Wiley & Sons Ltd. (1983)*, 504–512. [cited at p. 96]
- Radke, M., Welte, D. H., & Willsch, H. 1986. Maturity parameters based on aromatic hydrocarbons: Influence of the organic matter type. *Organic Geochemistry*, 10(1-3), 51–63. [cited at p. 97, 99]
- Radke, Matthias. 1988. Application of aromatic compounds as maturity indicators in source rocks and crude oils. *Marine and Petroleum Geology*, 5(3), 224–236. TY - JOUR. [cited at p. 97]
- Radke, Matthias, Welte, Dietrich H., & Willsch, Helmut. 1982a. Geochemical study on a well in the Western Canada Basin: relation of the aromatic distribution pattern to maturity of organic matter. *Geochimica et Cosmochimica Acta*, 46(1), 1–10. TY - JOUR. [cited at p. 97]
- Rigby, D., Batts, B. D., & Smith, J. W. 1981. The effect of maturation on the isotopic composition of fossil fuels. *Organic Geochemistry*, 3(1-2), 29–36. [cited at p. 107, 108]

- Rooney, M.A., Vuletich, A.K., & Griffith, C.E. 1998. Compound-specific isotope analysis as a tool for characterizing mixed oils: an example from the West of Shetlands area. *Organic Geochemistry Advances in Organic Geochemistry 1997 Proceedings of the 18th International Meeting on Organic Geochemistry Part I. Petroleum Geochemistry*, 29(1-3), 241–254. [cited at p. 107, 187]
- Ross, L. M., & Ames, R. L. 1988. Stratification of oils in Columbus basin off Trinidad. *Oil & Gas J.*, Sept.(26), 72–76. [cited at p. 2]
- Rullkotter, Jrgen, Spiro, Baruch, & Nissenbaum, Arie. 1985. Biological marker characteristics of oils and asphalts from carbonate source rocks in a rapidly subsiding graben, Dead Sea, Israel. *Geochimica et Cosmochimica Acta*, 49(6), 1357–1370. TY - JOUR. [cited at p. 119]
- Sadooni, Fadhil N., & Aqrabi, Adnan A.M. 2000. Cretaceous Sequence Stratigraphy and Petroleum Potential of the Mesopotamian Basin, Iraq. *Special Publication for Sedimentary Geology*, 69, 315–334. [cited at p. 12]
- Salel, J. F., & Seguret, M. 1994. Late Cretaceous to Palaeogene thin-skinned tectonics of the Palmyrides belt (Syria). *Tectonophysics*, 234(4), 265–290. TY - JOUR. [cited at p. 15]
- Santos Neto, Eugenio Vaz, & Hayes, John M. 1999. Use of hydrogen and carbon stable isotopes characterizing oils from the Potiguar Basin (onshore), northeastern Brazil. *AAPG Bulletin*, 83(3), 496–518. [cited at p. 111, 115, 187]
- Sarmiento, L. F., & Rangel, A. 2004. Petroleum systems of the Upper Magdalena Valley, Colombia. *Marine and Petroleum Geology*, 21(3), 373–391. TY - JOUR. [cited at p. 10]
- Sawaf, Tarif, Al-Saad, Damen, Gebran, Ali, Barazangi, Muawia, Best, John A., & Chaimov, Thomas A. 1993. Stratigraphy and structure of eastern Syria across the Euphrates depression. *Tectonophysics*, 220(1-4), 267–281. TY - JOUR. [cited at p. 16, 17, 18]
- Schimmelmann, Arndt, Lewan, Michael D., & Wintsch, Robert P. 1999. D/H isotope ratios of kerogen, bitumen, oil, and water in hydrous pyrolysis of source rocks containing kerogen types I, II, IIS, and III. *Geochimica et Cosmochimica Acta*, 63(22), 3751–3766. [cited at p. 108, 111]

- Schimmelmann, Arndt, Boudou, Jean-Paul, Lewan, Michael D., & Wintsch, Robert P. 2001. Experimental controls on D/H and $^{13}\text{C}/^{12}\text{C}$ ratios of kerogen, bitumen and oil during hydrous pyrolysis. *Organic Geochemistry*, 32(8), 1009–1018. TY - JOUR. [cited at p. 111]
- Schimmelmann, Arndt, Sessions, Alex L., Boreham, Christopher J., Edwards, Dianne S., Logan, Graham A., & Summons, Roger E. 2004. D/H ratios in terrestrially sourced petroleum systems. *Organic Geochemistry Selected papers from the sixteenth international symposium on environmental biogeochemistry*, 35(10), 1169–1195. TY - JOUR. [cited at p. 108]
- Schimmelmann, Arndt, Sessions, Alex L., & Mastalerz, Maria. 2006. Hydrogen Isotopic (D/H) Composition of Organic Matter During Diagenesis and Thermal Maturation. *Annu. Rev. Earth Planet. Sci.*, 34, 501–533. [cited at p. 107, 111]
- Schmoker, James W. 1994. Volumetric Calculation of Hydrocarbons Generated. *Pages 323–326 of: Magoon, LB, & Dow, WG (eds), The petroleum system - from source to trap.* Tulsa: American Association of Petroleum Geologists. [cited at p. 7]
- Schoell, M., Hwang, R. J., Carlson, R. M. K., & Welton, J. E. 1994. Carbon isotopic composition of individual biomarkers in gilsonites (Utah). *Organic Geochemistry*, 21(6-7), 673–683. [cited at p. 102]
- Schoell, Martin. 1984b. Recent advances in petroleum isotope geochemistry. *Organic Geochemistry*, 6, 645–663. [cited at p. 102]
- Schulz, Linda K., Wilhelms, Arnd, Rein, Elin, & Steen, Arne S. 2001. Application of diamondoids to distinguish source rock facies. *Organic Geochemistry*, 32(3), 365–375. [cited at p. xi, 91, 92, 142, 193]
- Searle, M. P. 1994. Structure of the interplate eastern Palmyride Fold Belt, Syria. *Geological Society of America Bulletin*, 106(10), 1332–1350. [cited at p. 15]
- Seifert, W.K., & Moldowan, J.M. 1986. Use of biological markers in petroleum exploration. *Biological markers in the sedimentary record, Published by Elsevier; Methods in Geochemistry & Geophysics, 24, Editors Johns R.B.*, 261–290. [cited at p. 82]

- Seifert, Wolfgang K., & Moldowan, Michael J. 1978. Applications of steranes, terpanes and monoaromatics to the maturation, migration and source of crude oils. *Geochimica et Cosmochimica Acta*, 42(1), 77–95. [cited at p. 94]
- Seifert, Wolfgang K., & Moldowan, Michael J. 1978a. Applications of steranes, terpanes and monoaromatics to the maturation, migration and source of crude oils. *Geochimica et Cosmochimica Acta*, 42(1), 77–95. [cited at p. 76, 79, 82, 94]
- Serryea, O.A. 1990. Geochemistry of Organic Matter and Oil as an Effective Tool for Hydrocarbon Exploration in Syria (Arabic). *Oil and Arab Cooperation*, 16(58), 119–181. [cited at p. 20, 156]
- Sessions, Alex L., Burgoyne, Thomas W., Schimmelmann, Arndt, & Hayes, John M. 1999. Fractionation of hydrogen isotopes in lipid biosynthesis. *Organic Geochemistry*, 30(9), 1193–1200. [cited at p. 107, 114]
- Sessions, Alex L., Sylva, Sean P., Summons, Roger E., & Hayes, John M. 2004. Isotopic exchange of carbon-bound hydrogen over geologic timescales. *Geochimica et Cosmochimica Acta*, 68(7), 1545–1559. [cited at p. 108, 115]
- Sharaf, L. M., Leboudy, M. M. El, & Shahin, A. N. 2007. Oil Families and Their Potential Sources in the Southern Gulf of Suez, Egypt. *Petroleum Science and Technology*, 25(5), 539 – 559. [cited at p. 10]
- Sieskind, Odette, Joly, Guy, & Albrecht, Pierre. 1979. Simulation of the geochemical transformations of sterols: superacid effect of clay minerals. *Geochimica et Cosmochimica Acta*, 43(10), 1675–1679. [cited at p. 80]
- Sinninghe Damste', Jaap S., Kenig, Fabien, Koopmans, Martin P., Koster, Jurgen, Schouten, Stefan, Hayes, J. M., & de Leeuw, Jan W. 1995. Evidence for gammacerane as an indicator of water column stratification. *Geochimica et Cosmochimica Acta*, 59(9), 1895–1900. [cited at p. 76]
- Slentz, L.W. 1981. Geochemistry of reservoir fluids as unique approach to optimum reservoir management. *SPE - 9582*, Presented at Middle East Oil Technical Conference, Manama, Bahrain. [cited at p. 2]
- Smith, J. W., Gould, K. W., & Rigby, D. 1981. The stable isotope geochemistry of Australian coals. *Organic Geochemistry*, 3(4), 111–131. [cited at p. 107, 108]

- Sofer, Zvi. 1984. Stable carbon isotope compositions of crude oils; application to source depositional environments and petroleum alteration. *AAPG Bulletin*, 68(1), 31–49. [cited at p. 102]
- Soylu, C., Yalcin, M.N., & Horsfield, B. 2005. Hydrocarbon generation habitat of two cretaceous carbonate source rocks in SE turkey. *Journal of petroleum geology*, 28, 67–82. [cited at p. 9]
- Summons, Roger E., & Capon, Robert J. 1988c. Fossil steranes with unprecedented methylation in ring-A. *Geochimica et Cosmochimica Acta*, 52(11), 2733–2736. [cited at p. 77]
- Sun, Yongge, Chen, Zhenyan, Xu, Shiping, & Cai, Pingxia. 2005. Stable carbon and hydrogen isotopic fractionation of individual n-alkanes accompanying biodegradation: evidence from a group of progressively biodegraded oils. *Organic Geochemistry*, 36(2), 225–238. [cited at p. 102, 107, 187]
- Survey, U.S. Geological. 2002. Undiscovered Oil and Gas Resources of Lower Silurian Qusaiba-Paleozoic Total Petroleum Systems, Arabian Peninsula. *USGS Fact Sheet F5-008-02*. [cited at p. 9]
- Talukdar, Suhas C., Dow, Wallace G., & Persad, Krishna M. 1990. Geochemistry of oils provides optimism for deeper exploration in Atlantic off Trinidad. *Oil & Gas Journal*, Nov 12, 118–122. [cited at p. xi, 70, 73]
- Tang, Yongchun, Huang, Yongsong, Ellis, Geoffrey S., Wang, Yi, Kralert, Paul G., Gillaizeau, Bruno, Ma, Qisheng, & Hwang, Rong. 2005. A kinetic model for thermally induced hydrogen and carbon isotope fractionation of individual n-alkanes in crude oil. *Geochimica et Cosmochimica Acta*, 69(18), 4505–4520. TY - JOUR. [cited at p. 108]
- ten Haven, H. L., Rohmer, M., Rullkotter, J., & Bissleret, P. 1989. Tetrahymanol, the most likely precursor of gammacerane, occurs ubiquitously in marine sediments. *Geochimica et Cosmochimica Acta*, 53(11), 3073–3079. [cited at p. 76]
- Terken, J. M. J., Frewin, N. L., & L., Indrelid. S. 2001. Petroleum systems of Oman: Charge timing and risks. *AAPG Bulletin*, 85(10), 1817–1845. [cited at p. 9, 12]

- Terken, Jos M.J. 1999. The Natih Petroleum System of North Oman. *GeoArabia*, 4(2), 157–180. [cited at p. 9]
- Thompson, K. F. M. 1979. Light hydrocarbons in subsurface sediments. *Geochimica et Cosmochimica Acta*, 43(5), 657–672. [cited at p. 69]
- Thompson, K. F. M. 1983. Classification and thermal history of petroleum based on light hydrocarbons. *Geochimica et Cosmochimica Acta*, 47(2), 303–316. [cited at p. 69]
- Thompson, K. F. M.;. 1987. Fractionated aromatic petroleums and the generation of gas-condensates. *Organic Geochemistry*, 11(6), 573–590. [cited at p. 69, 179]
- Thompson, K. F. M. 1988. Gas-condensate migration and oil fractionation in deltaic systems. *Marine and Petroleum Geology*, 5(3), 237–246. [cited at p. 69, 70]
- Thompson, K. F. M. 1991. Contrasting characteristics attributed to migration observed in petroleums reservoired in clastic and carbonate sequences in the Gulf of Mexico region. *From England, W. A. & Fleet, A. J. (eds), Petroleum Migration, Geological Society.*, Special Publication No. 59, 191–205. [cited at p. 69]
- Tissot, B., & Welte, D.H. 1984. Petroleum Formation and Occurrence. *Springer, Berlin*. [cited at p. 2, 3, 5, 7, 56, 58, 60, 62, 97, 118, 177]
- Trindade, L. A. F., Brassell, Simon C., & Santos Neto, E. V. 1992. Petroleum migration and mixing in the Potiguar Basin, Brazil. *AAPG Bulletin*, 76(12), 1903–1924. [cited at p. 102]
- van Aarssen, Ben G. K., Bastow, Trevor P., Alexander, Robert, & Kagi, Robert I. 1999. Distributions of methylated naphthalenes in crude oils: indicators of maturity, biodegradation and mixing. *Organic Geochemistry*, 30(10), 1213–1227. [cited at p. 93, 166]
- van Graas, Ger W. 1990. Biomarker maturity parameters for high maturities: Calibration of the working range up to the oil/condensate threshold. *Organic Geochemistry*, 16(4-6), 1025–1032. [cited at p. 79]
- van Kaam-Peters, Heidy M. E., Koster, Jurgen, van der Gaast, Sjierk J., Dekker, Marlen, de Leeuw, Jan W., & Sinninghe Damste, Jaap S. 1998b. The effect of

- clay minerals on diasterane/sterane ratios. *Geochimica et Cosmochimica Acta*, 62(17), 2923–2929. [cited at p. 80]
- Venkatesan, M. I. 1989. Tetrahymanol: Its widespread occurrence and geochemical significance. *Geochimica et Cosmochimica Acta*, 53(11), 3095–3101. [cited at p. 76]
- Verma, Mahendra K., Thomas S, Ahlbrandt, & Al-Gailani, Mohammad. 2004. Petroleum reserves and undiscovered resources in the total petroleum systems of Iraq: reserve growth and production implications. *GeoArabia*, 9(3), 51–74. [cited at p. 9, 12]
- Vieth, Andrea, & Wilkes, Heinz. 2006. Deciphering biodegradation effects on light hydrocarbons in crude oils using their stable carbon isotopic composition: A case study from the Gullfaks oil field, offshore Norway. *Geochimica et Cosmochimica Acta*, 70(3), 651–665. [cited at p. 102, 187]
- Wang, Zhendi., & Stout, Scott A. 2007. Oil Spill Environmental Forensics: Fingerprinting and Source Identification. *Academic Press, Elsevier*, pp.554. [cited at p. 167]
- Wei, Zhibin, Moldowan, J. Michael, Jarvie, Daniel M., & Hill, Ronald. 2006b. The fate of diamondoids in coals and sedimentary rocks. *Geology*, 34(12), 1013–1016. [cited at p. 87]
- Welte, D H, Horsfield, B., & Baker, D.R. 1997. Petroleum and Basin Evolution. *Springer Verlag, New York*. [cited at p. 2]
- Welte, D.H., Kratochvil, H., Rullkötter, J., Ladwein, H., & Schaefer, R.G. 1982. Organic geochemistry of crude oils from the Vienna Basin and an assessment of their origin. *Chemical Geology*, 35(1-2), 33–68. [cited at p. 181]
- Wenger, Lloyd M., Davis, Cara L., & Isaksan, Gary H. 2001. Multiple Controls on Petroleum Biodegradation and Impact on Oil Quality. *Society of Petroleum Engineers Paper 71450*. [cited at p. xiii, 175, 176, 177]
- Wilhelms, Arnd, & Larter, Steve. 2004. Shaken but not always stirred. Impact of petroleum charge mixing on reservoir geochemistry. *Geological Society, London, Special Publications*, 237(1), 27–35. [cited at p. 166, 167]

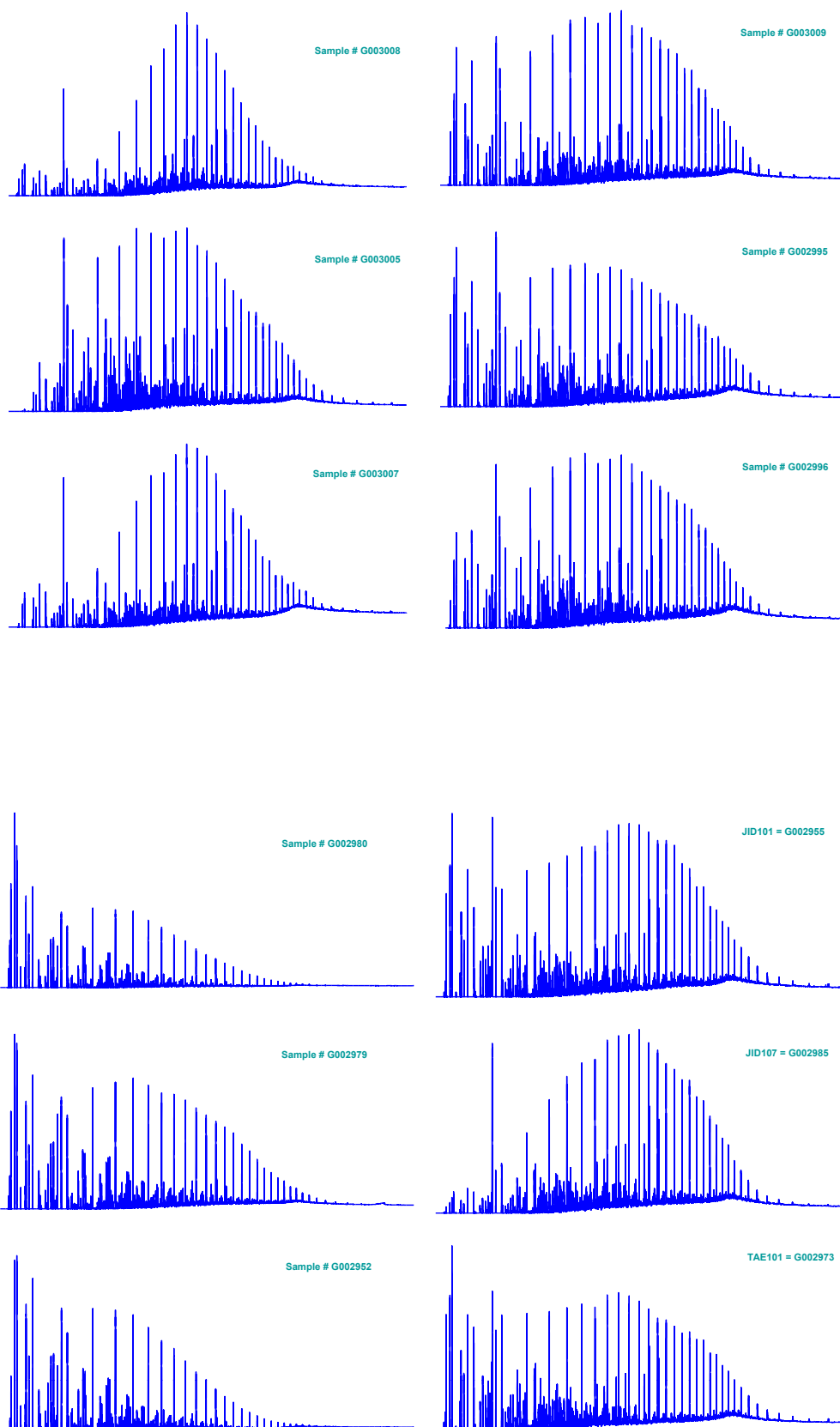
- Wilkes, H, Rabus, R, Fischer, T, Armstroff, A, Behrends, A, & Widdel, F. 2002. Anaerobic degradation of n-hexane in a denitrifying bacterium: further degradation of the initial intermediate (1-methylpentyl)succinate via C-skeleton rearrangement. *Arch Microbiol.*, 177(3), 235–243. [cited at p. 175]
- Wilkes, Heinz, Boreham, Chris, Harms, Gerda, Zengler, Karsten, & Rabus, Ralf. 2000. Anaerobic degradation and carbon isotopic fractionation of alkylbenzenes in crude oil by sulphate-reducing bacteria. *Organic Geochemistry*, 31(1), 101–115. [cited at p. 175]
- Wilkes, Heinz, Vieth, Andrea, & Elias, Rouven. 2008. Constraints on the quantitative assessment of in-reservoir biodegradation using compound-specific stable carbon isotopes. *Organic Geochemistry Advances in Organic Geochemistry 2007 - Proceedings of the 23rd International Meeting on Organic Geochemistry*, 39(8), 1215–1221. TY - JOUR. [cited at p. 2, 187]
- Wingert, William S. 1992. G.c.-m.s. analysis of diamondoid hydrocarbons in Smackover petroleum. *Fuel*, 71(1), 37–43. [cited at p. 87, 90]
- Xiong, Yongqiang, Geng, Ansong, Pan, Changchun, Liu, Deyong, & Peng, Pingan. 2005. Characterization of the hydrogen isotopic composition of individual n-alkanes in terrestrial source rocks. *Applied Geochemistry*, 20(3), 455–464. [cited at p. 107]
- Yeh, Hsueh-Wen, & Epstein, Samuel. 1981. Hydrogen and carbon isotopes of petroleum and related organic matter,. *Geochimica et Cosmochimica Acta*, 45(5), 753–762. [cited at p. 107]
- Zhang, Shuichang, & Huang, Haiping. 2005a. Geochemistry of Palaeozoic marine petroleum from the Tarim Basin, NW China: Part 1. Oil family classification. *Organic Geochemistry*, 36(8), 1204–1214. TY - JOUR. [cited at p. 10]
- Zhang, Shuichang, Liang, Digang, Gong, Zaisheng, Wu, Keqiang, Li, Maowen, Song, Fuqing, Song, Zhiguang, Zhang, Dajiang, & Wang, Peirong. 2003. Geochemistry of petroleum systems in the eastern Pearl River Mouth Basin: evidence for mixed oils. *Organic Geochemistry Chinese 2001 Symposium on Research and Technological Advances of Reservoir Geochemistry*, 34(7), 971–991. TY - JOUR. [cited at p. 3, 166]

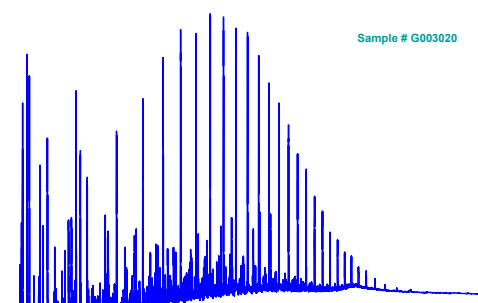
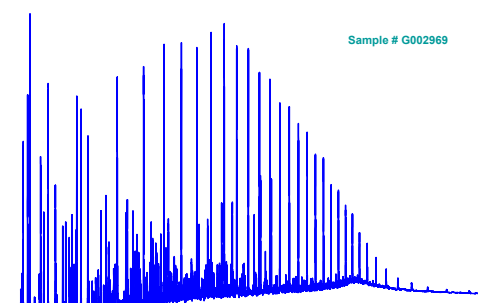
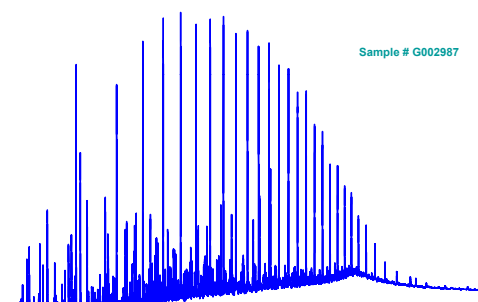
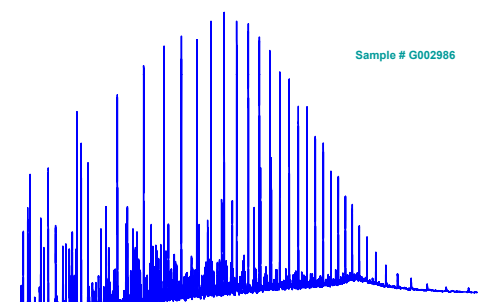
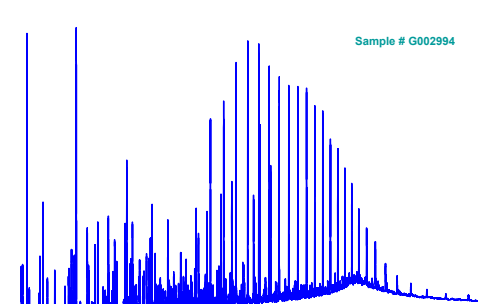
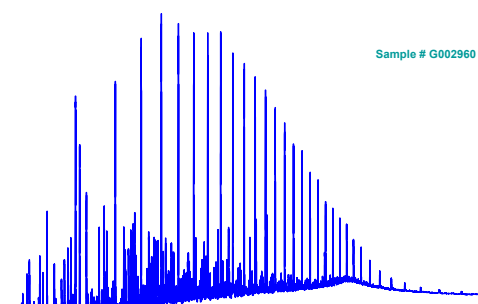
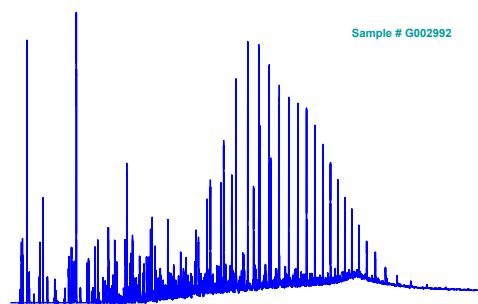
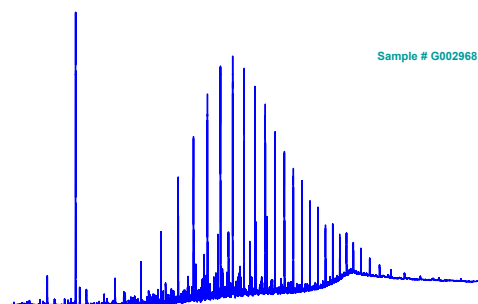
- Ziegler, Martin A. 2001. Late Permian to Holocene Paleofacies Evolution of the Arabian Plate and its Hydrocarbon Occurrences. *GeoArabia*, 6(3), 445–504. [cited at p. 18]
- Zumberge, John E. 1987. Prediction of source rock characteristics based on terpane biomarkers in crude oils: A multivariate statistical approach. *Geochimica et Cosmochimica Acta*, 51(6), 1625–1637. [cited at p. 74]

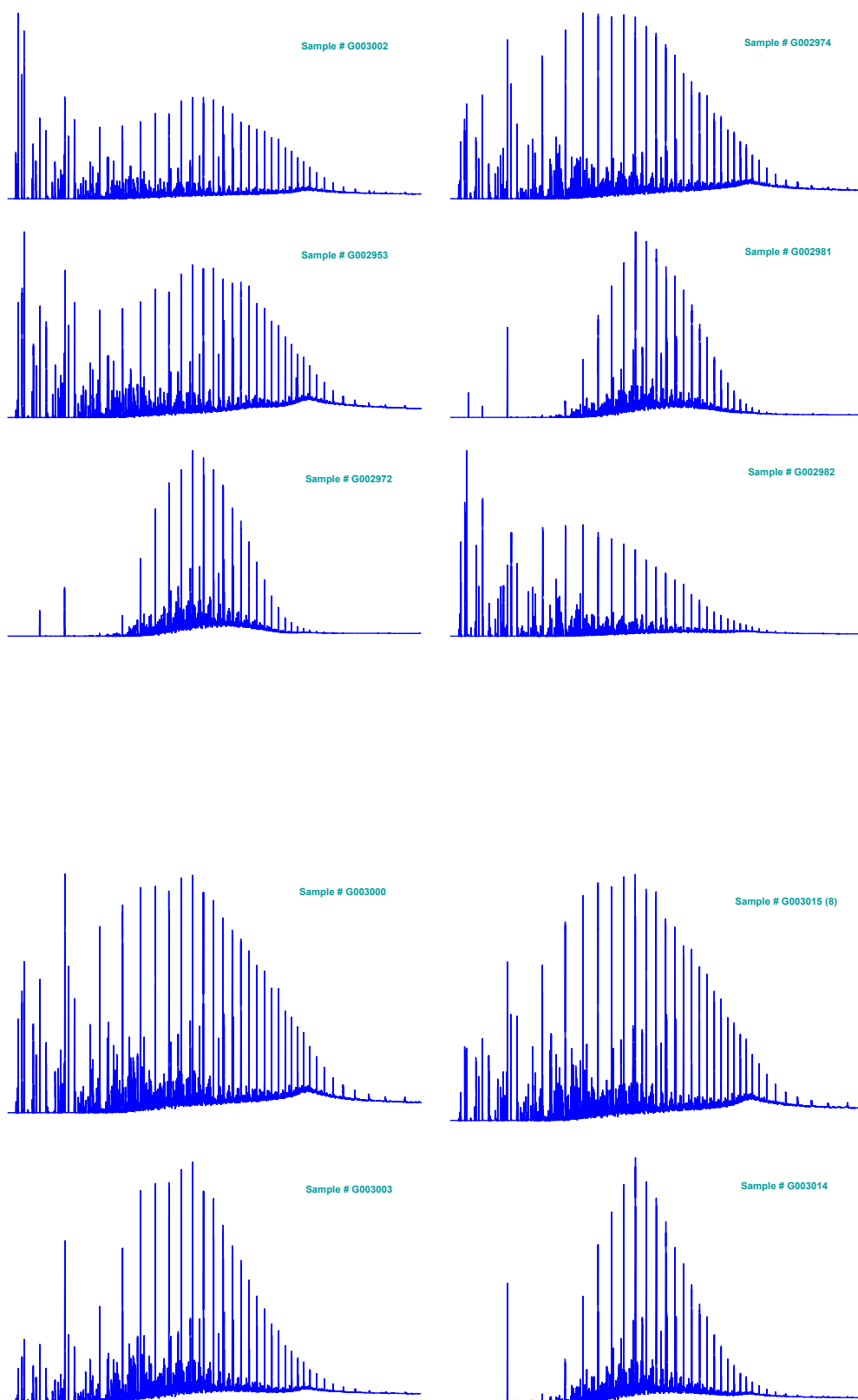
Appendices

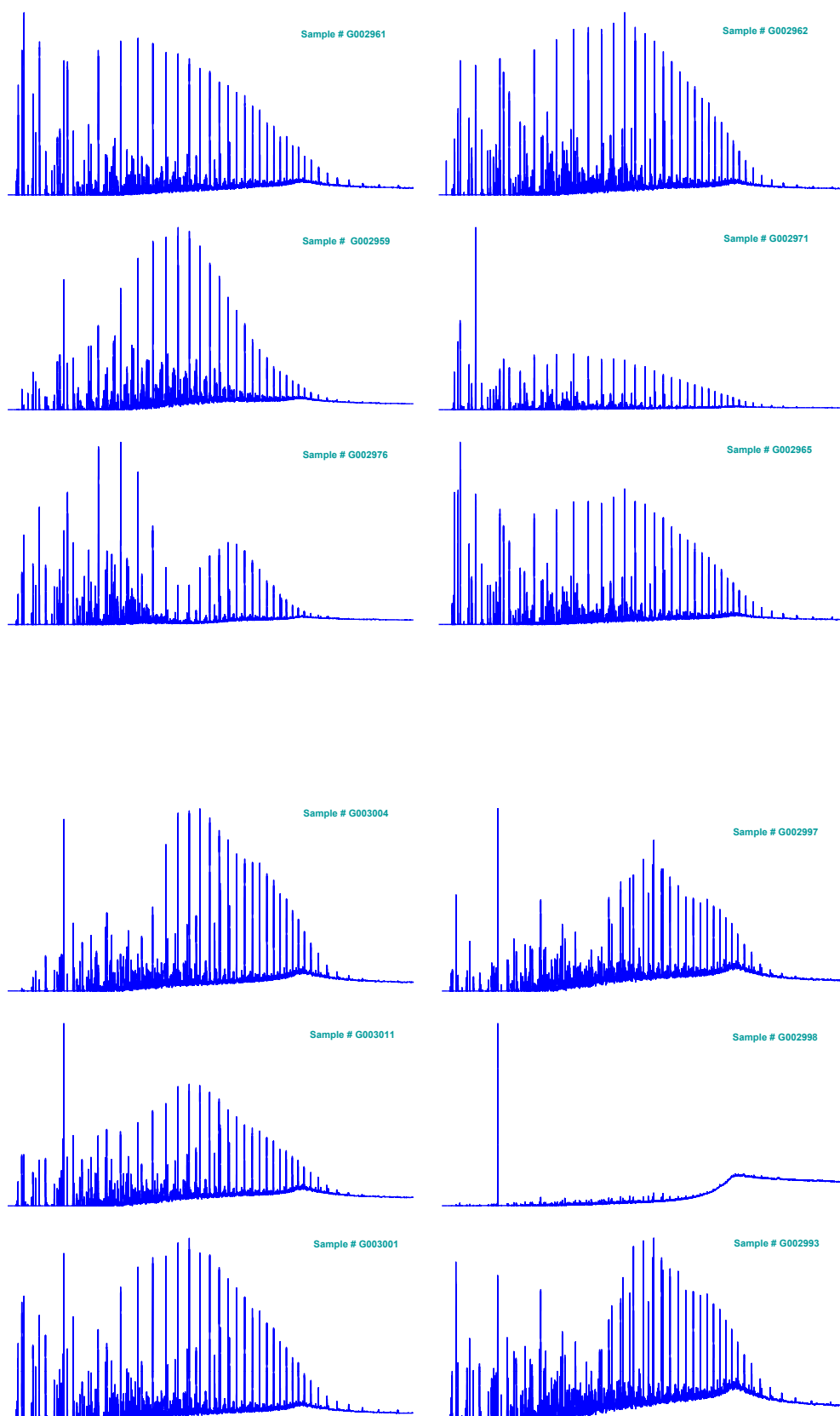
GCFID Fingerprints of Crude Oils

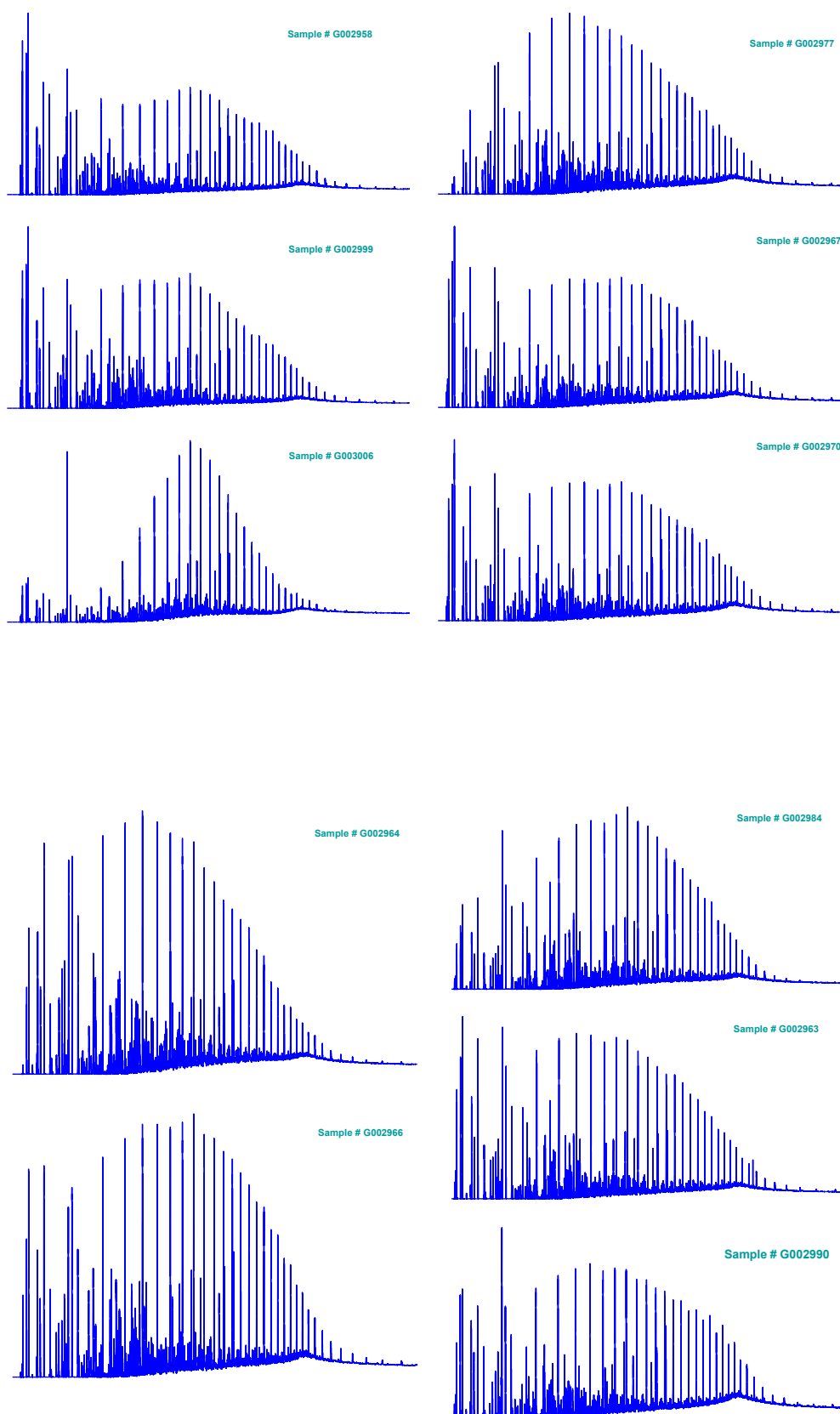


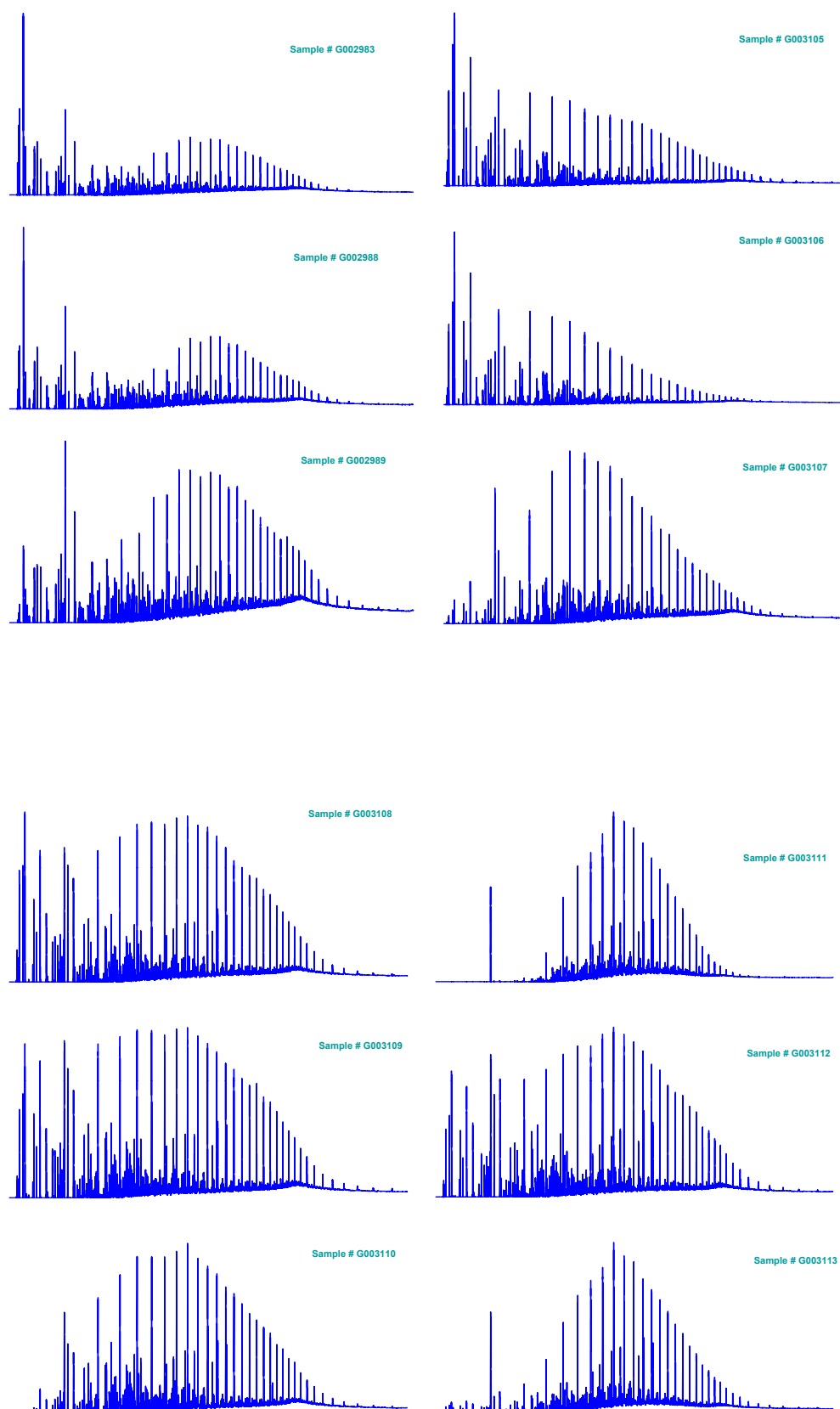












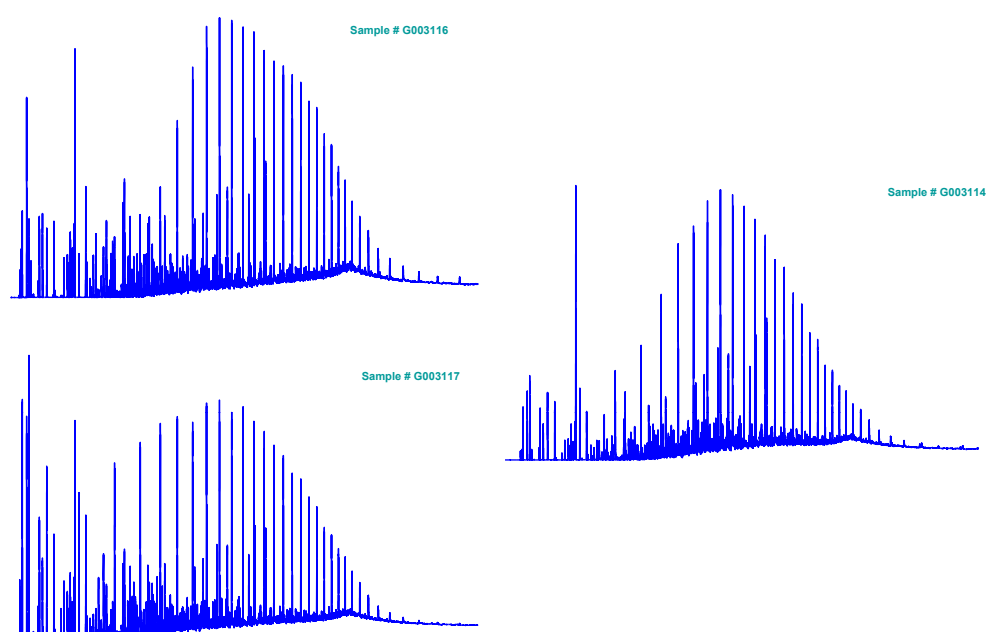


Figure A.1: illustrates the GC fingerprints for analyzed crude oils from the study area.

Appendix B

Geochemical Data of Analysed Oils

| Sample | Adamantane | | | | | | | | | | | | | | | | | | | | |
|---------|------------|------|-----|-----|-----|-----|-----|-----|-----|-----|-----|-----|-----|-----|-----|----|-----|----|-----|-----|----|
| | 1 | 2 | 3 | 4 | 5 | 6 | 7 | 8 | 9 | 10 | 11 | 12 | 13 | 14 | 15 | 16 | 17 | 18 | 19 | 20 | 21 |
| G002952 | 117 | 652 | 342 | 162 | 293 | 474 | 371 | 368 | 402 | 214 | 135 | 216 | 242 | 233 | 308 | 21 | 123 | 47 | 128 | 88 | 20 |
| G002953 | 16 | 56 | 61 | 33 | 70 | 36 | 44 | 48 | 60 | 27 | 10 | 20 | 28 | 25 | 37 | 3 | 10 | 4 | 18 | 14 | 2 |
| G002954 | 111 | 581 | 355 | 188 | 347 | 460 | 384 | 381 | 465 | 227 | 138 | 250 | 285 | 298 | 388 | 24 | 158 | 75 | 184 | 131 | 30 |
| G002956 | 1 | 6 | 5 | 4 | 7 | 7 | 6 | 6 | 8 | 6 | 3 | 5 | 6 | 7 | 10 | 1 | 5 | 2 | 6 | 5 | 1 |
| G002959 | 173 | 1196 | 527 | 272 | 469 | 961 | 679 | 624 | 706 | 427 | 290 | 427 | 494 | 483 | 597 | 50 | 274 | 96 | 232 | 148 | 50 |
| G002960 | 54 | 303 | 205 | 131 | 251 | 284 | 253 | 235 | 292 | 170 | 108 | 170 | 175 | 174 | 268 | 23 | 108 | 47 | 125 | 85 | 21 |
| G002961 | 24 | 138 | 82 | 54 | 88 | 109 | 89 | 88 | 103 | 66 | 37 | 59 | 65 | 61 | 87 | 6 | 36 | 14 | 36 | 27 | 6 |
| G002963 | 20 | 80 | 61 | 48 | 57 | 67 | 62 | 64 | 89 | 55 | 21 | 46 | 55 | 53 | 68 | 4 | 26 | 13 | 32 | 26 | 5 |
| G002964 | 9 | 50 | 57 | 41 | 82 | 45 | 61 | 64 | 82 | 53 | 19 | 46 | 54 | 56 | 90 | 6 | 32 | 15 | 44 | 34 | 7 |
| G002965 | 35 | 115 | 105 | 52 | 101 | 84 | 77 | 82 | 102 | 54 | 23 | 49 | 58 | 52 | 71 | 5 | 24 | 11 | 33 | 30 | 4 |
| G002966 | 9 | 31 | 35 | 18 | 48 | 24 | 25 | 26 | 38 | 21 | 6 | 15 | 20 | 18 | 23 | 1 | 7 | 5 | 13 | 11 | 1 |
| G002968 | 7 | 28 | 25 | 18 | 39 | 23 | 22 | 24 | 30 | 21 | 8 | 13 | 18 | 16 | 24 | 2 | 8 | 4 | 12 | 8 | 2 |
| G002969 | 28 | 115 | 84 | 52 | 90 | 89 | 77 | 81 | 102 | 60 | 26 | 48 | 55 | 51 | 72 | 5 | 27 | 12 | 34 | 26 | 5 |
| G002973 | 21 | 77 | 60 | 37 | 76 | 54 | 53 | 56 | 71 | 41 | 17 | 30 | 35 | 32 | 46 | 3 | 16 | 7 | 22 | 18 | 3 |
| G002974 | 45 | 203 | 129 | 79 | 133 | 146 | 130 | 128 | 145 | 90 | 44 | 75 | 87 | 85 | 116 | 7 | 45 | 21 | 53 | 39 | 8 |
| G002975 | 27 | 92 | 75 | 41 | 97 | 67 | 66 | 65 | 89 | 48 | 20 | 37 | 47 | 45 | 67 | 5 | 22 | 11 | 30 | 23 | 4 |
| G002976 | 15 | 46 | 35 | 19 | 40 | 34 | 26 | 26 | 32 | 16 | 9 | 13 | 15 | 13 | 20 | 2 | 7 | 3 | 8 | 5 | 2 |
| G002980 | 100 | 533 | 265 | 149 | 249 | 368 | 290 | 284 | 309 | 178 | 109 | 168 | 194 | 186 | 249 | 18 | 104 | 43 | 107 | 70 | 19 |
| G002981 | 29 | 129 | 109 | 95 | 175 | 113 | 109 | 112 | 145 | 95 | 40 | 67 | 83 | 79 | 118 | 10 | 43 | 20 | 52 | 41 | 10 |
| G002982 | 67 | 275 | 203 | 116 | 212 | 195 | 186 | 193 | 222 | 120 | 62 | 109 | 135 | 129 | 186 | 11 | 68 | 32 | 86 | 65 | 12 |
| G002988 | 51 | 227 | 169 | 100 | 190 | 167 | 155 | 159 | 197 | 103 | 51 | 88 | 110 | 104 | 146 | 10 | 57 | 25 | 71 | 53 | 11 |
| G002993 | 20 | 74 | 73 | 45 | 92 | 57 | 53 | 59 | 82 | 37 | 16 | 30 | 40 | 36 | 52 | 3 | 14 | 7 | 25 | 18 | 3 |
| G002995 | 16 | 59 | 39 | 28 | 51 | 46 | 37 | 36 | 43 | 27 | 14 | 18 | 23 | 20 | 30 | 4 | 10 | 4 | 12 | 9 | 2 |
| G002997 | 20 | 68 | 76 | 66 | 128 | 48 | 50 | 61 | 73 | 38 | 15 | 28 | 37 | 33 | 48 | 4 | 14 | 7 | 27 | 19 | 3 |
| G003005 | 27 | 96 | 68 | 41 | 79 | 75 | 56 | 61 | 83 | 44 | 21 | 33 | 39 | 38 | 48 | 6 | 16 | 8 | 25 | 21 | 4 |
| G003006 | 18 | 75 | 63 | 44 | 96 | 59 | 55 | 57 | 67 | 41 | 21 | 31 | 37 | 35 | 52 | 5 | 18 | 7 | 23 | 16 | 4 |
| G003009 | 31 | 132 | 90 | 49 | 95 | 97 | 77 | 76 | 96 | 56 | 28 | 45 | 51 | 50 | 66 | 7 | 26 | 11 | 28 | 22 | 6 |
| G003011 | 14 | 55 | 61 | 47 | 81 | 40 | 41 | 50 | 61 | 32 | 11 | 19 | 29 | 27 | 40 | 3 | 10 | 6 | 20 | 14 | 2 |
| G003015 | 22 | 87 | 71 | 47 | 82 | 59 | 55 | 57 | 76 | 37 | 18 | 32 | 35 | 35 | 44 | 4 | 16 | 5 | 22 | 20 | 3 |
| G003017 | 20 | 94 | 44 | 34 | 48 | 75 | 47 | 54 | 55 | 38 | 29 | 37 | 37 | 38 | 49 | 6 | 22 | 8 | 19 | 14 | 4 |

| Sample | Diamantane | | | | | | | | | | |
|---------|------------|----|----|----|----|----|----|----|----|----|--|
| | 22 | 23 | 24 | 25 | 26 | 27 | 28 | 29 | 30 | 31 | |
| G002952 | 13 | 21 | 16 | 15 | 9 | 10 | 11 | 18 | 8 | 20 | |
| G002953 | 5 | 7 | 4 | 4 | 2 | 2 | 3 | 3 | 2 | 4 | |
| G002954 | 18 | 27 | 24 | 23 | 11 | 14 | 17 | 29 | 11 | 37 | |
| G002956 | 6 | 10 | 8 | 7 | 4 | 6 | 7 | 9 | 5 | 13 | |
| G002959 | 32 | 54 | 41 | 38 | 22 | 27 | 32 | 39 | 22 | 54 | |
| G002960 | 27 | 43 | 23 | 23 | 13 | 15 | 21 | 25 | 14 | 28 | |
| G002961 | 6 | 10 | 7 | 7 | 4 | 5 | 5 | 7 | 4 | 9 | |
| G002963 | 7 | 8 | 7 | 7 | 3 | 4 | 4 | 6 | 3 | 8 | |
| G002964 | 14 | 19 | 13 | 12 | 6 | 7 | 10 | 13 | 6 | 13 | |
| G002965 | 8 | 9 | 8 | 8 | 3 | 4 | 5 | 6 | 3 | 6 | |
| G002966 | 2 | 3 | 3 | 3 | 1 | 2 | 2 | 2 | 1 | 2 | |
| G002968 | 7 | 9 | 5 | 5 | 2 | 3 | 4 | 3 | 2 | 3 | |
| G002969 | 8 | 11 | 7 | 8 | 4 | 5 | 6 | 6 | 4 | 7 | |
| G002973 | 5 | 7 | 5 | 5 | 2 | 3 | 4 | 4 | 3 | 4 | |
| G002974 | 7 | 11 | 9 | 10 | 4 | 6 | 7 | 9 | 4 | 14 | |
| G002975 | 8 | 10 | 7 | 6 | 3 | 4 | 5 | 5 | 3 | 6 | |
| G002976 | 5 | 7 | 4 | 4 | 2 | 3 | 3 | 4 | 2 | 3 | |
| G002980 | 12 | 19 | 15 | 14 | 8 | 10 | 11 | 15 | 8 | 19 | |
| G002981 | 40 | 52 | 30 | 29 | 15 | 16 | 25 | 18 | 14 | 17 | |
| G002982 | 8 | 11 | 11 | 11 | 5 | 6 | 7 | 13 | 4 | 15 | |
| G002988 | 11 | 17 | 13 | 12 | 6 | 8 | 10 | 13 | 7 | 15 | |
| G002993 | 5 | 7 | 6 | 5 | 2 | 3 | 4 | 4 | 3 | 4 | |
| G002995 | 4 | 6 | 5 | 4 | 2 | 3 | 3 | 3 | 2 | 2 | |
| G002997 | 5 | 7 | 5 | 4 | 2 | 3 | 4 | 3 | 3 | 3 | |
| G003005 | 9 | 12 | 8 | 8 | 4 | 5 | 6 | 5 | 4 | 4 | |
| G003006 | 17 | 22 | 12 | 12 | 6 | 7 | 10 | 7 | 6 | 6 | |
| G003009 | 11 | 16 | 10 | 9 | 5 | 5 | 8 | 6 | 5 | 7 | |
| G003011 | 4 | 6 | 4 | 4 | 2 | 3 | 3 | 3 | 2 | 4 | |
| G003015 | 6 | 8 | 6 | 6 | 2 | 4 | 5 | 4 | 2 | 4 | |
| G003017 | 19 | 25 | 12 | 10 | 7 | 7 | 11 | 8 | 6 | 6 | |

Table B.1: Concentrations [$\mu\text{g/g oil}$] for adamantane and diamantane compounds. Compound names and numbers are shown in Fig.3.2 and Tab.3.3

| Sample | $n\text{-}C_3$ | $i\text{-}C_4$ | $n\text{-}C_4$ | $i\text{-}C_5$ | $n\text{-}C_5$ | 2MP | 3MP | $n\text{-}C_6$ | MCP | BZ | Chex | 3Mhex |
|---------|----------------|----------------|----------------|----------------|----------------|--------|--------|----------------|--------|--------|--------|--------|
| G002952 | | -24.80 | -25.03 | -27.41 | -26.66 | -27.49 | -27.99 | -27.34 | -25.03 | -27.73 | -25.89 | -28.21 |
| G002953 | -25.13 | -30.72 | -27.35 | -28.69 | -28.61 | -29.02 | -27.83 | -30.15 | -26.63 | -28.35 | -27.50 | -28.05 |
| G002954 | -24.53 | -27.97 | -26.29 | -27.69 | -26.16 | -27.28 | -27.52 | -27.19 | -25.07 | -28.50 | -24.68 | -27.88 |
| G002956 | | -28.61 | -27.52 | -27.84 | -27.84 | -27.37 | -27.28 | -28.51 | -26.16 | -25.72 | -25.49 | -26.77 |
| G002959 | | | | -23.42 | -20.78 | -24.82 | -25.83 | -24.16 | -25.80 | | -23.77 | -26.43 |
| G002960 | | | -25.47 | -26.40 | -26.12 | -26.38 | -26.45 | -26.89 | -25.84 | -24.17 | -24.28 | -26.77 |
| G002961 | | -28.16 | -28.16 | -27.87 | -27.75 | -27.51 | -27.86 | -28.10 | -26.70 | -27.19 | -26.69 | -27.39 |
| G002963 | -25.66 | -28.91 | -26.64 | -27.81 | -26.97 | -27.52 | -26.71 | -27.60 | -27.06 | -29.91 | -26.51 | -26.58 |
| G002964 | | | | -27.14 | -26.23 | -27.85 | -27.97 | -27.51 | -27.33 | -28.95 | -26.09 | -28.51 |
| G002965 | -28.55 | -30.69 | -28.49 | -28.87 | -28.66 | -28.31 | -27.25 | -28.82 | -26.68 | -28.25 | -26.38 | -27.26 |
| G002966 | | -31.26 | -28.89 | -29.38 | -28.97 | -28.72 | -27.80 | -29.28 | -28.24 | -27.32 | -29.16 | -27.12 |
| G002968 | | | | | | | | | | | | |
| G002969 | -27.70 | -29.87 | -28.34 | -28.57 | -28.30 | -28.18 | -26.92 | -29.04 | -28.36 | -27.38 | -27.99 | -27.71 |
| G002973 | | -30.60 | -27.81 | -28.24 | -28.29 | -28.49 | -26.82 | -29.18 | -26.21 | -27.66 | -26.63 | -27.19 |
| G002974 | | -27.83 | -27.20 | -27.40 | -27.33 | -27.17 | -27.01 | -27.14 | -26.51 | -25.94 | -27.87 | -26.87 |
| G002975 | -28.03 | -30.18 | -28.10 | -28.21 | -27.77 | -27.54 | -26.02 | -27.98 | -26.43 | | -26.67 | -26.71 |
| G002976 | | | -31.42 | -30.23 | -30.25 | -29.77 | -28.58 | -30.19 | -28.81 | -30.98 | -28.98 | -28.17 |
| G002980 | -26.05 | -27.65 | -26.69 | -27.86 | -26.49 | -27.55 | -27.69 | -27.27 | -25.90 | -26.91 | -25.69 | -28.41 |
| G002981 | | | | | | | | | | | | |
| G002982 | | -29.52 | -28.55 | -29.13 | -28.01 | -28.51 | -28.45 | -28.77 | -28.31 | | -27.41 | -28.94 |
| G002988 | | -32.16 | -26.73 | -29.33 | -26.93 | -28.22 | -27.39 | -29.61 | -28.50 | | -27.50 | -27.22 |
| G002993 | -28.41 | -31.32 | -28.48 | -29.96 | -28.64 | -29.10 | -27.07 | -29.89 | -29.64 | -28.08 | -29.63 | -27.59 |
| G002995 | | -30.74 | -24.02 | -28.53 | -24.16 | -27.17 | -27.03 | -25.97 | -25.97 | | -26.10 | -26.02 |
| G002997 | | | | | | -26.25 | -24.69 | -27.39 | -25.72 | -24.21 | -28.90 | -26.98 |
| G003005 | | | -32.22 | -30.54 | -31.72 | -30.51 | -29.67 | -31.65 | -28.50 | | -30.94 | -28.48 |
| G003006 | | | -25.02 | -27.22 | -26.84 | -26.88 | -25.75 | -27.43 | -26.52 | -25.92 | -27.24 | -25.74 |
| G003009 | | | -29.52 | -29.62 | -29.58 | -29.92 | -28.36 | -30.26 | -28.34 | | -29.27 | -28.35 |
| G003011 | | | -27.67 | -28.40 | -28.11 | -28.18 | -27.07 | -28.41 | -27.29 | | -28.21 | -27.06 |
| G003015 | | | | | | | | | | | | |
| G003017 | -24.74 | -30.00 | -24.98 | -28.97 | -24.80 | -26.65 | -28.67 | -27.01 | -27.23 | | -27.45 | -28.26 |

| Sample | $n-C_7$ | MCHex | Tol | $n-C_8$ | ECHex | EtB | $m/p-X$ | $o-X$ | $n-C_9$ | $n-C_{10}$ | $n-C_{11}$ | $n-C_{12}$ |
|---------|---------|--------|--------|---------|--------|--------|---------|--------|---------|------------|------------|------------|
| G002952 | -28.10 | -27.55 | -28.33 | -28.22 | -27.90 | -28.06 | | -28.31 | -28.51 | -28.57 | -28.76 | -29.42 |
| G002953 | -30.58 | -28.26 | -34.82 | -29.50 | -28.98 | -26.16 | -31.59 | | -30.20 | -30.24 | -30.43 | -30.24 |
| G002954 | -27.39 | -25.82 | | -27.57 | -26.77 | | | | -27.69 | -27.68 | -27.80 | -28.04 |
| G002956 | -28.81 | -26.86 | | -30.26 | -29.00 | | | | -27.77 | -27.71 | -27.44 | -27.88 |
| G002959 | -25.63 | -25.48 | | -26.27 | -26.04 | -25.82 | -26.74 | -25.85 | -27.07 | -26.97 | -27.72 | -28.66 |
| G002960 | -27.36 | -25.11 | -25.57 | -27.28 | -27.49 | -25.72 | | -28.29 | -27.23 | -27.18 | -26.82 | -27.38 |
| G002961 | -28.21 | -27.08 | -27.35 | -27.77 | -30.21 | | | | -27.69 | -27.53 | -27.55 | -27.77 |
| G002963 | -28.43 | -29.48 | -37.60 | -28.63 | -31.22 | -32.54 | | -33.52 | -29.02 | -28.65 | -28.65 | -28.92 |
| G002964 | -27.79 | -27.13 | | -27.48 | -28.20 | | | | -27.74 | -27.53 | -27.61 | -27.96 |
| G002965 | -29.22 | -28.05 | -31.43 | -28.70 | -28.51 | -28.21 | | -30.54 | -28.98 | -28.60 | -28.85 | -29.22 |
| G002966 | -29.28 | -28.00 | -28.74 | -28.60 | -28.79 | -25.15 | | -28.84 | -28.84 | -28.55 | -28.62 | -28.89 |
| G002968 | | | | | | | | | | | | |
| G002969 | -29.33 | -28.28 | | -28.58 | -29.01 | -28.48 | -31.40 | | -28.80 | -28.63 | -28.66 | -28.69 |
| G002973 | -29.40 | -27.19 | -29.20 | -28.35 | -28.21 | -26.42 | | | -28.98 | -28.68 | -29.23 | -29.53 |
| G002974 | -27.20 | -26.17 | -26.82 | -27.22 | -26.96 | -25.02 | -26.78 | -26.69 | -27.31 | -27.09 | -27.18 | -27.19 |
| G002975 | -28.34 | -28.01 | | -28.01 | -28.21 | -27.40 | | -29.57 | -28.43 | -27.63 | -27.56 | -27.70 |
| G002976 | -30.16 | -28.63 | -34.94 | -29.48 | -29.55 | -28.75 | | | -29.49 | -28.98 | -28.96 | -29.55 |
| G002980 | -27.99 | -27.71 | -31.32 | -28.05 | -28.86 | | | -32.13 | -28.52 | -28.38 | -28.67 | -29.14 |
| G002981 | | | | | | | | | -28.63 | -28.05 | -27.74 | -27.64 |
| G002982 | -28.88 | -29.32 | | -28.74 | -28.49 | | | -30.25 | -28.71 | -28.15 | -28.54 | -28.71 |
| G002988 | -28.02 | -27.51 | | -26.24 | -28.37 | | -29.47 | | | -27.07 | -27.40 | -28.38 |
| G002993 | -29.60 | -28.77 | | -28.88 | -29.71 | | | | -29.07 | -30.05 | -30.08 | -28.60 |
| G002995 | -22.26 | -26.18 | | -25.73 | | | | | | | | |
| G002997 | -28.76 | -27.79 | -27.80 | -28.92 | -29.03 | -24.73 | -29.50 | | -29.09 | -28.65 | -28.73 | -28.88 |
| G003005 | -32.69 | -28.41 | | -29.97 | -29.41 | -28.24 | | | -29.22 | -28.58 | -28.18 | -28.03 |
| G003006 | -27.53 | -25.93 | -25.88 | -27.23 | -27.52 | -24.03 | -27.33 | -27.22 | -27.26 | -27.07 | -26.79 | -27.24 |
| G003009 | -29.63 | -27.43 | | -28.54 | -29.16 | | -29.98 | | | -29.20 | -29.41 | -29.18 |
| G003011 | -28.61 | -25.77 | -27.40 | -28.11 | -28.48 | -25.90 | -28.85 | | -28.63 | -27.95 | -28.03 | -28.33 |
| G003015 | -27.96 | | | -28.60 | -28.20 | | -28.35 | | -27.67 | -27.59 | -27.47 | -27.15 |
| G003017 | -25.92 | -28.61 | | -26.13 | -29.37 | | | | -26.96 | -27.71 | -28.25 | -28.26 |

| Sample | $n\text{-C}_{13}$ | $n\text{-C}_{14}$ | $n\text{-C}_{15}$ | $n\text{-C}_{16}$ | $n\text{-C}_{17}$ | Pr | $n\text{-C}_{18}$ | Ph | $n\text{-C}_{19}$ | $n\text{-C}_{20}$ | $n\text{-C}_{21}$ | $n\text{-C}_{22}$ |
|---------|-------------------|-------------------|-------------------|-------------------|-------------------|--------|-------------------|--------|-------------------|-------------------|-------------------|-------------------|
| G002952 | -28.78 | -29.40 | -29.26 | -29.50 | -29.34 | -29.40 | -29.54 | -29.39 | -29.75 | -30.23 | -30.76 | |
| G002953 | -30.29 | -30.59 | -30.75 | -31.93 | -31.97 | -31.07 | -31.93 | -30.96 | -30.93 | -30.90 | -30.21 | -30.28 |
| G002954 | -27.46 | -28.30 | -28.18 | -28.47 | -27.83 | -27.58 | -27.82 | -28.01 | -27.76 | -29.16 | | |
| G002956 | -27.48 | -27.58 | -28.40 | -29.16 | -29.67 | -29.71 | -30.46 | -30.64 | -30.74 | -31.36 | -33.67 | -33.09 |
| G002959 | -28.73 | -29.08 | -29.20 | -29.15 | -29.13 | -28.67 | -29.45 | -28.60 | -28.03 | -29.19 | -29.18 | -27.35 |
| G002960 | -27.57 | -27.61 | -27.53 | -32.42 | -31.52 | -29.99 | -31.66 | -30.50 | -31.08 | -31.42 | -32.45 | -31.80 |
| G002961 | -27.81 | -28.14 | -27.86 | -29.22 | -27.51 | -27.81 | -27.27 | -27.48 | -27.88 | -27.30 | -27.76 | -28.74 |
| G002963 | -28.78 | -30.26 | -29.20 | -29.97 | -30.34 | -29.67 | -28.59 | -29.63 | -29.59 | -29.07 | -29.87 | -29.70 |
| G002964 | -27.77 | -28.41 | -28.52 | -28.32 | -28.01 | -27.84 | -28.05 | -28.41 | -28.28 | -27.95 | -28.32 | -28.25 |
| G002965 | -29.06 | -29.96 | -29.20 | -30.01 | -29.32 | -28.27 | -29.22 | -29.98 | -30.22 | -29.85 | -30.65 | -29.50 |
| G002966 | -29.32 | -28.57 | -28.70 | -29.05 | -28.01 | -29.67 | -29.77 | -30.38 | -29.38 | -29.94 | -28.98 | -30.62 |
| G002968 | | | | | | | | | | | | |
| G002969 | -28.58 | -29.01 | -29.33 | -29.40 | -29.73 | -29.17 | -29.48 | -29.13 | -29.03 | -29.16 | -29.55 | -29.16 |
| G002973 | -29.20 | -29.57 | -30.01 | -29.68 | -30.49 | -31.19 | -30.06 | -30.56 | -29.57 | -29.66 | -29.97 | -29.87 |
| G002974 | -26.99 | -27.37 | -28.06 | -28.67 | -29.87 | -28.29 | -27.56 | -28.52 | -28.13 | -28.96 | -28.91 | -28.66 |
| G002975 | -27.66 | -27.85 | -28.16 | -28.16 | -30.57 | -27.95 | -29.01 | -27.53 | -28.47 | -29.30 | -29.33 | -29.17 |
| G002976 | -29.04 | -31.16 | -28.64 | -28.98 | -30.76 | -26.34 | -29.50 | -29.51 | -28.81 | -28.85 | -28.85 | -29.23 |
| G002980 | -29.31 | -30.09 | -30.31 | -30.26 | -29.97 | -29.01 | -30.10 | -30.88 | -29.59 | -30.27 | -29.02 | -30.71 |
| G002981 | -27.58 | -28.02 | -28.02 | -28.46 | -28.77 | -29.85 | -28.56 | -29.51 | -28.84 | -28.66 | -29.29 | -28.93 |
| G002982 | -28.67 | -29.27 | -28.88 | -29.18 | -28.43 | -27.83 | -29.27 | -29.23 | -29.63 | -28.56 | -27.90 | -29.22 |
| G002988 | -28.68 | -28.85 | -28.67 | -28.76 | -28.76 | -30.08 | -29.60 | -29.81 | -30.02 | -30.29 | -30.59 | -29.62 |
| G002993 | -28.23 | -29.64 | -28.23 | -28.49 | -27.90 | -28.57 | -29.69 | -28.49 | -28.63 | -28.33 | -28.62 | -28.29 |
| G002995 | -26.97 | -29.37 | -29.08 | -29.68 | -30.21 | -31.29 | -29.53 | -31.13 | -29.49 | -29.76 | -29.81 | -29.93 |
| G002997 | -28.82 | -28.80 | -29.11 | -29.39 | -30.45 | -30.54 | -31.23 | -30.74 | -29.81 | -28.86 | | |
| G003005 | -28.34 | -29.02 | -27.81 | -28.31 | -28.67 | -30.06 | -28.77 | -29.82 | -28.39 | -28.87 | -29.55 | -30.18 |
| G003006 | -27.19 | -27.48 | -27.01 | -27.58 | -28.61 | -26.61 | -28.65 | -29.47 | -28.62 | -28.72 | -29.06 | -29.21 |
| G003009 | -28.83 | -28.81 | -28.53 | -28.95 | -30.05 | -30.72 | -29.37 | -30.40 | -29.74 | -29.87 | -29.81 | -29.57 |
| G003011 | -28.52 | -28.00 | -28.07 | -28.60 | -27.60 | -28.90 | -29.07 | -30.48 | -29.31 | -29.04 | -29.48 | |
| G003015 | -27.22 | -27.36 | -27.39 | -27.23 | -26.31 | -30.95 | -28.15 | -29.02 | -27.89 | -27.50 | -27.51 | -27.68 |
| G003017 | -29.43 | -29.26 | -28.90 | -30.37 | -29.38 | -28.37 | -28.80 | -29.68 | -30.44 | -29.56 | -30.51 | -30.45 |

| Sample | $n-C_{23}$ | $n-C_{24}$ | $n-C_{25}$ | $n-C_{26}$ | $n-C_{27}$ | $n-C_{28}$ | $n-C_{29}$ | $n-C_{30}$ | $n-C_{31}$ |
|---------|------------|------------|------------|------------|------------|------------|------------|------------|------------|
| G002952 | -30.29 | -30.04 | -30.14 | -28.86 | -29.64 | -29.73 | -29.41 | -29.66 | -28.88 |
| G002953 | -32.41 | -31.51 | -30.35 | -29.63 | -29.75 | -29.04 | -29.56 | -32.29 | -33.35 |
| G002954 | -29.49 | -29.44 | -29.30 | -28.58 | -26.44 | -29.53 | -29.23 | -28.80 | -30.79 |
| G002956 | -28.81 | -28.39 | -25.94 | -29.09 | -31.92 | -28.07 | -25.19 | -30.82 | -31.19 |
| G002960 | -28.81 | -27.99 | -29.06 | -27.58 | -28.36 | -27.87 | -26.91 | -30.45 | -30.64 |
| G002963 | -29.48 | -29.27 | -29.30 | -28.81 | -29.12 | -28.84 | -28.98 | -29.99 | -29.28 |
| G002964 | -28.38 | -28.18 | -28.40 | -27.50 | -28.04 | -27.66 | -27.89 | -28.06 | -28.30 |
| G002965 | -29.99 | -28.84 | -28.83 | -27.74 | -28.89 | -27.82 | -29.31 | -30.07 | -30.60 |
| G002966 | -30.97 | -30.11 | -29.60 | -30.59 | -29.99 | -29.91 | -28.77 | -30.32 | -30.63 |
| G002968 | -28.62 | -29.08 | -28.59 | -29.87 | -29.09 | -29.35 | -29.48 | -29.93 | -29.29 |
| G002969 | -29.05 | -29.26 | -29.49 | -28.68 | -29.36 | -29.33 | -29.48 | -30.76 | -27.59 |
| G002973 | -29.20 | -28.51 | -28.19 | -28.52 | -27.75 | -28.53 | -28.79 | -25.90 | -28.27 |
| G002974 | -28.57 | -27.97 | -27.63 | -27.26 | -27.64 | -27.59 | -27.18 | -27.71 | -29.46 |
| G002975 | -28.27 | -28.50 | -26.90 | -28.10 | -28.01 | -28.21 | -29.27 | -30.62 | -30.99 |
| G002976 | -27.74 | -29.25 | -27.61 | -29.30 | -30.78 | | | | |
| G002980 | -27.96 | -29.07 | -28.63 | -27.72 | -29.78 | -29.51 | | | |
| G002981 | -28.58 | -31.12 | -29.75 | -30.32 | -30.53 | | | | |
| G002982 | -30.91 | -31.50 | -32.15 | -29.69 | -32.38 | -31.15 | -31.39 | | |
| G002988 | -28.69 | -29.55 | | | | | | | |
| G002993 | -29.15 | -28.83 | -29.49 | -29.34 | -29.24 | -29.11 | -29.58 | | |
| G002995 | | | | | | | | | |
| G002997 | -29.23 | -28.94 | -28.92 | -29.17 | -31.58 | | | | |
| G003005 | -29.27 | | | | | | | | |
| G003006 | -29.52 | -29.05 | -28.53 | -28.63 | | | | | |
| G003009 | | | | | | | | | |
| G003011 | | | | | | | | | |
| G003015 | | | | | | | | | |
| G003017 | -30.67 | -28.55 | -32.39 | -29.35 | -31.33 | -30.53 | -31.85 | -30.25 | -31.08 |

Table B.2: $\delta^{13}\text{C}$ values [‰] for $n-C_3$ to $n-C_{31}$ in the studied crude oils. G002968 is contaminated with water, hence, no data can be provided.

[illegible]

| Sample | $n-C_7$ | MCHex | Tol | $n-C_8$ | ECHex | EtB | $m/p-X$ | $o-X$ | $n-C_9$ | $n-C_{10}$ | $n-C_{11}$ | $n-C_{12}$ |
|---------|---------|---------|---------|---------|---------|--------|---------|---------|---------|------------|------------|------------|
| G002952 | -117.20 | -84.90 | -104.49 | -113.98 | -97.05 | -32.12 | -87.92 | -91.32 | -110.63 | -106.72 | -111.64 | -101.49 |
| G002953 | -182.15 | -115.03 | -113.34 | -166.25 | -104.19 | | -122.44 | | -161.84 | -157.74 | -158.32 | -156.45 |
| G002954 | -112.16 | -78.28 | -103.24 | -103.16 | -98.69 | -42.24 | -92.48 | -91.69 | -94.43 | -107.76 | -88.90 | -98.50 |
| G002956 | -147.49 | -109.81 | -107.83 | -132.84 | -108.18 | -60.76 | -118.40 | -110.60 | -122.16 | -122.63 | -122.77 | -117.76 |
| G002959 | -99.70 | -68.46 | | -107.14 | -73.53 | | -30.95 | | -89.29 | -90.55 | -94.03 | -91.40 |
| G002960 | -114.34 | -102.83 | -108.46 | -112.56 | -97.79 | -64.34 | -93.62 | -104.68 | -102.86 | -103.52 | -100.41 | -95.83 |
| G002961 | -123.53 | -84.65 | -95.22 | -114.68 | -86.16 | | -87.22 | | -102.24 | -93.55 | -108.33 | -101.78 |
| G002963 | -120.46 | -95.58 | -110.21 | -124.97 | -102.36 | | -113.60 | -93.78 | -115.23 | -107.37 | -111.81 | -102.02 |
| G002964 | -110.84 | -84.71 | | -99.19 | -91.36 | -56.17 | -87.16 | | -100.68 | -96.45 | -95.29 | -90.64 |
| G002965 | -138.18 | -96.79 | -104.84 | -125.07 | -92.92 | | -113.44 | -89.14 | -126.12 | -111.42 | -118.75 | -118.84 |
| G002966 | -122.93 | -88.14 | -97.12 | -112.34 | -90.00 | -52.79 | -97.90 | | -107.88 | -106.25 | -108.41 | -105.03 |
| G002968 | | | | | | | | | | | | |
| G002969 | -135.85 | -106.48 | -99.15 | -128.47 | -94.54 | | | | -122.79 | -115.16 | -121.81 | -120.05 |
| G002973 | -168.69 | -110.95 | | -147.05 | -90.44 | | -113.33 | | -145.57 | -143.75 | -145.84 | -146.69 |
| G002974 | -106.67 | -89.61 | -94.34 | -104.43 | -88.92 | -62.73 | -91.78 | | -105.06 | -86.15 | -92.25 | -99.45 |
| G002975 | -131.14 | -99.87 | -89.91 | -124.90 | -96.68 | -49.84 | -97.43 | | -124.29 | -113.43 | -111.99 | -114.00 |
| G002976 | -133.03 | -100.09 | -122.53 | -123.66 | -106.90 | -84.06 | -116.38 | | -113.31 | -108.41 | -106.17 | -99.84 |
| G002980 | -105.65 | -73.46 | -87.96 | -99.52 | -76.84 | | | | -98.74 | -94.65 | -95.01 | -96.24 |
| G002981 | | | | | | | | | -99.70 | -99.30 | -101.24 | -104.41 |
| G002982 | -114.78 | -81.56 | -95.93 | -108.95 | -64.09 | | -83.71 | -79.49 | -101.48 | -102.30 | -98.60 | -87.99 |
| G002988 | -72.83 | -88.20 | | | -112.24 | | | | -73.95 | -93.99 | -91.67 | -78.28 |
| G002993 | -135.20 | -103.10 | | | -117.41 | | | | | -125.10 | -123.32 | -131.34 |
| G002995 | -133.05 | -98.17 | -118.89 | -131.52 | -110.40 | -76.57 | -102.68 | | -117.50 | -111.39 | -119.25 | -103.12 |
| G002997 | -74.76 | -76.98 | | -100.48 | -111.80 | | -115.66 | | | | | |
| G003005 | -120.71 | -104.68 | -102.24 | -120.97 | -95.76 | | -111.66 | | | | | |
| G003006 | | | | | | | | | | | | |
| G003009 | -120.43 | -90.38 | -84.22 | -114.47 | -91.94 | -59.43 | -86.06 | | -121.46 | -112.95 | -123.27 | -115.03 |
| G003011 | -159.83 | -97.25 | -110.99 | | -107.82 | -58.86 | -125.34 | | -109.50 | -97.86 | -103.14 | -105.60 |
| G003015 | -135.06 | -105.59 | -103.25 | -127.84 | -102.23 | | | | -109.51 | -101.63 | -100.97 | -96.01 |
| G003017 | -120.67 | -108.44 | | -126.62 | -106.70 | | | | -117.85 | -116.43 | -125.98 | -115.77 |
| | | | | | | | | | -121.16 | -111.98 | -115.16 | -108.63 |

| Sample | $n\text{-}C_{13}$ | $n\text{-}C_{14}$ | $n\text{-}C_{15}$ | $n\text{-}C_{16}$ | $n\text{-}C_{17}$ | Pr | $n\text{-}C_{18}$ | Ph | $n\text{-}C_{19}$ | $n\text{-}C_{20}$ | $n\text{-}C_{21}$ | $n\text{-}C_{22}$ |
|---------|-------------------|-------------------|-------------------|-------------------|-------------------|---------|-------------------|---------|-------------------|-------------------|-------------------|-------------------|
| G002952 | -99.48 | -99.09 | -112.55 | -99.68 | -97.75 | -116.47 | -95.16 | -120.75 | -97.36 | -96.63 | -99.06 | -96.90 |
| G002953 | -153.57 | -145.67 | -144.17 | -146.22 | -143.34 | -166.96 | -142.94 | -159.13 | -139.81 | -135.90 | -140.42 | -138.83 |
| G002954 | -89.66 | -84.60 | -92.81 | -87.35 | -85.82 | -90.56 | -86.74 | -120.01 | -86.75 | -85.80 | -90.33 | -90.88 |
| G002956 | -113.78 | -114.84 | -118.75 | -114.39 | -119.58 | -151.17 | -113.06 | -158.00 | -115.22 | -112.68 | -119.11 | -111.92 |
| G002959 | -87.66 | -84.03 | -92.98 | -96.67 | -89.54 | -94.61 | -90.14 | -102.64 | -100.76 | -92.28 | -101.53 | -88.33 |
| G002960 | -92.33 | -91.10 | -92.08 | -92.94 | -80.78 | -117.11 | -87.45 | -106.18 | -90.02 | -85.90 | -83.38 | -79.94 |
| G002961 | -91.75 | -92.17 | -96.17 | -96.72 | -98.28 | -121.75 | -99.41 | -120.40 | -91.36 | -89.40 | -89.62 | -81.04 |
| G002963 | -101.31 | -99.74 | -106.52 | -102.21 | -99.45 | -123.14 | -97.73 | -123.25 | -100.01 | -98.53 | -97.76 | -96.07 |
| G002964 | -91.55 | -84.54 | -89.69 | -91.31 | -87.76 | -123.37 | -86.95 | -123.44 | -91.91 | -87.52 | -92.25 | -92.33 |
| G002965 | -112.31 | -100.36 | -111.45 | -110.73 | -106.67 | -132.05 | -101.62 | -126.84 | -106.21 | -101.50 | -106.46 | -99.27 |
| G002966 | -99.66 | -87.15 | -96.72 | -98.29 | -90.38 | -112.89 | -88.02 | -113.83 | -87.94 | -86.54 | -89.96 | -85.37 |
| G002968 | | | | | | | | | | | | |
| G002969 | -114.32 | -103.02 | -116.71 | -105.78 | -104.82 | -139.09 | -103.24 | -132.89 | -103.71 | -102.20 | -108.76 | -102.90 |
| G002973 | -148.64 | -136.84 | -139.28 | -137.84 | -135.73 | -168.16 | -130.19 | -162.29 | -131.42 | -129.42 | -135.65 | -127.64 |
| G002974 | -94.75 | -86.64 | -93.02 | -96.20 | -88.44 | -119.52 | -88.90 | -118.63 | -90.44 | -82.57 | -92.32 | -86.90 |
| G002975 | -112.39 | -100.33 | -108.32 | -107.93 | -102.36 | -125.85 | -101.41 | -114.49 | -102.15 | -97.01 | -102.53 | -94.41 |
| G002976 | -94.20 | -95.24 | -99.28 | -102.66 | -101.82 | -133.11 | -101.50 | -128.50 | -105.16 | -103.66 | -104.07 | -100.74 |
| G002980 | -93.07 | -90.46 | -101.95 | -91.23 | -88.46 | -116.74 | -87.62 | -127.70 | -90.87 | -79.66 | -87.92 | -75.52 |
| G002981 | -103.28 | -99.72 | -99.88 | -98.13 | -94.81 | -121.62 | -91.73 | -115.57 | -93.93 | -93.98 | -97.46 | -95.58 |
| G002982 | -90.65 | -88.16 | -98.20 | -90.26 | -89.68 | -105.23 | -85.39 | -112.31 | -91.39 | -93.53 | -95.43 | -88.42 |
| G002988 | -92.37 | -96.57 | -101.64 | -114.25 | -111.55 | -118.55 | -111.29 | -113.92 | -110.17 | -116.38 | -116.41 | -112.24 |
| G002993 | -136.93 | -131.80 | -132.35 | -136.40 | -130.69 | -153.35 | -122.68 | -161.00 | -138.27 | -132.31 | -131.89 | -127.89 |
| G002995 | -108.33 | -102.57 | -107.27 | -105.53 | -103.79 | -135.10 | -97.67 | -129.62 | -102.03 | -100.14 | -99.50 | -94.18 |
| G002997 | -128.76 | -127.72 | -126.02 | -122.65 | -118.24 | -146.15 | -115.09 | -143.06 | -119.77 | -114.16 | -115.34 | -111.32 |
| G003005 | -114.62 | -104.40 | -112.12 | -110.05 | -106.00 | -128.86 | -103.16 | -128.74 | -107.41 | -104.60 | -105.94 | -104.05 |
| G003006 | -102.51 | -96.45 | -97.95 | -99.18 | -92.51 | -131.23 | -87.71 | -127.99 | -88.90 | -82.67 | -91.32 | -81.65 |
| G003009 | -90.66 | -83.75 | -88.68 | -86.54 | -83.52 | -107.67 | -80.52 | -104.83 | -84.30 | -82.51 | -83.36 | -80.22 |
| G003011 | -139.08 | -126.10 | -119.76 | -117.18 | -113.30 | -137.00 | -117.68 | -157.74 | -123.95 | -120.04 | -123.99 | -121.20 |
| G003015 | -118.72 | -108.99 | -110.61 | -113.65 | -109.05 | -137.89 | -104.52 | -127.56 | -106.04 | -103.02 | -107.41 | -105.26 |
| G003017 | -103.68 | -99.86 | -98.26 | -94.57 | -90.79 | -129.73 | -89.24 | -120.70 | -89.83 | -91.07 | -91.14 | -87.73 |

| Sample | $n-C_{23}$ | $n-C_{24}$ | $n-C_{25}$ | $n-C_{26}$ | $n-C_{27}$ | $n-C_{28}$ | $n-C_{29}$ | $n-C_{30}$ | $n-C_{31}$ |
|---------|------------|------------|------------|------------|------------|------------|------------|------------|------------|
| G002952 | -91.75 | -78.06 | -87.55 | -126.74 | -129.53 | -137.22 | -122.64 | -117.48 | -136.89 |
| G002953 | -124.81 | -127.91 | -127.62 | -77.80 | -99.95 | -62.40 | | | |
| G002954 | -93.55 | -96.50 | -88.77 | -99.76 | -107.11 | -102.50 | -101.96 | -99.69 | -119.31 |
| G002956 | -117.18 | -113.64 | -106.99 | -80.23 | -96.60 | -90.84 | -79.01 | -76.74 | |
| G002959 | -88.38 | -84.08 | -85.11 | -66.23 | -74.34 | -75.57 | -69.41 | -68.02 | -82.75 |
| G002960 | -80.39 | -84.50 | -72.52 | -75.38 | -78.07 | -82.04 | -82.06 | -69.70 | -86.78 |
| G002961 | -91.76 | -76.87 | -80.15 | -79.04 | -72.44 | -86.05 | -89.21 | -82.12 | -93.75 |
| G002963 | -90.16 | -86.16 | -80.28 | -100.17 | -95.42 | -109.81 | -76.78 | -82.53 | -72.27 |
| G002964 | -84.23 | -93.25 | -92.36 | -96.94 | -93.98 | -99.54 | -79.29 | -90.59 | -95.55 |
| G002965 | -97.85 | -96.89 | -94.74 | -80.21 | -88.69 | -80.27 | -73.97 | -84.51 | -59.14 |
| G002966 | -89.22 | -83.13 | -80.12 | | | | | | |
| G002968 | | | | | | | | | |
| G002969 | -96.92 | -91.41 | -92.92 | -90.59 | -106.32 | -88.39 | -83.95 | -88.47 | -98.01 |
| G002973 | -131.27 | -119.70 | -117.60 | -119.13 | -120.03 | -121.28 | -114.71 | -122.68 | -137.84 |
| G002974 | -102.84 | -82.42 | -81.18 | -80.48 | -73.00 | -95.72 | -65.13 | -87.65 | -72.05 |
| G002975 | -101.07 | -85.32 | -91.13 | -85.46 | -88.92 | -84.37 | -86.63 | -85.12 | -93.69 |
| G002976 | -105.58 | -108.32 | -93.43 | -89.31 | -66.86 | -106.19 | -76.89 | | |
| G002980 | -72.70 | -77.70 | -75.40 | | | | | | |
| G002981 | -95.76 | | | | | | | | |
| G002982 | -88.74 | -89.14 | -97.48 | -78.96 | -108.42 | | | | |
| G002988 | -111.51 | -109.56 | -107.15 | -109.36 | -111.90 | -114.32 | -103.42 | -86.20 | -106.62 |
| G002993 | -135.22 | -127.86 | -128.94 | -124.23 | -131.66 | -148.54 | -134.37 | -126.01 | -155.70 |
| G002995 | -96.58 | -103.60 | -94.87 | -92.50 | -56.61 | -87.21 | -91.89 | -80.51 | -106.00 |
| G002997 | -113.79 | -111.81 | -110.50 | -115.39 | -107.03 | -120.85 | -119.48 | -119.93 | -134.13 |
| G003005 | -105.84 | -94.44 | -101.39 | -97.60 | -88.22 | -99.26 | -71.57 | -103.96 | -102.12 |
| G003006 | -85.50 | -84.77 | -90.87 | | | | | | |
| G003009 | -80.56 | -77.91 | -78.65 | -70.51 | -69.07 | -67.04 | -63.41 | -67.59 | -63.48 |
| G003011 | -119.48 | -118.73 | -118.03 | -119.49 | -124.85 | -132.32 | -121.83 | -119.53 | -130.49 |
| G003015 | -103.12 | -100.58 | -97.61 | -94.89 | -97.82 | -95.92 | -93.28 | -99.50 | -99.11 |
| G003017 | -87.22 | -83.95 | -76.42 | -75.03 | -81.73 | -71.09 | -78.19 | -87.67 | -92.18 |

Table B.3: δ D values [‰] for $n-C_3$ to $n-C_{31}$ in the studied crude oils. G002968 is contaminated with water, hence, no data can be provided.

Appendix C

Oil Families Geochemistry

| Sample | Family | Reservoir | CPI | % C_{27} St | % C_{28} St | % C_{29} St | % C_{27} dia | % C_{28} dia | % C_{29} dia | Dia/Reg |
|---------|--------|-------------|------|---------------|---------------|---------------|----------------|----------------|----------------|---------|
| G002975 | 2A | ICD | 0.93 | 33.75 | 29.77 | 36.48 | 39.08 | 32.18 | 28.74 | 0.77 |
| G002968 | | L.Doubay | 1.01 | 35.47 | 33.59 | 30.93 | 40.38 | 36.74 | 22.88 | 0.60 |
| G002995 | | R'mah | 0.91 | 35.19 | 33.57 | 31.24 | 41.43 | 35.20 | 23.36 | 0.38 |
| G002973 | | Mulussa F | 1.01 | 38.37 | 31.61 | 30.03 | 43.44 | 34.54 | 22.02 | 0.30 |
| G003006 | | Kometan | 0.89 | 38.25 | 32.27 | 29.48 | 42.99 | 35.14 | 21.87 | 0.15 |
| G003015 | | Rutbah | 1.00 | 34.84 | 33.38 | 31.78 | 38.09 | 38.78 | 23.12 | 0.57 |
| G002956 | | Rutbah | 0.94 | 34.14 | 34.63 | 31.23 | 38.82 | 37.81 | 23.37 | 0.62 |
| G002965 | | L.Rutbah | 0.98 | 34.73 | 34.51 | 30.76 | 38.86 | 38.44 | 22.70 | 1.04 |
| G003005 | | U.Shiranish | 0.96 | 33.76 | 34.66 | 31.58 | 38.47 | 39.01 | 22.52 | 0.54 |
| G002997 | | Jeribe | 1.03 | 32.60 | 34.35 | 33.05 | 37.58 | 39.54 | 22.88 | 0.38 |
| G002953 | | Rutbah | 0.98 | 32.62 | 35.94 | 31.44 | 34.86 | 41.41 | 23.74 | 0.77 |
| G002993 | | L.Fars | 1.03 | 32.73 | 35.25 | 32.02 | 35.64 | 40.94 | 23.42 | 0.41 |
| G002969 | | Mulussa F | 0.95 | 33.21 | 35.33 | 31.46 | 37.49 | 40.27 | 22.23 | 0.69 |
| G003011 | | Dhiban | 1.00 | 32.95 | 35.01 | 32.04 | 38.26 | 39.16 | 22.58 | 0.46 |
| G002963 | 2B | L.Rutbah | 0.93 | 36.52 | 33.20 | 30.28 | 44.65 | 33.96 | 21.40 | 0.41 |
| G002960 | | Erek | 0.93 | 37.92 | 31.03 | 31.05 | 46.55 | 30.50 | 22.96 | 0.90 |
| G002966 | | L.Rutbah | 1.00 | 38.47 | 31.28 | 30.25 | 45.54 | 32.33 | 22.12 | 1.14 |
| G002964 | | PJS | 0.91 | 38.57 | 31.62 | 29.81 | 44.74 | 33.50 | 21.76 | 0.37 |
| G002974 | | PJS | 0.96 | 37.64 | 32.38 | 29.97 | 45.47 | 33.15 | 21.38 | 1.40 |
| G002961 | | Derro | 0.91 | 40.61 | 29.83 | 29.56 | 47.48 | 32.45 | 20.07 | 0.33 |
| G002980 | | Rutbah | 0.92 | 40.90 | 32.12 | 26.98 | 45.05 | 34.93 | 20.02 | 0.70 |
| G002952 | | Lower Fars | 0.91 | 45.97 | 27.72 | 26.31 | 48.07 | 27.53 | 24.39 | 0.77 |
| G002976 | | U.Shiranish | 0.94 | 44.74 | 28.50 | 26.77 | 49.82 | 26.57 | 23.61 | 0.78 |
| G002981 | | Khabour | 0.82 | 42.36 | 30.88 | 26.77 | 47.68 | 32.48 | 19.84 | 0.71 |
| G003009 | | Rutbah | 0.95 | 40.18 | 28.17 | 31.65 | 48.93 | 27.81 | 23.26 | 0.62 |
| G003017 | | Doubay | 0.91 | 38.51 | 30.15 | 31.33 | 44.69 | 30.86 | 24.45 | 0.37 |
| G002959 | 1 | PJS | 1.01 | 44.00 | 0.00 | 56.00 | 35.96 | 27.38 | 36.66 | 2.18 |
| G002954 | | PJS | 0.92 | 33.47 | 19.66 | 46.88 | 30.58 | 21.08 | 48.34 | 2.51 |
| G002982 | | U.Doubay | 0.96 | 35.52 | 26.37 | 38.11 | 34.86 | 27.02 | 38.12 | 1.17 |
| G002988 | | Jeribe | 1.01 | 31.03 | 29.13 | 39.83 | 36.78 | 27.47 | 35.75 | 0.60 |

Table C.1: Source-related parameters used to classify the oil samples into main genetic oil families shown Fig.5.15. $CPI = ([n-C_{25}H_{52}] + [n-C_{27}H_{56}] + [n-C_{29}H_{60}] + [n-C_{31}H_{64}]) / (0.5[n-C_{24}H_{50}] + [n-C_{26}H_{54}] + [n-C_{28}H_{58}] + [n-C_{30}H_{62}] + 0.5[n-C_{32}H_{66}])$, % C_{27} St, % C_{28} St, and % C_{29} St are the relative abundance of regular steranes, % C_{27} dia, % C_{28} dia, and % C_{29} dia are the relative abundance of rearranged steranes, Dia/Reg = $\beta\alpha$ diasterane / $(\alpha\alpha + \beta\beta)$ regular sterane for $C_{27}-C_{29}$.

| Sample | Family | Reservoir | C_{28}/C_{29} | C_{22}/C_{21} | TT | C_{24}/C_{23} | TT | C_{26}/C_{25} | TT | HHI | GI | ST/H | 24/(24+27) |
|---------|--------|-------------|-----------------|-----------------|----|-----------------|----|-----------------|----|------|------|------|------------|
| G002975 | 2A | ICD | 0.82 | 0.30 | | 1.03 | | 1.18 | | 0.09 | 0.04 | 0.37 | 0.44 |
| G002968 | | L.Doubayat | 1.09 | 0.43 | | 0.70 | | 1.37 | | 0.08 | 0.08 | 1.70 | 0.45 |
| G002995 | | R'mah | 1.07 | 0.48 | | 0.81 | | 1.26 | | 0.12 | 0.13 | 2.44 | 0.41 |
| G002973 | | Mulussa F | 1.05 | 0.32 | | 0.86 | | 1.28 | | 0.08 | 0.07 | 0.94 | 0.41 |
| G003006 | | Kometan | 1.09 | 0.49 | | 0.73 | | 1.16 | | 0.13 | 0.11 | 1.46 | 0.44 |
| G003015 | | Rutbah | 1.05 | 0.48 | | 0.71 | | 1.22 | | 0.10 | 0.14 | 1.82 | 0.42 |
| G002956 | | Rutbah | 1.11 | 0.56 | | 0.65 | | 1.49 | | 0.11 | 0.06 | 1.16 | 0.41 |
| G002965 | | L.Rutbah | 1.12 | 0.35 | | 0.96 | | 1.08 | | 0.13 | 0.13 | 2.84 | 0.45 |
| G003005 | | U.Shiranish | 1.10 | 0.45 | | 0.63 | | 1.59 | | 0.08 | 0.08 | 2.03 | 0.39 |
| G002997 | | Jeribe | 1.04 | 0.32 | | 0.74 | | 1.56 | | 0.07 | 0.07 | 1.62 | 0.43 |
| G002953 | | Rutbah | 1.14 | 0.29 | | 0.74 | | 1.33 | | 0.07 | 0.05 | 1.89 | 0.40 |
| G002993 | | L.Fars | 1.10 | 0.39 | | 0.76 | | 1.59 | | 0.07 | 0.07 | 1.56 | 0.43 |
| G002969 | | Mulussa F | 1.12 | 0.43 | | 0.87 | | 1.14 | | 0.08 | 0.05 | 1.74 | 0.39 |
| G003011 | | Dhiban | 1.09 | 0.34 | | 0.84 | | 1.56 | | 0.07 | 0.05 | 1.29 | 0.39 |
| G002963 | 2B | L.Rutbah | 1.10 | 0.46 | | 0.71 | | 1.22 | | 0.13 | 0.24 | 1.64 | 0.45 |
| G002960 | | Erek | 1.00 | 0.58 | | 0.67 | | 1.45 | | 0.16 | 0.11 | 0.69 | 0.40 |
| G002966 | | L.Rutbah | 1.03 | 0.42 | | 0.96 | | 1.26 | | 0.15 | 0.12 | 1.25 | 0.38 |
| G002964 | | PJS | 1.06 | 0.50 | | 0.94 | | 1.36 | | 0.13 | 0.14 | 1.26 | 0.46 |
| G002974 | | PJS | 1.08 | 0.54 | | 0.60 | | 1.48 | | 0.14 | 0.14 | 1.36 | 0.45 |
| G002961 | | Derro | 1.01 | 0.53 | | 0.66 | | 1.22 | | 0.10 | 0.11 | 0.95 | 0.40 |
| G002980 | | Rutbah | 1.19 | n.d | | n.d | | n.d | | 0.09 | 0.09 | 1.42 | 0.37 |
| G002952 | | Lower Fars | 1.05 | n.d | | n.d | | n.d | | 0.12 | 0.11 | 1.68 | n.d |
| G002976 | | U.Shiranish | 1.06 | 0.49 | | 0.57 | | 2.03 | | 0.14 | 0.18 | 1.67 | n.d |
| G002981 | | Khabour | 1.15 | 0.46 | | 0.53 | | 1.74 | | 0.10 | 0.09 | 1.43 | 0.43 |
| G003009 | | Rutbah | 0.89 | 0.36 | | 0.82 | | 1.42 | | 0.19 | 0.16 | 1.54 | 0.40 |
| G003017 | | Doubayat | 0.96 | 0.51 | | 0.68 | | 1.47 | | 0.20 | 0.16 | 0.98 | 0.39 |
| G002959 | 1 | PJS | 0.20 | n.d | | n.d | | n.d | | 0.00 | 0.17 | 0.46 | n.d |
| G002954 | | PJS | 0.42 | n.d | | n.d | | n.d | | 0.00 | 0.00 | 2.11 | 0.43 |
| G002982 | | U.Doubayat | 0.69 | n.d | | n.d | | n.d | | 0.16 | 0.00 | 1.50 | 0.42 |
| G002988 | | Jeribe | 0.73 | 0.00 | | 0.73 | | 1.61 | | 0.14 | 0.19 | 1.27 | 0.40 |

Table C.2: Source-related parameters used to classify the oil samples into main genetic oil families shown Fig.5.15. C_{22}/C_{21} ; C_{24}/C_{23} ; C_{26}/C_{25} TT=tricyclic terpanes, $C_{28}/C_{29}=C_{28}/C_{29}$ $\alpha\beta\beta$ sterane, HHI= $C_{35}/(C_{31}-C_{35})(S+R)$ homohopanes, GI= gammacerane index, St./H= $C_{29}-C_{33}$ steranes/17 α (H) hopanes, 24/(24+27)= C-24/(C-24+C-27) norcholestane

| Sample | Family | Reservoir | 24d/(24d+27d) | DMDI-1 | DMDI-2 | EAI | 4.9DMD% | 4.8DMD% | 3.4DMD% |
|---------|--------|-------------|---------------|--------|--------|-----|---------|---------|---------|
| G002975 | 2A | ICD | 0.38 | 64 | 62 | 70 | 0.23 | 0.30 | 0.47 |
| G002968 | | L.Doubayat | 0.32 | 58 | 63 | 69 | 0.24 | 0.40 | 0.36 |
| G002995 | | R'mah | 0.37 | 59 | 59 | 64 | 0.19 | 0.30 | 0.51 |
| G002973 | | Mulussa F | 0.44 | 60 | 61 | 67 | 0.22 | 0.35 | 0.43 |
| G003006 | | Kometan | 0.39 | 55 | 63 | 69 | 0.24 | 0.34 | 0.42 |
| G003015 | | Rutbah | 0.31 | 65 | 66 | 64 | 0.23 | 0.35 | 0.43 |
| G002956 | | Rutbah | 0.32 | 66 | 61 | 62 | 0.23 | 0.33 | 0.44 |
| G002965 | | L.Rutbah | 0.36 | 68 | 67 | 66 | 0.20 | 0.35 | 0.45 |
| G003005 | | U.Shiranish | 0.32 | 57 | 62 | 66 | 0.21 | 0.35 | 0.45 |
| G002997 | | Jeribe | 0.31 | 61 | 65 | 66 | 0.20 | 0.39 | 0.42 |
| G002953 | | Rutbah | 0.35 | 60 | 63 | 68 | 0.20 | 0.41 | 0.40 |
| G002993 | | L.Fars | 0.31 | 61 | 63 | 67 | 0.25 | 0.41 | 0.34 |
| G002969 | | Mulussa F | 0.32 | 63 | 64 | 64 | 0.22 | 0.40 | 0.38 |
| G003011 | | Dhiban | 0.30 | 60 | 60 | 63 | 0.25 | 0.39 | 0.36 |
| G002963 | 2B | L.Rutbah | 0.35 | 69 | 63 | 54 | 0.22 | 0.32 | 0.46 |
| G002960 | | Erek | 0.37 | 65 | 61 | 66 | 0.23 | 0.38 | 0.40 |
| G002966 | | L.Rutbah | 0.38 | 67 | 67 | 73 | 0.24 | 0.38 | 0.38 |
| G002964 | | PJS | 0.41 | 68 | 62 | 67 | 0.24 | 0.31 | 0.45 |
| G002974 | | PJS | 0.37 | 68 | 60 | 63 | 0.26 | 0.43 | 0.31 |
| G002961 | | Derro | 0.35 | 65 | 58 | 62 | 0.19 | 0.29 | 0.52 |
| G002980 | | Rutbah | 0.36 | 65 | 56 | 62 | 0.21 | 0.33 | 0.46 |
| G002952 | | Lower Fars | 0.20 | 67 | 57 | 64 | 0.24 | 0.40 | 0.36 |
| G002976 | | U.Shiranish | 0.34 | 61 | 61 | 68 | 0.26 | 0.37 | 0.37 |
| G002981 | | Khabour | 0.43 | 55 | 62 | 65 | 0.22 | 0.43 | 0.35 |
| G003009 | | Rutbah | 0.35 | 56 | 60 | 66 | 0.25 | 0.41 | 0.33 |
| G003017 | | Doubayat | 0.35 | 55 | 63 | 58 | 0.25 | 0.43 | 0.31 |
| G002959 | 1 | PJS | 0.23 | 64 | 59 | 63 | 0.27 | 0.39 | 0.34 |
| G002954 | | PJS | 0.21 | 73 | 61 | 65 | 0.25 | 0.38 | 0.37 |
| G002982 | | U.Doubayat | 0.26 | 74 | 61 | 65 | 0.21 | 0.41 | 0.38 |
| G002988 | | Jeribe | 0.25 | 68 | 61 | 66 | 0.26 | 0.43 | 0.31 |

Table C.3: Source-related parameters used to classify the oil samples into main genetic oil families shown Fig.5.15. $24d/(24d+27d)=C-24/(C-24+C-27)$ nordiacholestane, $DMDI-1=$ dimethyl diamantane index $1=3,4DMD/(3,4DMD+4,9DMD)$, $DMDI-2=$ dimethyl diamantane index $2=4,8DMD/(4,8DMD+4,9DMD)$, $EAI=$ ethyldiamantane index $=2EA/(2EA+1EA)$, % 4,9 DMD $=4,9DMD/(4,9-+4,8-+3,4DMD)$, % 4,8 DMD $=4,8DMD/(4,9-+4,8-+3,4DMD)$, % 3,4 DMD $=3,4DMD/(4,9-+4,8-+3,4DMD)$

Appendix D

Mixing Model Calculations

Equation (Eq.5.8) can be solved readily using the matrix algebra functions (MMULT, MINVERSE, and TRANSPOSE) in Microsoft EXCEL. To solve the mixing potential problem presented in section.5.3 using an EXCEL spreadsheet, put matrix G (which is the end-members columns in Tab.5.3) in cells B4:D22, and put the matrix d (which is the data of each proposed mixed oil sample) in the cells E4:E22. Then select cells E20:E22 for matrix M (which represents the proportional contribution of each end-member in the mixed oil sample), and type the following line with no breaks or spaces:

```
=MMULT(MMULT(MINVERSE(MMULT(TRANSPOSE(B4:D22);B4:D22));  
TRANSPOSE(B4:D22));E4:E22)
```

into the cell E22. Then press CONTROL+ALT+ENTER to make E20:E22 an array containing M matrix.

Appendix E

Concentration of Crude Oil Constituents

| sample | biodegraded (ppm) | | | | non-biodegraded (ppm) | | | |
|------------------|-------------------|---------|---------|---------|-----------------------|---------|---------|---------|
| | G002993 | G002997 | G003001 | G003011 | G002953 | G002956 | G002973 | G002995 |
| iC5 | 2955 | 2692 | 3703 | 1507 | 4683 | 4706 | 4650 | 4455 |
| nC5 | 1168 | 478 | 4206 | 1631 | 7191 | 6512 | 6857 | 5957 |
| 2,2-DMB | 112 | 123 | 107 | 52 | 72 | 252 | 132 | 90 |
| CP | 343 | 177 | 844 | 369 | 1438 | 1193 | 1414 | 1160 |
| 2,3-DMB | 551 | 541 | 482 | 320 | 508 | 662 | 510 | 568 |
| 2MP | 1437 | 795 | 3533 | 1468 | 3988 | 4329 | 4072 | 4743 |
| 3MP | 2441 | 2139 | 2731 | 1372 | 3110 | 3200 | 3091 | 3379 |
| nC6 | 1510 | 602 | 5577 | 2280 | 6919 | 8743 | 6632 | 7019 |
| 2,2-DMP | 91 | 76 | 118 | 63 | 113 | 213 | 115 | 90 |
| MCP | 1860 | 836 | 4829 | 2545 | 6624 | 5042 | 6407 | 4613 |
| 2,4-DMP | 292 | 289 | 269 | 167 | 295 | 318 | 300 | 256 |
| 2,2,3-TMB | 45 | 39 | 40 | 54 | 45 | 82 | 62 | 22 |
| Benzene | 10 | 12 | 17 | 91 | 1659 | 2315 | 1763 | 1486 |
| 3,3-DMP | 99 | 97 | 93 | 68 | 99 | 118 | 86 | 66 |
| CH | 993 | 559 | 2389 | 1268 | 3889 | 3006 | 3542 | 2726 |
| 2MH | 1135 | 732 | 2141 | 1016 | 2124 | 2771 | 2231 | 2225 |
| 2,3-DMP | 1443 | 1356 | 1283 | 935 | 1423 | 1243 | 1409 | 1575 |
| 1,1-DMCP | 731 | 592 | 741 | 689 | 941 | 499 | 733 | 409 |
| 3MH | 1790 | 1199 | 3052 | 1609 | 3032 | 3511 | 3187 | 3627 |
| 1,cis,3-DMCP | 1596 | 898 | 2302 | 2080 | 2626 | 1659 | 2411 | 1304 |
| 1,trans,3-DMCP | 1705 | 1174 | 2154 | 1967 | 2471 | 1590 | 2278 | 1241 |
| 1,cis,2-DMCP | 1694 | 706 | 4603 | 4498 | 5294 | 3521 | 4993 | 2705 |
| nC7 | 872 | 299 | 4328 | 2778 | 7042 | 7654 | 6782 | 7649 |
| MCH | 3544 | 1962 | 7449 | 4951 | 10445 | 7149 | 9144 | 5810 |
| 1,trans,1,3-TMCP | 1494 | 1563 | 1145 | 1320 | 1737 | 947 | 1336 | 641 |
| ECp | 565 | 365 | 1087 | 725 | 1030 | 953 | 1204 | 1039 |
| 2,5-DMHhex | 299 | 287 | 357 | 222 | 316 | 513 | 389 | 413 |
| 2,4-DMHhex | 492 | 524 | 447 | 324 | 426 | 601 | 442 | 451 |
| 1,trans,2,4-TMCP | 2472 | 2667 | 1592 | 1723 | 1739 | 1030 | 1484 | 819 |
| 3,3-DMHhex | 118 | 133 | 120 | 87 | 133 | 148 | 108 | 135 |
| 1,2,3-TMCP | 2233 | 1982 | 2356 | 2832 | 2411 | 1482 | 2307 | 1191 |
| 2,3,4-TMCP | 445 | 470 | 322 | 346 | 428 | 225 | 346 | 287 |
| Toluene | 134 | 107 | 1630 | 600 | 2202 | 3245 | 2439 | 4275 |

Table E.1

| sample | biodegraded (ppm) | | | non-biodegraded (ppm) | | |
|------------|-------------------|---------|---------|-----------------------|---------|---------|
| | G002993 | G002997 | G003001 | G002953 | G002956 | G002973 |
| 2MHep | 989 | 658 | 2901 | 4026 | 4005 | 3854 |
| 3MHep | 993 | 774 | 1758 | 1520 | 2304 | 1611 |
| nC8 | 2868 | 2595 | 5592 | 8102 | 8213 | 7567 |
| ECHex | 3148 | 2667 | 4581 | 5219 | 4163 | 4758 |
| m+p-Xylene | 2107 | 1849 | 4587 | 4902 | 3784 | 4127 |
| 2+4-MOct | 1084 | 970 | 2158 | 1796 | 2911 | 1980 |
| 3MOct | 549 | 682 | 1641 | 1538 | 2116 | 1615 |
| o-Xylene | 1234 | 332 | 1136 | 1222 | 1347 | 1057 |
| nC9 | 979 | 1222 | 6519 | 6640 | 7059 | 6033 |
| nC10 | 2194 | 2285 | 7001 | 6769 | 7317 | 6062 |
| nC11 | 1168 | 1346 | 7432 | 6952 | 6886 | 5880 |
| nC12 | 1441 | 1482 | 7415 | 6837 | 6497 | 5523 |
| nC13 | 3051 | 2187 | 8193 | 8234 | 6938 | 6354 |
| nC14 | 4043 | 3643 | 8601 | 9087 | 7505 | 6892 |
| nC15 | 4335 | 3989 | 8385 | 9269 | 7202 | 6716 |
| nC16 | 4327 | 4496 | 7878 | 8781 | 6833 | 6288 |
| iC18 | 3214 | 3715 | 2986 | 3895 | 2726 | 2799 |
| nC17 | 3938 | 4204 | 7129 | 8455 | 6308 | 5908 |
| Pr. | 5500 | 6597 | 4768 | 6589 | 3882 | 4785 |
| nC18 | 3736 | 4139 | 6306 | 8108 | 5741 | 5326 |
| Ph. | 4314 | 5055 | 4327 | 5438 | 3536 | 3845 |
| nC19 | 4201 | 4471 | 6583 | 9005 | 5805 | 5708 |
| nC20 | 3274 | 3358 | 5375 | 7359 | 5012 | 4690 |
| nC21 | 2879 | 2850 | 4834 | 6282 | 4514 | 4395 |
| nC22 | 2756 | 2660 | 4612 | 5912 | 4362 | 4536 |
| nC23 | 2599 | 2649 | 3976 | 5085 | 3748 | 4025 |
| nC24 | 2596 | 2666 | 3633 | 4770 | 3532 | 4038 |
| nC25 | 2744 | 2712 | 3140 | 4014 | 2849 | 3445 |
| nC26 | 2358 | 2407 | 2727 | 3604 | 2788 | 3127 |
| nC27 | 1936 | 2026 | 2309 | 3088 | 2313 | 2755 |
| nC28 | 1576 | 1671 | 1900 | 2518 | 1974 | 2238 |
| nC29 | 1415 | 1438 | 1506 | 2116 | 1528 | 2056 |
| nC30 | 1330 | 1255 | 1480 | 1920 | 1561 | 1829 |
| | | | 1019 | | | 1591 |

Table E.2: Concentrations (ppm) of crude oil constituents used in Eq.5.17 to calculate the mean degradative loss to assess the degree of biodegradation after (Elias *et al.*, 2007).

Curriculum Vitae

Ahmad Aldahik

Address: Werneuchenerstr.19

13055 Berlin / Germany

Tel. +49 17622952624

Email: aadahik@hotmail.com

aadahik@gfz-potsdam.de

Date of Birth: 01 March 1978



Professional Background

10/05 – 11/10 Researcher (limited contract) at Helmholtz Centre Potsdam, German Research Centre for Geosciences GFZ, Organic Geochemistry section

- **Geochemical study (PhD)** on crude oils and source rocks from the Euphrates Graben Petroleum System, Syria

04/03 – 11/04 Lecturer Assistant Al Baath University, Petroleum Engineering Faculty, Syria

- Teaching “Petroleum Geochemistry” for third- year students

10/01 – 04/03 Operation Engineer (shift engineer), Homs Refinery Company, Syria

- Kerosene; Coker gas oil; Heavy Coker gas oil hydro treating units
- Observing the work in normal circumstances
- Making decisions when technical or operation mistakes are occurred

Academic Background

10/05 – 11/10 Ph.D. Berlin University of Technology & Helmholtz Centre Potsdam

German Research Centre for Geosciences GFZ, Organic Geochemistry sec.
 Doctoral thesis: "Crude Oil Families in the Euphrates Graben Petroleum System, Syria"

2001 – 2003 Diploma in Petroleum Engineering, Al Baath University, Petroleum Engineering Faculty, Syria
 Diploma thesis: S
 Average grade: GPA: 72.3 %, this is considered "good"

1996 - 2001 Bachelor in Petroleum Engineering, Al Baath University, Petroleum Engineering Faculty, Syria
 Bachelor thesis:
 S S S
 Average grade: GPA: 69.9 %, this is considered "good"

Scientific Courses

| | |
|----------------|--|
| Winter 2005 | Exploration Geology |
| Summer 2005 | Fossil Fuel Exploration: Applications of Petroleum Biomarkers |
| Summer 2005 | Environmental Geochemistry |
| Winter 2006 | Basin Analysis |
| Summer 2006 | Basin modeling and organic geochemistry in petroleum exploration |
| September 2007 | Petroleum System Evaluation: Fluid Compositional Prediction |
| September 2009 | Establishing petroleum systems using biomarkers and chemometrics |
| September 2009 | Terrestrial source rocks and oils: concepts and tools for improved assessment and prediction |

Languages

- Arabic: mother tongue
- English: very good
- German: very good

Publications

Papers in journals

- Aldahik, A., Wilkes, H., Schulz, H.-M., Horsfield, B., Nederlof, P., Dransfield, M., Dominik, W.: Geochemical Characterisations of Crude Oils in the Euphrates Graben, Syria. (in prep.)

Presentations at international congresses

- Aldahik, A.; Wilkes, H.; Horsfield, B.; Dominik, W.; Nederlof, P. (2006): Oil Families in the Euphrates Graben, Syria, The first annual Ph.D day at GeoForschungZentrum Potsdam GFZ, (Potsdam, Germany, 2006). POSTER
- Aldahik, A.; Wilkes, H.; Schulz, H.-M.; Horsfield, B.; Dominik, W.; Nederlof, P. (2007): Oil Families in the Euphrates Graben, Syria, Book of Abstracts, 23rd International Meeting on Organic Geochemistry - IMOG (Torquay, Devon, United Kingdom 2007). POSTER
- Aldahik, A.; Wilkes, H.; Schulz, H.-M.; Horsfield, B.; Dominik, W.; Nederlof, P.; Dransfield, M. (2008): Silurian Tanf Formation: Prospectivity in the Euphrates Graben Petroleum System, Syria, Book of Abstracts, 8th Middle East Geoscience Conference and Exhibition – Geo 2008 (Manama, Bahrain, 2008). ORAL
- Aldahik, A.; Wilkes, H.; Schulz, H.-M.; Horsfield, B.; Dominik, W.; Nederlof, P.; Dransfield, M. (2008): Crude oil families and mixing in the Euphrates Graben, Syria, 5th General Assembly European Geosciences Union - EGU (Vienna, Austria 2008). POSTER
- Aldahik, A.; Wilkes, H.; Schulz, H.-M.; Horsfield, B.; Dominik, W.; Nederlof, P. (2008): Geochemical Characteristics of Crude Oils in the Euphrates Graben, Syria, The third annual Ph.D day at GFZ GeoForschungZentrum Potsdam , (Potsdam, Germany, 2008). POSTER
- Aldahik, A.; Wilkes, H.; Schulz, H.-M.; Horsfield, B.; Dominik, W.; Nederlof, P. (2009): Geochemical Investigations of Crude Oils in the Euphrates Graben, Syria, Book of Abstracts, 24th International Meeting on Organic Geochemistry - IMOG (Bremen, Germany 2009). POSTER

Presentations at internal meetings (with industry partners: Shell & AFPC)

Aldahik et al.,: Petroleum Systems of Syria: Oil Families in the Euphrates Graben. Presentations for the Industry Partners at regular meetings in Potsdam (Germany), Rijswijk (the Netherlands), and Damascus (Syria).

Scientific Reports (unpublished)

- Aldahik et al., (2007): Petroleum Systems of Syria. 2nd annual report for the Industry Partners, “Oil Families in the Euphrates Graben, Syria”, GFZ Potsdam.
- Aldahik et al., (2006): Petroleum Systems of Syria. 1st annual report for the Industry Partners, “Oil Families in the Euphrates Graben, Syria”, GFZ Potsdam.
- Aldahik et al., (2006): Petroleum Systems of Syria. Progress report for the Industry Partners, “Oil Families in the Euphrates Graben, Syria”, GFZ Potsdam.

References

| | | | |
|-----------------------|--|-----------------|--|
| Prof. Brian Horsfield | Head of Chemistry and Material Cycles department at the German research centre (GFZ Potsdam) | +49 331 2881780 | horsf@gfz-potsdam.de |
| Dr. Peter Nederlof | Shell’s chief geochemist | | P.Nederlof@shell.com |
| Ph Dr. Heinz Wilkes | Organic Geochemistry section at the German research centre for Geosciences (GFZ Potsdam) | +49 331 2881784 | wilkes@gfz-potsdam.de |

Ahmad Aldahik